# University of Cincinnati

**Date: 7/21/2015**

**I, Kevin E Wilson , hereby submit this original work as part of the requirements for the degree of Master of Science in Civil Engineering.**

It is entitled:

**A Finite Element Investigation of Non-Orthogonal Moment Connections in Steel Construction**

Student's name: **Kevin E Wilson**

This work and its defense approved by:

**Committee chair: Gian Rassati, Ph.D.**

**Committee member: James Swanson, Ph.D.**

UNIVERSITY OF Cincinnati

18440

# A Finite Element Investigation of Non-Orthogonal Moment Connections in Steel Construction

A thesis submitted to the

Graduate School of the University of Cincinnati in partial fulfillment of

the requirements of the degree of

Master of Science in Civil Engineering

Department of Civil and Architectural Engineering and Construction

Management

By

Kevin E. Wilson

Bachelor of Science in Civil Engineering

University of Cincinnati, College of Engineering

Committee Chair: Gian A. Rassati, PhD

Committee Members:
James A. Swanson, PhD
Uwe Aschemeier

## Abstract

Modern architectural designs for buildings often require innovative and unconventional structural solutions such as the use of non-orthogonally framed connections. Moment frames are seismic force resisting systems that provide architectural liberty when these unconventional designs are encountered. While a braced frame or a structural wall can be more cost efficient, a moment frame allows for the building space to be more efficiently utilized. Additionally, the moment frame allows for architectural liberty.

When the seismic demand requires the use of an intermediate or special moment frame per the ASCE/SEI 7 specification, the document requires that the designing engineer implement a prequalified connection from the ANSI/AISC 358 document. However, the connections presented within this document do not account for non-orthogonally framed connections. Therefore, the designing engineer must either perform cyclic qualification of the proposed connection, or make a potentially ambiguous decision for the use of the connection based on their engineering judgment alone.

The research investigates the effects of non-orthogonal connection framing of two connections presented in the ANSI/AISC 358 document with solid element finite element analyses. The responses of the connections are compared with traditional orthogonally framed connections validated from experimental testing.

The results of the analyses provide insights on the expected behaviors as well as design recommendations that should be considered for practicing engineers.

## Acknowledgements

I would like to thank my committee members, Dr. Gian A. Rassati and Dr. James A. Swanson. They provided a tremendous resource when the research encountered difficulties. Furthermore, I would also like to thank them for their contributions to my education and development as a student and engineer. I would not have the knowledge and confidence without their commitment to my growth. For this, I am grateful.

I would also like to thank my final committee member Uwe Aschemeier for his time as well as considerations throughout this research project. His particular knowledge and expertise on the research topic provided a great resource to the investigation.

I would like to thank my fiancée Allison Brown for her support throughout my graduate studies. I would also like to thank the friends that I made in graduate school. Without the comradery of my fellow peers, the work in graduate school would likely have been too overwhelming.

**Table of Contents**

## Table of Figures

# Chapter 1: Introduction

The ANSI/AISC 358 document produced by the American Institute of Steel Construction (AISC) contains prequalified moment connections for use in buildings that require an intermediate or special moment frame (ANSI/AISC 358, 2010). The connections presented in the document provide design requirements and limitations for use by the designing engineer. The document also provides the expected behaviors of the connections such as location of hinging in the beam and the amount of rotation expected in the connection.

The prequalified connections that are presented in the document are qualified based on cyclic testing performed in literature as well as extensive finite element analyses that accompany the testing. If a specific connection that is not presented in the ANSI/AISC 358 document is intended for use in an intermediate or special moment frame, it must be qualified by cyclic testing as required by the ANSI/AISC 341 specification (ANSI/AISC 341, 2010).

During the design of buildings, architectural constraints can require the use of non-orthogonal framing modifications. The seismic demands of the area may require the use of an intermediate or special moment frame. Therefore, the use of the ANSI/AISC 358 document would be a great resource for the design engineers. However, the document currently considers only traditional orthogonally framed

connections explicitly. If the designing engineer is required to implement non-orthogonal framing, the applicable specifications do not provide explicit guidance.

There have been recent additions to the commentary of the ANSI/AISC 358 document for the 2016 edition that implicitly addresses non-orthogonal connections. For skewed connection configurations, the commentary indicates that limited analytical studies indicate skew angles less than 10 degrees might be acceptable for reduced beam sections (RBS). Similarly, for sloped connection configurations, studies suggest that orienting the RBS detail perpendicular to the beam performs better than orienting parallel to the column centerline. The limited analytical studies have only included RBS connections.

Furthermore, the ANSI/AISC 358 document is ambiguous whether the non-orthogonally framed connection would require cyclic qualification. This creates an economical dilemma, as further resources would be required prior to commencement of construction. Therefore, the non-orthogonal configurations of moment frames need to be addressed in the ANSI/AISC 358 document.

# Chapter 2: Background

## 2.1 Tom Bradley International Terminal Modernization Program

As part of the architectural design of the Tom Bradley International Terminal (TBIT) Modernization Program at Los Angeles International Airport (LAX), there were numerous sloped moment frames. The architectural expressions required the use of special moment frames that spanned long lengths. Not only were some of the beams and columns sloped up to 28 degrees, but the steel members curved along the spans.

The reduced beam section (RBS) moment connection detail was selected for the project. Since the RBS connection can be found in the ANSI/AISC 358 document, it does not require prequalification testing (ANSI/AISC 341, 2010). The ANSI/AISC 358 document explicitly considers orthogonal framing. Therefore, whether the building codes require non-orthogonal moment frames to be prequalified is ambiguous. Because of this, the engineer decided to perform qualification testing given the sloped and curved configurations of the special moment frames.

The qualification testing was documented in a research article (Ball, 2011). The results of each of the four connections tested met the building code requirements for use in seismic application. (ANSI/AISC 341, 2010) The intent of the article was to provide awareness of the issue of non-orthogonal connection

framing. The TBIT-LAX project incurred additional expense due to the necessity of qualification for the connections utilized in the building. The authors suggest that the governing building codes support the design of non-orthogonal moment frames in order to avoid this increased project cost.

### 2.2 Evaluation of Sloped RBS Moment Connections

In conjunction with the physical testing of the sloped beam-to-column connections in the TBIT-LAX project, finite element modeling and analyses were conducted in an attempt to quantify the effects of sloped geometry. The physical testing in the TBIT-LAX project prompted the authors to model the sloped connection using finite element analysis due to the atypical brittle fracture of the top flange weld which is uncommon of an RBS connection (Kim et al, 2015).

The connections tested in the TBIT-LAX project met the requirements of the ANSI/AISC 341 specification, but a brittle fracture of the top flange weld was observed. This prompted the authors to modify the connection by further increasing the radius cut dimension “c” (see Figure 2-1) in the RBS design to induce plasticity further away from the connection. The increased radius cut dimension “c” successfully increased plasticity and improved the overall ductility of the connection, but a brittle fracture of the top flange weld was also observed.

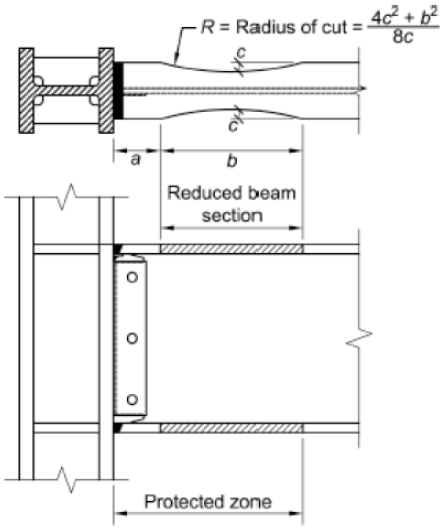


**Figure 2-1: RBS connection detail (ANSI/AISC 358, 2010)**

The RBS connection tested in the TBIT-LAX project was configured with the radius cut region parallel to the column. The authors investigated an alternative configuration with the radius cut region perpendicular to the beam section as shown in Figure 2-2. The authors advise the use of the configuration with radius cut region perpendicular to the beam section as it reduces the strain demand at the heel location of the connection. Finally, their analyses indicated that for further increase in the angle of the slope at the beam-to-column connection increases strain demand at the heel location and decreases the strain demand at the toe location (Kim et al., 2015).

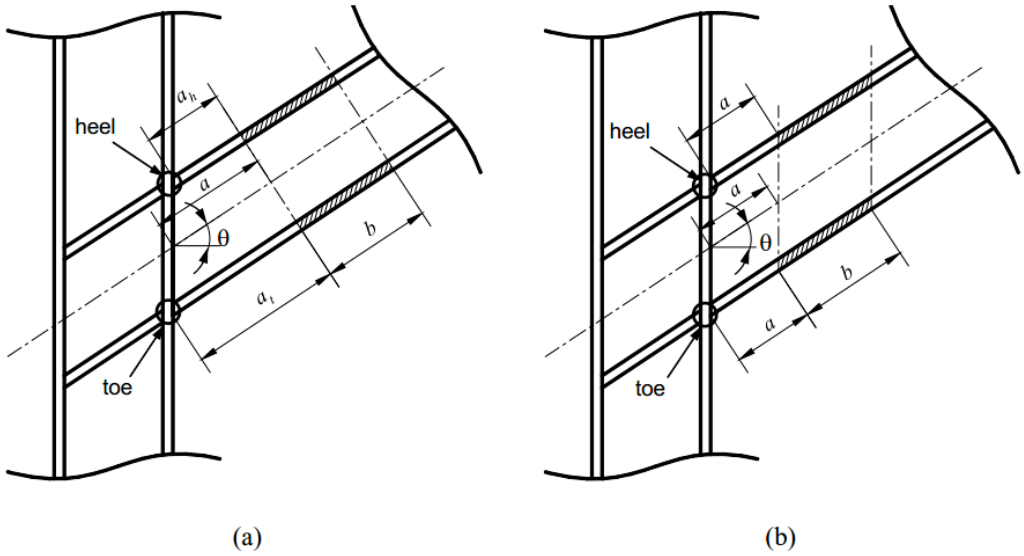


**Figure 2-2: RBS configurations: (a) Radius cut perpendicular to the beam section; (b) Radius cut parallel to the column section (Kim et al., 2015)**

## 2.3 Demands on Reduced Beam Section Connections with Out-of-Plane Skew

In an attempt to determine the amount of skew angle that could be incorporated in a non-orthogonal special moment frame connection, finite element analyses were performed on several moment frames with various skew angles (Prinz and Richards, 2014). Several beam and column sizes were selected that would barely meet the seismic compactness requirements within the ANSI/AISC 341 specification. These connections were selected with the idea that they would be more critical than beam and column sizes that moderately exceed the compactness requirements.

The finite element modeling considered an exterior beam-to-column connection (L-shaped) and an interior beam-to-column connection (T-shaped). The finite element analyses utilized shell elements. The selected moment frames included varying skew angles for the beam up to 30 degrees by 10 degree increments.

The authors utilized two response parameters to quantify the results: 80% of the plastic moment capacity and a low cycle fatigue damage model. The results indicated an increase in column twisting for increased beam skew angles. Notably, the authors indicated that the connections with the largest beam skew configuration resulted in the highest rotation capacities. This increased rotation capacity came at the expense of the column. Yielding of the column flanges was observed in the

finite element models at skew angles of 30 degrees as shown in Figure 2-3. The authors recommended that in the absence of experimental data for beam skew, an approach that was consistent with their results would be acceptable for beams with skew angles up to 10 degrees.

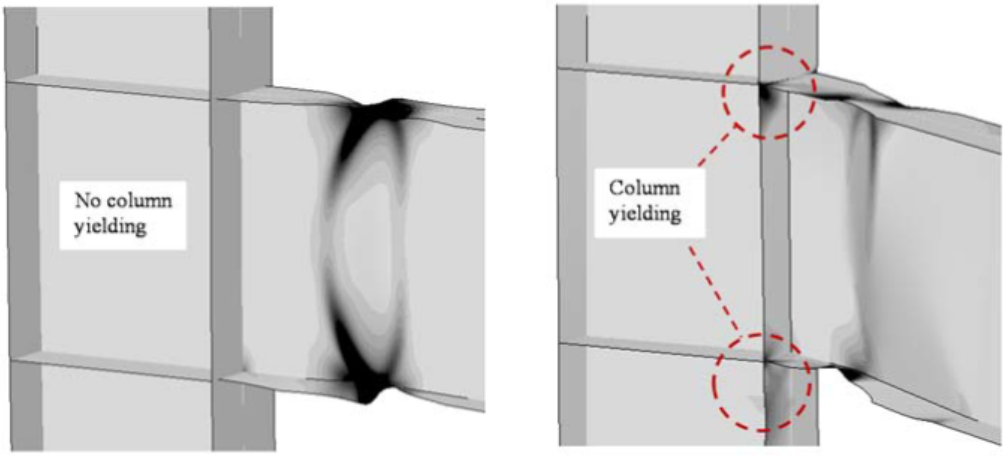


**Figure 2-3: Observed column yielding: (left) 0 degree skew; (right) 30 degree skew (Prinz and Richards, 2014)**

## 2.4 A Finite Element Approach for Modeling Bolted Top-and-Seat Angle Components and Moment Connections

Partially restrained connections are difficult to effectively consider when modeling using finite element software because they cannot be considered a simple connection or a fixed connection. Because of this, the top-and-seat angle connection is not currently prequalified for use by engineers for moment resistance per the ANSI/AISC 341 specification. A finite element modeling methodology was developed at the University of Cincinnati for use in modeling top-and-seat angle connections (Ruffley, 2011).

The finite element software use in the research was ABAQUS. The analysis implemented solid elements and nonlinear plasticity. Prior to modeling full scale connections, mesh sensitivity analyses were performed to determine the type and quantity of elements to optimize accuracy and computation time. The sensitivity analyses considered the use of both linear and quadratic elements. The results of the sensitivity analyses were compared to theoretical moment and displacement values from structural analysis computed traditionally by hand. The investigation concluded that the use of C3D8R elements could be used with a combination of coarse and fine meshes in lieu of the more computationally exhausting C3D20R. However, in regions where high stress and strain demands were expected, C3D20R elements were implemented.

A full-scale top-and-seat angle moment connection was modeled following a mesh sensitivity analyses. The model was created to match previous experimental testing of a full-scale connection from literature (Schrauben, 1999). The finite element model created in ABAQUS is shown in Figure 2-4. Careful consideration of the geometries and material properties allowed the author to have a comparable finite element model. The analysis was performed by reproducing the loading as detailed in the literature. The results of the finite element analyses were compared with the physical testing results as shown in Figure 2-5.

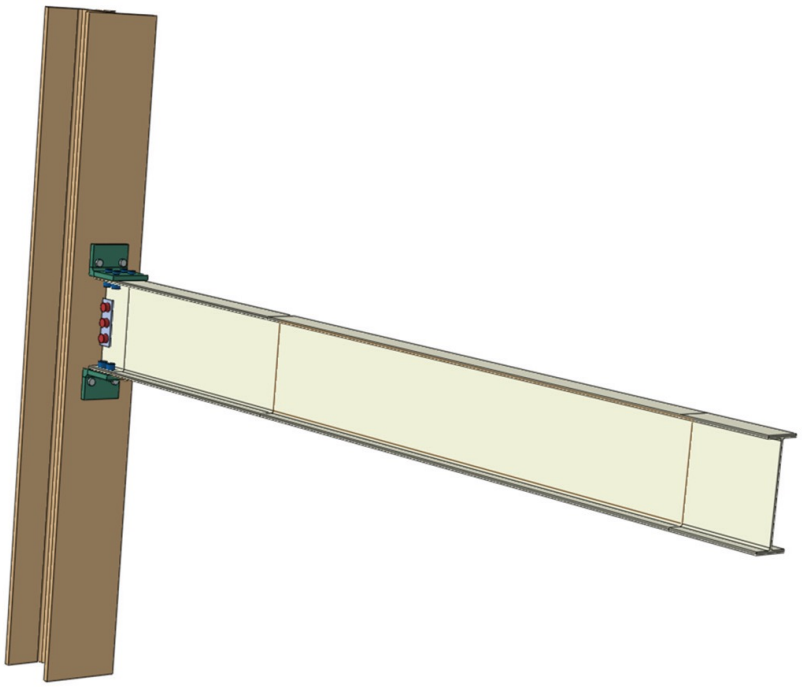

**Figure 2-4: FS-01 model assembly in ABAQUS (Ruffley, 2011)**

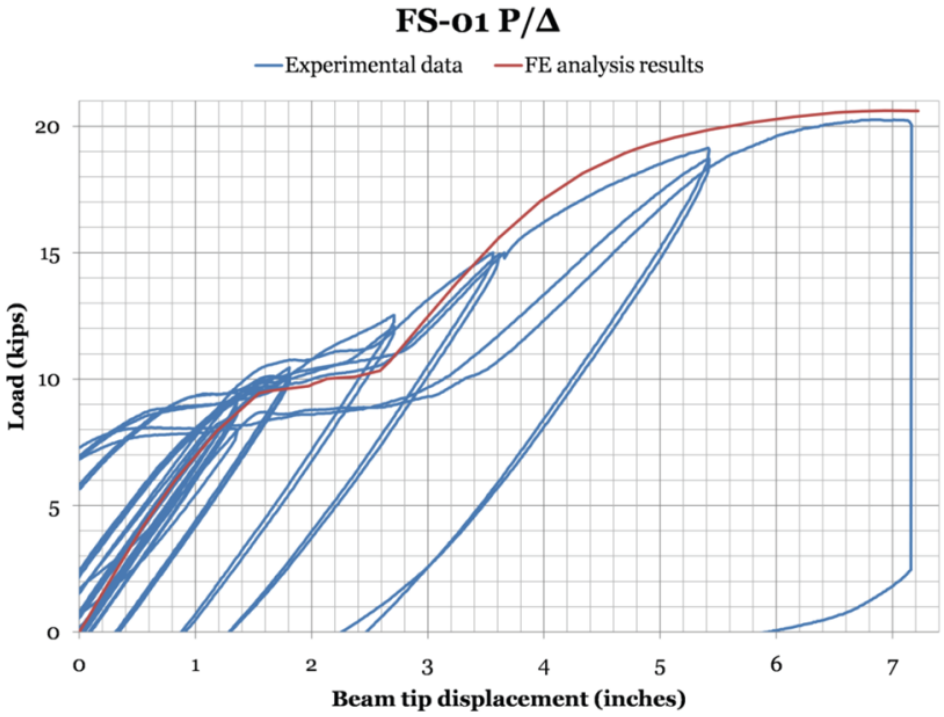


**Figure 2-5: Load vs. beam tip displacement comparison between experimental data and finite element model (Ruffley, 2011)**

The results were successful in reproducing the response of the physical testing using finite element modeling software. Therefore, the modeling methodology formulated from the research could be applied to other connections. This modeling methodology will be utilized for the investigation of the proposed research.

# Chapter 3: Goals and Methodologies

## 3.1 Goals

The goals of this research were to observe and quantify the effects of non-orthogonal connection geometry on prequalified moment frame connections taken from the ANSI/AISC 358 document. Two connection details were be selected based on the popularity of use among practicing engineers in the United States. These selected connection details include: the Welded Unreinforced Flange Welded-Web (WUF-W) and the Reduced Beam Section (RBS).

Finite element modeling and analysis will be performed on the selected connection details using methodologies from literature. (Ruffley, 2011) The selected connections will be validated by comparing the results of the orthogonally framed models to the response of physical tests documented in literature. Upon validation of both connection details, the orthogonal framing will be modified by sloping and/or skewing the beam section as it frames into the column. The analysis will be performed on the non-orthogonal connection configurations and the results will be compared to the traditional orthogonally framed configuration.

## 3.2 Response Parameters and Sign Convention

The response parameters that were investigated include: stiffness and plastic moment capacity, stress distribution, and plastic strain distribution. The connection

stiffness and plastic moment capacity were investigated by comparing the moment versus rotation response of the non-orthogonal connection models to the orthogonal connection model. For all finite element models, the loading applied to the connection is performed by applying a vertical displacement to the beam tip. The moment force is calculated by taking the vertical reaction force at the beam tip and multiplying by the length of the beam perpendicular to the column face. The rotation is calculated as the vertical displacement of the beam tip divided by the perpendicular length to the column face. These calculations ensure a direct comparison of moment versus rotation between the non-orthogonal and orthogonal connection models.

The sign convention used for positive and negative moments follows typical engineering practice in the United States. This sign convention defines a positive moment resulting in tension below the neutral axis of the beam and a negative moment resulting in tension above the neutral axis of the beam. A downward vertical displacement at the beam tip applied a negative moment, while an upward vertical displacement at the beam tip applied a positive moment.

The stress distribution and plastic strain distribution were investigated by implementing the Von Mises yield criterion. The stress values were scaled to the yield strengths of the materials in use in order to better view the distribution of stress throughout the connection. The plastic strain values were scaled to the

maximum observed plastic strain values of the orthogonal model to provide a direct comparison between the orthogonal and non-orthogonal connection geometry.

Finally, to quantitatively observe the effects of stress distribution in the beam from the non-orthogonal geometry, stress values were recorded from the analysis at specified locations. At the first indication of nonlinearity from the analysis, the stress values associated with that moment force were recorded and compared between models. Additionally, at 50% of yield, the stress values were recorded and compared between models.

For the WUF-W models, the stress values were recorded in the beam flange under tension at a distance of one-half of the depth from the face of the column. Three values were recorded for the skewed configurations and labeled $\sigma_L$, $\sigma_M$, and $\sigma_R$ which correspond to the left, middle, and right of the flange, respectively. The "left" node is taken at a length from the edge of the flange equal to 1/3 of the width of flange. The "right" node is taken at a length from the edge of the flange equal to 1/3 of the width of the flange. The locations are shown in Figure 3-1. For reference, under these definitions for locations of stress recordings, the skewed angle forms at the right side of the beam flange.

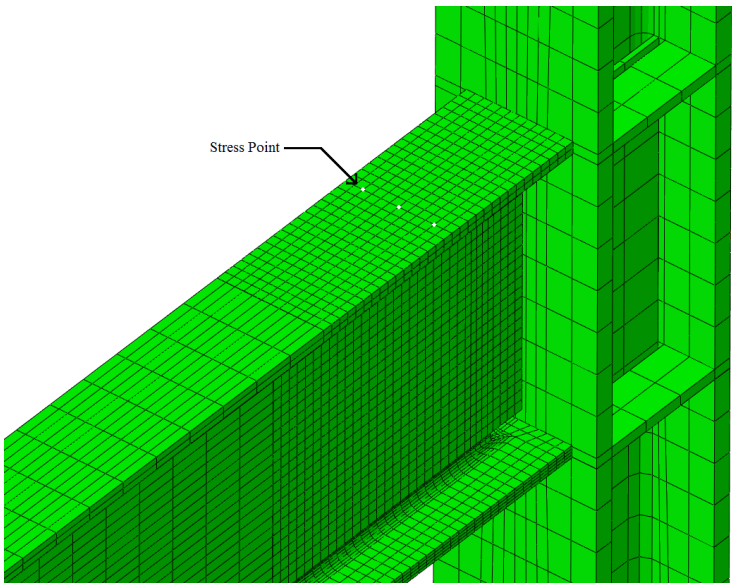


**Figure 3-1: Selected nodes for Von Mises stress values for the WUF-W model.**

For the sloped configurations, the $\sigma_L$ and $\sigma_R$ values are recorded on the top and bottom of the beam flange in tension. These two values were averaged for both top and bottom flange and recorded as $\sigma_T$ and $\sigma_B$. These values correspond to the top and bottom of the beam flange in tension, respectively.

For the RBS model, the stress values are defined the same way. The only difference between the WUF-W and RBS models are the locations of the stress recordings. In the RBS models, the stress values are recorded at the center of the radius cut section. The locations of the stress recordings for the skewed configurations are shown in Figure 3-2.

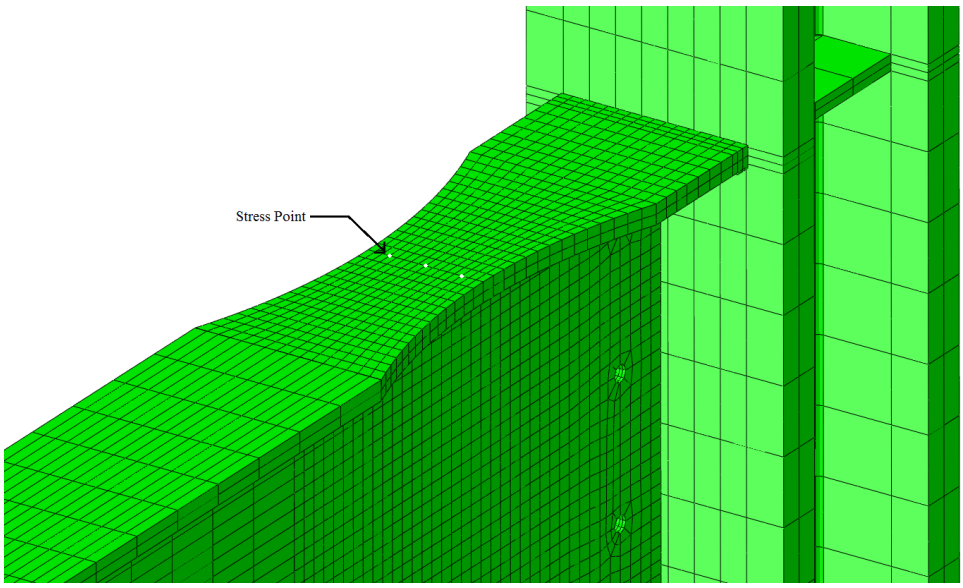


**Figure 3-2: Selected nodes for Von Mises stress values for the RBS model.**

## 3.3 Definitions of Skewed and Sloped Framing

The definitions for the skewed and sloped configurations are consistent with the ANSI/AISC 360 specification. A sloped beam-to-column configuration varies the angle of the beam within the plane of loading as shown in Figure 3-3. In relation to the beam/column assembly, the slope angle varies the beam vertically with respect to the longitudinal axis of the column. The skewed beam-to-column configuration varies the angle of the beam horizontally with respect to the transverse axis of the column as shown in Figure 3-4.

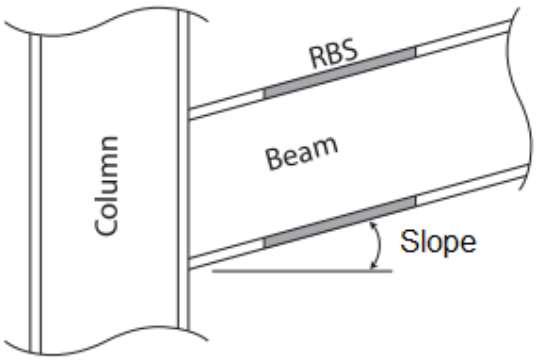


**Figure 3-3: Sloped beam-to-column configuration (Prinz and Richards, 2014)**

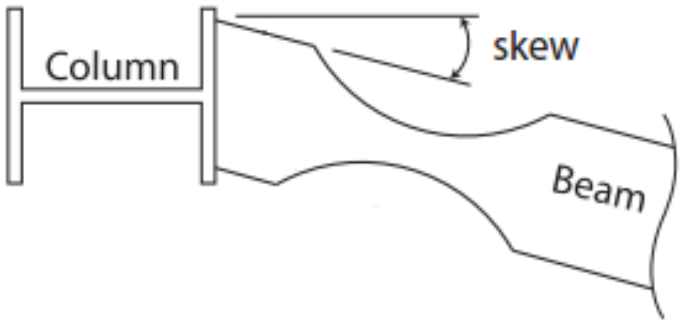


**Figure 3-4: Skewed beam-to-column configuration (Prinz and Richards, 2014)**

## 3.4 Finite Element Modeling Methodology

### 3.4.1 Welded Unreinforced Flange Welded-Web (WUF-W) Model

The Welded Unreinforced Flange Welded-Web (WUF-W) detail is a fully welded beam-to-column connection that is a popular selection for seismic application among engineers in the United States. The WUF-W moment

connection is a prequalified connection as detailed in the ANSI/AISC 358 document. In order to compare the effects of non-orthogonal geometry, a control model was selected from literature and reproduced with finite element analysis. The control model selected was from experimental testing conducted in conjunction with the SAC Task 7.05. (Hassan, 2012)

The physical testing consisted of a W30 × 148 beam framing into a W14 × 257 column with continuity plates and doubler plates as shown in Figure 3-5. The material grades were specified within the research, and expected values were implemented into the finite element model. The W30 × 148 beam had coupons cut and tested for yield and tensile strength. The stress-strain curve was documented in the literature and incorporated in the material plasticity for the beam section in the finite element model.

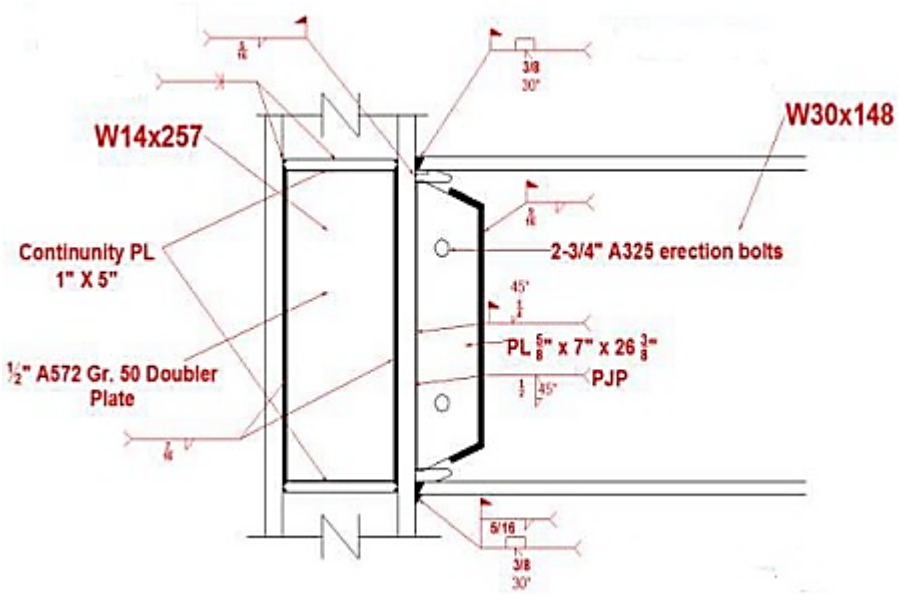


**Figure 3-5: WUF-W moment connection detail (Hassan, 2012)**

The W30 × 148 beam was modeled with a combination of C3D8R and C3D20R cubic solid elements. In order to control the meshing scheme, the beam was partitioned in several locations consistent with the methodologies from literature. (Ruffley, 2011) In regards to the recommendations from Ruffley, C3D20R elements were implemented within a distance equal to the depth of the cross section from the face of the column. The remainder of the beam was meshed with C3D8R elements. The seed size for the C3D8R elements was 1 inch while the seed size for the C3D20R elements was 4 inches. The erection bolts in the shear tab and beam web were omitted because they were not expected to carry non-negligible forces. The beam mesh assembly is shown in Figure 3-6. The beam was connected to the column face using a tie that would create the fully welded connection.

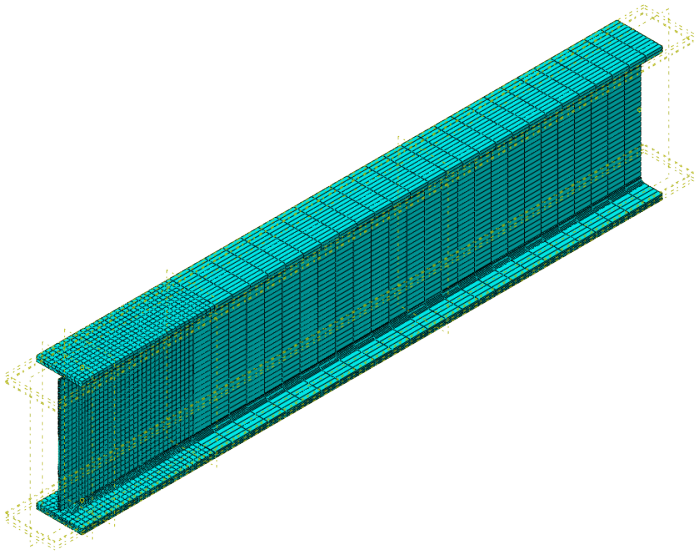

**Figure 3-6: W30 × 148 beam mesh assembly for the WUF-W moment connection**

The W14 × 257 column was modeled with the use of C3D20R elements throughout. The seed size used was 4 inches which was consistent with the recommendations by Ruffley. Due to the large relative size of the elements using a 4 inch seed, the use of C3D20R elements was not considered to have a significant impact on computation time. The mesh assembly for the column is shown in Figure 3-7.

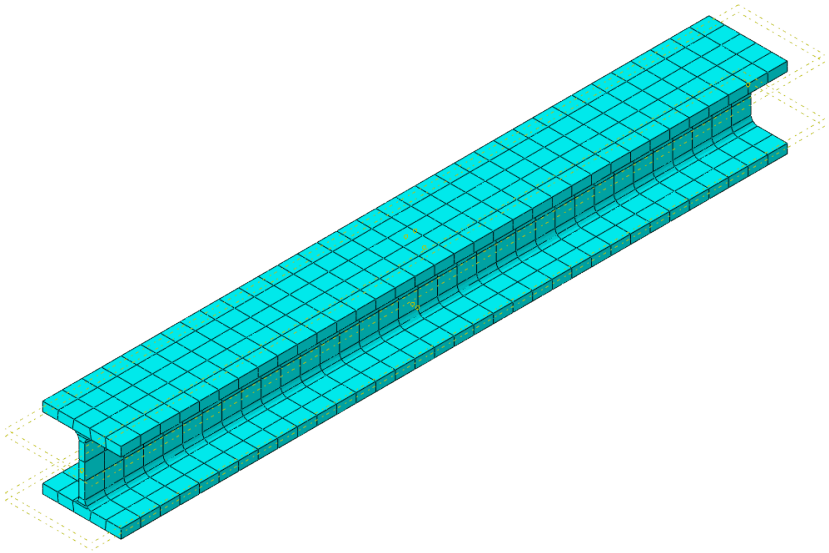

**Figure 3-7: W14 × 257 column mesh assembly for the WUF-W moment connection**

The shear tab, continuity plates, and doubler plates all implemented the C3D20R elements due to the small size and relative number of elements created with respect to the entire model. A seed size of 1 inch was used for each the shear tab, continuity plates, and doubler plates. The mesh assemblies for each part are

shown in Figures 3-8, 3-9, and 3-10. The shear tab was connected to the column face using a tie constraint. The shear tab was connected to the web of the beam with a tie constraint along the length of the prescribed fillet weld from the physical connection detail. The continuity and doubler plates were connected to the column with tie constraints along the length of the welds prescribed in the physical connection detail.

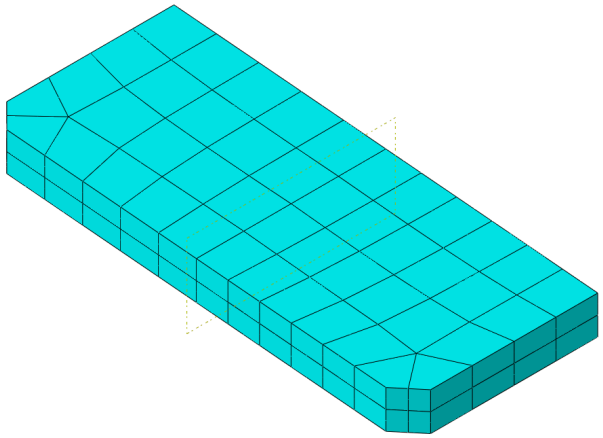

**Figure 3-8: Continuity plate mesh assembly for the WUF-W moment connection**

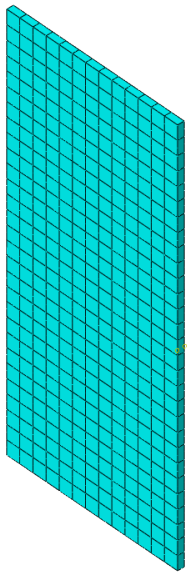

**Figure 3-9: Doubler plate mesh assembly for the WUF-W moment connection**

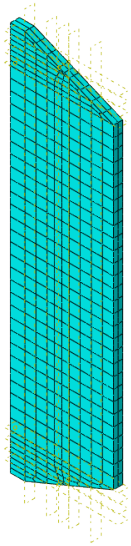

**Figure 3-10: Shear tab mesh assembly for the WUF-W moment connection**

### 3.4.2 Reduced Beam Section (RBS) Model

The reduced beam section (RBS) detail was also selected in the investigation for its popularity among engineers in seismic design. Similar to the WUF-W

moment connection, a control model was created in order to compare the effects of non-orthogonal geometry. A connection was selected from literature and the response was reproduced with finite element modeling. The connection detail was selected from an experimental investigation of the RBS moment connection under cyclic loading. (Engelhardt et al. 1998)

There were several different connections that were tested and documented in the literature. The DB4 connection designation was selected for validation which consisted of a W36 × 194 beam framing into a W14 × 426 column. The detail from the physical connection is shown in Figure 3-11. The column was designated as ASTM A572 grade 50 steel. The mill certificates were unavailable for the remaining components. Therefore, the specified grades of steel were unknown. However, the measured beam flange yield stresses were documented for the tested connections.

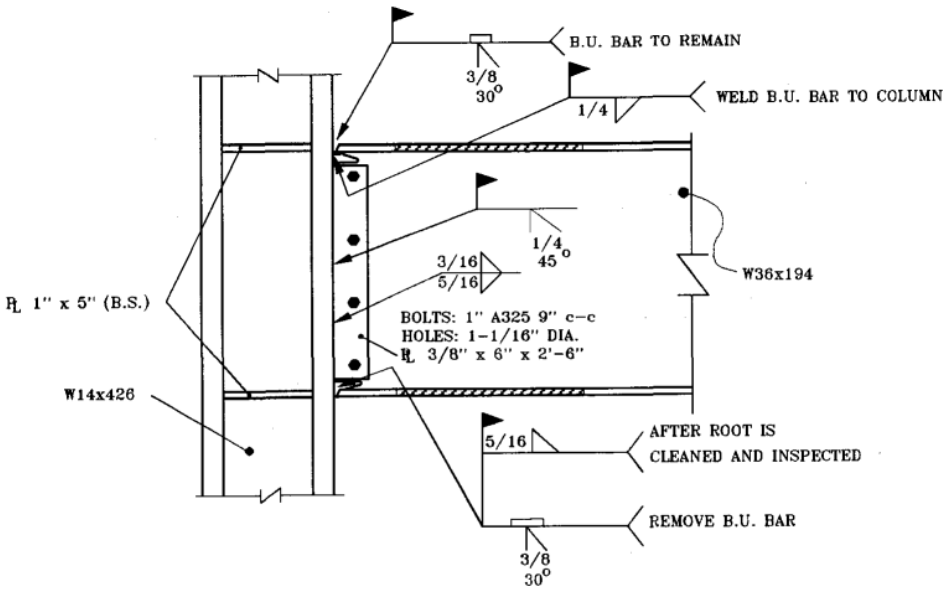


**Figure 3-11: RBS moment connection detail (Engelhardt et al. 1998)**

The W36 × 194 beam was modeled with a combination of C3D8R and C3D20R cubic solid elements. In order to control the meshing scheme, the beam was partitioned in several locations consistent with the methodologies from literature. (Ruffley, 2011) Because Ruffley had not modeled an RBS connection, the authors decided to provide C3D20R elements a distance from the face of the column extending through the radius cut region. The remainder of the beam was meshed with C3D8R elements. The seed size for the C3D8R elements was 1 inch while the seed size for the C3D20R elements was 4 inches which as consistent with the recommendations by Ruffley. The beam mesh assembly is shown in Figure 3-12. The beam was connected to the column face using a tie that would create the fully welded connection.

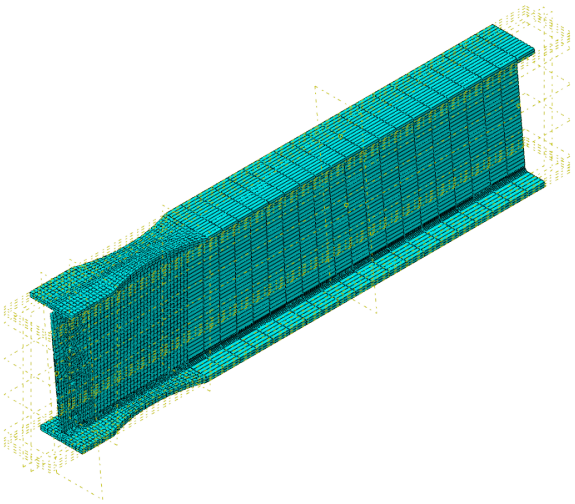

**Figure 3-12: W36 × 194 beam mesh assembly for the RBS moment connection**

The bolts within the connection were designated as pretensioned. The RBS model included the bolts. By following the recommendations by Ruffley, bolts were created in the ABAQUS model implementing C3D20R elements and a seed size of 0.15 inches. The bolt mesh assembly is shown in Figure 3-13. The pretension force and the restricted degrees of freedom were applied based on the recommendations by Ruffley.

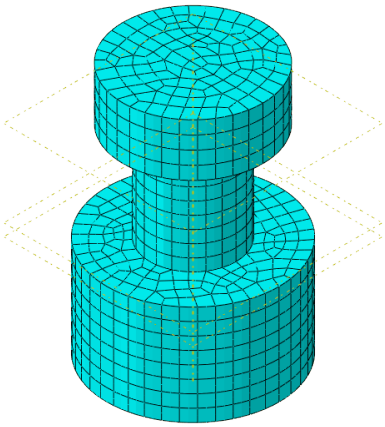

**Figure 3-13: Bolt mesh assembly for the RBS moment connection**

The W14 × 426 column was modeled with the use of C3D20R elements throughout. The seed size used was 4 inches which was consistent with the recommendations by Ruffley. Due to the large relative size of the elements using a 4 inch seed, the use of C3D20R elements was not considered to have a significant impact on computation time. The mesh assembly for the column is shown in Figure 3-14.

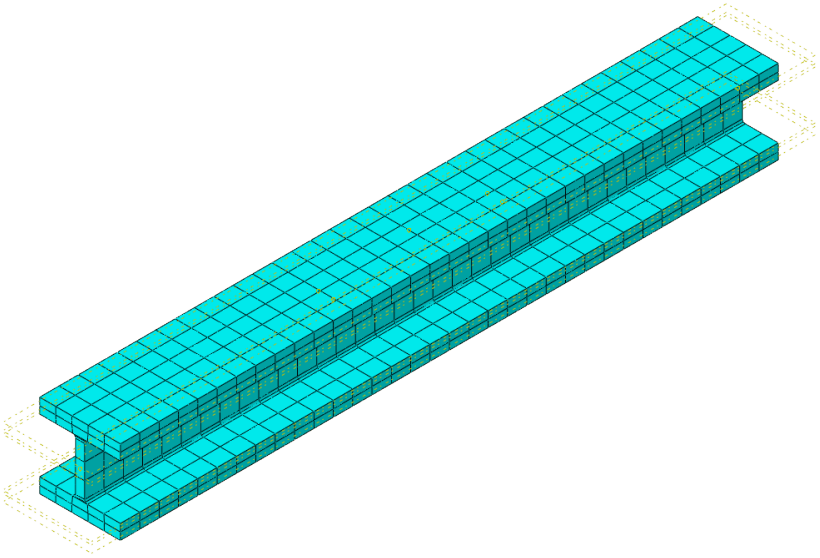

**Figure 3-14: W14 × 426 column mesh assembly for the RBS moment connection**

The shear tab and continuity plates all implemented the C3D20R elements due to the small size and relative number of elements created with respect to the entire model. A seed size of 1 inch was used for each the shear tab and continuity plates. The mesh assemblies for each part are shown in Figures 3-15 and 3-16. The shear tab was connected to the column face using a tie constraint. The shear tab was connected to the beam web by friction created from the bolt pretension. The coefficient of static friction was 0.2 based on the recommendations by Ruffley. The continuity plates were connected to the column with tie constraints along the length of the welds prescribed in the physical connection detail.

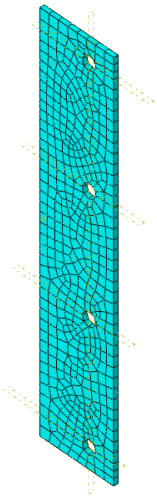

**Figure 3-15: Shear tab mesh assembly for the RBS moment connection**

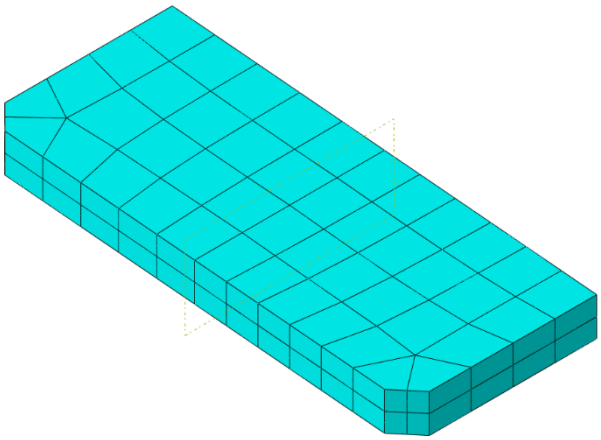

**Figure 3-16: Continuity plate mesh assembly for the RBS moment connection**

# Chapter 4: Finite Element Validation of the RBS and WUF-W Moment Connections

## 4.1 Welded Unreinforced Flange Welded-Web (WUF-W) Moment Connection

The loading applied to the connection followed the displacement-based loading protocol as detailed in the ANSI/AISC 341 specification (ANSI/AISC 341, 2010). Failure of the connection was observed at 5.0% interstory drift during the physical testing. Therefore, a downward vertical displacement of 7 inches was applied to the beam tip corresponding to 5.0% of the interstory drift. The moment in the connection was calculated by multiplying the vertical reaction force applied to the beam tip by the distance to the centerline of the column as detailed in the literature. The rotation was calculated similarly by dividing the beam tip displacement by the distance to the column centerline. The results of the finite element analysis compared to the physical testing is shown in Figure 4-1. The results indicate that the finite element simulation with ABAQUS is capable of predicting stiffness and ultimate strength of the connection within approximately 2% of error.

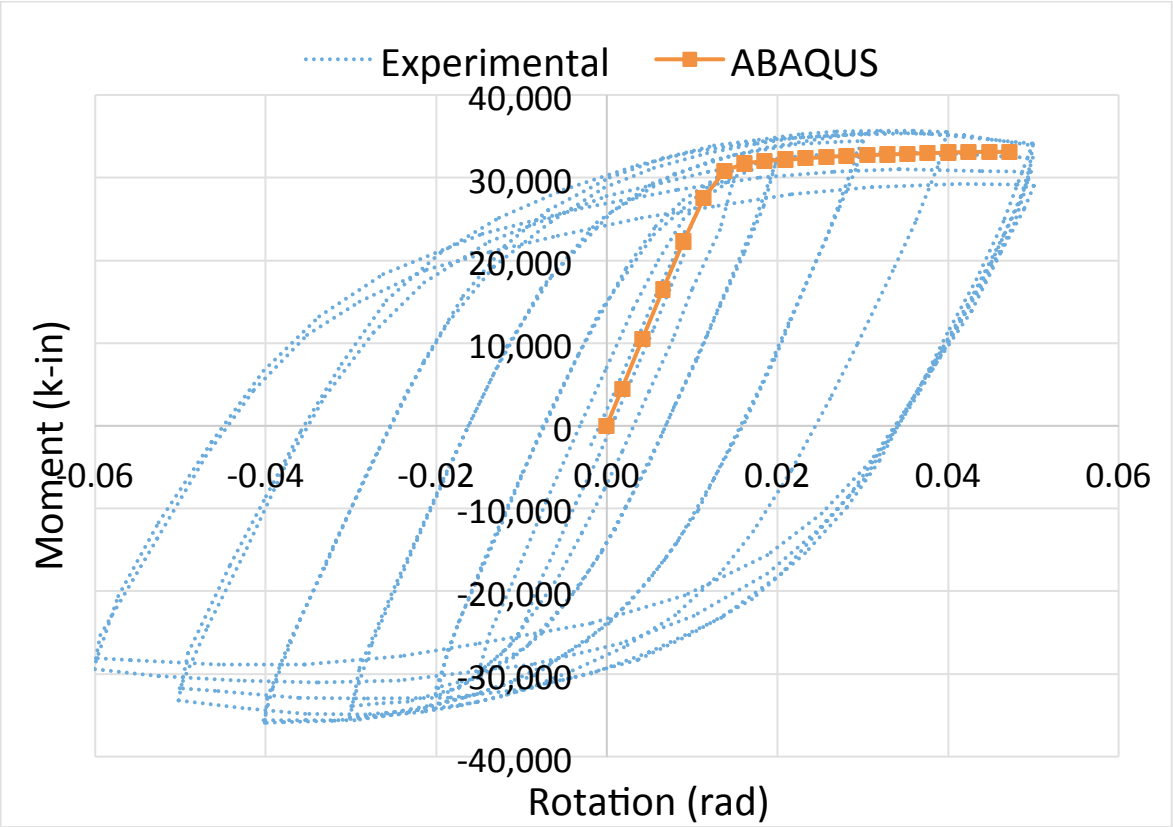


**Figure 4-1: Moment versus rotation comparison between finite element model and physical testing (Hassan, 2012)**

## 4.2 Reduced Beam Section (RBS) Moment Connection

The loading protocol followed the displacement based loading protocol specified in ATC-24. This loading history subjects the beam tip to a vertical displacement. The results of the physical testing were documented as moment versus plastic rotation. The moment was calculated by taking the vertical force in the beam tip and multiplying by the distance to the face of the column. The plastic rotation was computed by taking the plastic portion of the beam tip deflection and dividing it by the distance to the face of the column.

The model was loaded by applying a vertical displacement to the beam tip. The finite element analysis was successful in reproducing the physical response as indicated in Figure 4-2. The results indicate that the finite element simulation with ABAQUS is capable of predicting stiffness and ultimate strength of the connection within approximately 2% of error.

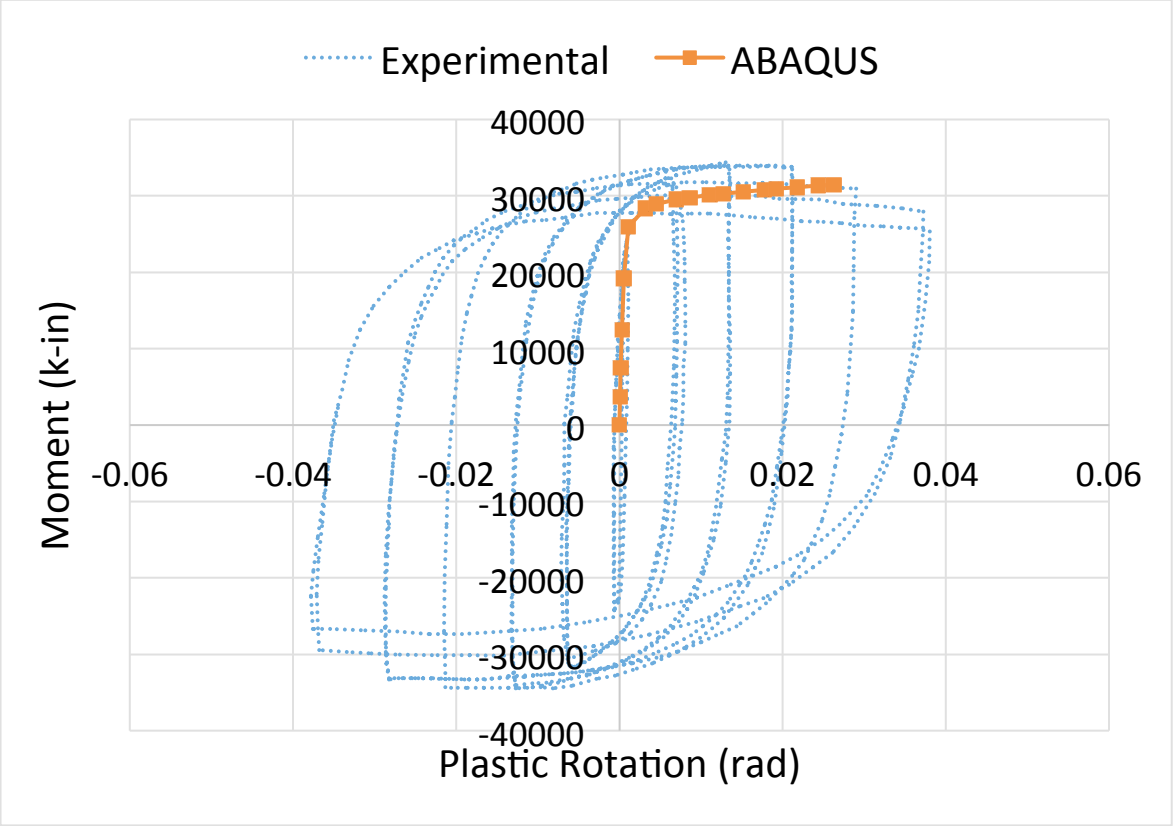


**Figure 4-2: Moment versus plastic rotation comparison between finite element model and physical testing (Engelhardt et al. 1998)**

# Chapter 5: Non-orthogonal Response of the Welded Unreinforced Flange-Welded Web (WUF-W)

A total of nine models were built varying the skew angles between 5 and 45 degrees through 5-degree increments. Similarly, a total of nine models were built varying the slope angles between 5 and 45 degrees through 5-degree increments. The finite element analyses were performed using quasi-static loading, since cyclical loading is computationally demanding. Therefore, in an attempt to quantify the effects of cyclic loading, the connection was subject to both positive and negative moments.

The Von Mises stress variable was scaled with a minimum stress value of 36 kips/in$^2$ (ksi) and a maximum stress value of 60 ksi. These values were selected as a minimum stress value for a steel component of A36 material to yield and an expected value exceeding yield value of A572/A992 steel. The results of the orthogonal model are shown in Figure 5-1. The stress distribution concentrates largely in the beam at the face of the column. This result is in good agreement with the expected response of the connection in accordance with the ANSI/AISC 358 document which expects yielding to occur in the beam at the face of the column.

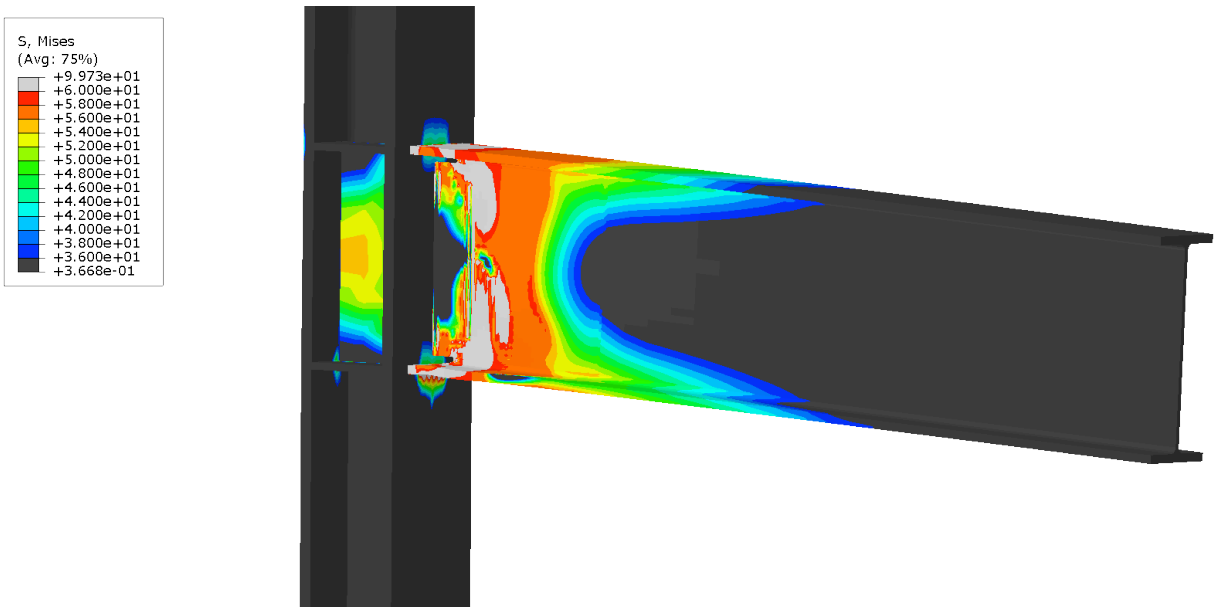


**Figure 5-1: Von Mises stress distribution for the orthogonal WUF-W moment connection**

The equivalent plastic strains (PEEQ) were investigated by implementing the Von Mises yield criterion. The PEEQ variable was scaled between models to the maximum observed PEEQ of the orthogonal connection. The maximum observed PEEQ value in the orthogonal connection was 0.1567 in/in. The scaling provides a direct comparison between the orthogonal and non-orthogonal models. All of the investigated response parameters were compared to the response of the traditional orthogonally framed connection. All yielding in the connection models occurred in the beam so a zoomed view of the beam from multiple angles will be displayed for the PEEQ observations.

The same design details were maintained for the WUF-W moment connection for all orthogonal and non-orthogonal models. The sloped

modifications altered the shear tab, but the details were incorporated maintaining the same detailing requirements currently required by the ANSI/AISC 358 document for orthogonally framed connections.

The weld access holes for both connections were modified so that the perpendicular distance extending away from the column was maintained constant. This remediation simulates a practical solution to be used in the field when the welder would require access to perform the welding.

The PEEQ values for the orthogonal connection are displayed in Figure 5-2. The plastic hinge mechanism and the distribution of strain throughout the cross-section are in good agreement with the expected response of the connection in accordance the ANSI/AISC 358 document. (ANSI/AISC 358, 2010) The PEEQ values for the orthogonal connection will provide a direct comparison to the response of the non-orthogonal connections.

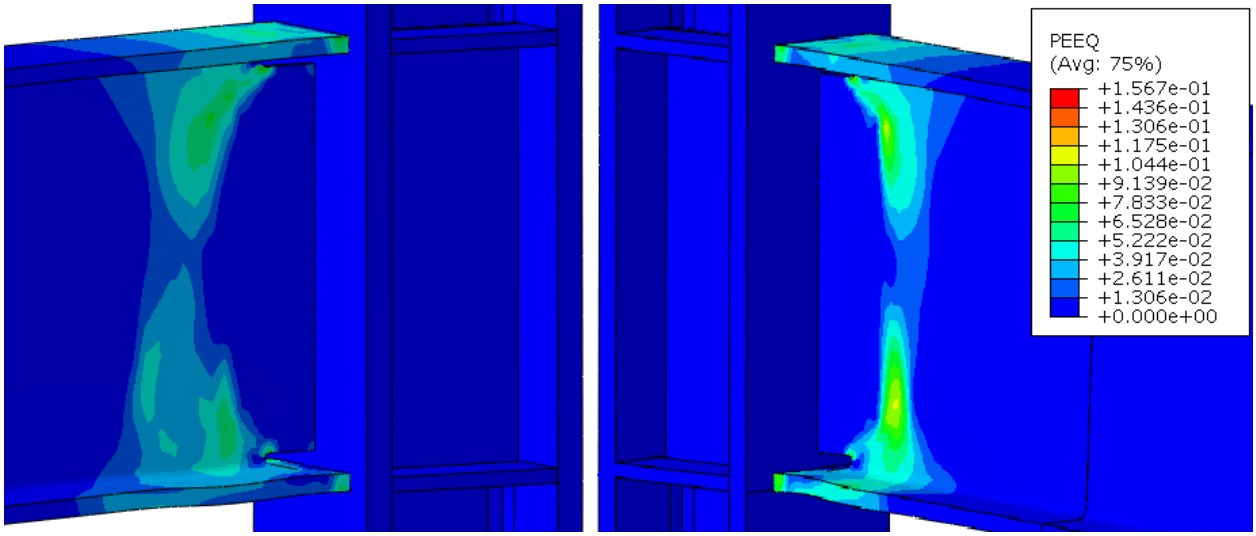


**Figure 5-2: PEEQ of the WUF-W connection with orthogonal framing**

## 5.1 WUF-W Moment Connection with Skewed Configurations

The WUF-W moment connection was arranged with a skewed beam-to-column configuration in order to investigate the effects on the connection. The skew in the beam was varied up to 45 degrees by 5 degree increments. The analyses were performed and the results compared to the response of the orthogonal connection.

The plastic moment capacity of the connection was largely unaffected as shown in Figure 5-3. The results indicate that the full plastic moment capacity of the connection can be reached with the use of bracing as required by the ANSI/AISC 341 specification. The point at which yielding occurs becomes increasingly less well defined as the skew angle increases, as indicated by the more gradual change of slope from the elastic to plastic behavior. This is most likely attributed to the addition of axial and torsional forces that are present once the beam has been skewed.

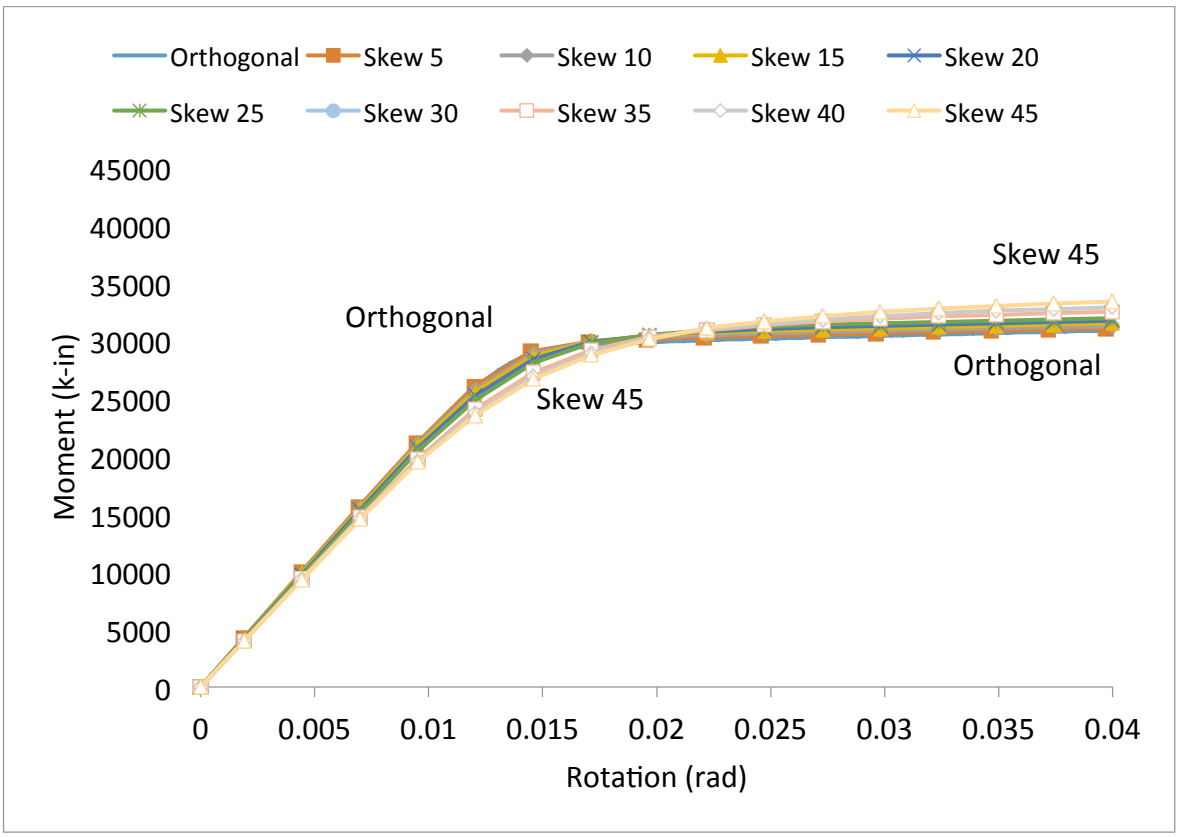


**Figure 5-3: Moment versus rotation of the WUF-W connection with skewed configurations**

The stress distribution in the WUF-W connection detail is largely impacted by the amount of skew in the beam as shown in Figures 5-4 through 5-12. The most pronounced observation is that the stress distribution in the column flange increases near the acute angle formed between the beam and column for each increase in skew angle. For skew angles less than 10 degrees, this appears to be negligible. Additionally, as the skew angle increases, the stress distributes over a larger region in the column flange along the length of the column. Once the skew angle exceeds 20 degrees, the stress distribution in the column flange at the

beam/column interface begins to concentrate at both the acute and the obtuse angle formed between the beam and the column.

Within the beam section, as the skew angle increases, the stress distribution in the beam flanges concentrates towards the vertex of the acute angle formed between the beam and column. This effect is immediately impacted by a skew angle greater than or equal to 5 degrees. Within the web of the beam, the skew angle does not appear to impact the stress distribution. For each increase in skew angle, the stress distribution concentrates in the beam web at the face of the column which is expected of a traditional, orthogonally framed WUF-W connection detail.

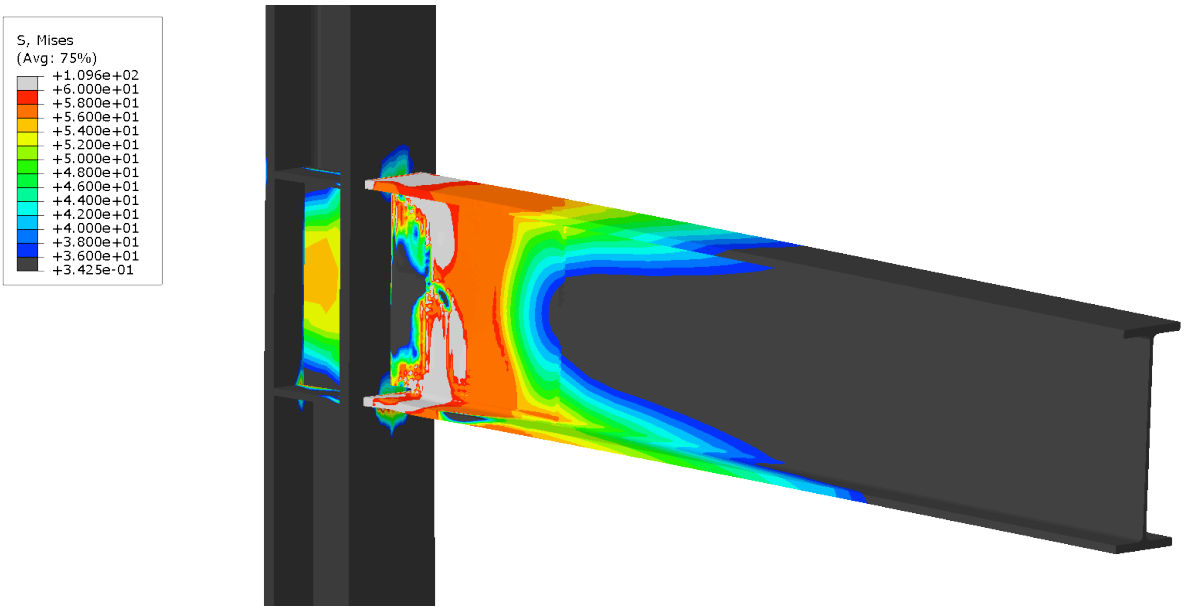


**Figure 5-4: Von Mises stress distribution for the WUF-W with connection 5 degree skew**

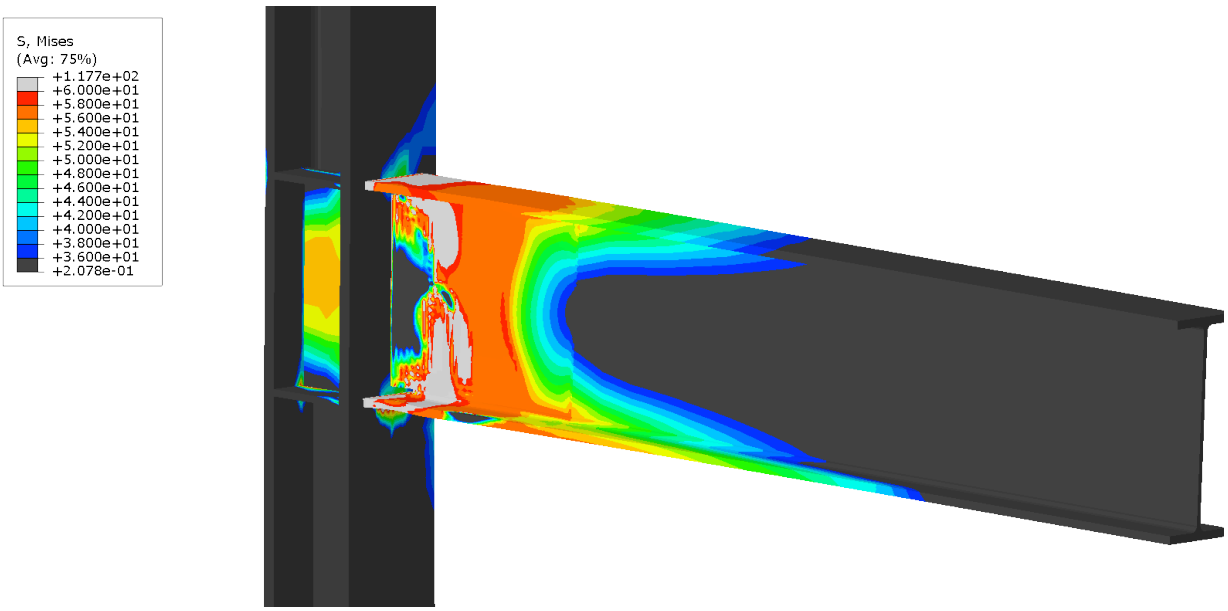


**Figure 5-5: Von Mises stress distribution for the WUF-W with connection 10 degree skew**

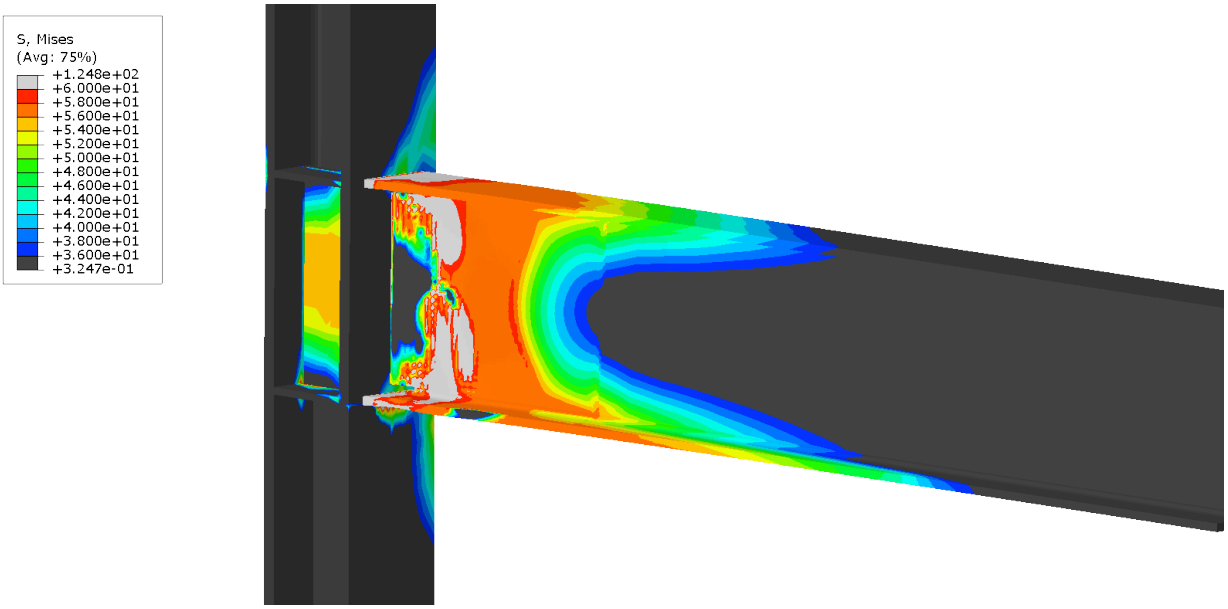


**Figure 5-6: Von Mises stress distribution for the WUF-W with connection 15 degree skew**

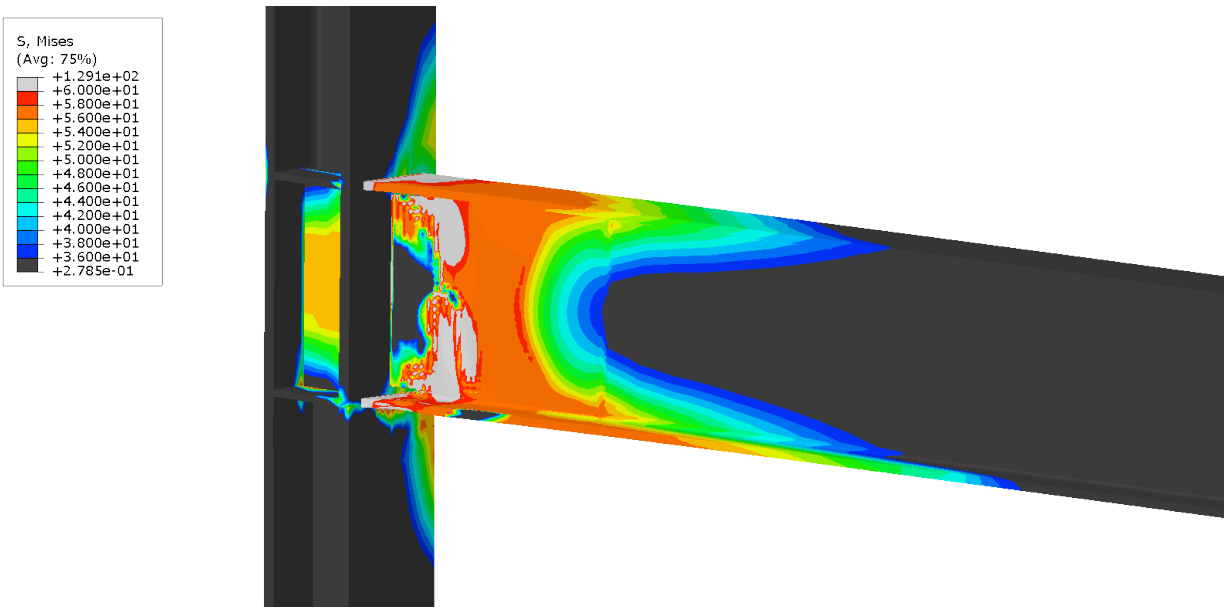


**Figure 5-7: Von Mises stress distribution for the WUF-W with connection 20 degree skew**

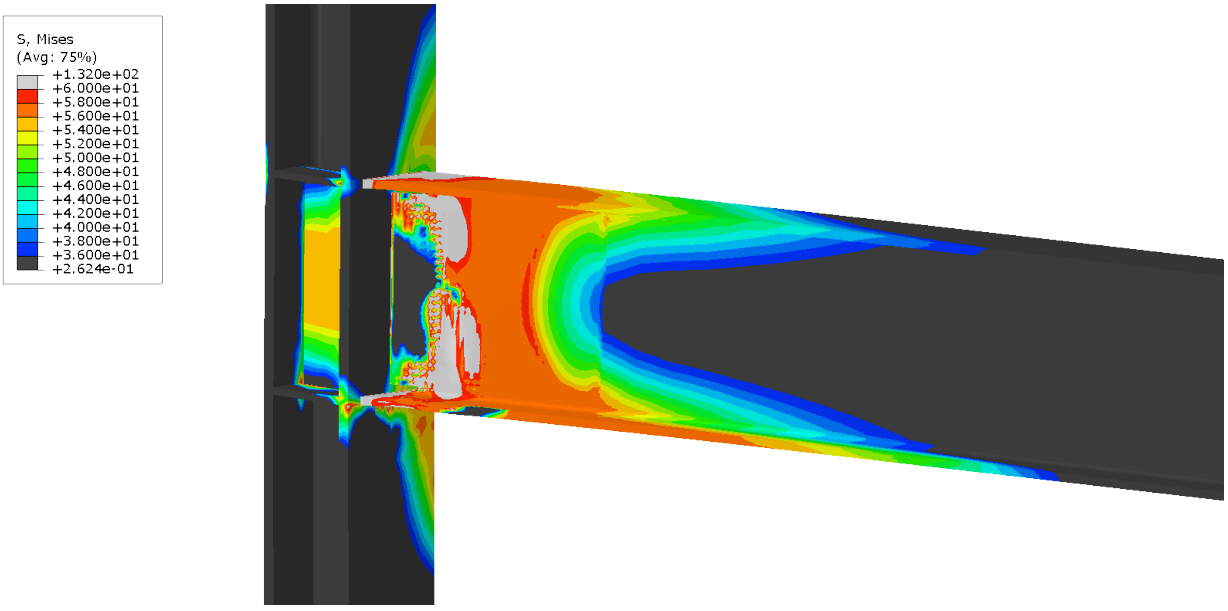


**Figure 5-8: Von Mises stress distribution for the WUF-W with connection 25 degree skew**

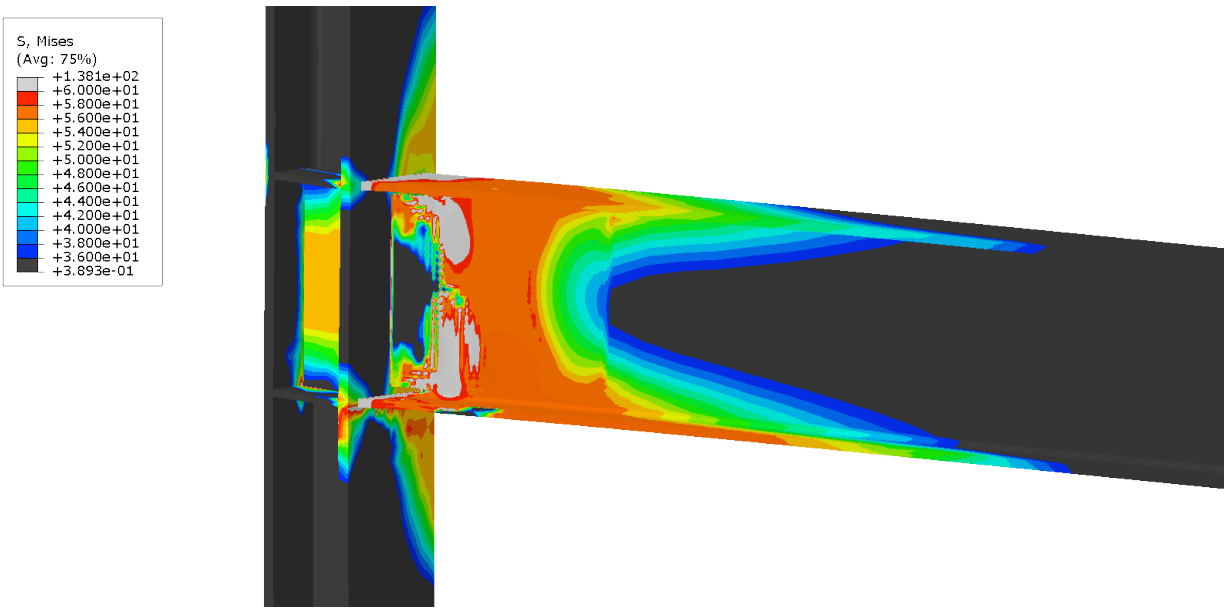


**Figure 5-9: Von Mises stress distribution for the WUF-W with connection 30 degree skew**

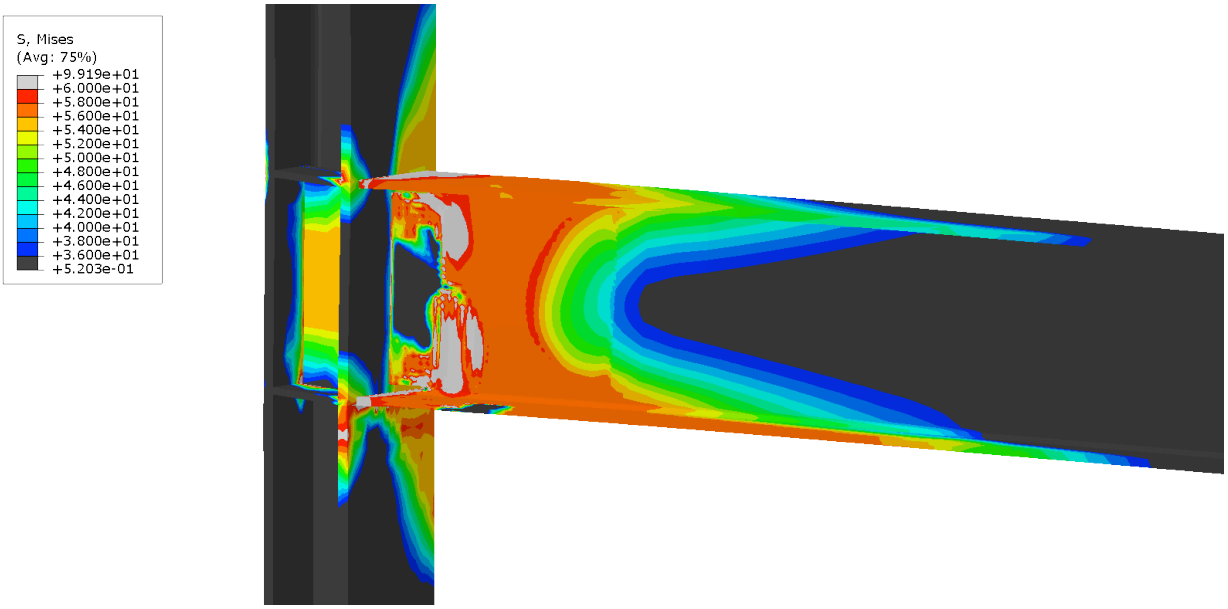


**Figure 5-10: Von Mises stress distribution for the WUF-W with connection 35 degree skew**

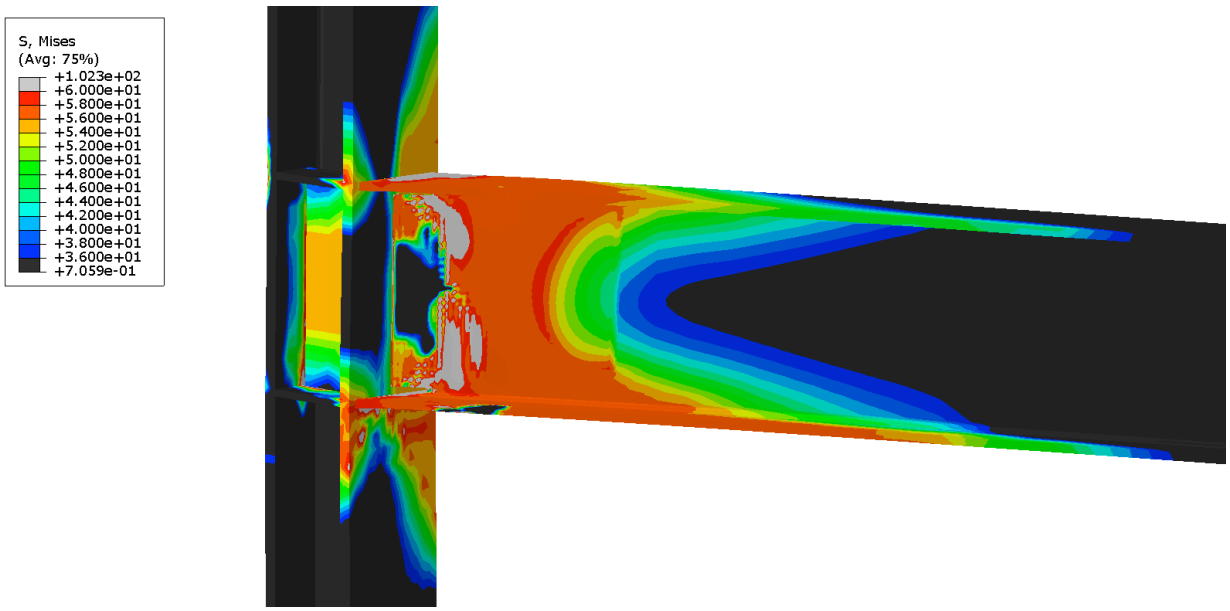


**Figure 5-11: Von Mises stress distribution for the WUF-W with connection 40 degree skew**

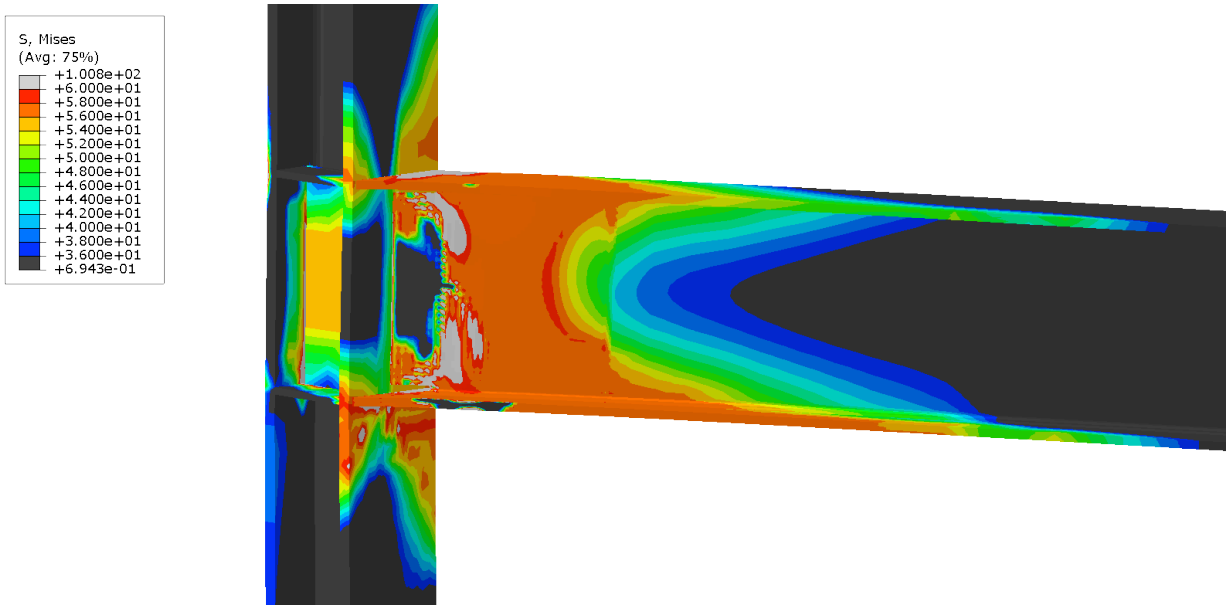


**Figure 5-12: Von Mises stress distribution for the WUF-W with connection 45 degree skew**

The first indication of non-linearity from the moment vs. rotation relationship occurs at a moment force of 24150 k-in. The stress values associated

with that moment force were recorded and plotted with respect to the skewed angle in Figure 5-13. The stress distribution throughout the flange width trends towards the right side and away from the left side as the skew angle increases. The stress concentration at the center of the beam flange remains essentially the same for each variation in skew angle.

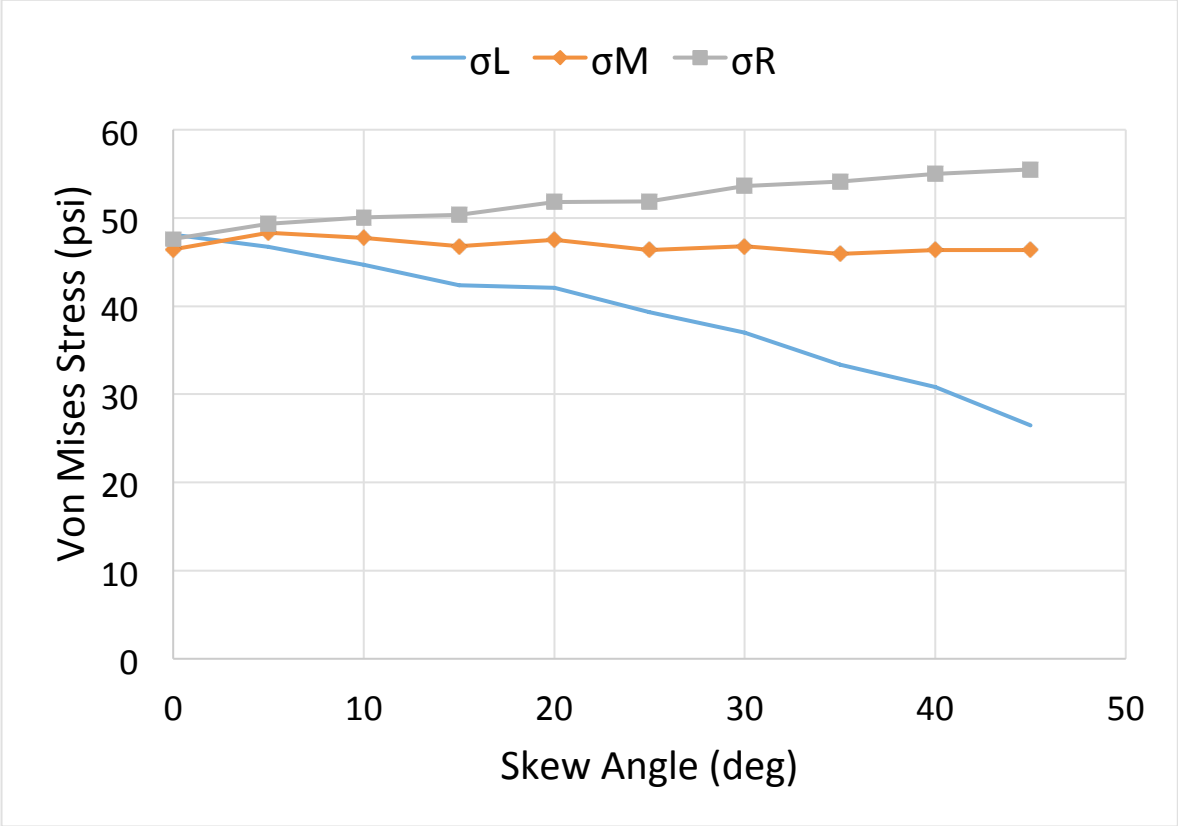


**Figure 5-13: Von Mises stress values within the WUF-W beam flange for skewed configurations at first yield.**

At 50% of the yield moment as calculated by dividing the moment force associated with the first indication of non-linearity by 2, the stress values were recorded corresponding to a moment force of 12140 k-in. The stress values were

plotted with respect to the skewed angle in Figure 5-14. The stress distribution throughout the flange width trends towards the right side and away from the left side as the skew angle increases. The stress concentration at the center of the beam flange remains essentially the same for each variation in skew angle.

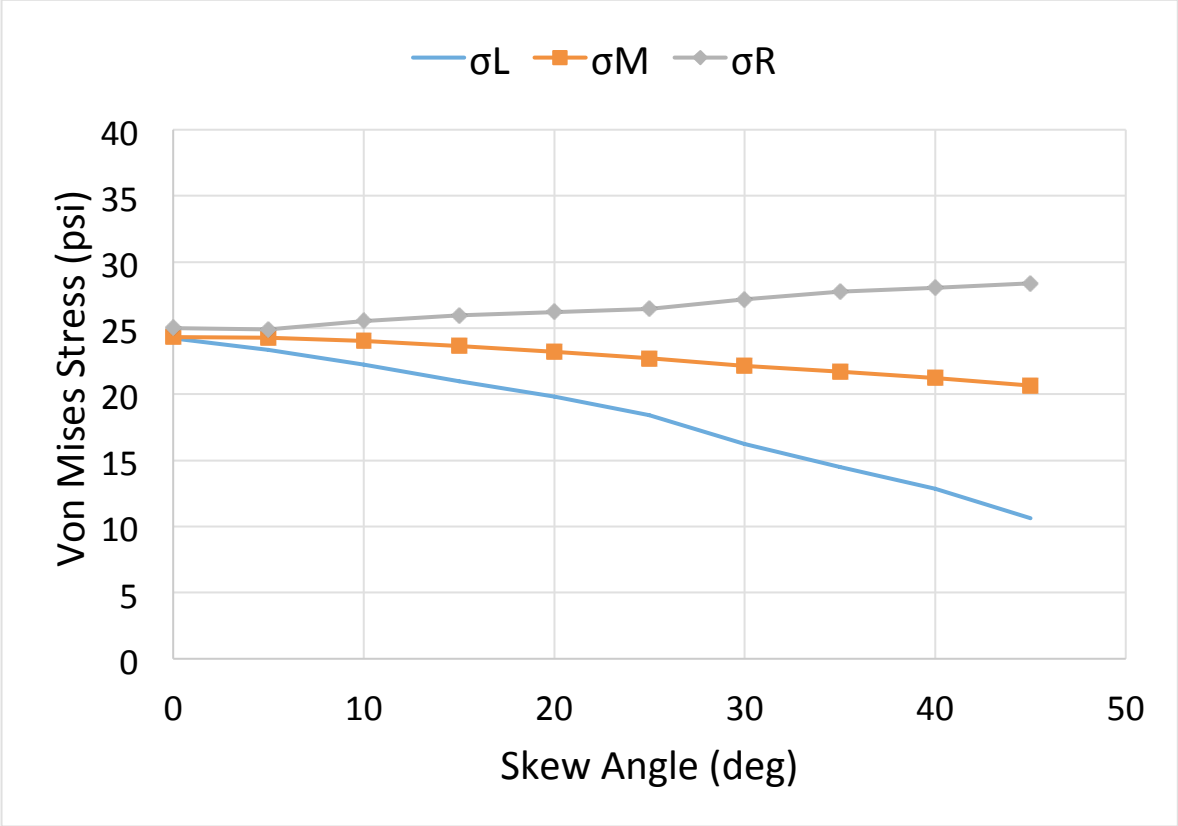


**Figure 5-14: Von Mises stress values within the WUF-W beam flange for skewed configurations at 50% yield.**

For each increase in the skew angle of the beam-to-column connection, the strain demand progressively localizes near the acute angle formed between the beam and column as indicated in Figures 5-15 through 5-23. The plastic hinge

forms throughout the beam at the face of the column in a manner that is expected by the WUF-W connection per the ANSI/AISC 358 document. (ANSI/AISC 358, 2010) However, the strain demand increases in the top and bottom flanges near the acute angle formed from the skewed configuration for each increase in angle. These effects appear to be negligible for angles not exceeding 10 degrees. However, once the skew angle exceeds 10 degrees, the strain demand observed near the acute angle of the connection begins to exceed that of the orthogonally framed connection. For the extreme case of the 45 degree skew, the strain demand near the acute angle exceeds 100% of the observed strain demand in the orthogonal connection.

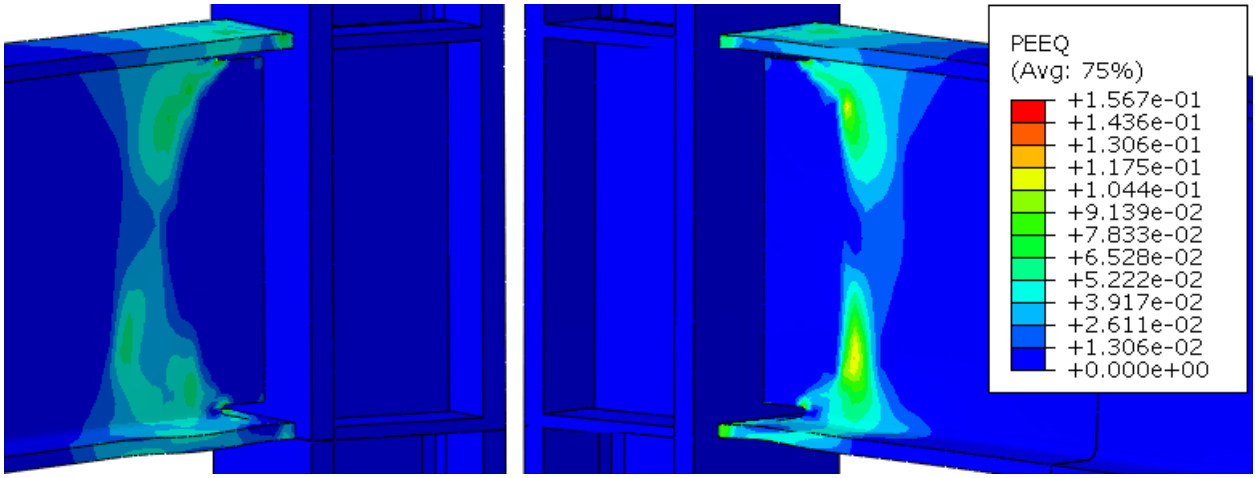


**Figure 5-15: PEEQ of the WUF-W connection with 5 degree skew**

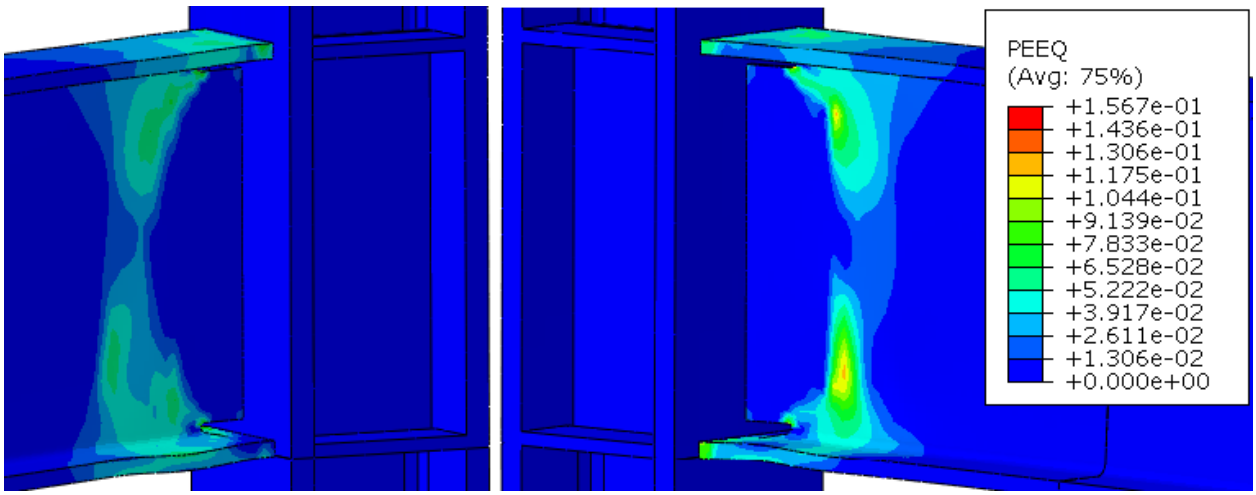


**Figure 5-16: PEEQ of the WUF-W connection with 10 degree skew**

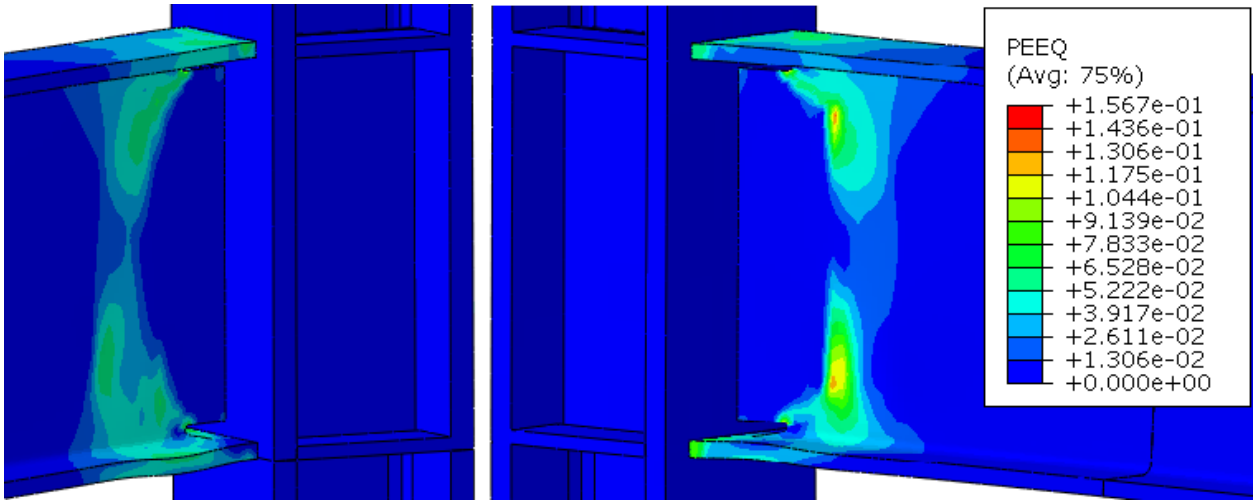


**Figure 5-17: PEEQ of the WUF-W connection with 15 degree skew**

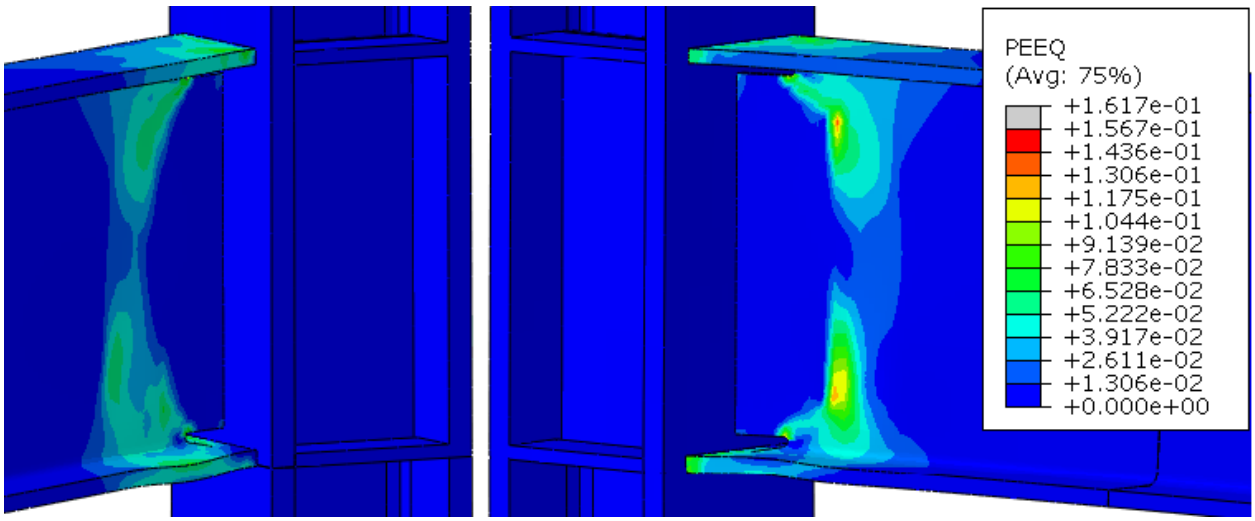


**Figure 5-18: PEEQ of the WUF-W connection with 20 degree skew**

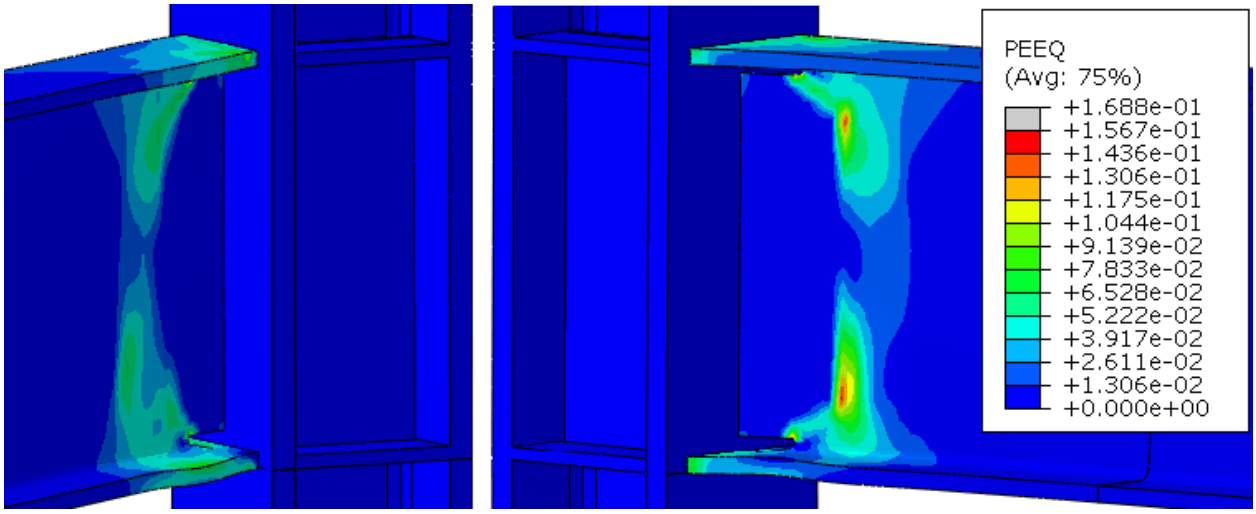


**Figure 5-19: PEEQ of the WUF-W connection with 25 degree skew**

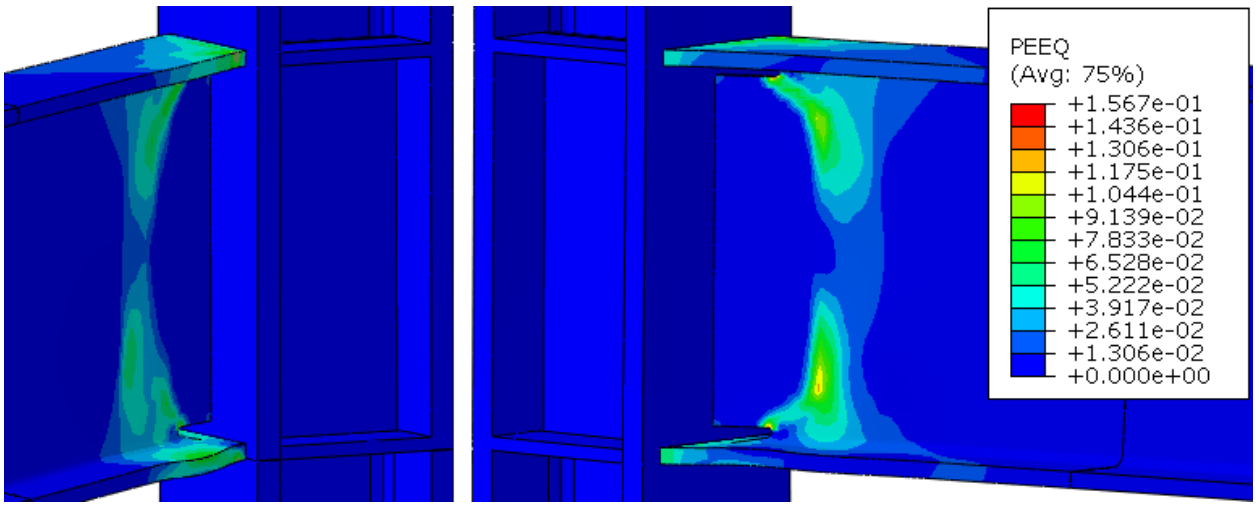


**Figure 5-20: PEEQ of the WUF-W connection with 30 degree skew**

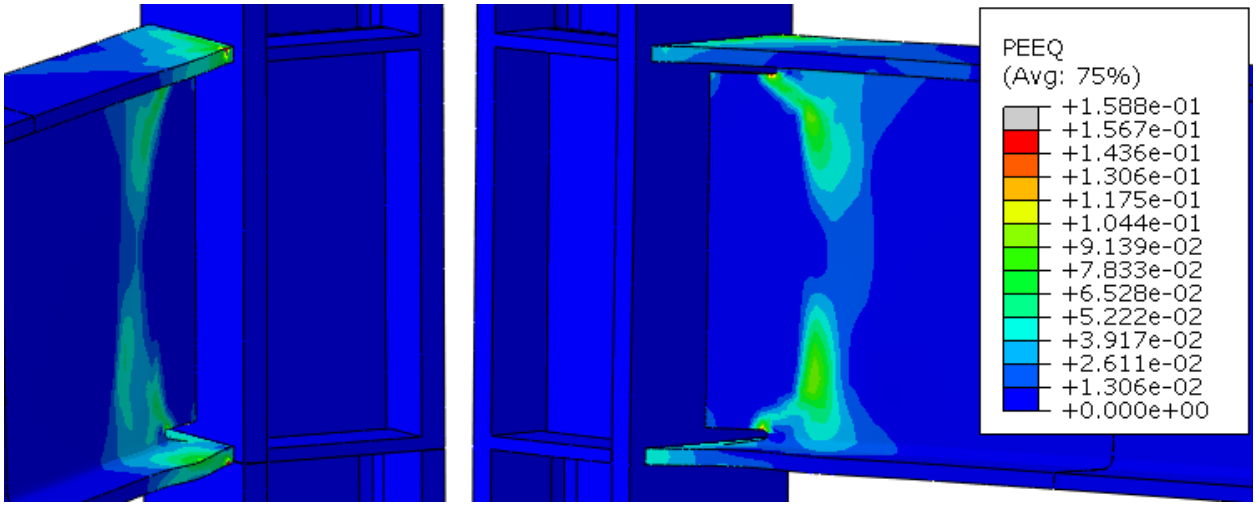


**Figure 5-21: PEEQ of the WUF-W connection with 35 degree skew**

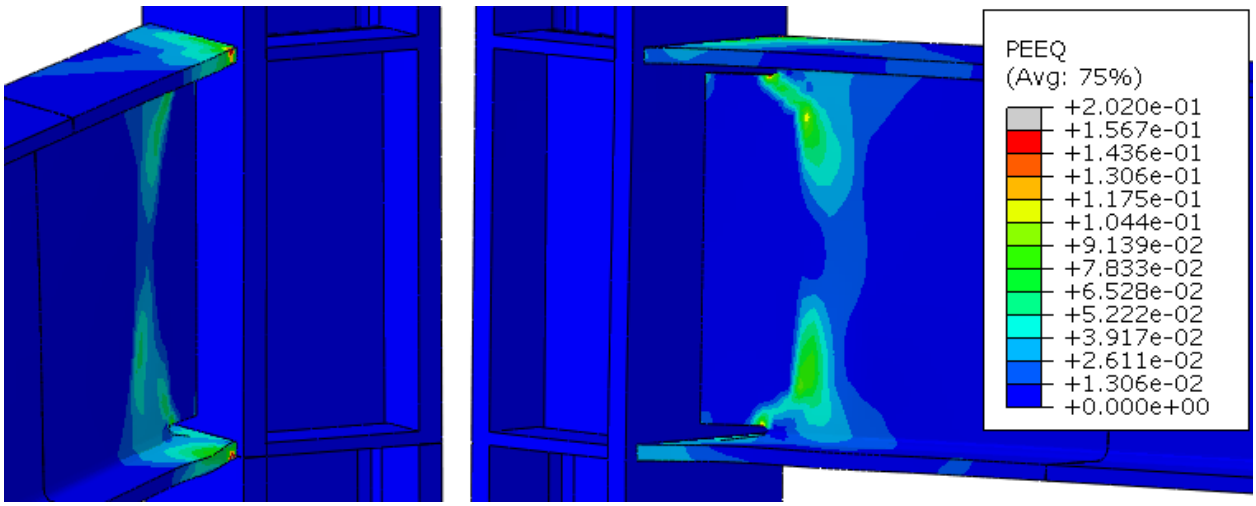


**Figure 5-22: PEEQ of the WUF-W connection with 40 degree skew**

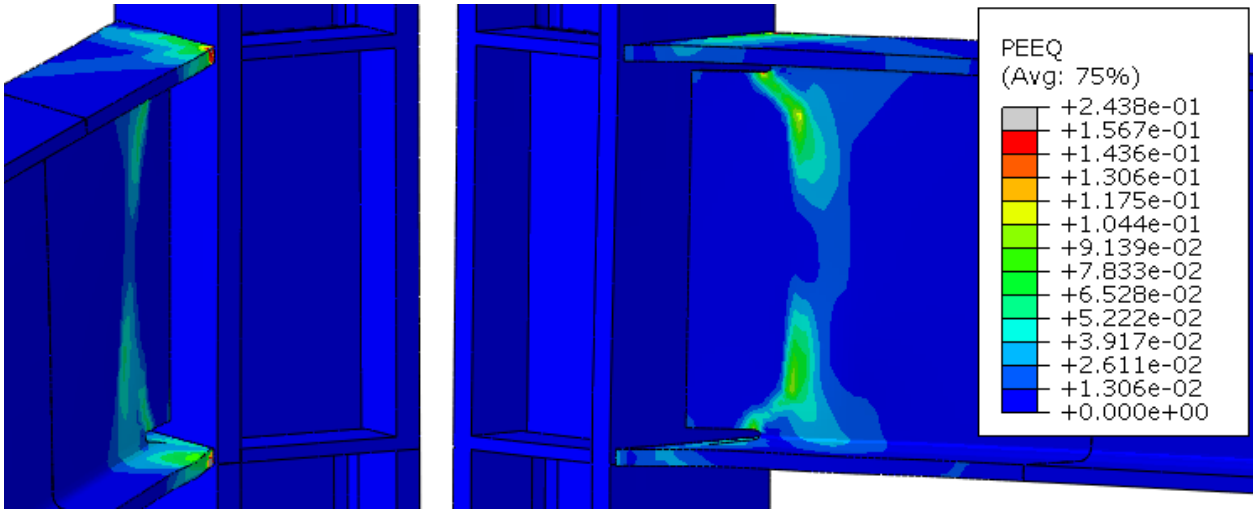


**Figure 5-23: PEEQ of the WUF-W connection with 45 degree skew**

## 5.2 WUF-W Moment Connection with Sloped Configurations subject to Negative Moment

The WUF-W moment connection was arranged with a downward sloped beam-to-column configuration to investigate the effects of slope on the connection. The connection model was subject to a negative moment by applying a downward vertical displacement at the beam tip. The slope of the beam was varied up to 45 degrees through 5 degree increments. The analyses were performed and the results compared to the response of the orthogonal connection.

In the case of a sloped beam configuration subject to a negative moment, the results indicate an increase in plastic moment capacity for an increase in slope angle. This can be observed from Figure 5-24. This is most likely attributed to the increase in the overall effective depth of the beam cross-section with respect to the bending axis. As the beam section is modified to create a slope surface, the depth becomes a function of the slope angle which can be seen in Figure 5-25. The depth of the cross-section is proportional to the slope angle from trigonometry. Since the value of cosine varies between 0 and 1, the effective depth can only increase. This depth directly affects the moment of inertia with respect to the beam strong axis. With an increased bending moment of inertia, the initial stiffness and plastic moment capacity increase.

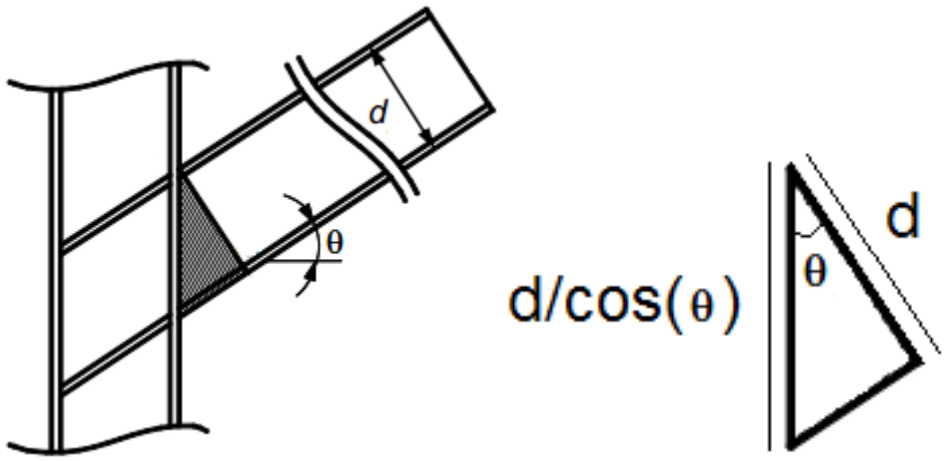


**Figure 5-24: Effective depth of beam cross-section (Kim et al. 2015)**

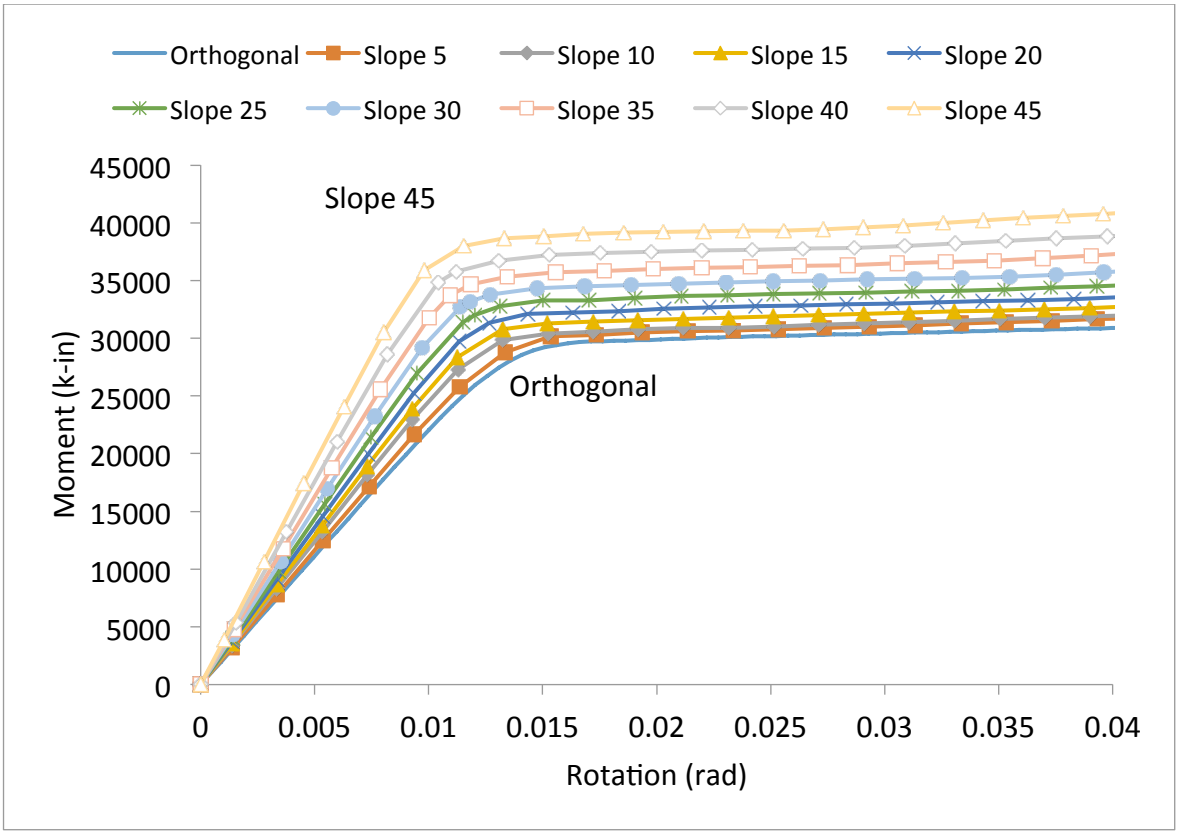


**Figure 5-25: Moment versus rotation of the WUF-W connection with sloped configurations subject to a negative moment**

For the WUF-W connection detail with sloped configurations, the stress distribution remains perpendicular to the beam section as shown in Figures 5-26 through 5-34. This effect does not appear to be impacted by the sloped geometry. As a result of this, the stress distribution concentrates within the bottom flange of the beam section near the beam/column interface for slope angles exceeding 10 degrees. Conversely, the stress distribution in the top flange concentrates further away from the beam/column interface and distributes over a larger region. For slope angles between 5 and 30 degrees, this stress distribution in the beam top flange actually reduces the concentration of stress as it distributes over a larger region. However, once the slope angle exceeds 30 degrees, the stress concentration increases in the beam top flange.

The panel zone of the connection is also impacted by the sloped configurations. As the slope angle increases, the stress distribution in the doubler plates within the panel zone concentrates towards the backside of the connection near the bottom.

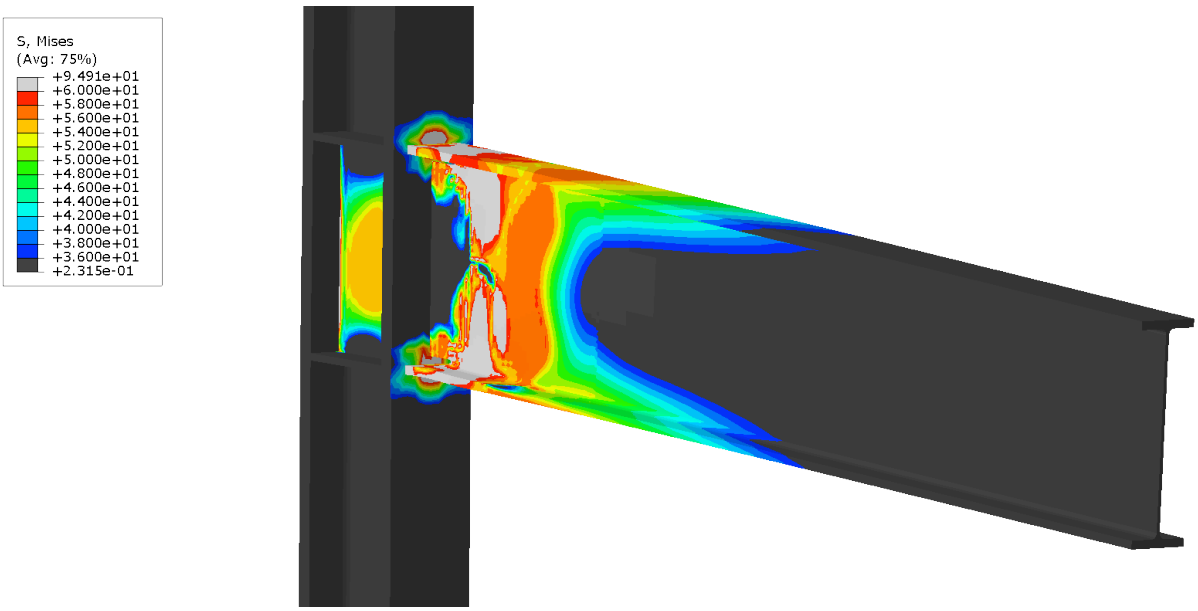


**Figure 5-26: Von Mises stress distribution for the WUF-W with connection 5 degree slope subject to a negative moment**

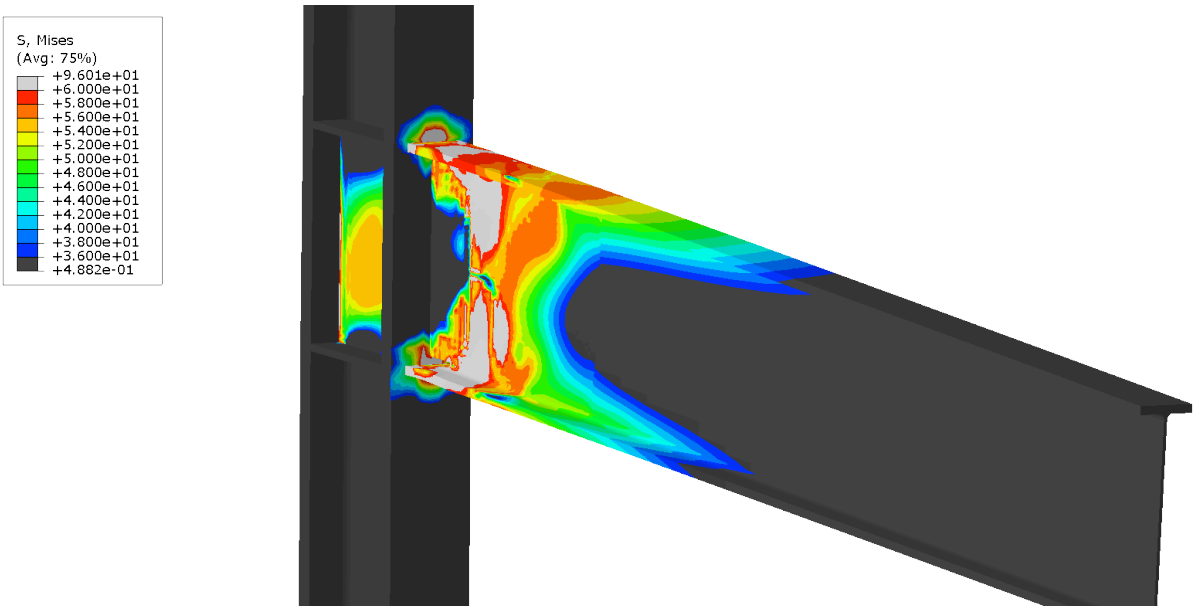


**Figure 5-27: Von Mises stress distribution for the WUF-W with connection 10 degree slope subject to a negative moment**

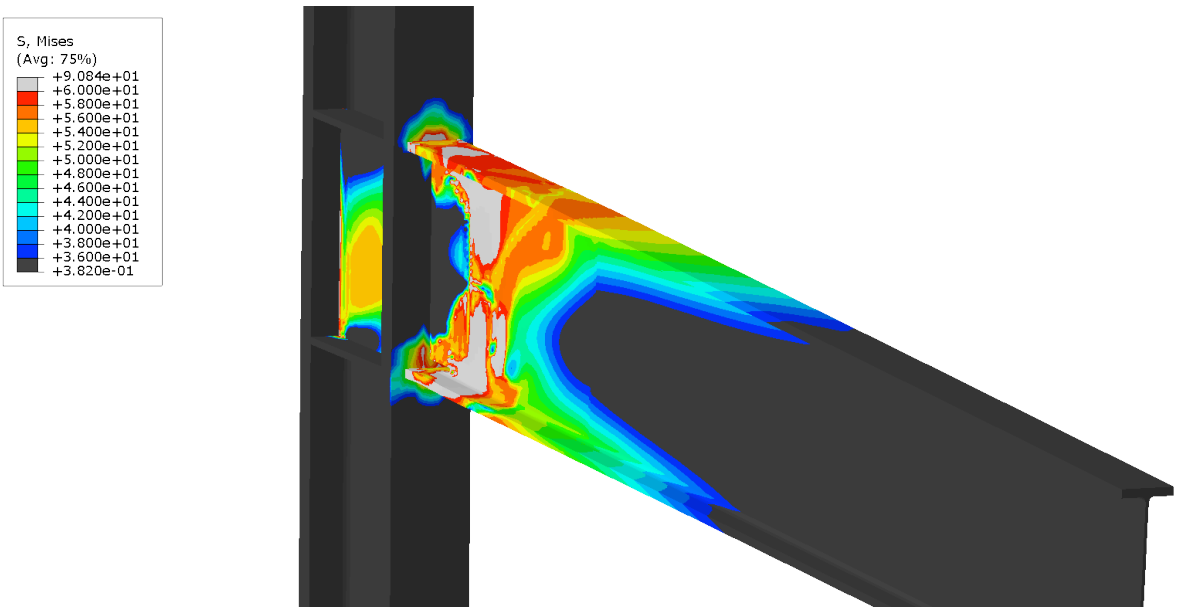


**Figure 5-28: Von Mises stress distribution for the WUF-W with connection 15 degree slope subject to a negative moment**

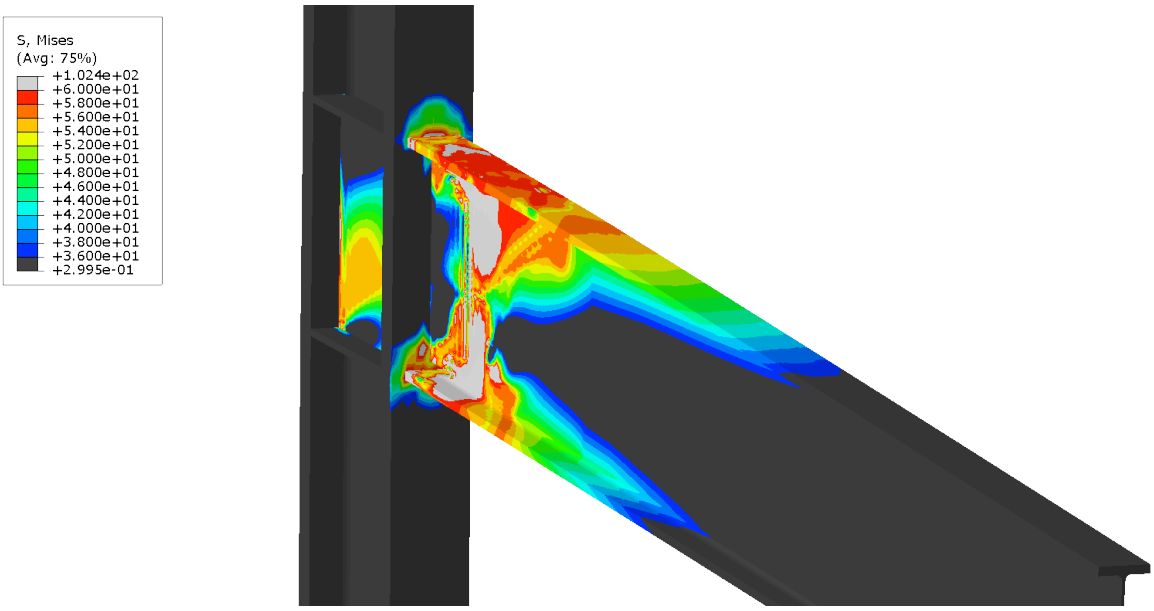


**Figure 5-29: Von Mises stress distribution for the WUF-W with connection 20 degree slope subject to a negative moment**

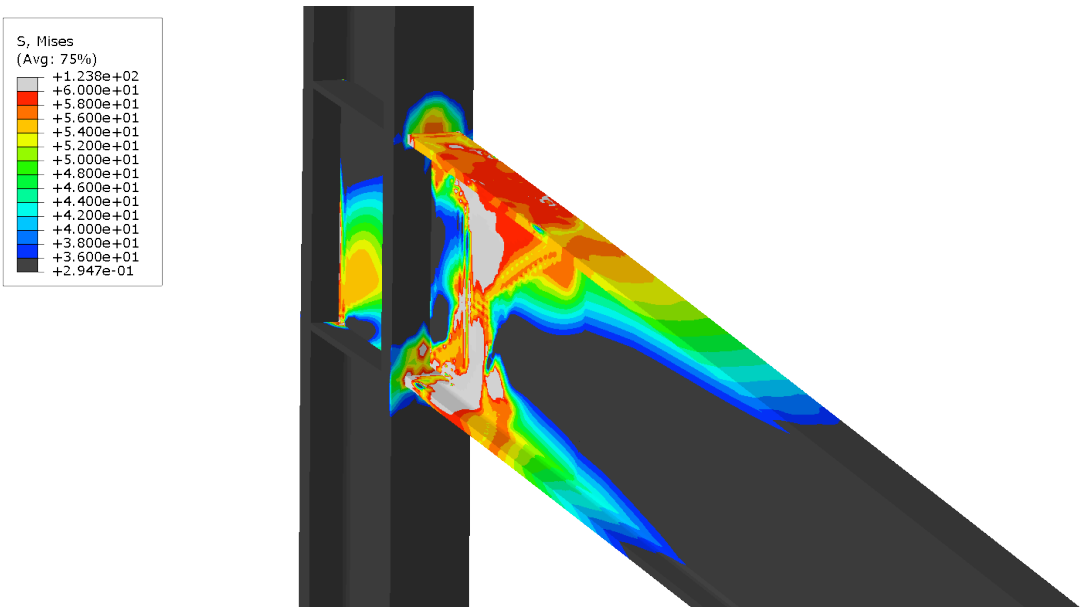


**Figure 5-30: Von Mises stress distribution for the WUF-W with connection 25 degree slope subject to a negative moment**

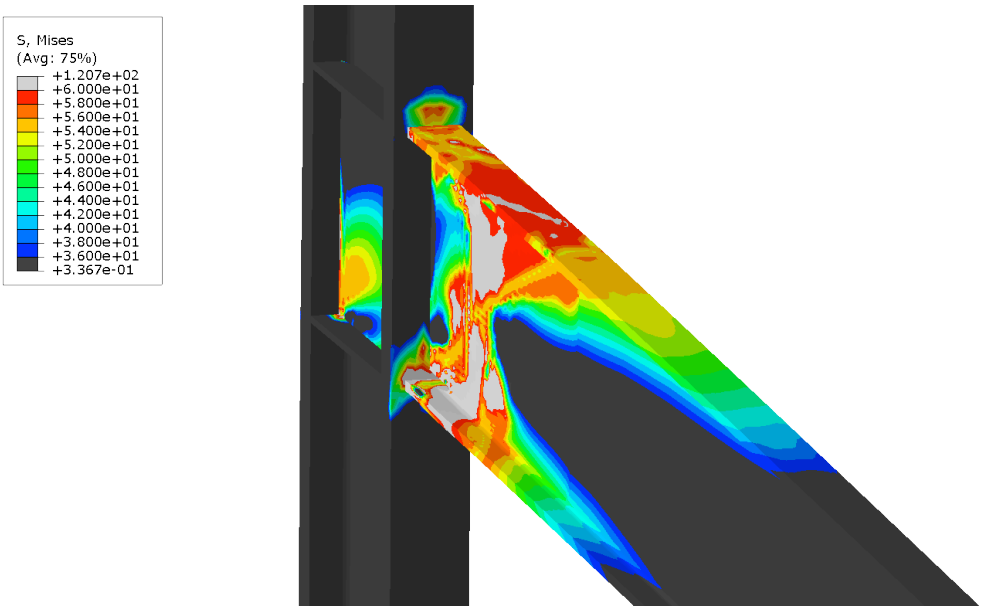


**Figure 5-31: Von Mises stress distribution for the WUF-W with connection 30 degree slope subject to a negative moment**

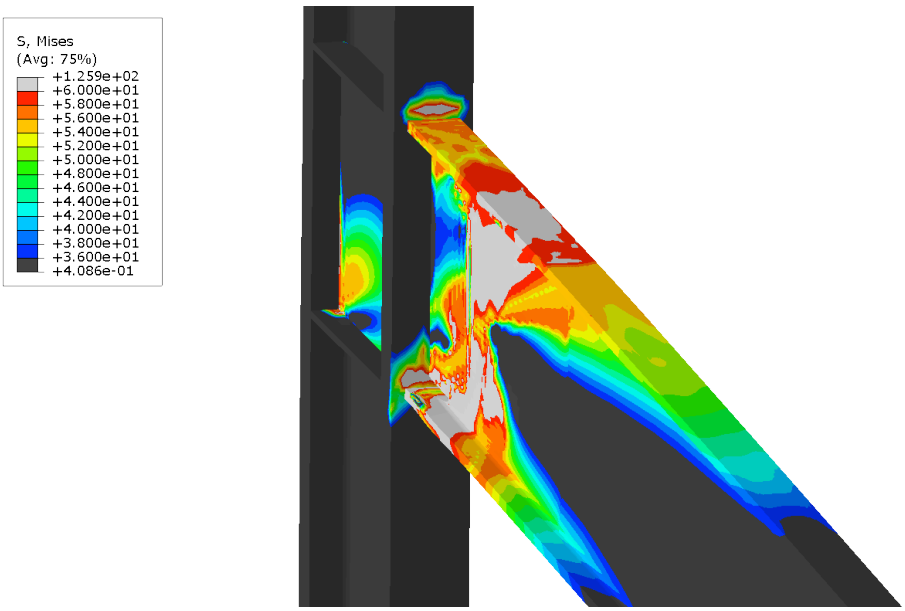


**Figure 5-32: Von Mises stress distribution for the WUF-W with connection 35 degree slope subject to a negative moment**

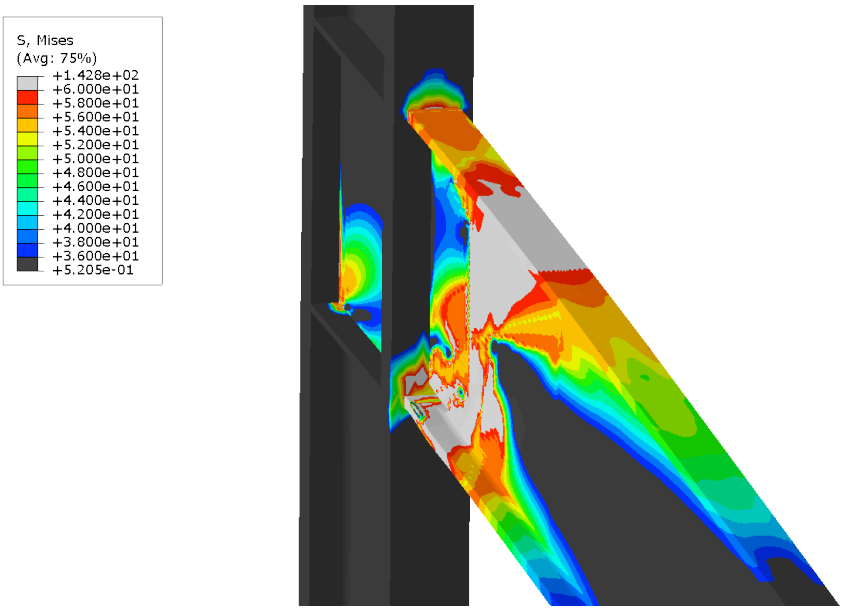


**Figure 5-33: Von Mises stress distribution for the WUF-W with connection 40 degree slope subject to a negative moment**

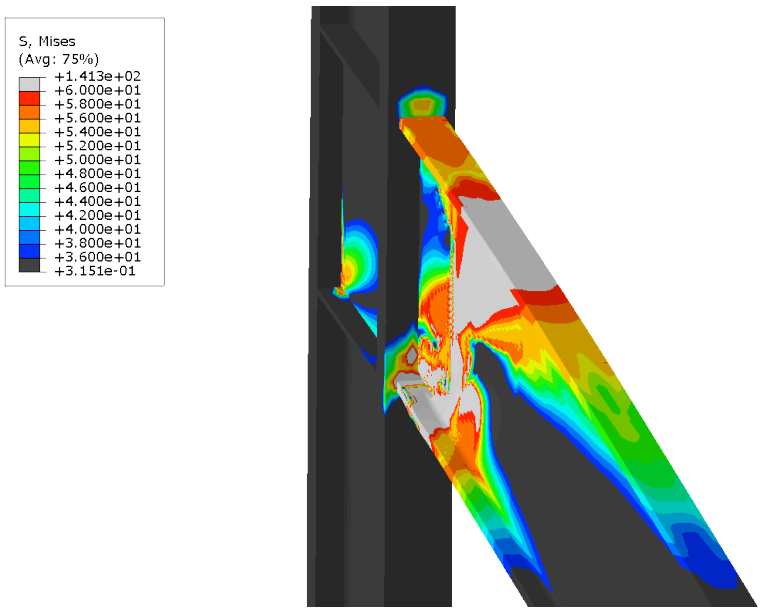


**Figure 5-34: Von Mises stress distribution for the WUF-W with connection 45 degree slope subject to a negative moment**

The first indication of non-linearity from the moment vs. rotation relationship occurs at a moment of 24150 k-in. The stress values associated with that moment force were recorded and plotted with respect to the sloped angle in Figure 5-35. The stress concentration increases between 0 and 20 degrees and eventually decreases after 20 degrees. The stress distribution throughout the flange in tension remains essentially unchanged.

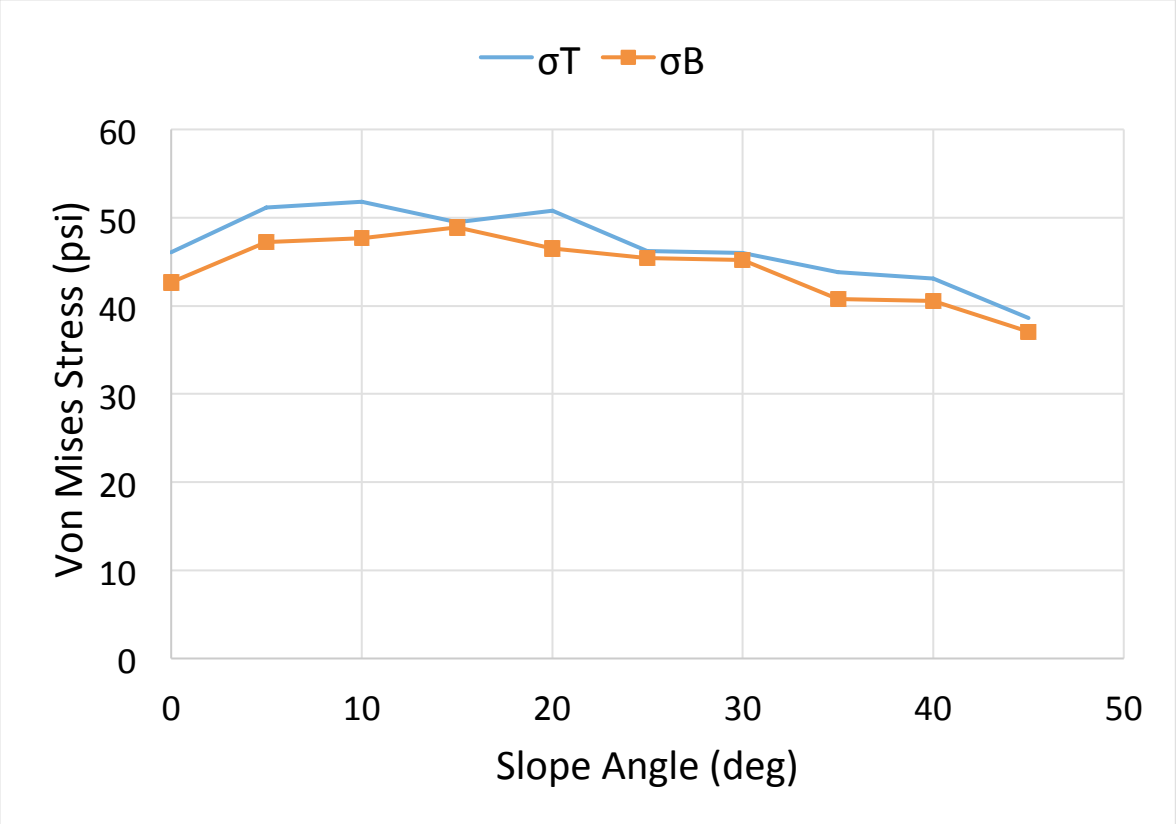


**Figure 5-35: Von Mises stress values within the WUF-W beam flange for sloped configurations subject to a negative moment at first yield.**

At 50% of the yield moment as calculated by dividing the moment force associated with the first indication of non-linearity by 2, the stress values were recorded corresponding to a moment of 12140 k-in. The stress values were plotted with respect to the sloped angle in Figure 5-36. The stress concentration increases between 0 and 20 degrees of slope and eventually decreases for slope angles after 20 degrees. The stress distribution between the top and bottom of the beam flange in tension remains essentially unchanged.

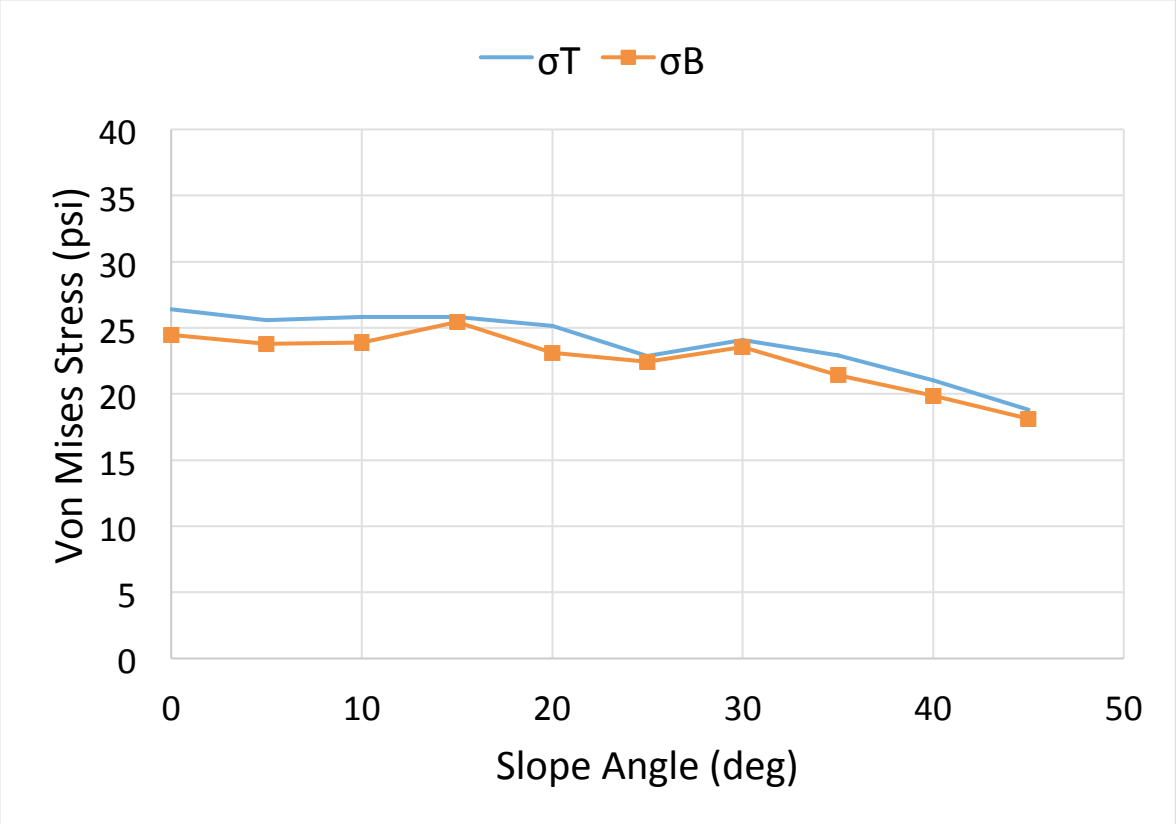


**Figure 5-36: Von Mises stress values within the WUF-W beam flange for sloped configurations subject to a negative moment at 50% yield.**

For sloped configurations of the WUF-W, the hinging mechanism of the beam is largely contained within a plane perpendicular to the beam cross-section as evident from Figures 5-37 through 5-45. As a result, the strain demand begins to concentrate closer to the beam/column interface at the bottom flange of the beam as the slope angle increases the strain demand in the web of the beam also increases with the increase of the slope angle. On the contrary, the strain demand in the beam top flange distributes over a larger region as the slope angle increases.

This distribution decreases the concentration of strain demand in the top flange in comparison to configurations with smaller slope angles.

The increased strain demands near the beam/column interface in the bottom flange and in the web are negligible for slope angles not exceeding 10 degrees. For slope angles exceeding 10 degrees, the strain demand at the face of the column in the bottom flange exceeds 60% of the maximum observed plastic strain in the orthogonally framed connection.

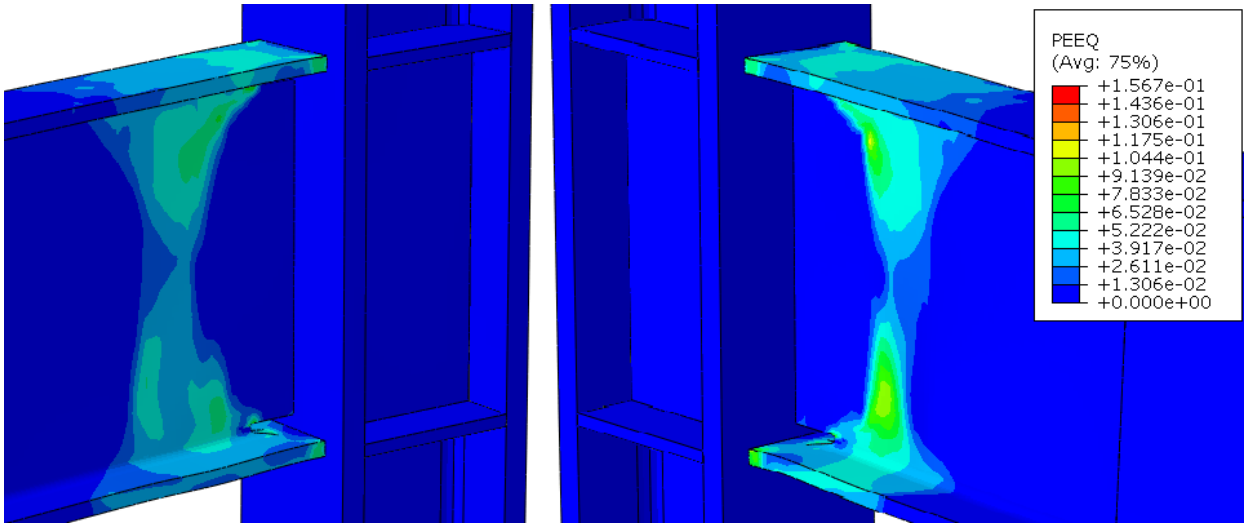


**Figure 5-37: PEEQ of the WUF-W connection with 5 degree slope subject to a negative moment**

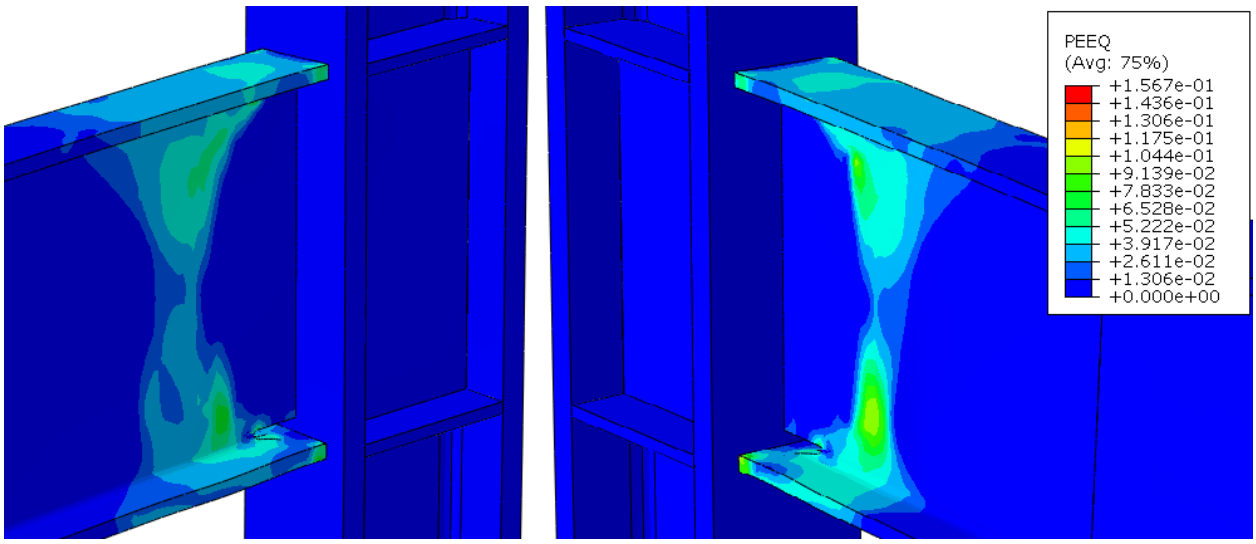


**Figure 5-38: PEEQ of the WUF-W connection with 10 degree slope subject to a negative moment**

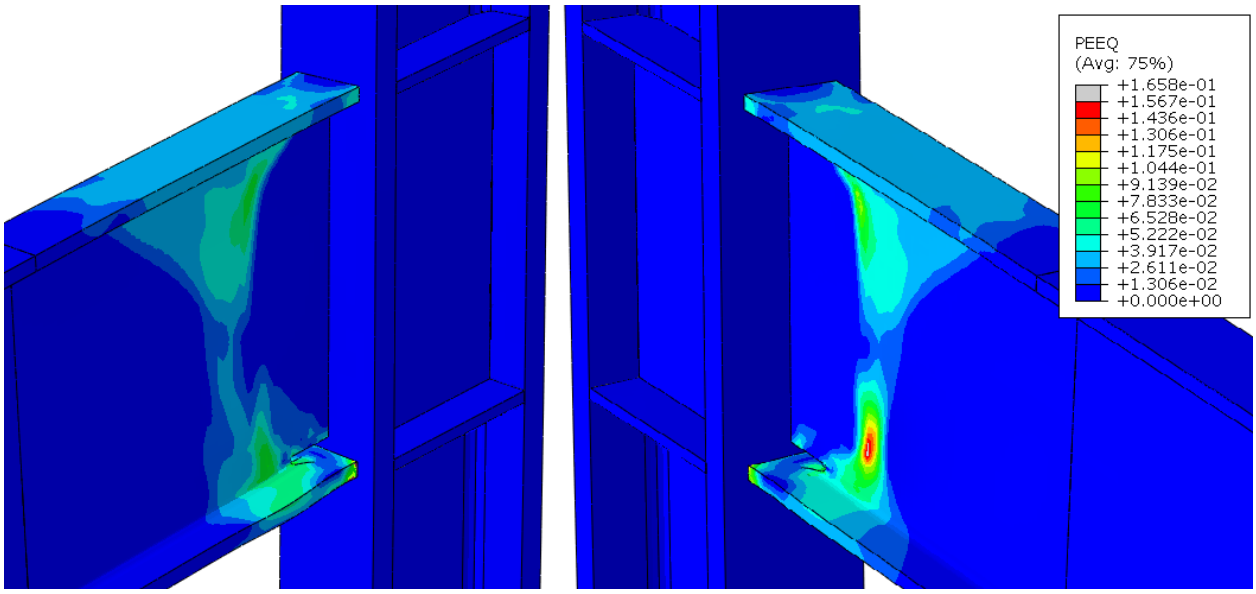


**Figure 5-39: PEEQ of the WUF-W connection with 15 degree slope subject to a negative moment**

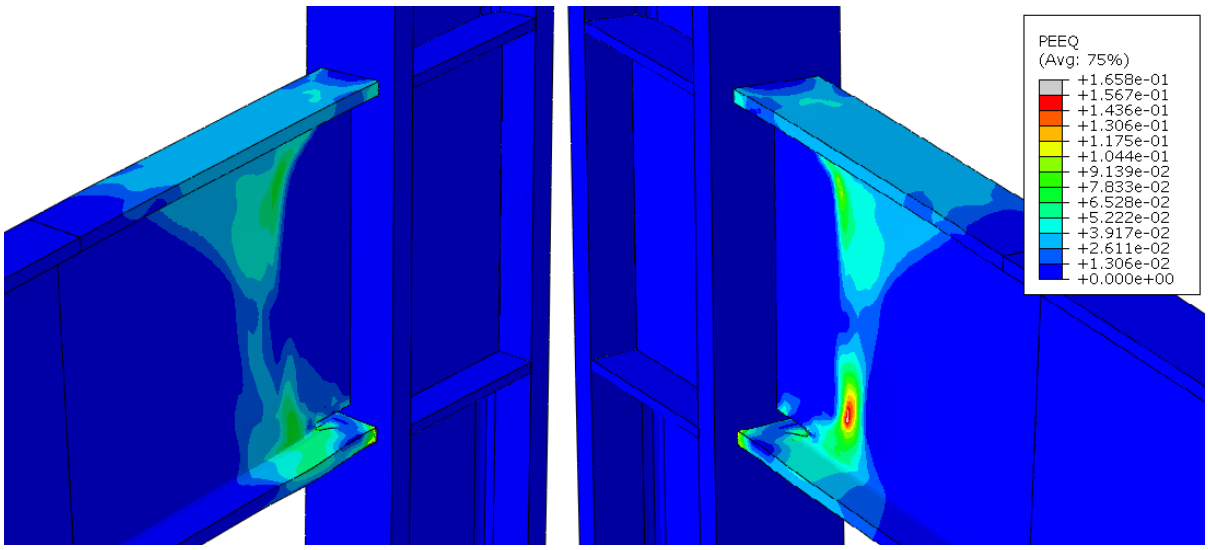


**Figure 5-40: PEEQ of the WUF-W connection with 20 degree slope subject to a clockwise moment**

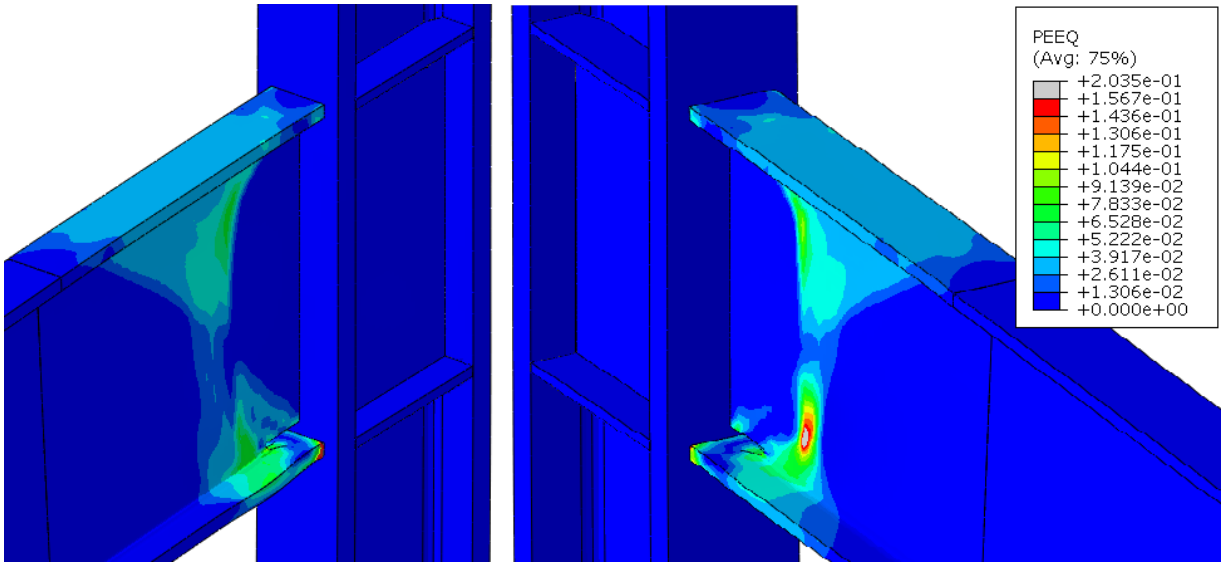


**Figure 5-41: PEEQ of the WUF-W connection with 25 degree slope subject to a negative moment**

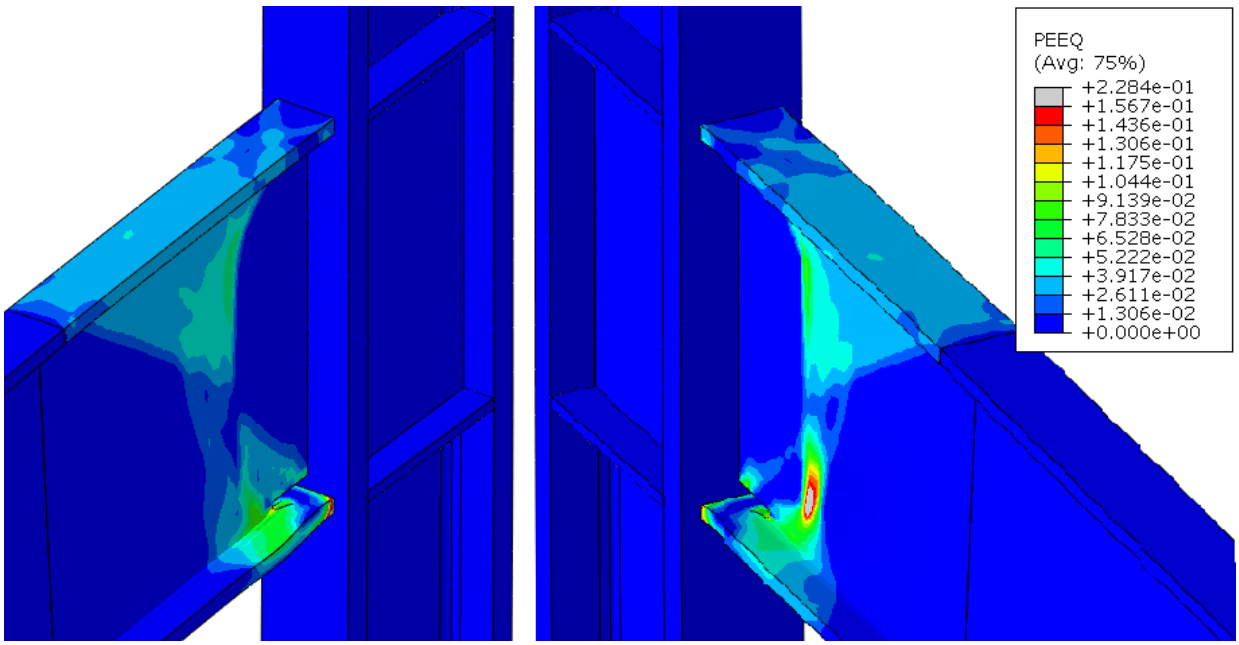


**Figure 5-42: PEEQ of the WUF-W connection with 30 degree slope subject to a clockwise moment**

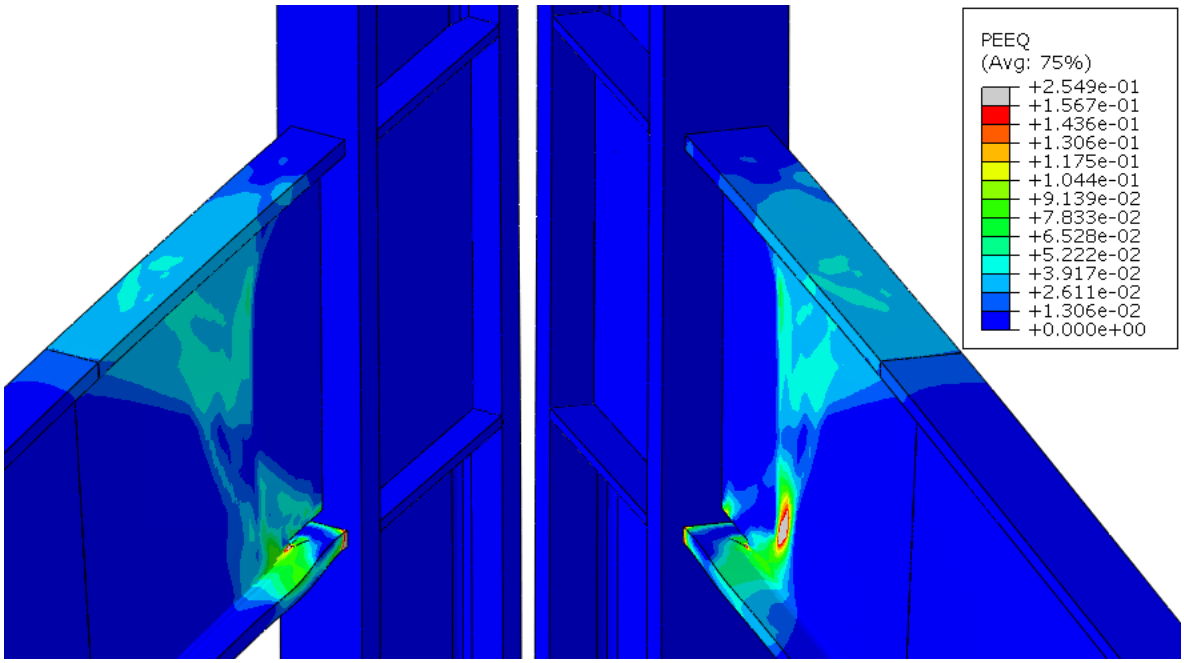


**Figure 5-43: PEEQ of the WUF-W connection with 35 degree slope subject to a negative moment**

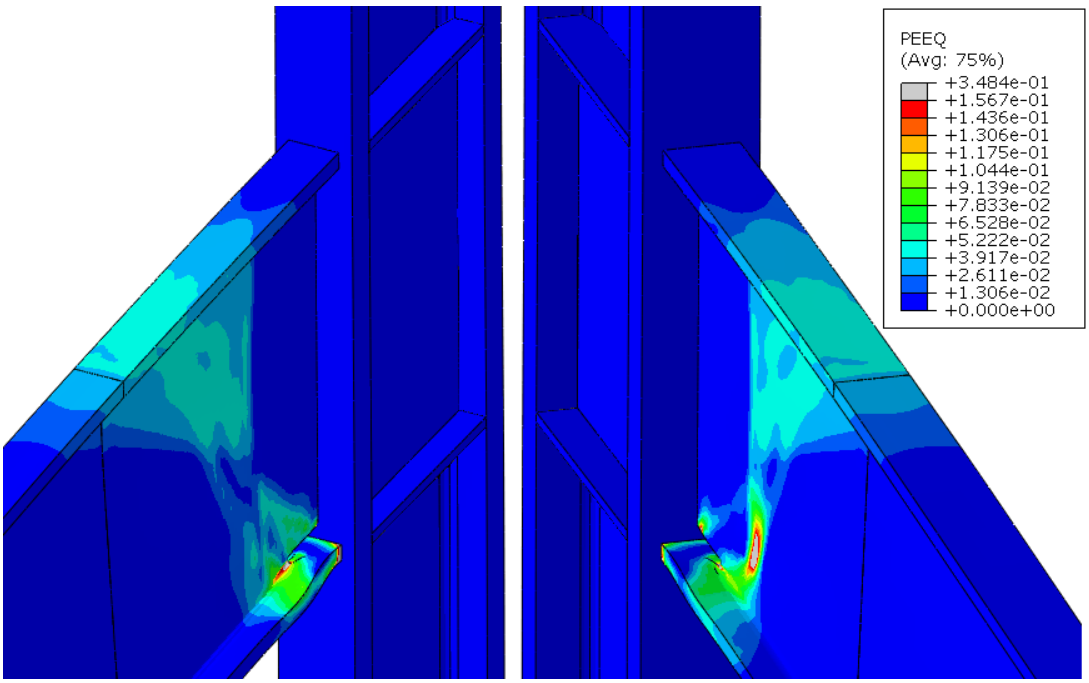


**Figure 5-44: PEEQ of the WUF-W connection with 40 degree slope subject to a clockwise moment**

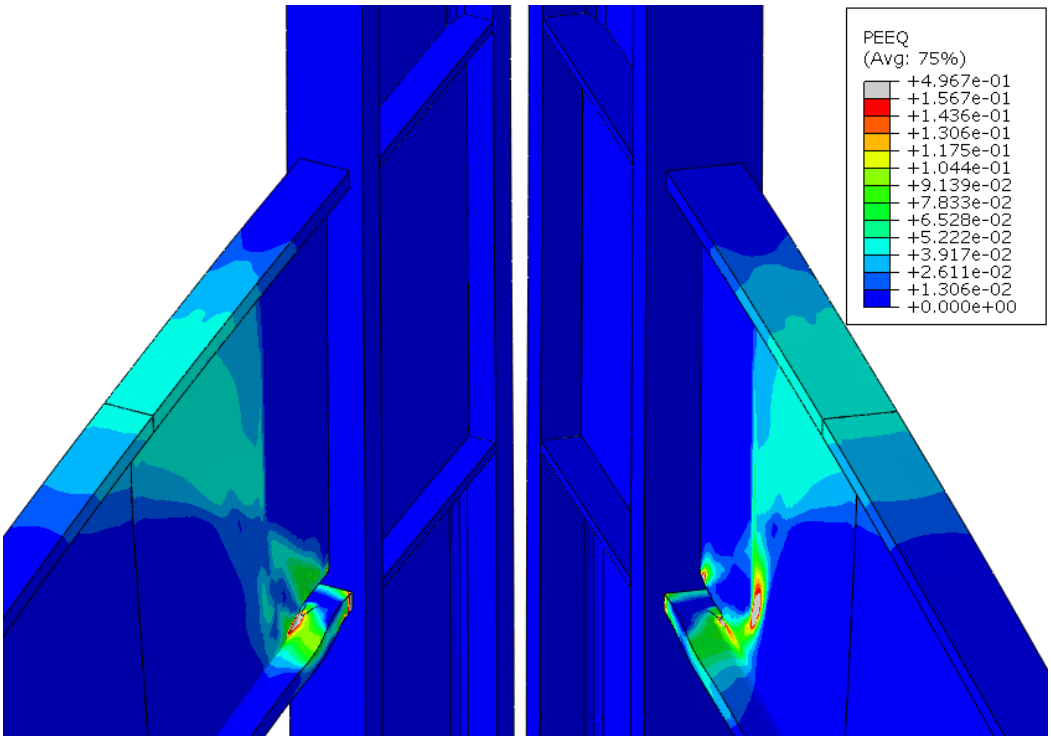


**Figure 5-45: PEEQ of the WUF-W connection with 45 degree slope subject to a negative moment**

## 5.3 WUF-W Moment Connection with Sloped Configurations subject to Positive Moment

The WUF-W connection models with a downward sloped beam-to-column configuration were subject to a positive moment in order to observe its effects. This was performed by applying an upward vertical displacement at the beam tip. The slope of the beam was varied between 5 and 45 degrees through 5 degree increments. The analyses were performed and their results compared to the response of the orthogonally framed connection.

In the case of a sloped beam configuration subject to a positive moment, the results indicate an increase in plastic moment capacity with an increase in slope angle. This can be observed from Figure 5-46. Similar to the configuration subject to a negative moment, this is most likely attributed to the increase effective depth of the beam cross-section with respect to the bending axis.

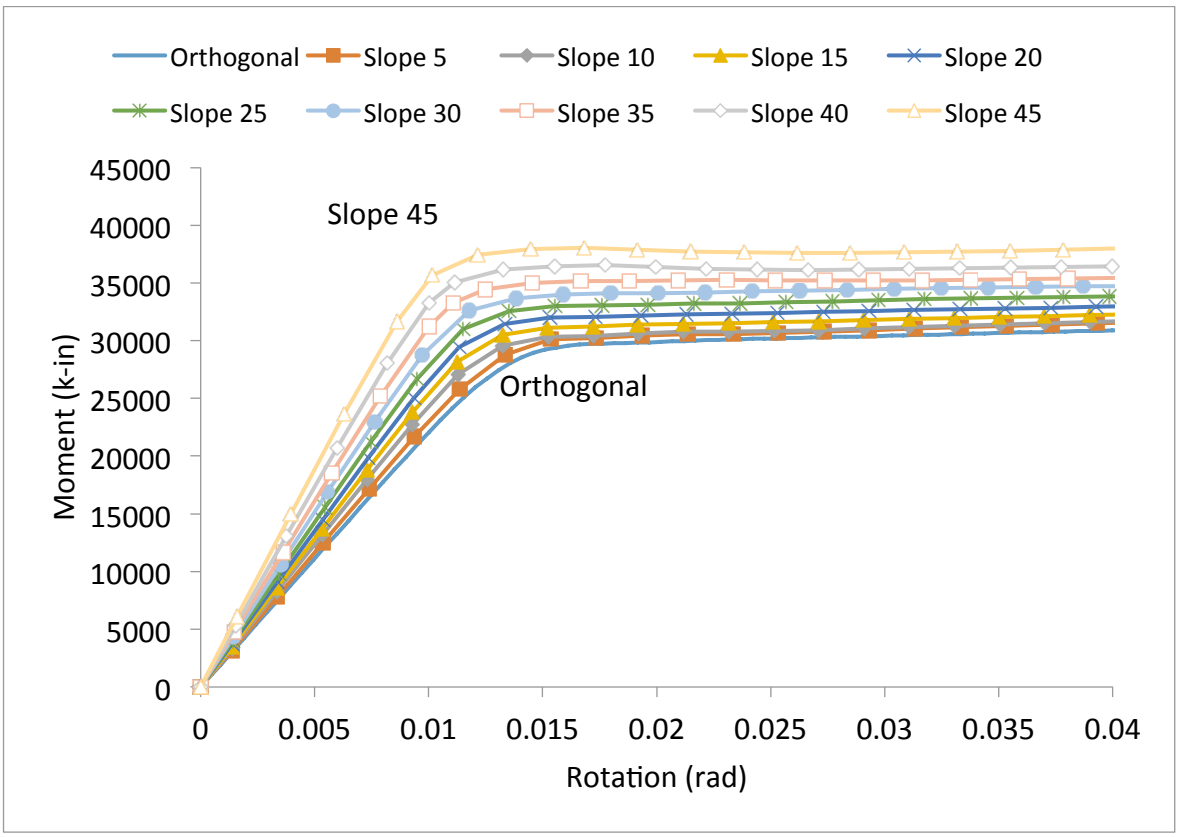


**Figure 5-46: Moment versus rotation of the WUF-W connection with sloped configurations subject to a positive moment**

Similar to the WUF-W connection detail with sloped configurations subject to a negative moment, the stress distribution remains perpendicular to the beam section as shown in Figures 5-47 through 5-55 as the beam is subject to a positive moment. This effect does not appear to be impacted by the sloped geometry. As a result of this, the stress distribution concentrates within the beam bottom flange of the beam section near the beam/column interface for slope angles exceeding 10 degrees. Conversely, the stress distribution in the beam top flange concentrates farther away from the beam/column interface and distributes over a larger region.

The panel zone of the connection is also impacted by the sloped configurations. As the slope angle increases, the stress distribution in the doubler plates within the panel zone concentrates towards the backside of the connection near the bottom.

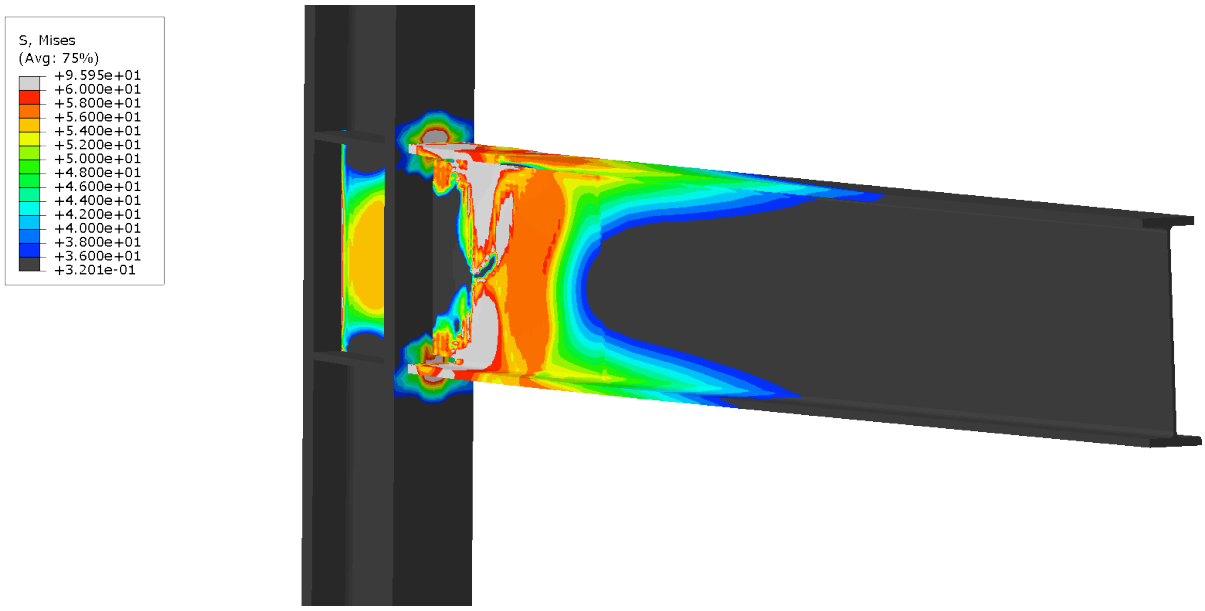


**Figure 5-47: Von Mises stress distribution for the WUF-W with connection 5 degree slope subject to a positive moment**

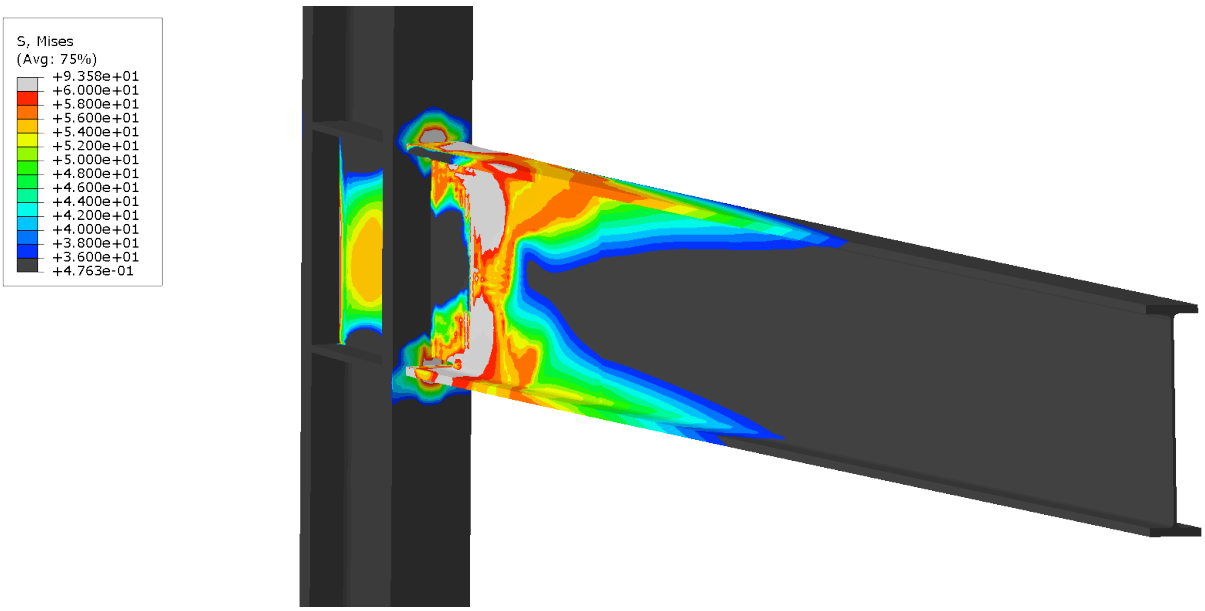


**Figure 5-48: Von Mises stress distribution for the WUF-W with connection 10 degree slope subject to a positive moment**

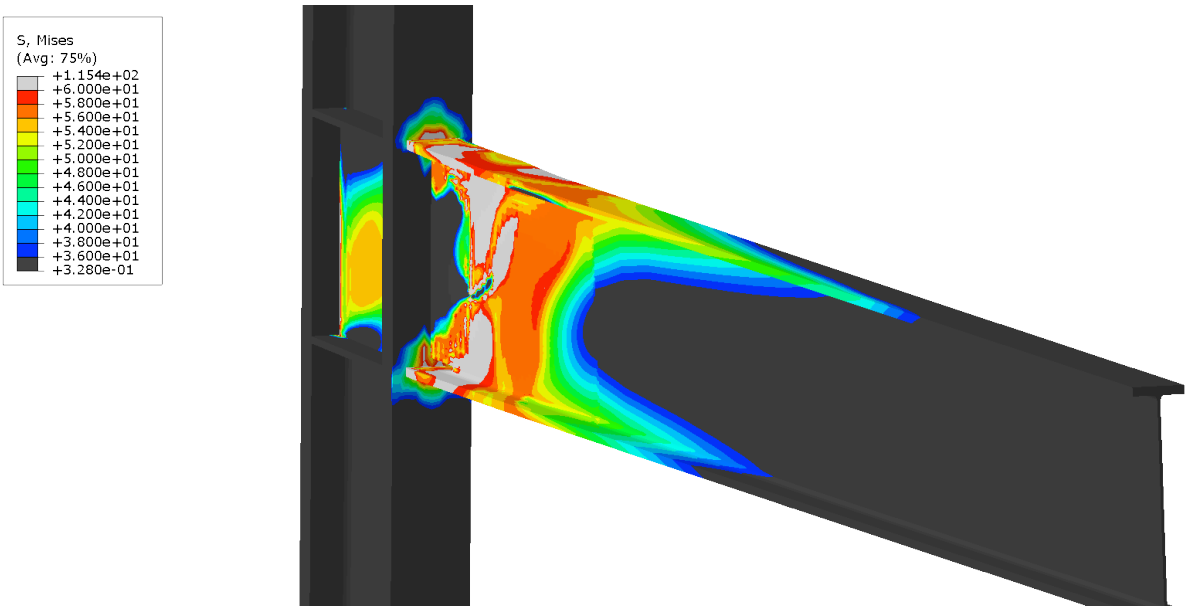


**Figure 5-49: Von Mises stress distribution for the WUF-W with connection 15 degree slope subject to a positive moment**

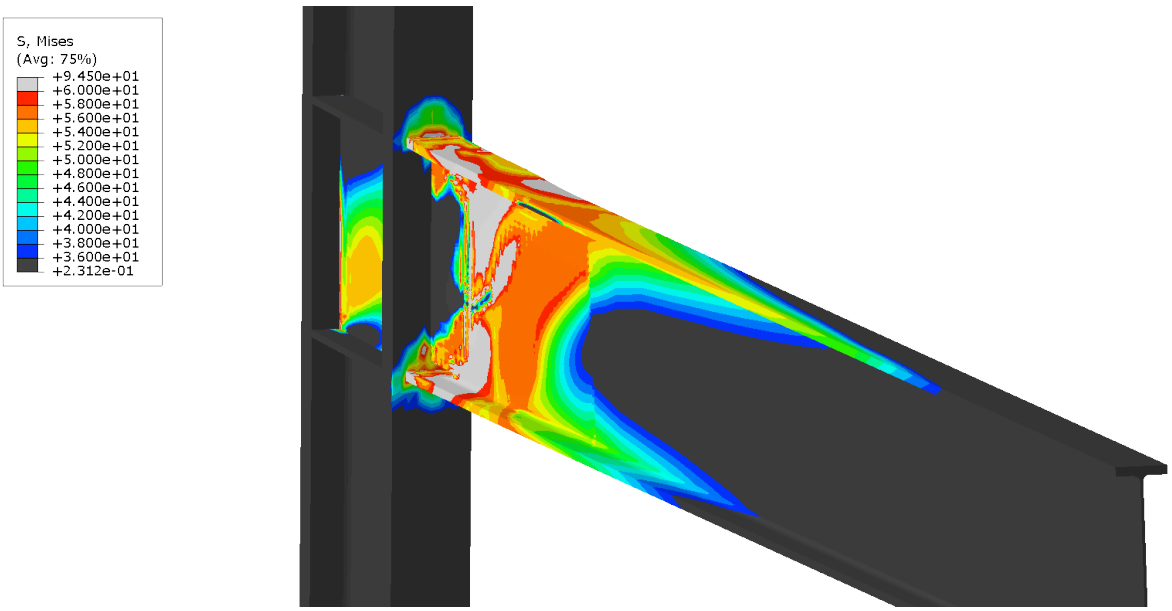


**Figure 5-50: Von Mises stress distribution for the WUF-W with connection 20 degree slope subject to a positive moment**

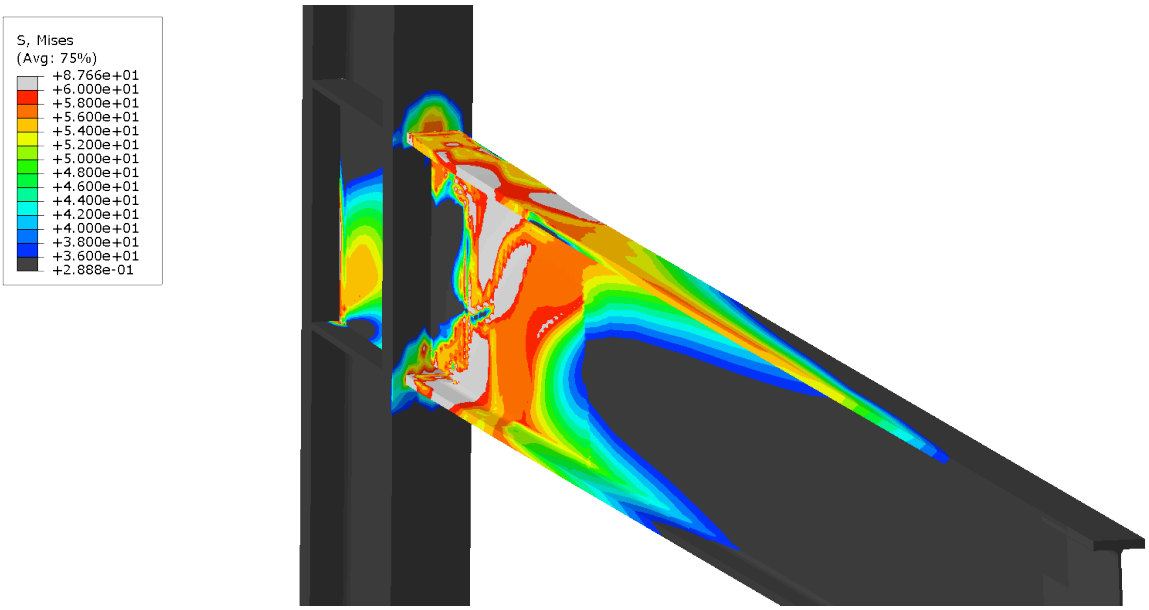


**Figure 5-51: Von Mises stress distribution for the WUF-W with connection 25 degree slope subject to a positive moment**

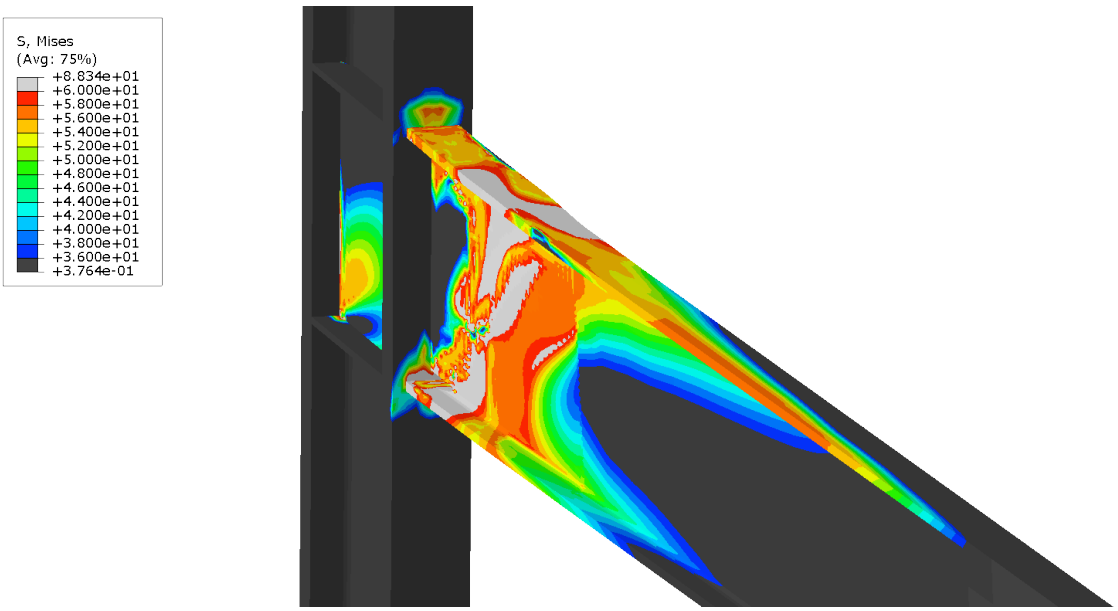


**Figure 5-52: Von Mises stress distribution for the WUF-W with connection 30 degree slope subject to a positive moment**

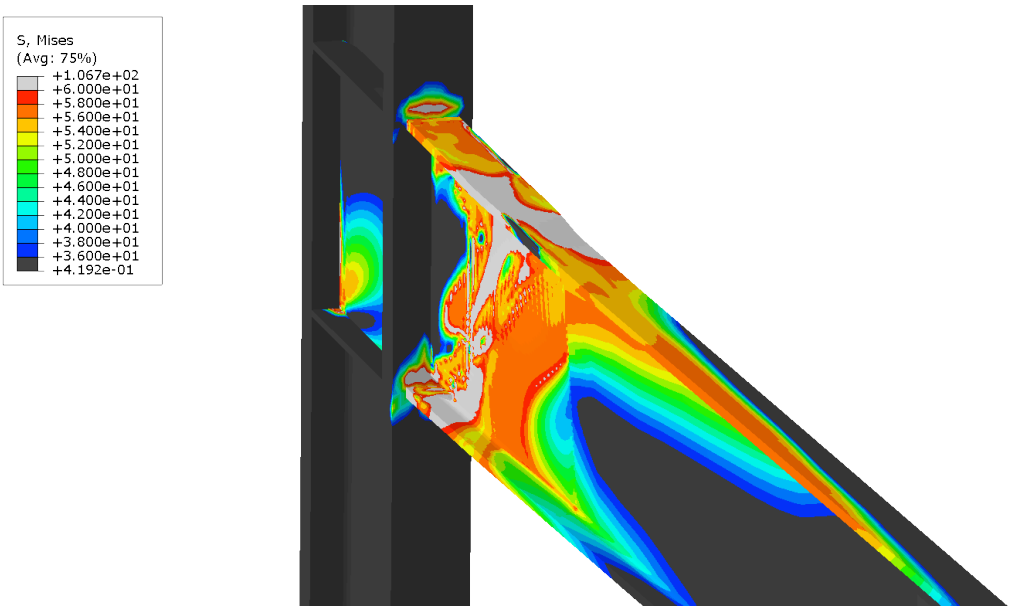


**Figure 5-53: Von Mises stress distribution for the WUF-W with connection 35 degree slope subject to a positive moment**

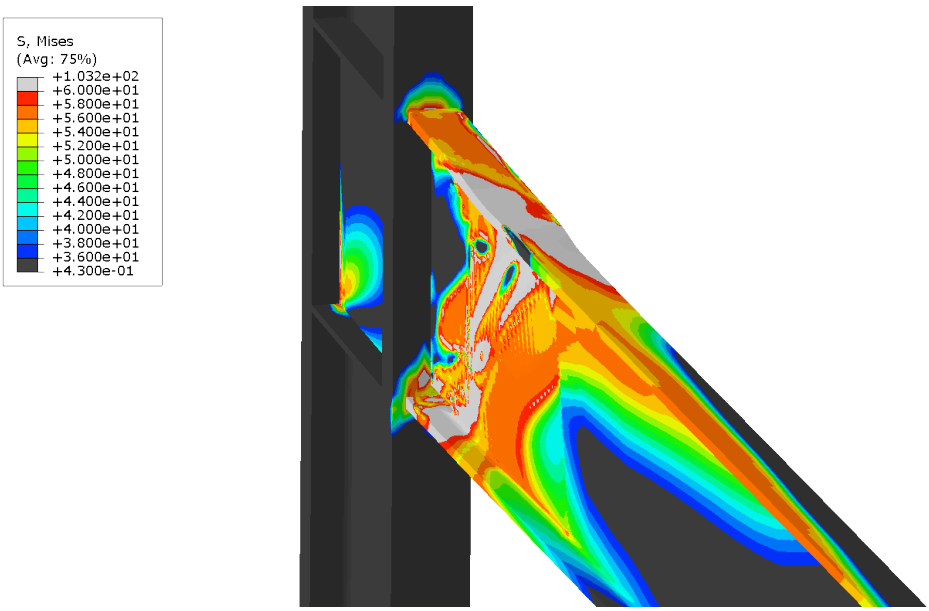


**Figure 5-54: Von Mises stress distribution for the WUF-W with connection 40 degree slope subject to a positive moment**

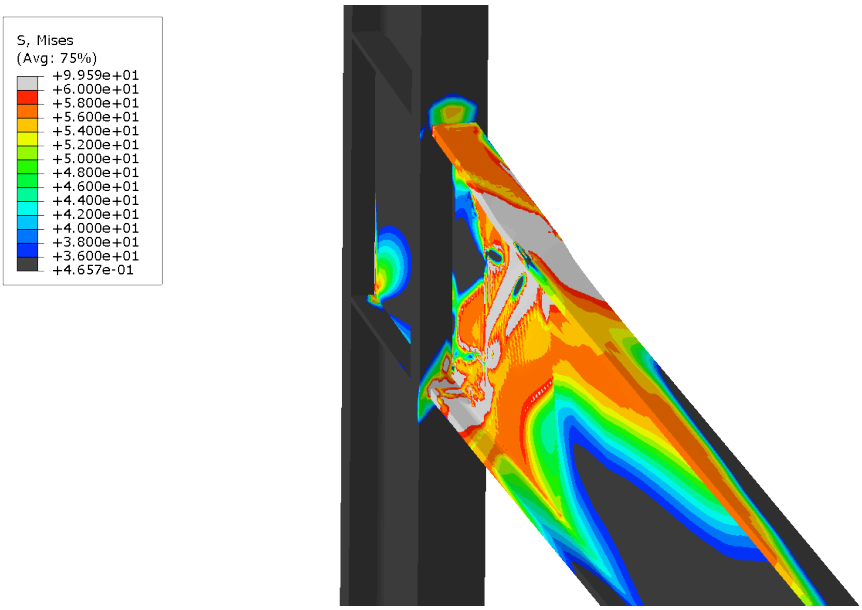


**Figure 5-55: Von Mises stress distribution for the WUF-W with connection 45 degree slope subject to a positive moment**

The first indication of non-linearity from the moment vs. rotation relationship occurs at a moment of 24150 k-in. The stress values associated with that moment were recorded and plotted with respect to the sloped angle in Figure 5-56. An increase in stress concentration is observed from 0 to 5 degrees followed by a progressive decrease in stress concentration for slope angles exceeding 5 degrees. The stress distribution throughout the flange in tension remains essentially unchanged.

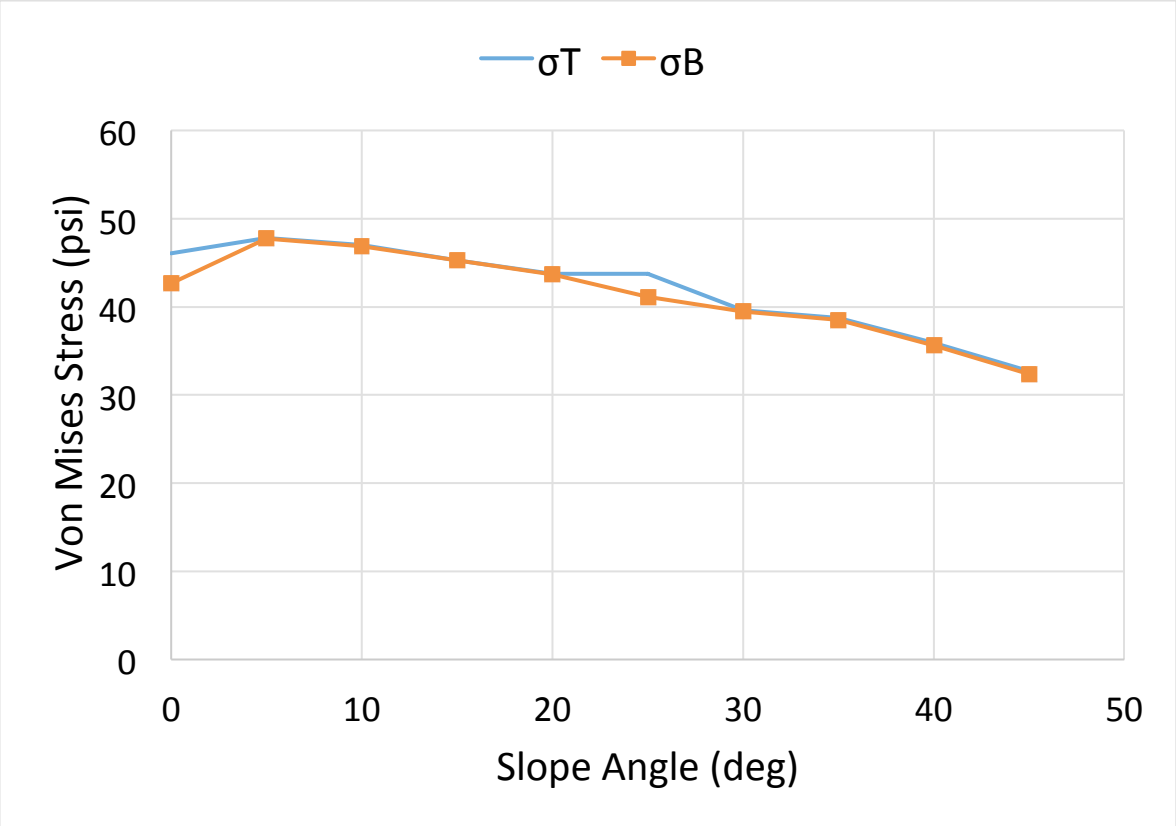


**Figure 5-56: Von Mises stress values within the WUF-W beam flange for sloped configurations subject to a positive moment at first yield.**

At 50% of the yield moment as calculated by dividing the moment associated with the first indication of non-linearity by 2, the stress values were recorded corresponding to a moment of 12140 k-in. The stress values were plotted with respect to the slope angle in Figure 5-57. A progressive decrease in stress concentration is observed for slope angles exceeding 5 degrees. The stress distribution throughout the flange in tension remains essentially unchanged.

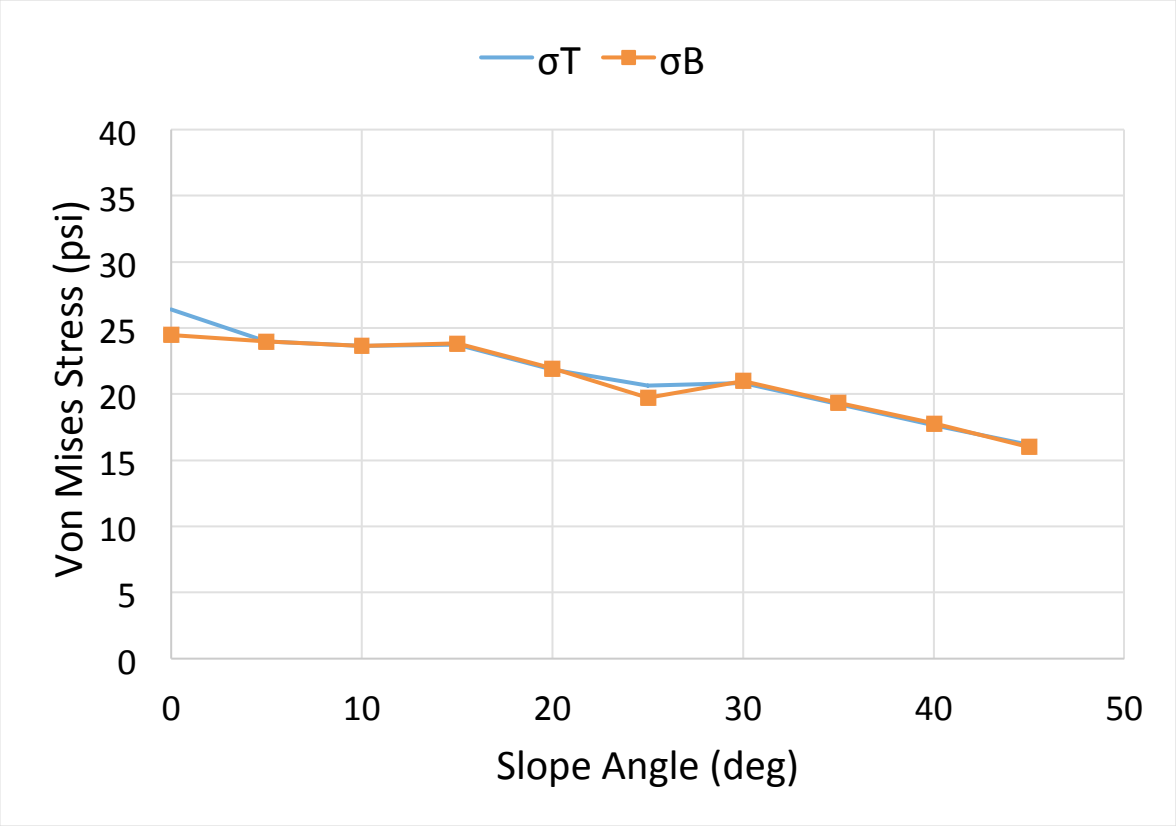


**Figure 5-57: Von Mises stress values within the WUF-W beam flange for sloped configurations subject to a positive moment at 50% yield.**

In all sloped configurations of the WUF-W detail, the hinging mechanism of the beam is contained in a plane perpendicular to the beam cross-section as shown

in Figures 5-58 through 5-66. Similar to the case of connections subject to negative moments, the strain demand distributes over a larger region in the top flange. However, the strain demand increases for each increasing angle. The strain demand concentrates near the connection in the bottom flange much like the case of connections subject to negative moments. The increased strain demand starts exceeding that of the orthogonally framed connection when slope angles exceed 20 degrees.

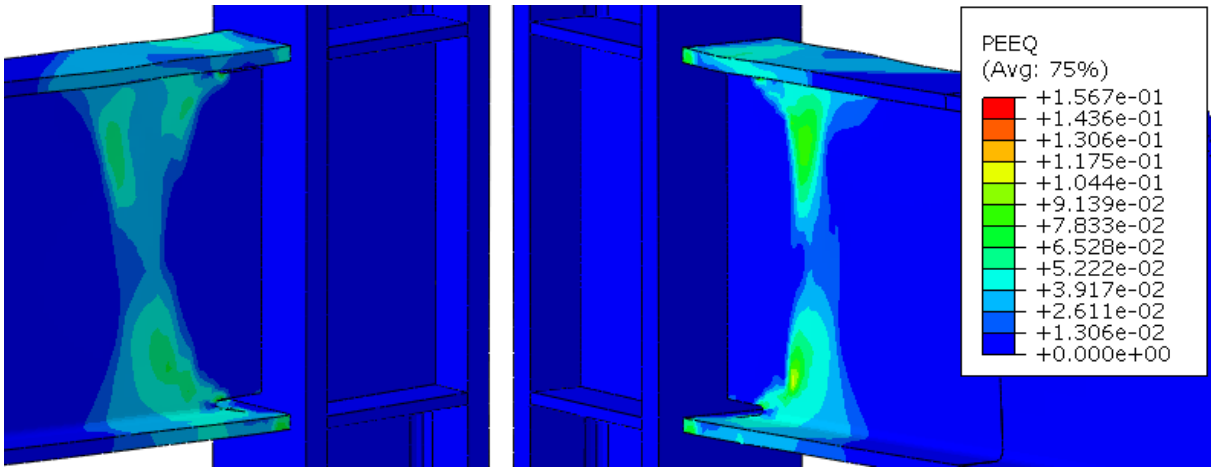


**Figure 5-58: PEEQ of the WUF-W connection with 5 degree slope subject to a positive moment**

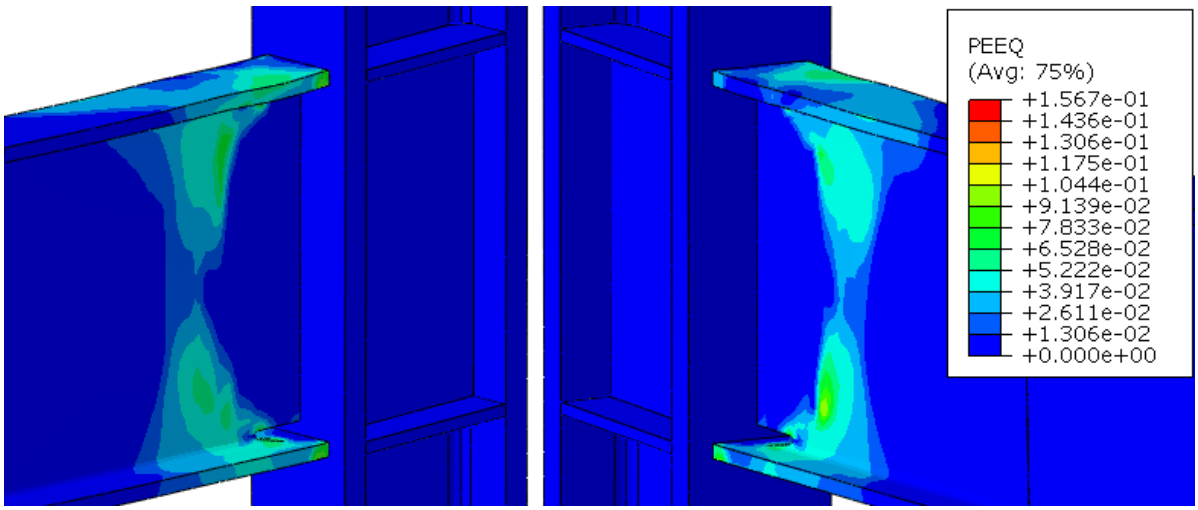


**Figure 5-59: PEEQ of the WUF-W connection with 10 degree slope subject to a positive moment**

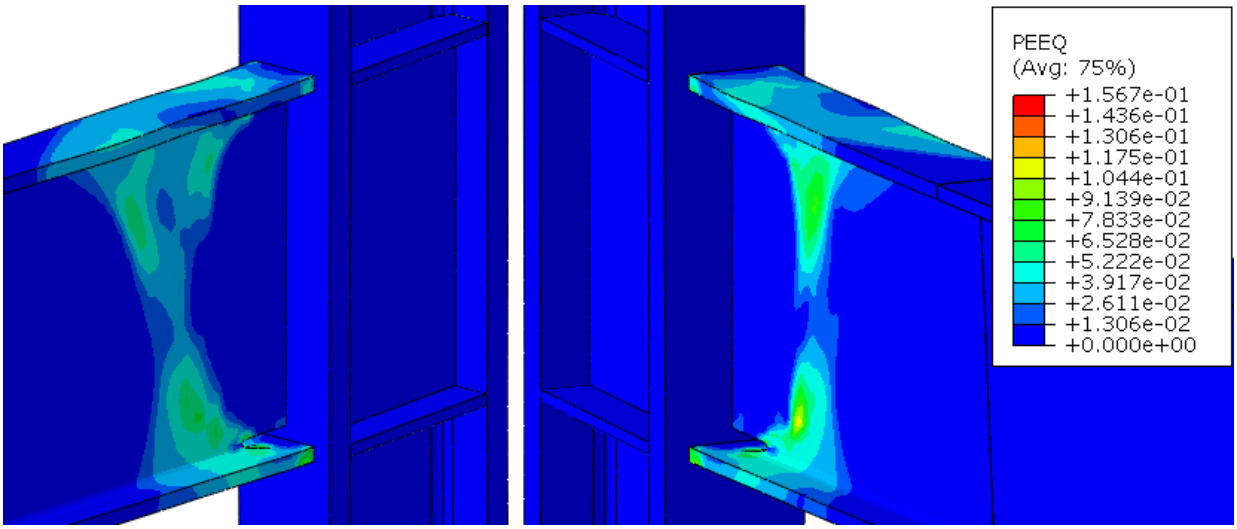


**Figure 5-60: PEEQ of the WUF-W connection with 15 degree slope subject to a positive moment**

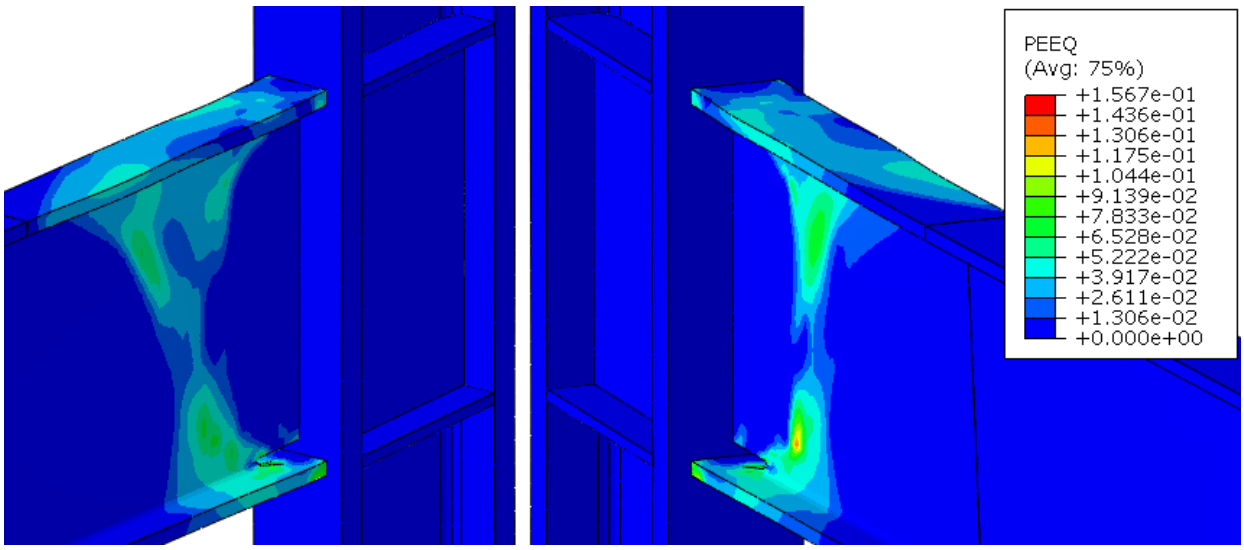


**Figure 5-61: PEEQ of the WUF-W connection with 20 degree slope subject to a positive moment**

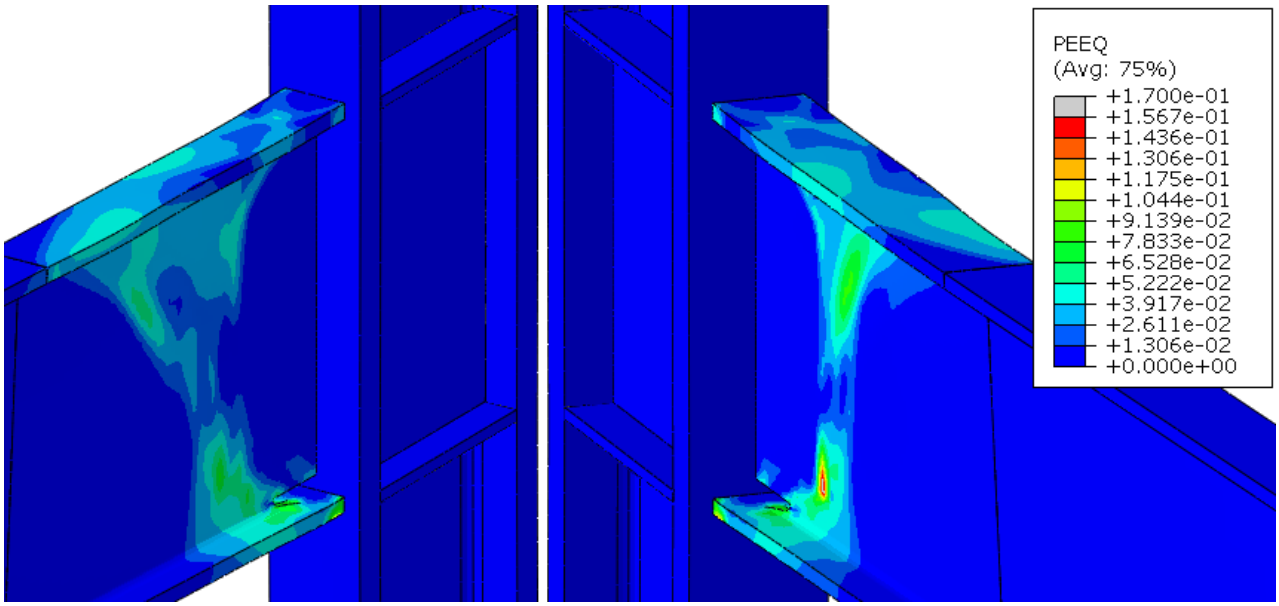


**Figure 5-62: PEEQ of the WUF-W connection with 25 degree slope subject to a positive moment**

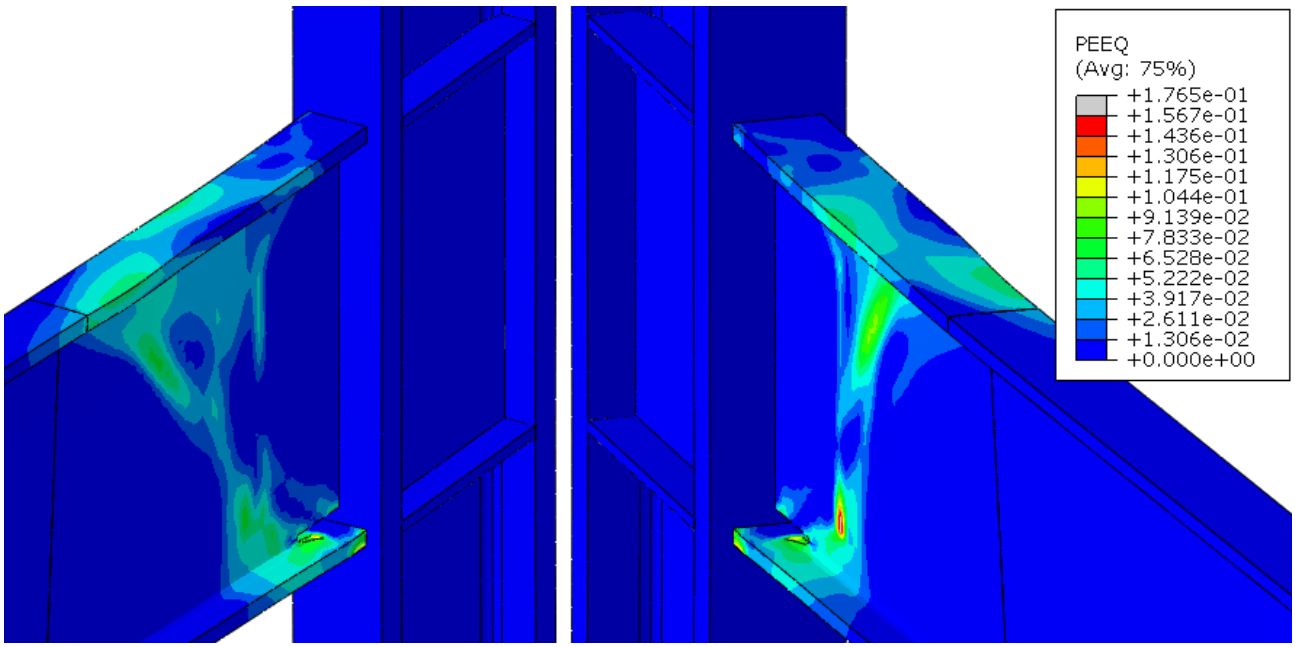


**Figure 5-63: PEEQ of the WUF-W connection with 30 degree slope subject to a positive moment**

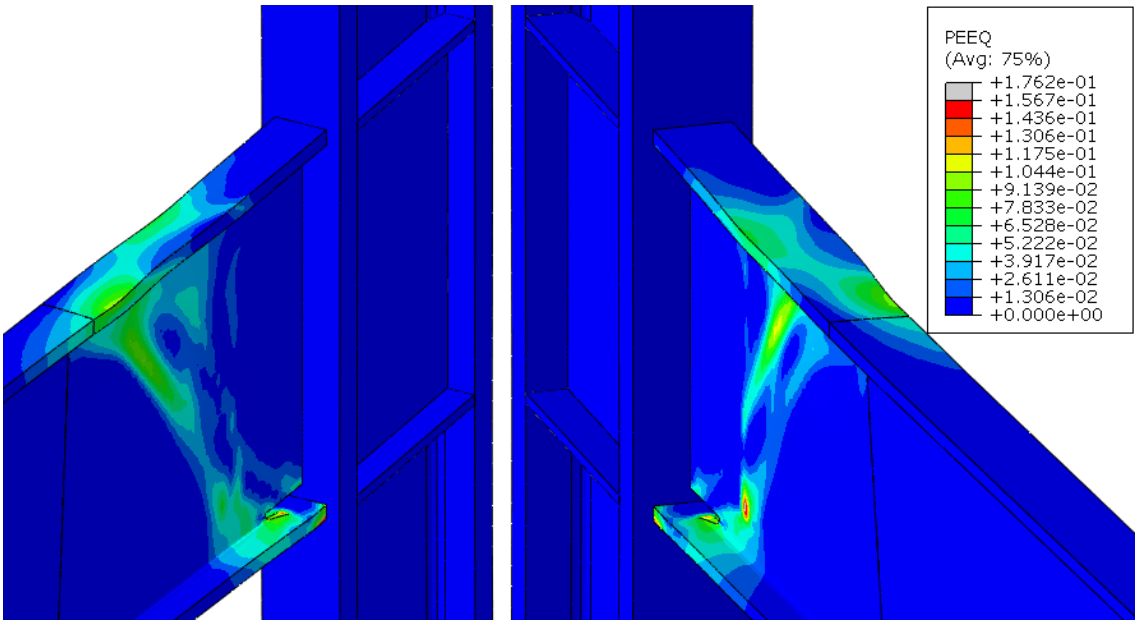


**Figure 5-64: PEEQ of the WUF-W connection with 35 degree slope subject to a positive moment**

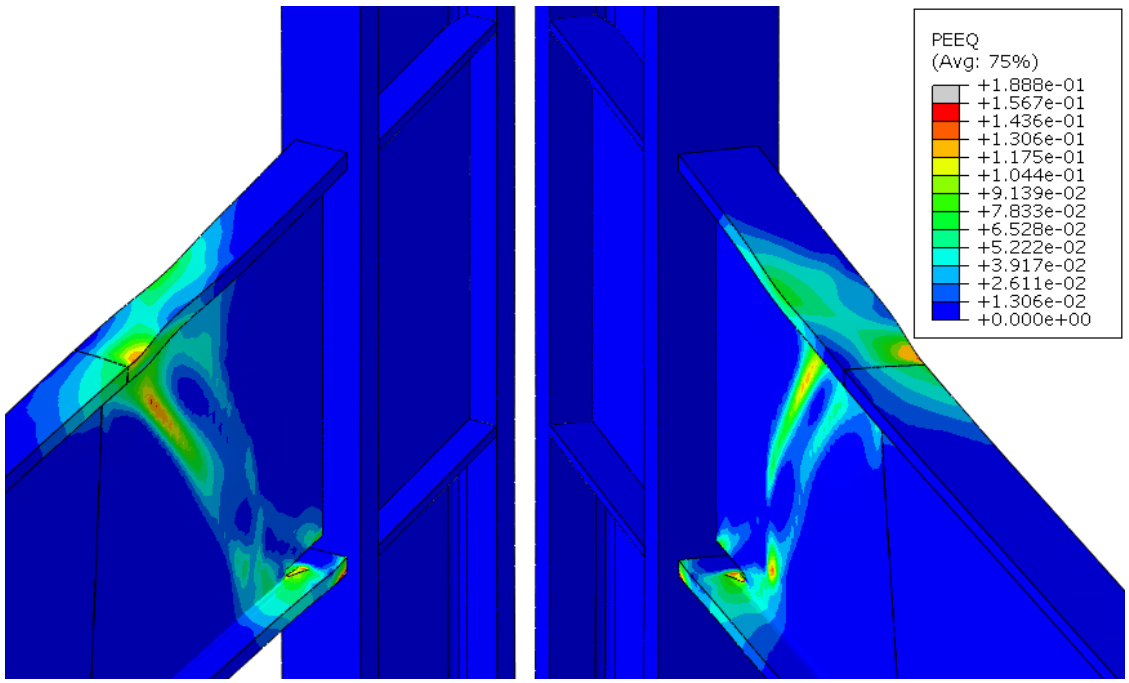


**Figure 5-65: PEEQ of the WUF-W connection with 40 degree slope subject to a positive moment**

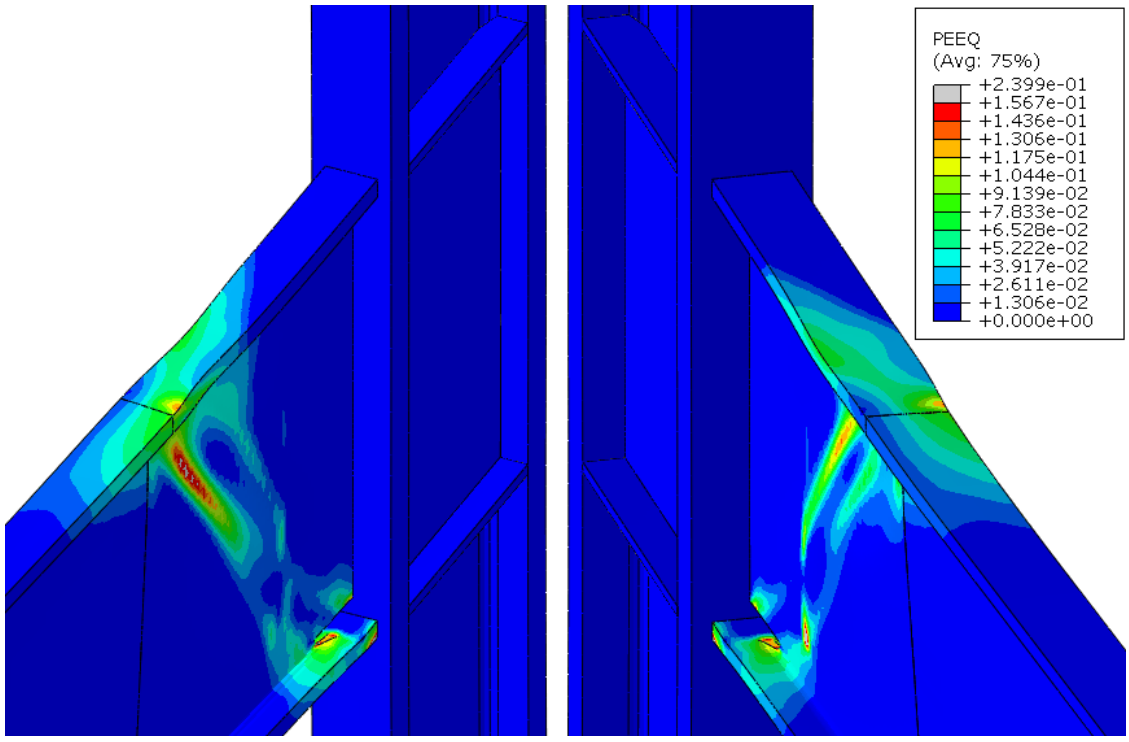


**Figure 5-66: PEEQ of the WUF-W connection with 45 degree slope subject to a positive moment**

# Chapter 6: Non-Orthogonal Response of the Reduced Beam Section (RBS) Moment Connection

A total of eight models were built varying the skew angles between 5 and 40 degrees through 5-degree increments. Only configurations up to 40-degree skew were able to be investigated due to limitations in the column flange size. Similarly, a total of nine models were built varying the slope angles between 5 and 45 degrees through 5-degree increments. The finite element analyses were performed using quasi-static loading, since cyclical loading is computationally demanding. Therefore, in an attempt to quantify the effects of cyclic loading, the connection was subject to both positive and negative moments.

The Von Mises stress variable was scaled with a minimum stress value of 36 kips/in$^2$ (ksi) and a maximum stress value of 60 ksi. These values were selected as a minimum stress value for a steel component of A36 material to yield and an expected value exceeding yield value of A572/A992 steel. The results of the orthogonal model are shown in Figure 6-1. The stress distribution concentrates largely in the beam at a distance away from the face of the column. This result is in good agreement with the expected response of the connection in accordance with the ANSI/AISC 358 document which expects yielding to occur in the beam at a specified distance away from the face of the column.

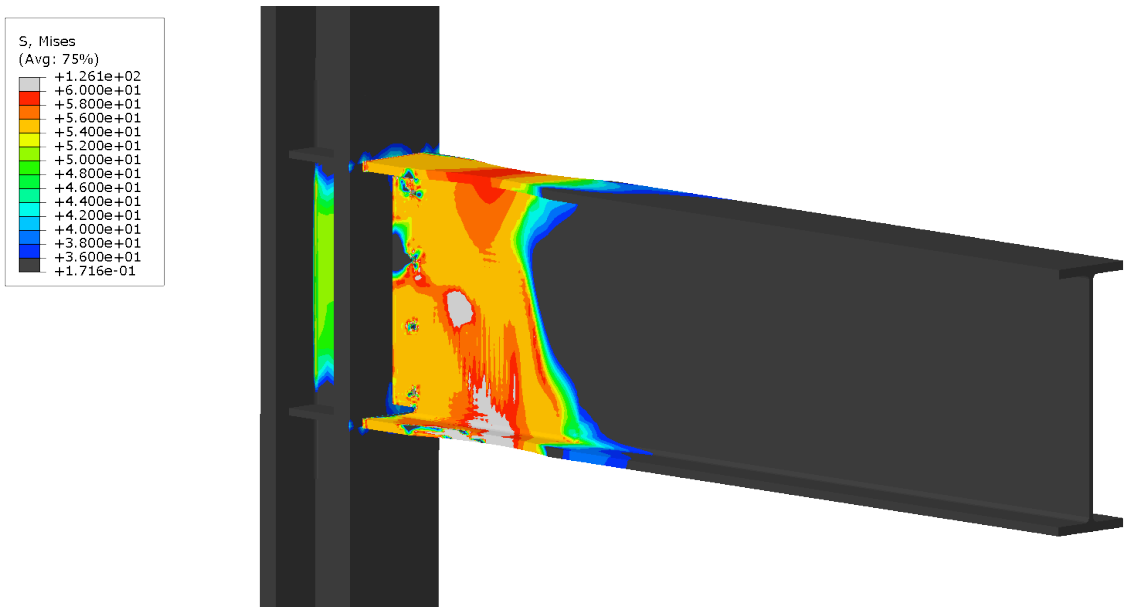


**Figure 6-1: Von Mises stress distribution for the orthogonal RBS connection detail**

For PEEQ comparisons, the observed PEEQ for all model configurations was scaled to the maximum observed PEEQ of the orthogonal model. The maximum observed PEEQ value in the orthogonal connection was 0.1988 in/in. All yielding in the connection models occurred in the beam so a zoomed view of the beam from multiple angles will be displayed for the PEEQ observations. The scaling provides a direct comparison between the orthogonal and non-orthogonal models. All of the investigated response parameters were compared to the response of the traditional orthogonally framed connection.

Upon considering the investigation of the RBS connection with non-orthogonal configurations, it was noted that there would be two possibilities for the radius cut to be arranged. For sloped configurations, the radius cut could be made

parallel to the column cross-section as shown in Figure 6-2. The distance from the face of the column to the radius cut could be maintained regardless of the slope angle with this arrangement. On the other hand, the radius cut could be made perpendicular to the beam axis as show in Figure 6-3. In the latter case, the distance from the face of the column to the radius cut was maintained for the flange that had the radius cut closer to the beam/column interface. This would be the flange forming the acute angle of the connection. By detailing in this manner, the minimum distance to the face of the column is maintained.

For skewed configurations, the corresponding radius cut arrangements are shown in Figures 6-4 and 6-5. Both arrangements of the radius cut were investigated for both the skewed and sloped configurations in order to observe the effects on performance.

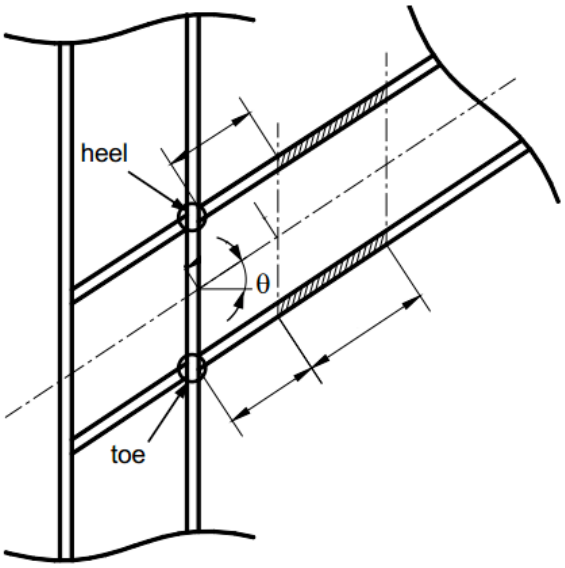


**Figure 6-2: RBS (slope) with radius cut parallel to column section (Kim et al. 2015)**

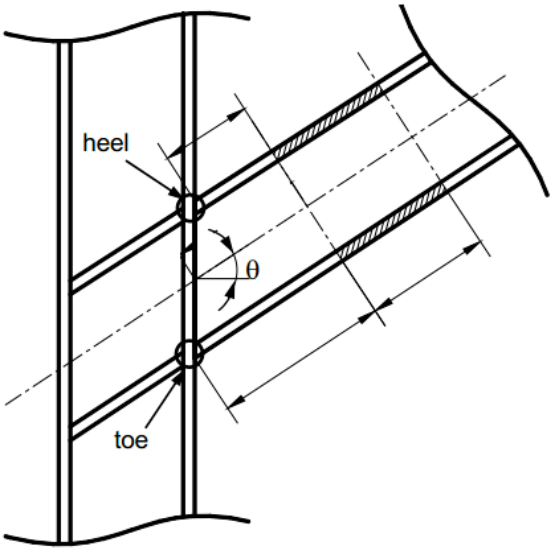


**Figure 6-3: RBS (slope) with radius cut perpendicular to beam section (Kim et al. 2015)**

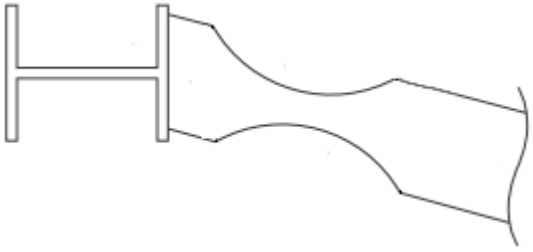

**Figure 6-4: RBS (skew) with radius cut parallel to column section (Prinz and Richards, 2014)**

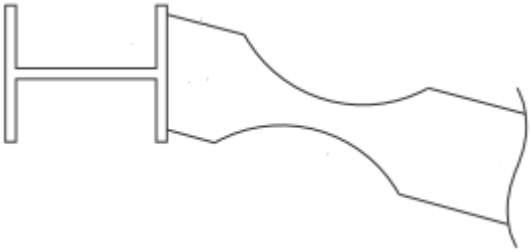

**Figure 6-5: RBS (skew) with radius cut perpendicular to beam section (Prinz and Richards, 2014)**

The weld access holes for both connections were modified so that the perpendicular distance extending away from the column was maintained to be constant. This remediation simulates a practical solution to be used in the field when the welder would require access to perform the welding.

The observed PEEQ values for the orthogonal configuration are displayed in Figure 6-6. The plastic hinge mechanism and the distribution of strain throughout the cross-section are in good agreement with the expected response of the connection in accordance to the ANSI/AISC 358 document. (ANSI/AISC 358, 2010) The RBS connection is detailed to concentrate the strain demand away from the column face. The PEEQ values for the orthogonal connection will provide a direct comparison to the response of the non-orthogonal configurations.

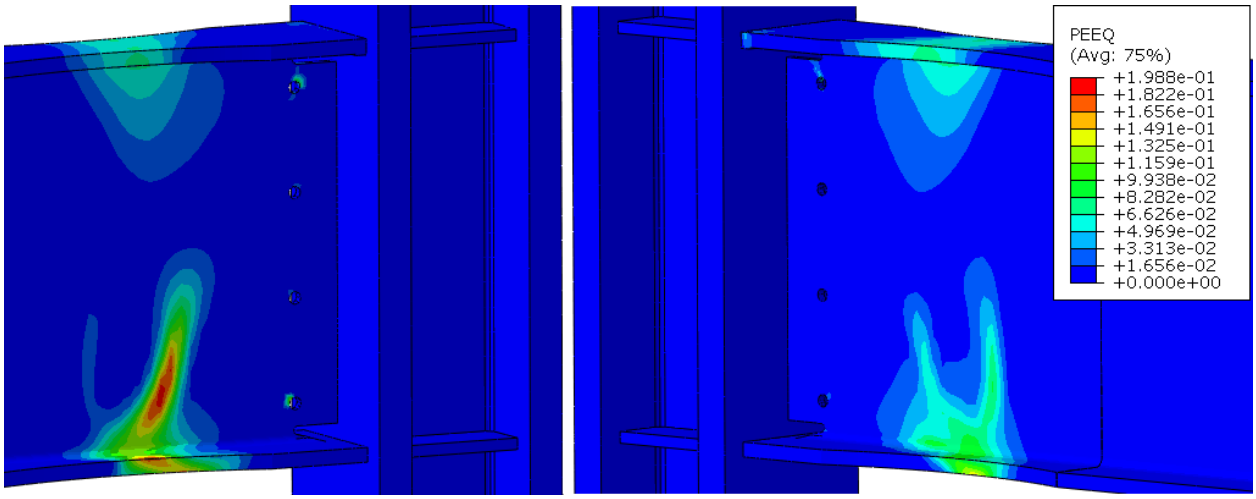


**Figure 6-6: PEEQ of the RBS connection with orthogonal framing**

## 6.1 RBS with Skewed Configurations

The RBS connections with skewed configurations were subject to a negative moment only due to the doubly symmetric column and beam sections. The negative moment was applied by displacing the beam tip vertically downward. Skew configurations were considered up to a 40 degree skew because of limitations in the column flange size. The effects of both radius cut arrangements were investigated.

### 6.1.1 RBS with Radius Cut Perpendicular to the Beam Section

The effects on plastic moment capacity for the RBS connections with skewed configurations and radius cut perpendicular to the beam section were minimal as shown in Figure 6-7. The plastic moment capacity increased approximately 3% for each 5-degree increase of skew angle. The onset of yielding was not impacted by the skew angle. The yielding point was largely unaffected by the skew angle as evident from the transition from elastic to plastic stiffness.

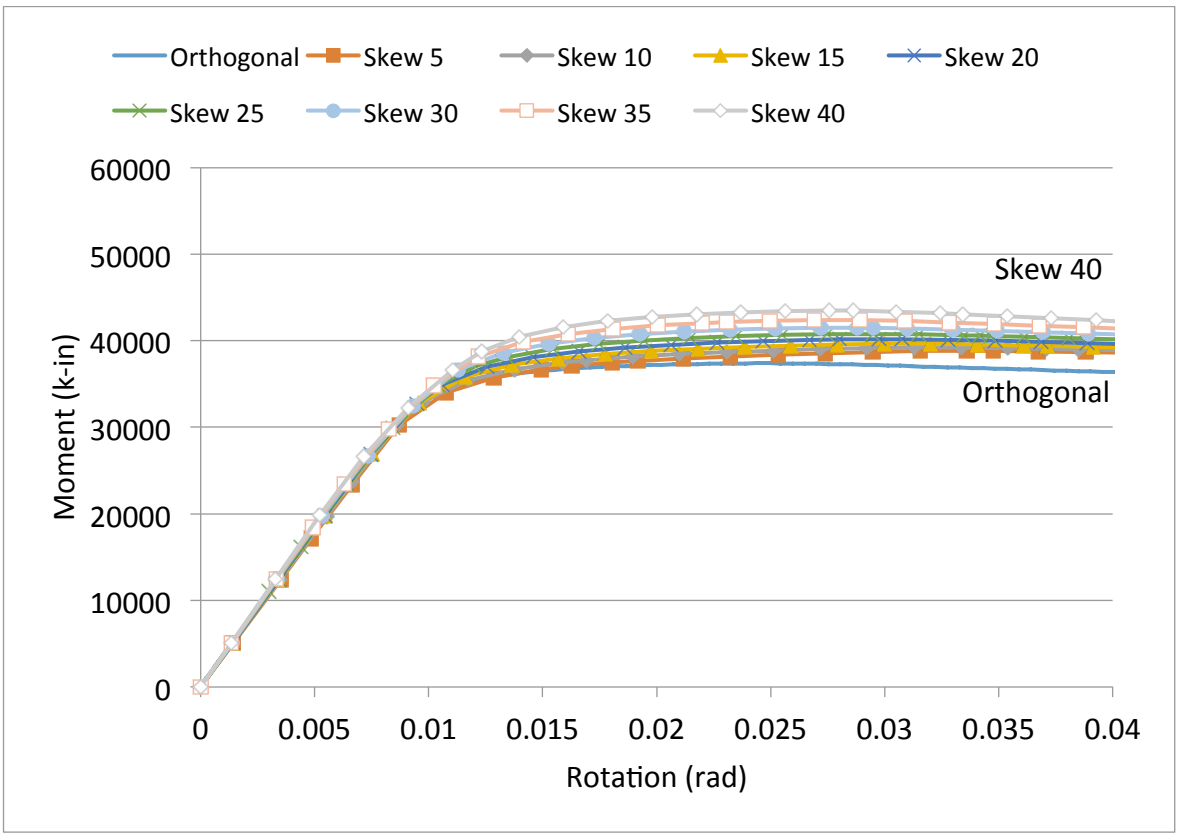


**Figure 6-7: Moment versus rotation of the RBS connection with skewed configurations and radius cut perpendicular to the beam section**

The stress distribution in the RBS connection detail is largely impacted by the amount of skew in the beam as shown in Figures 6-8 through 6-15. For skew angles between 5 and 40 degrees, the radius cut region is successful at concentrating most of the stress distribution within the beam. As the skew angle increases, the stress concentration within the beam flanges at the acute angle formed between the beam and column minimally increases. However, the stress concentration increases in the column flange at the acute angle formed between the beam and column. Additionally, as the skew angle exceeds 20 degrees, the stress

distribution in the column flange begins to concentrate at the obtuse angle formed between the beam and column. This effect progressively increases as the skew angle increases past 20 degrees. Finally, once the skew angle reaches or exceeds 30 degrees, the stress distribution in the column flange progressively concentrates between the beam flanges along the beam web.

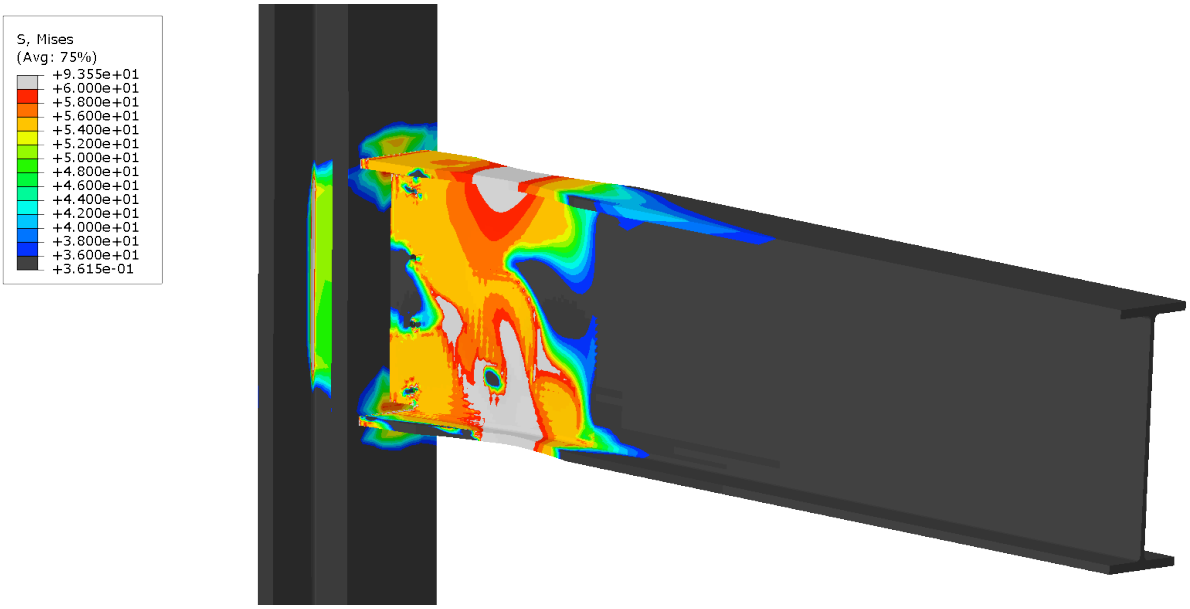


**Figure 6-8: Von Mises stress distribution of the RBS connection with 5 degree skew and radius cut perpendicular to the beam section**

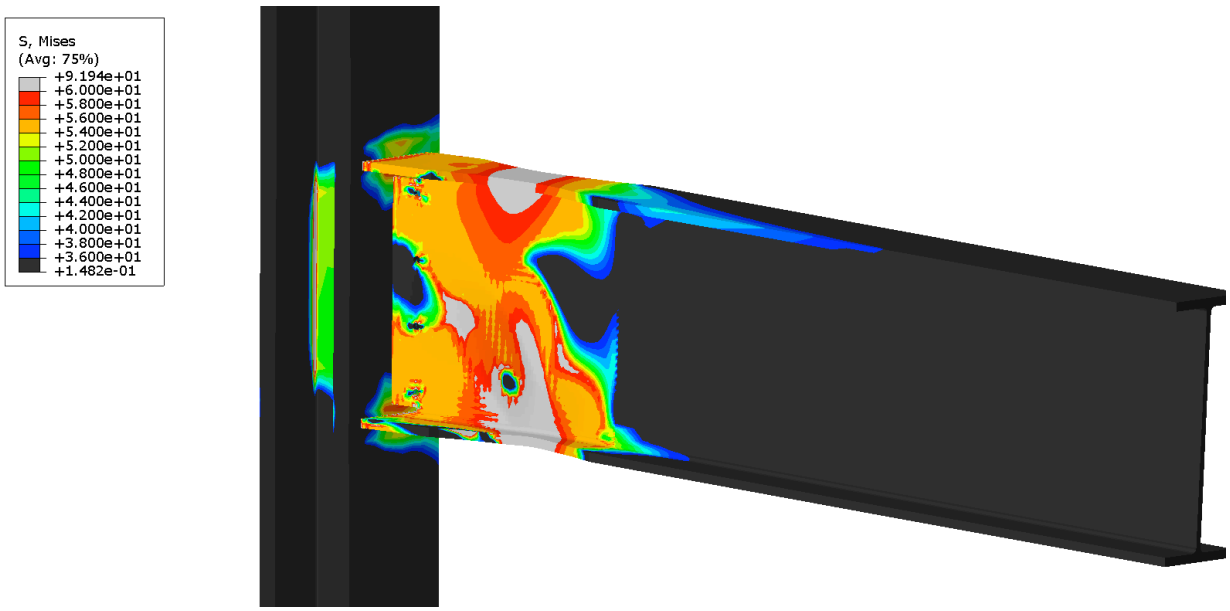


**Figure 6-9: Von Mises stress distribution of the RBS connection with 10 degree skew and radius cut perpendicular to the beam section**

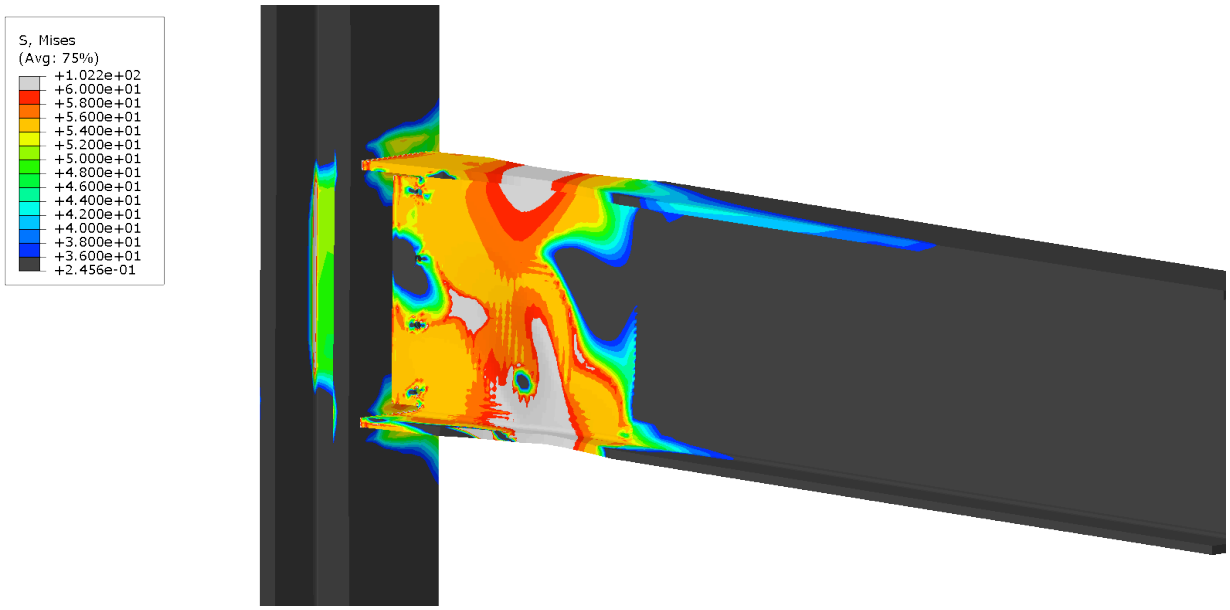


**Figure 6-10: Von Mises stress distribution of the RBS connection with 15 degree skew and radius cut perpendicular to the beam section**

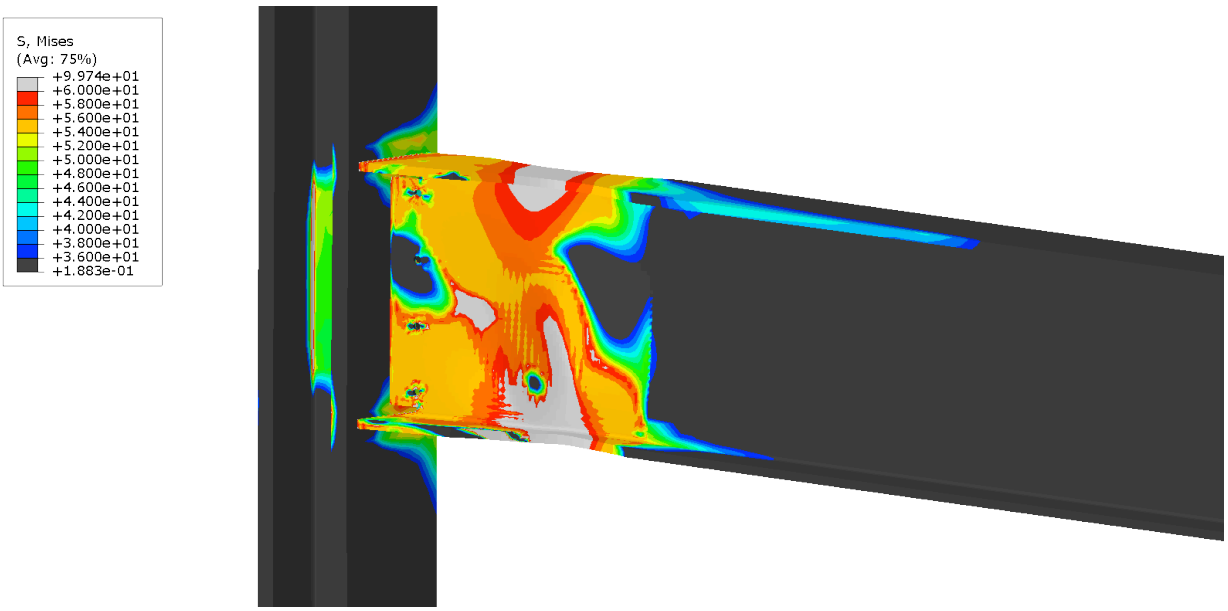


**Figure 6-11: Von Mises stress distribution of the RBS connection with 20 degree skew and radius cut perpendicular to the beam section**

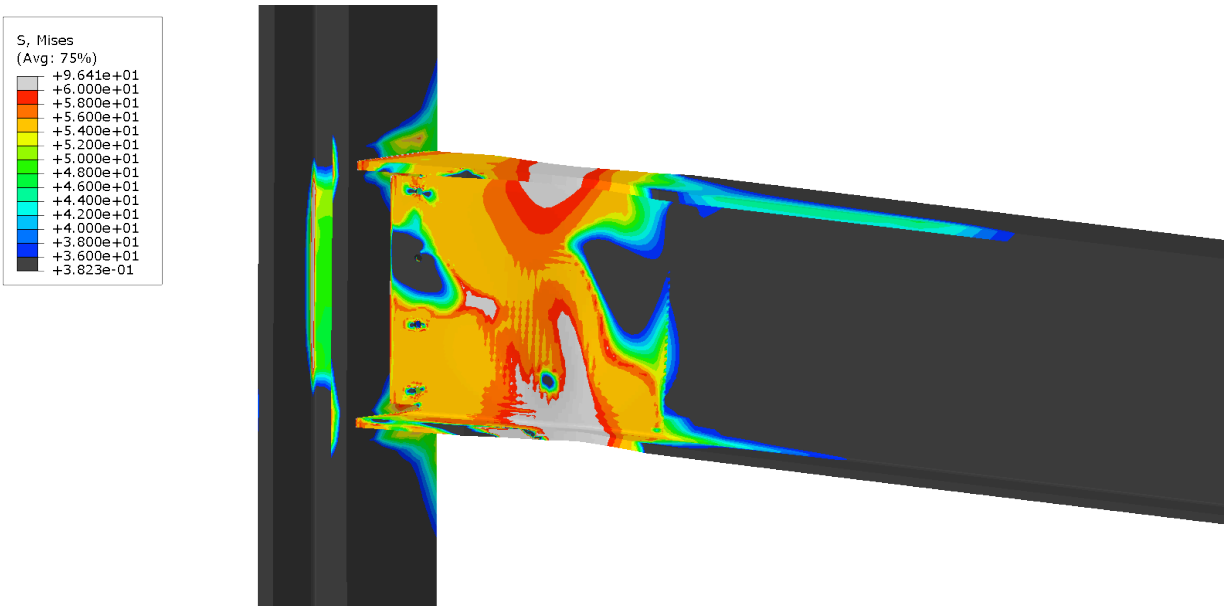


**Figure 6-12: Von Mises stress distribution of the RBS connection with 25 degree skew and radius cut perpendicular to the beam section**

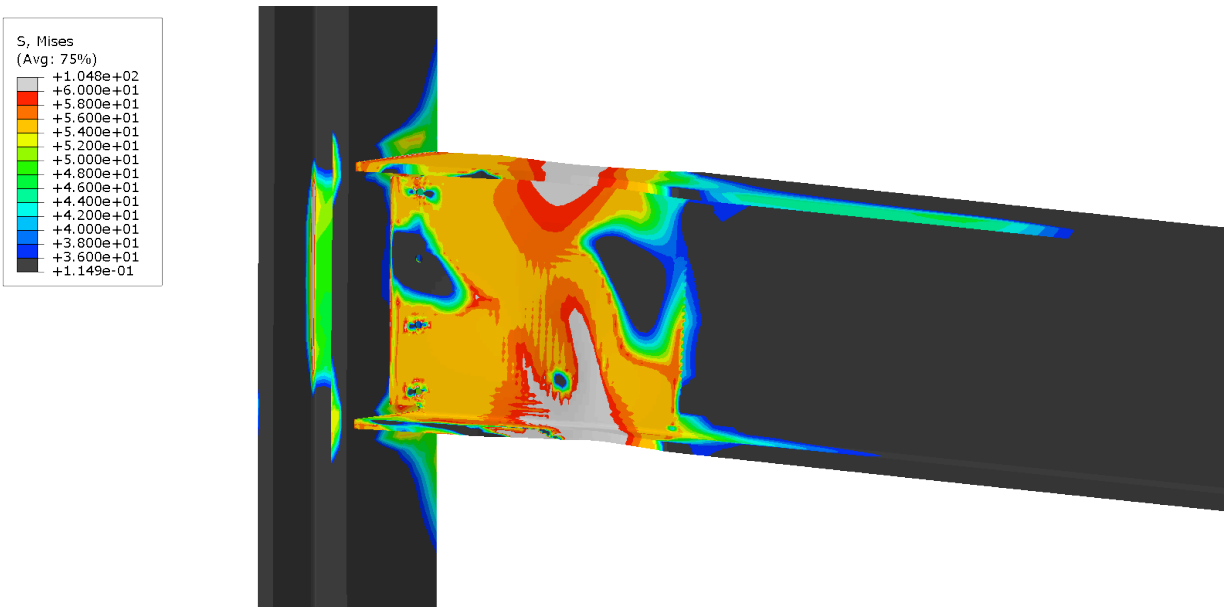


**Figure 6-13: Von Mises stress distribution of the RBS connection with 30 degree skew and radius cut perpendicular to the beam section**

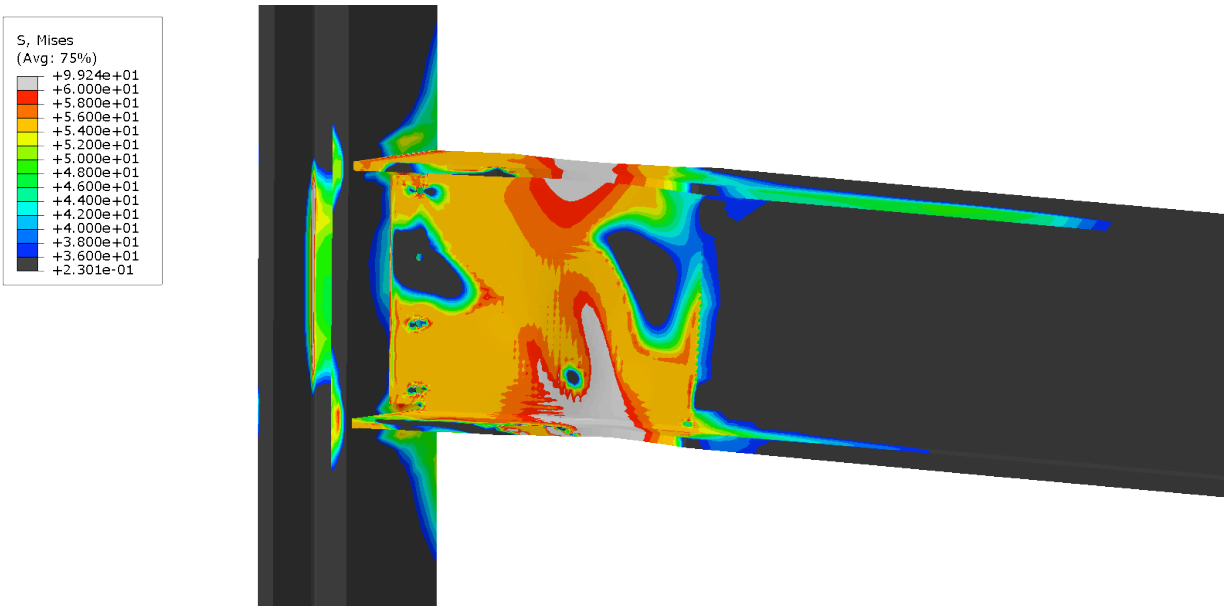


**Figure 6-14: Von Mises stress distribution of the RBS connection with 35 degree skew and radius cut perpendicular to the beam section**

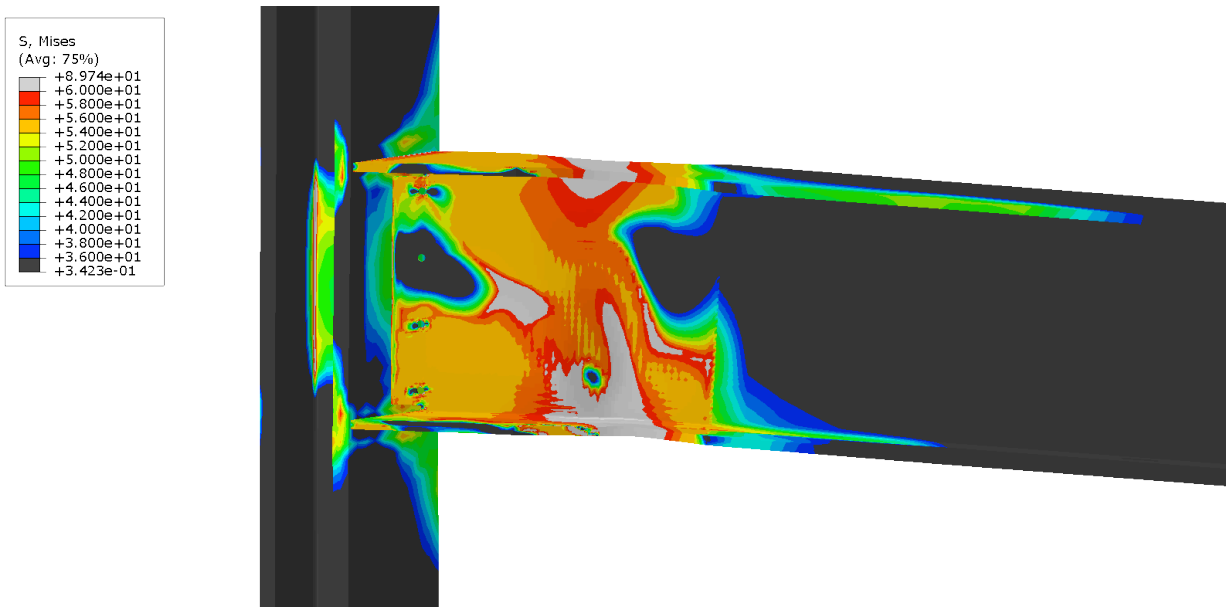


**Figure 6-15: Von Mises stress distribution of the RBS connection with 40 degree skew and radius cut perpendicular to the beam section**

The first indication of non-linearity from the moment vs. rotation relationship occurs at a moment of 32125 k-in. The stress values associated with that moment force were recorded and plotted with respect to the skewed angle in Figure 6-16. The stress concentration between the left, middle, and right of the radius cut region remains unchanged for skew angles up to 20 degrees. For skew angles exceeding 20 degrees, the stress concentration on the left side of the radius cut region progressively decreases. The stress distribution in the middle and right side remain unchanged.

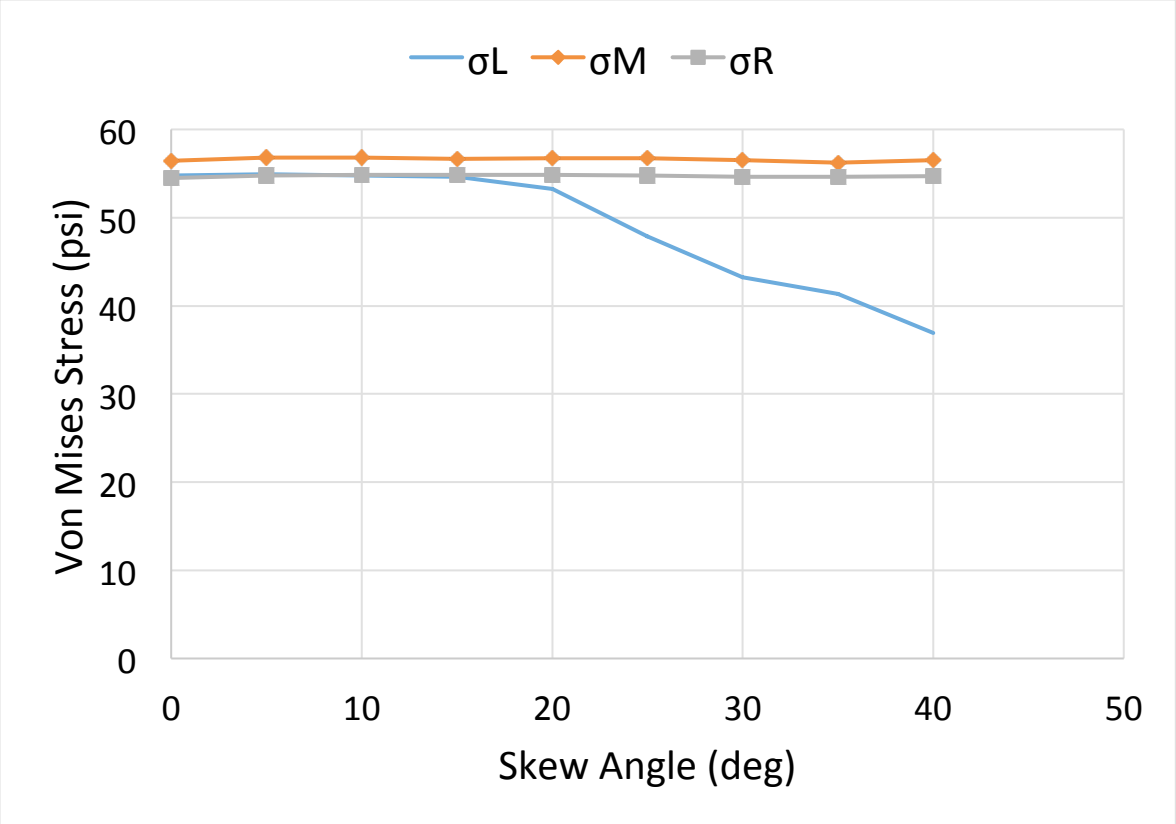


**Figure 6-16: Von Mises stress values within the RBS with radius cut perpendicular to the beam flange for skewed configurations at first yield.**

At 50% of the yield moment as calculated by dividing the moment force associated with the first indication of non-linearity by 2, the stress values were recorded corresponding to a moment of 14295 k-in. The stress values were plotted with respect to the skewed angle in Figure 6-17. The stress concentration in the left of the radius cut region decreases for each increase in skew angle. The stress concentration in the middle of the radius cut essentially remains unchanged as the skew angle increases. The stress concentration in the right side of the radius increases for each increase in skew angle.

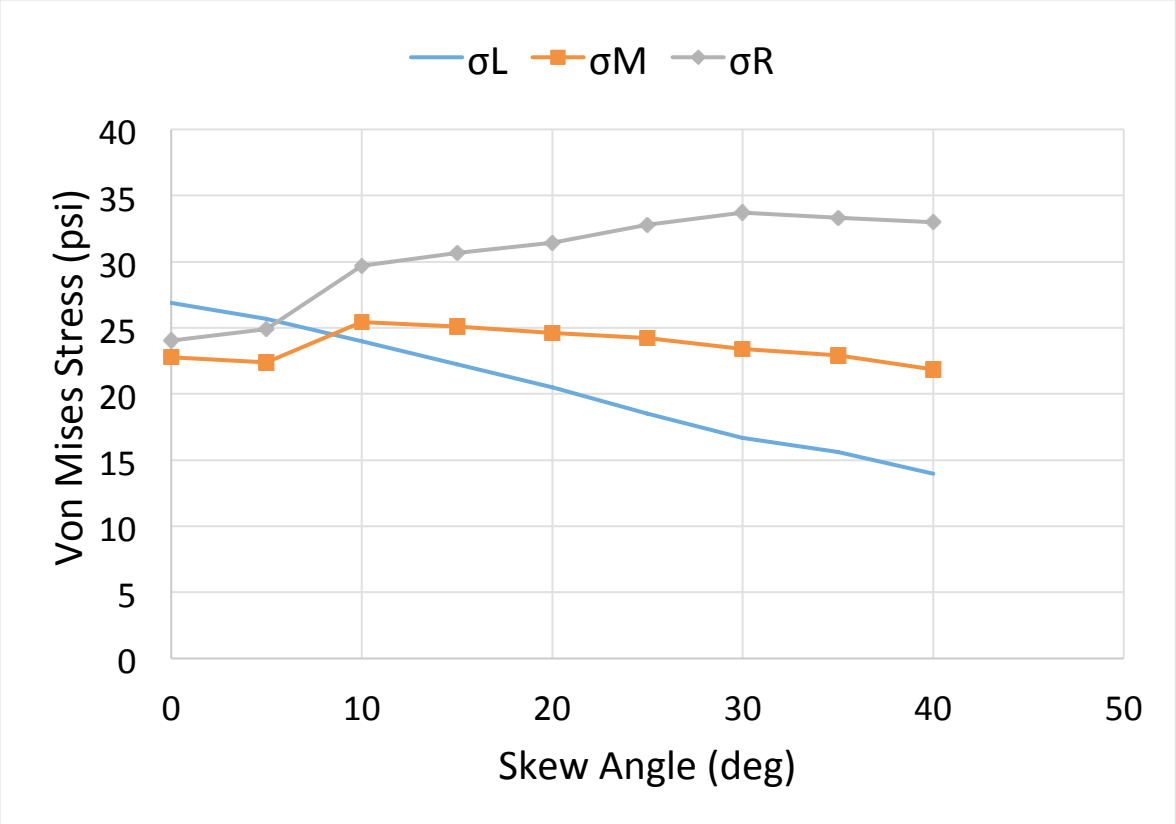


**Figure 6-17: Von Mises stress values within the RBS with radius cut perpendicular to the beam flange for skewed configurations at 50% yield.**

For skewed configurations with RBS radius cut perpendicular to the beam, the strain demands are concentrated within the radius cut region as shown in Figures 6-18 through 6-25. For skew angles exceeding 25 degrees, localized strain demands occur in the beam flanges near the acute angle of the connection as indicated in Figure 6-22. For a 25 degree skew configuration, the strain demand in the flanges near the connection is on the order of 8% of the maximum observed strain. The strain demand near the connection increases for each increasing skew

angle. Furthermore, the 40 degree skew configuration showed approximately 24% of the maximum observed plastic strain.

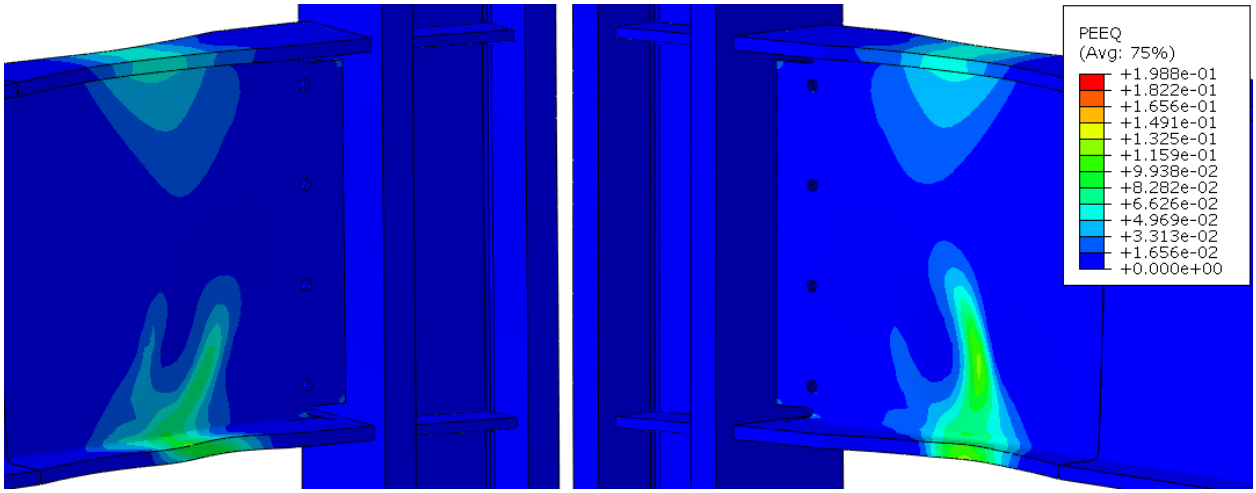


**Figure 6-18: PEEQ of the RBS connection with 5 degree skew and radius cut perpendicular to the beam section**

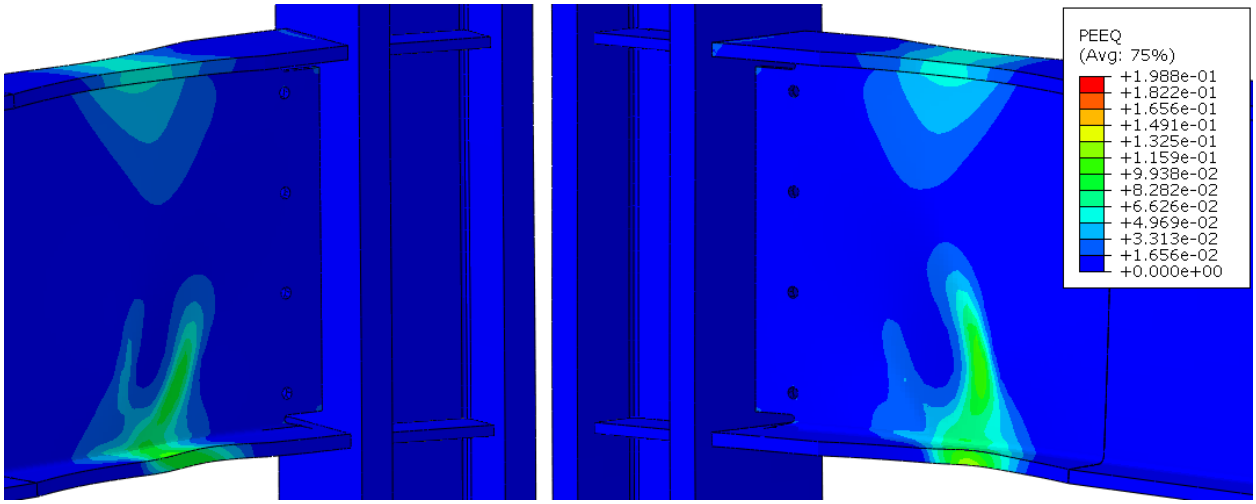


**Figure 6-19: PEEQ of the RBS connection with 10 degree skew and radius cut perpendicular to the beam section**

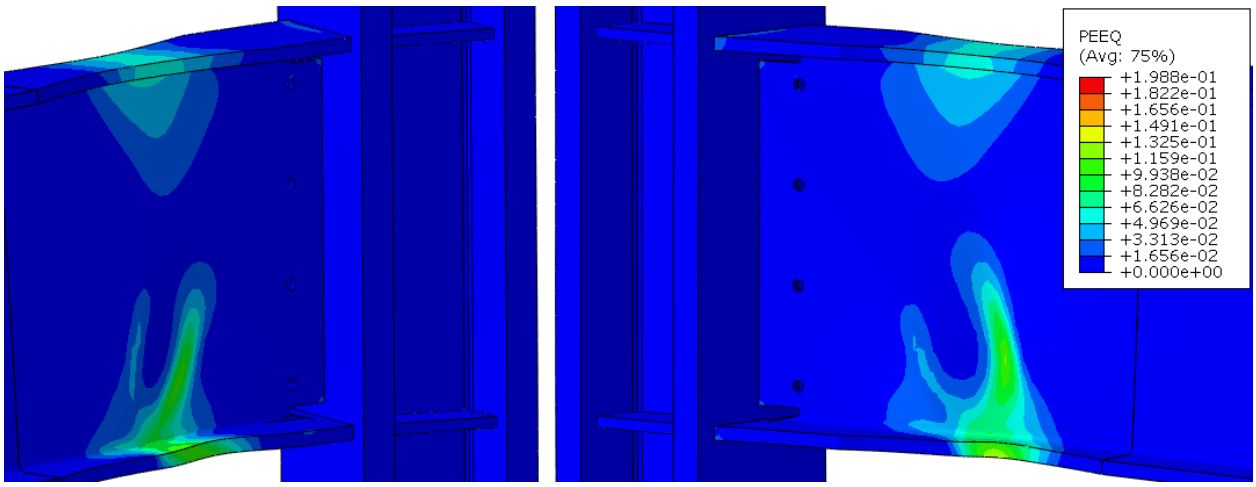


**Figure 6-20: PEEQ of the RBS connection with 15 degree skew and radius cut perpendicular to the beam section**

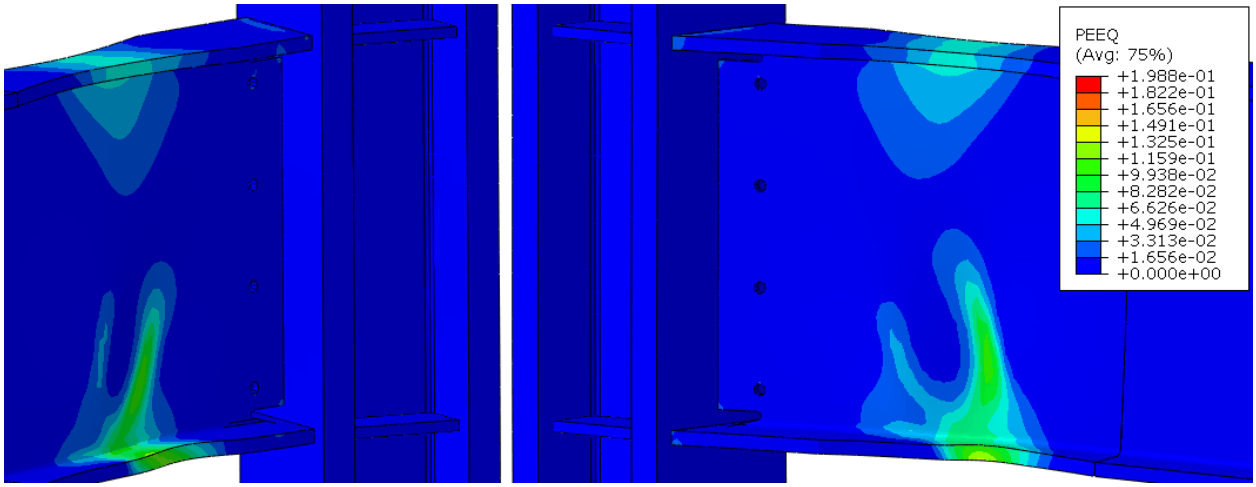


**Figure 6-21: PEEQ of the RBS connection with 20 degree skew and radius cut perpendicular to the beam section**

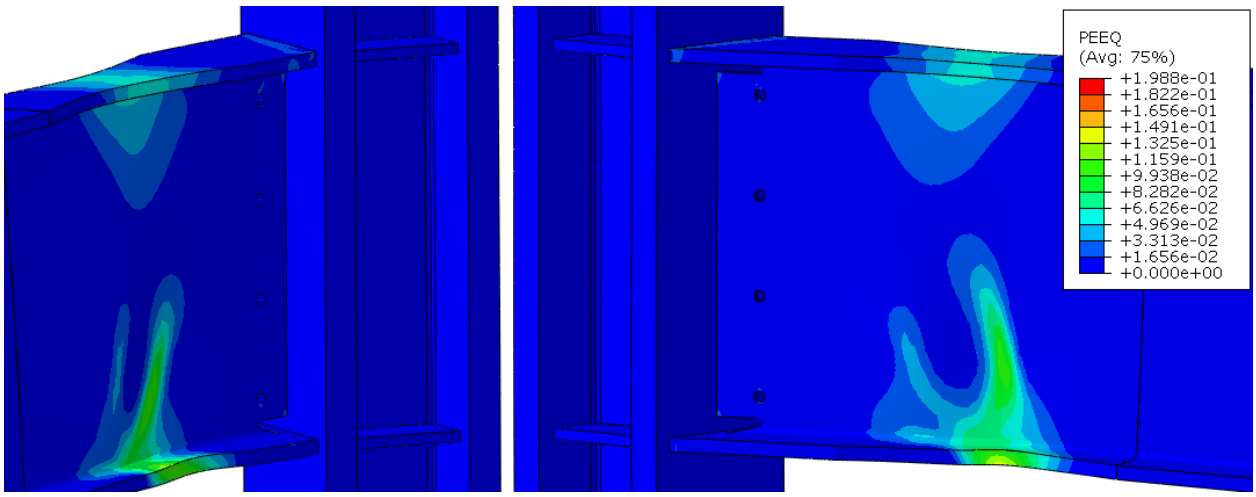


**Figure 6-22: PEEQ of the RBS connection with 25 degree skew and radius cut perpendicular to the beam section**

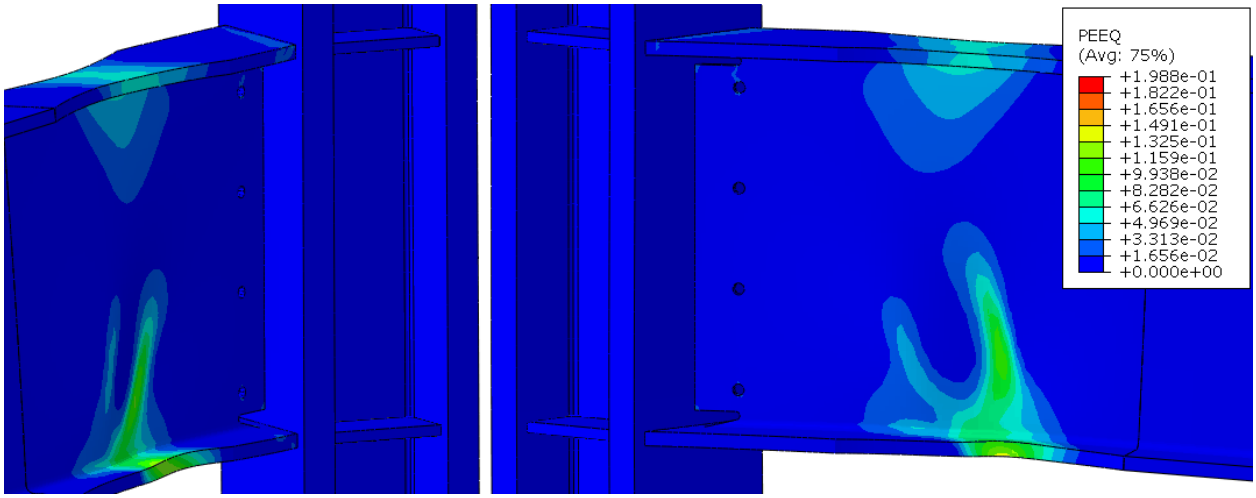


**Figure 6-23: PEEQ of the RBS connection with 30 degree skew and radius cut perpendicular to the beam section**

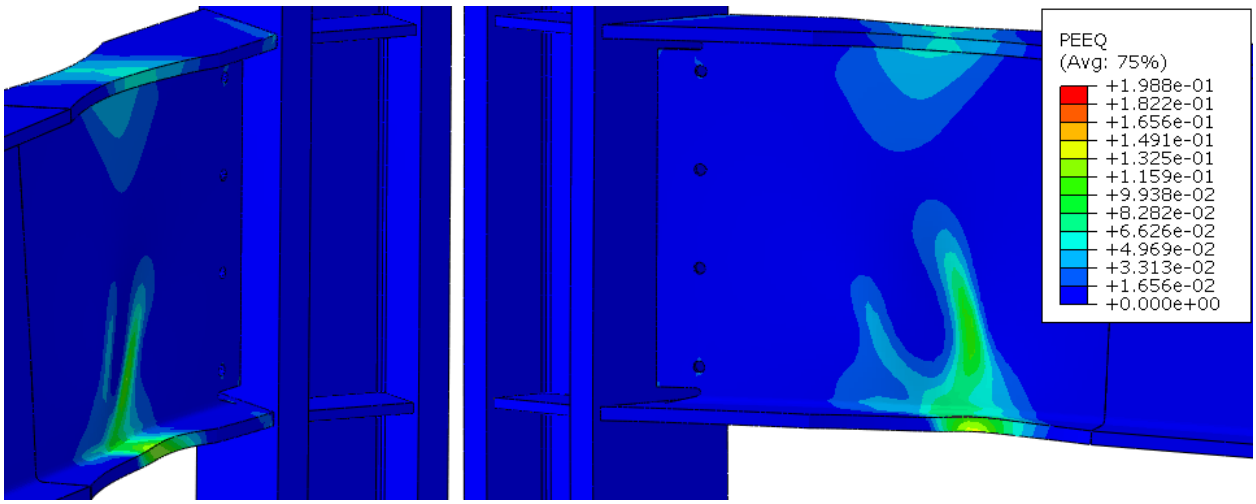


**Figure 6-24: PEEQ of the RBS connection with 35 degree skew and radius cut perpendicular to the beam section**

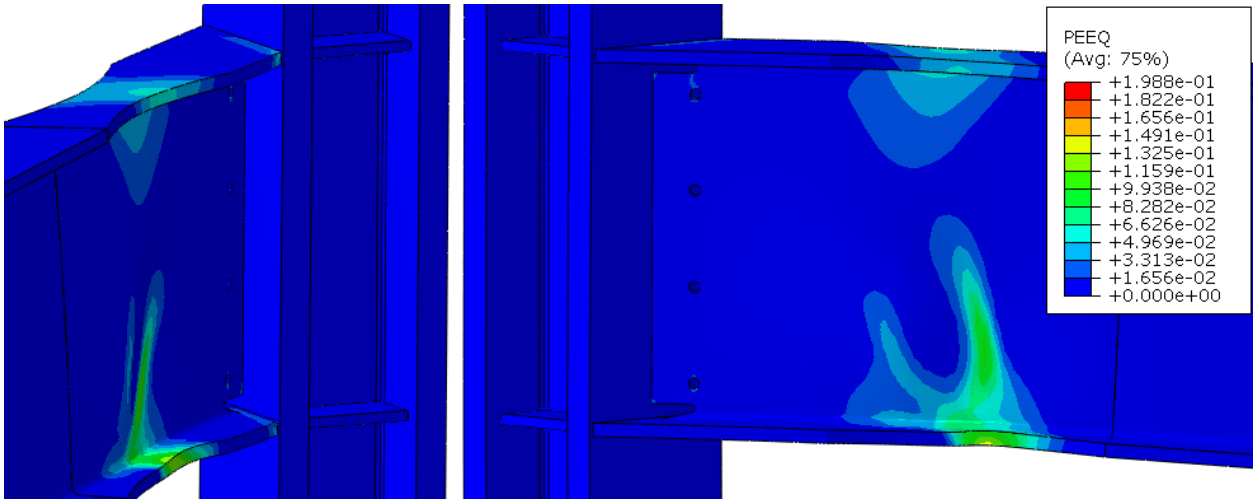


**Figure 6-25: PEEQ of the RBS connection with 40 degree skew and radius cut perpendicular to the beam section**

### 6.1.2 RBS with Radius Cut Parallel to the Column Section

The effects on plastic moment capacity for skewed configurations with RBS radius cut parallel to the column section were minimal as shown in Figure 6-26. The yielding point was largely unaffected by the skew angle as evident from the transition from elastic to plastic stiffness. The plastic moment capacity increased approximately 3% for each 5-degree increase of the skew angle.

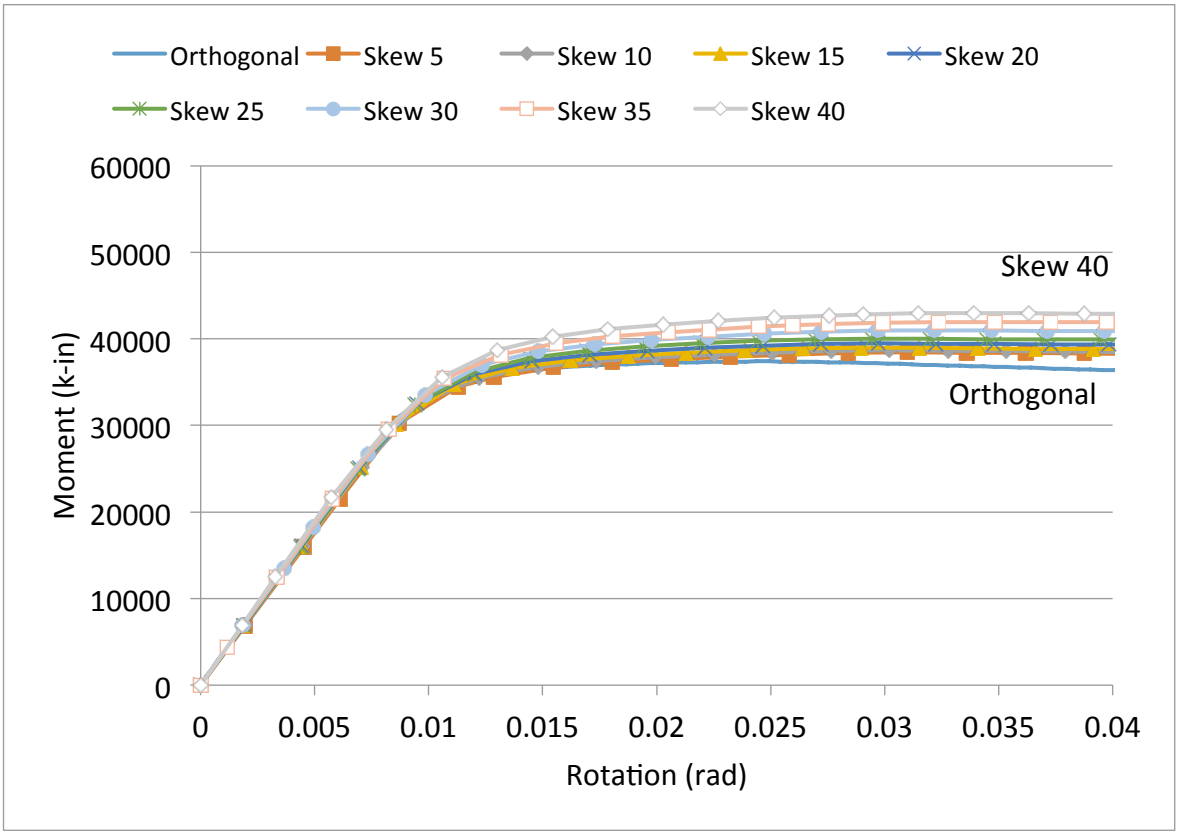


**Figure 6-26: Moment versus rotation of the RBS connection with skewed configurations and radius cut parallel to the column section**

The effects of skew on the RBS connection detail with radius cut parallel to the column section largely impact the stress distribution as shown in Figures 6-27

through 6-34. For skew angles between 5 and 40 degrees, the radius cut region is successful at concentrating most of the stress distribution within the beam. For skew angles between 0 and 30 degrees, the stress concentration within the beam flanges at the acute angle formed between the beam and column minimally increases. For skew angle exceeding 30 degrees, the stress concentration is increased at the acute angle. However, the stress concentration increases in the column flange at the acute angle formed between the beam and column. Additionally, as the skew angle exceeds 20 degrees, the stress distribution in the column flange begins to concentrate at the obtuse angle formed between the beam and column. This effect progressively increases as the skew angle increases past 20 degrees. Finally, once the skew angle reaches or exceeds 35 degrees, the stress distribution in the column flange progressively concentrates between the beam flanges along the beam web.

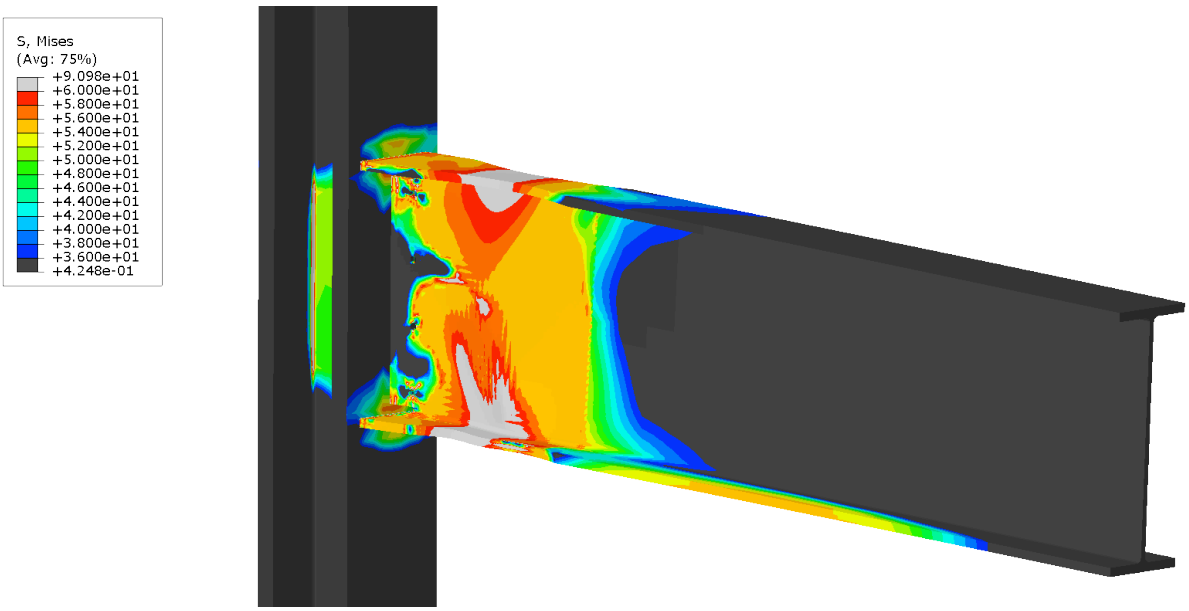


**Figure 6-27: Von Mises stress distribution of the RBS connection with 5 degree skew and radius cut parallel to the column section**

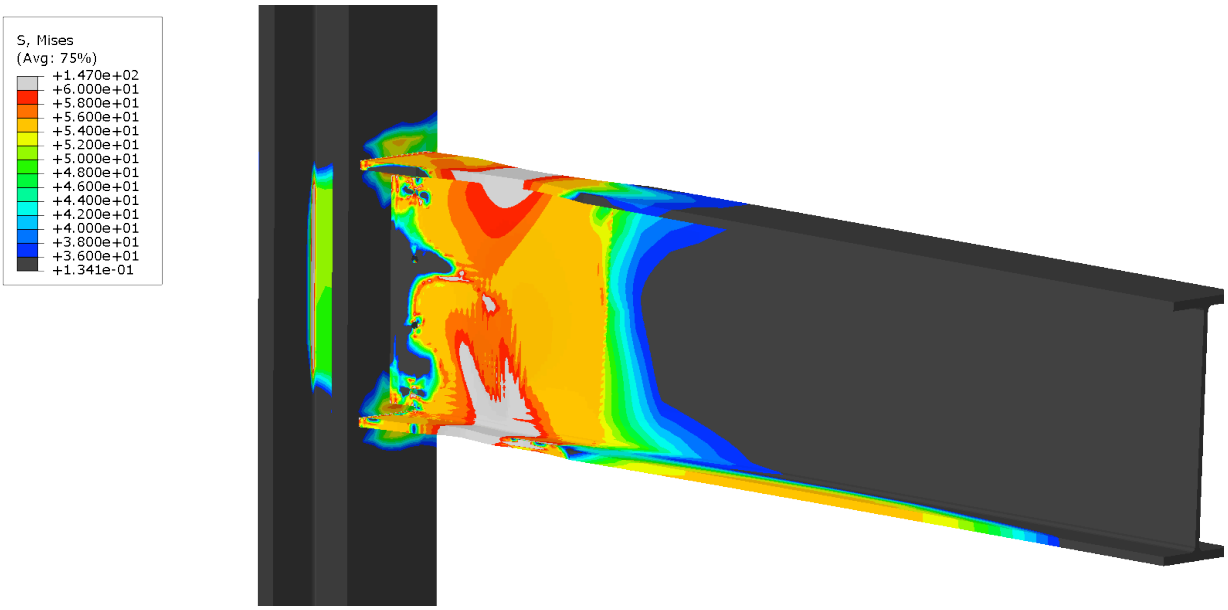


**Figure 6-28: Von Mises stress distribution of the RBS connection with 10 degree skew and radius cut parallel to the column section**

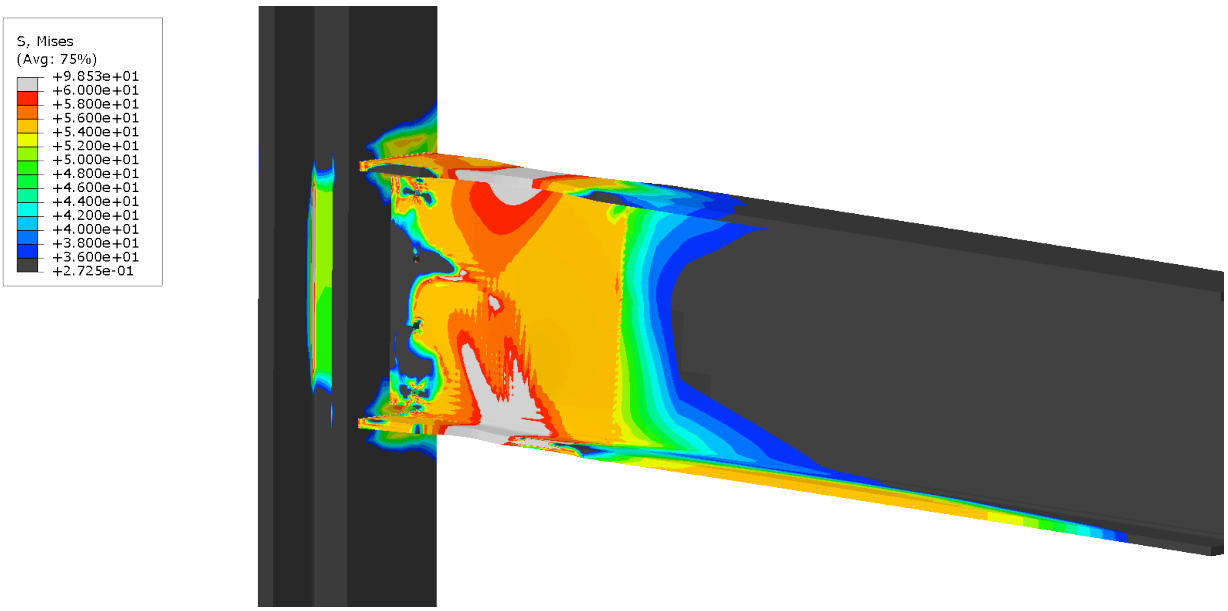


**Figure 6-29: Von Mises stress distribution of the RBS connection with 15 degree skew and radius cut parallel to the column section**

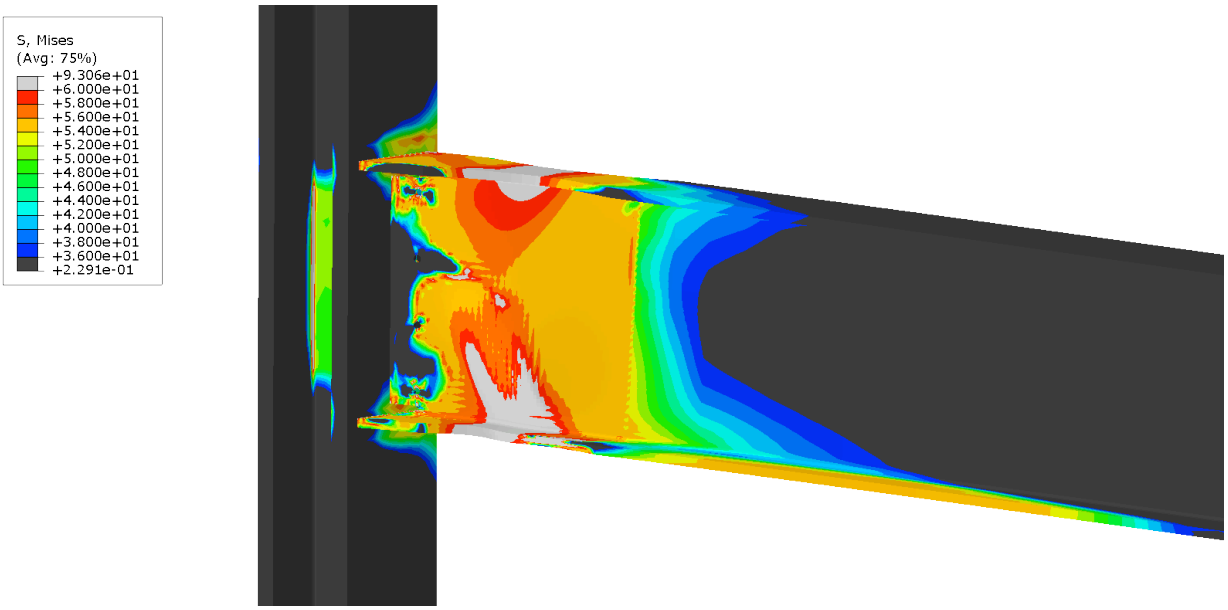


**Figure 6-30: Von Mises stress distribution of the RBS connection with 20 degree skew and radius cut parallel to the column section**

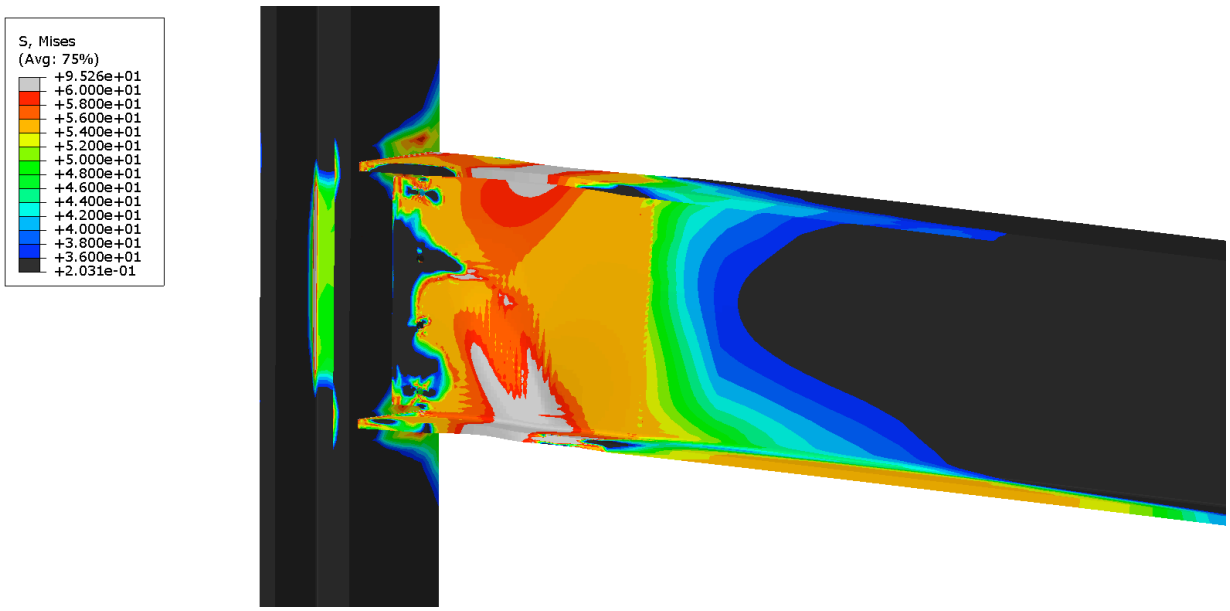


**Figure 6-31: Von Mises stress distribution of the RBS connection with 25 degree skew and radius cut parallel to the column section**

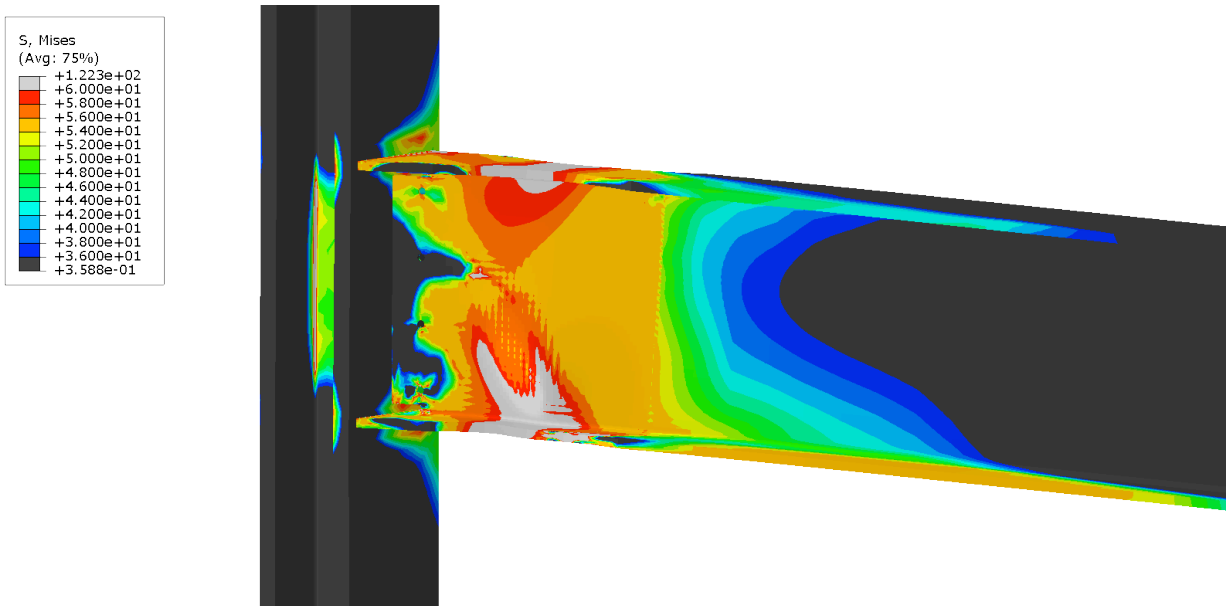


**Figure 6-32: Von Mises stress distribution of the RBS connection with 30 degree skew and radius cut parallel to the column section**

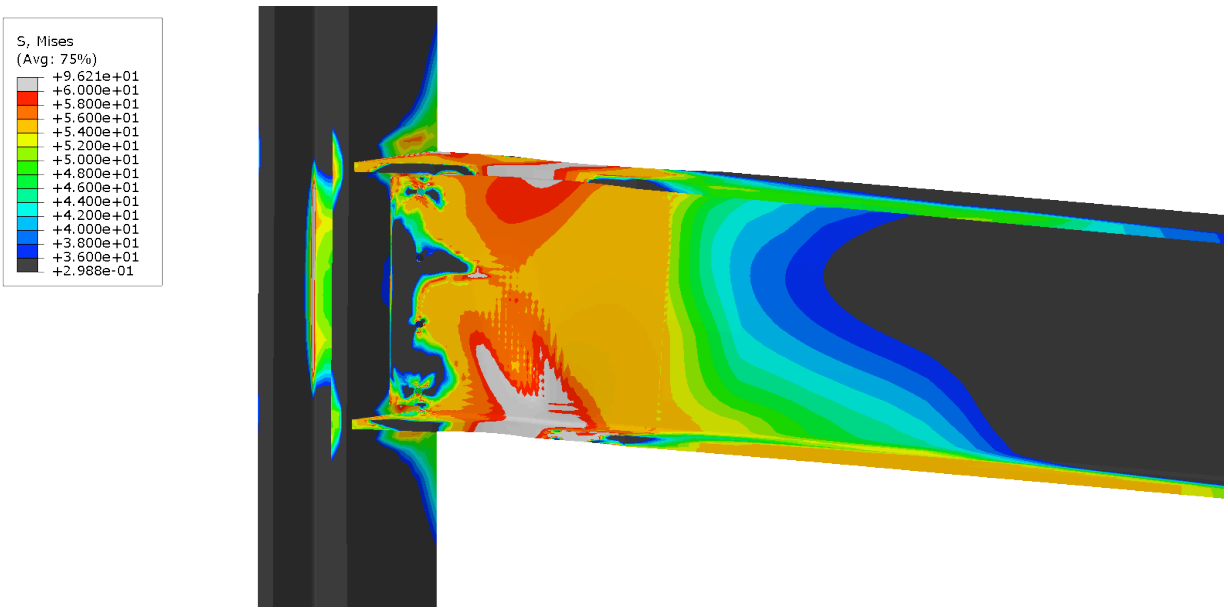


**Figure 6-33: Von Mises stress distribution of the RBS connection with 35 degree skew and radius cut parallel to the column section**

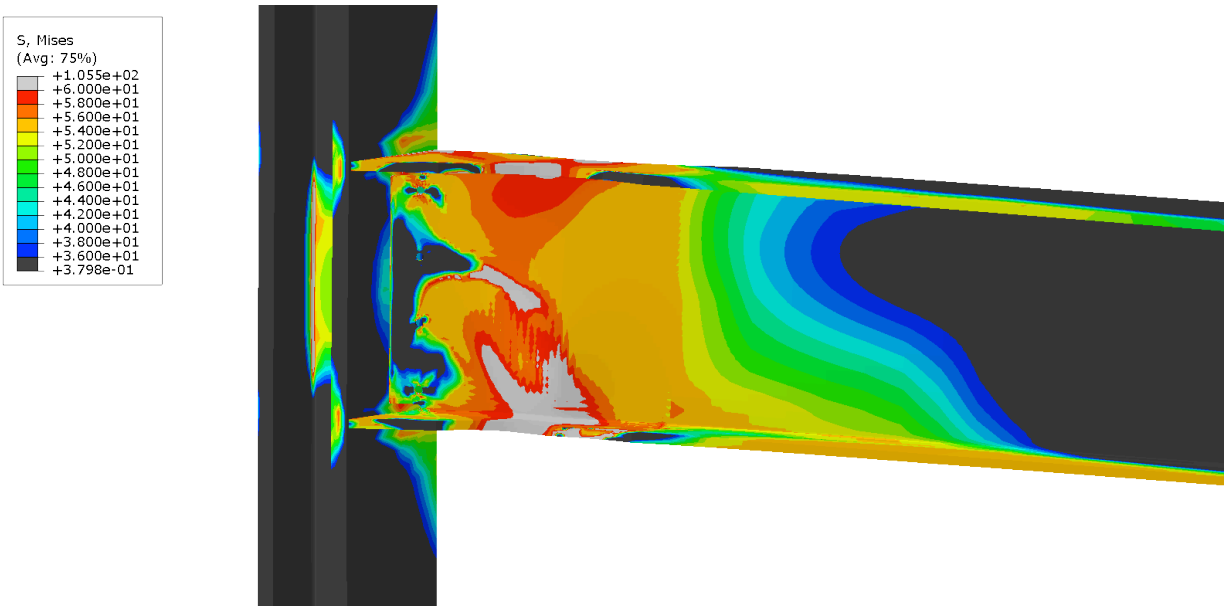


**Figure 6-34: Von Mises stress distribution of the RBS connection with 40 degree skew and radius cut parallel to the column section**

The first indication of non-linearity from the moment vs. rotation relationship occurs at a moment of 32125 k-in. The stress values associated with that moment force were recorded and plotted with respect to the skewed angle in Figure 6-35. The stress distribution between the left, middle, and right of the radius cut region remains unchanged for skew angles up to 15 degrees. For skew angles exceeding 15 degrees, the stress concentration on the left side of the radius cut region progressively decreases. The stress distribution in the middle and right side remain unchanged.

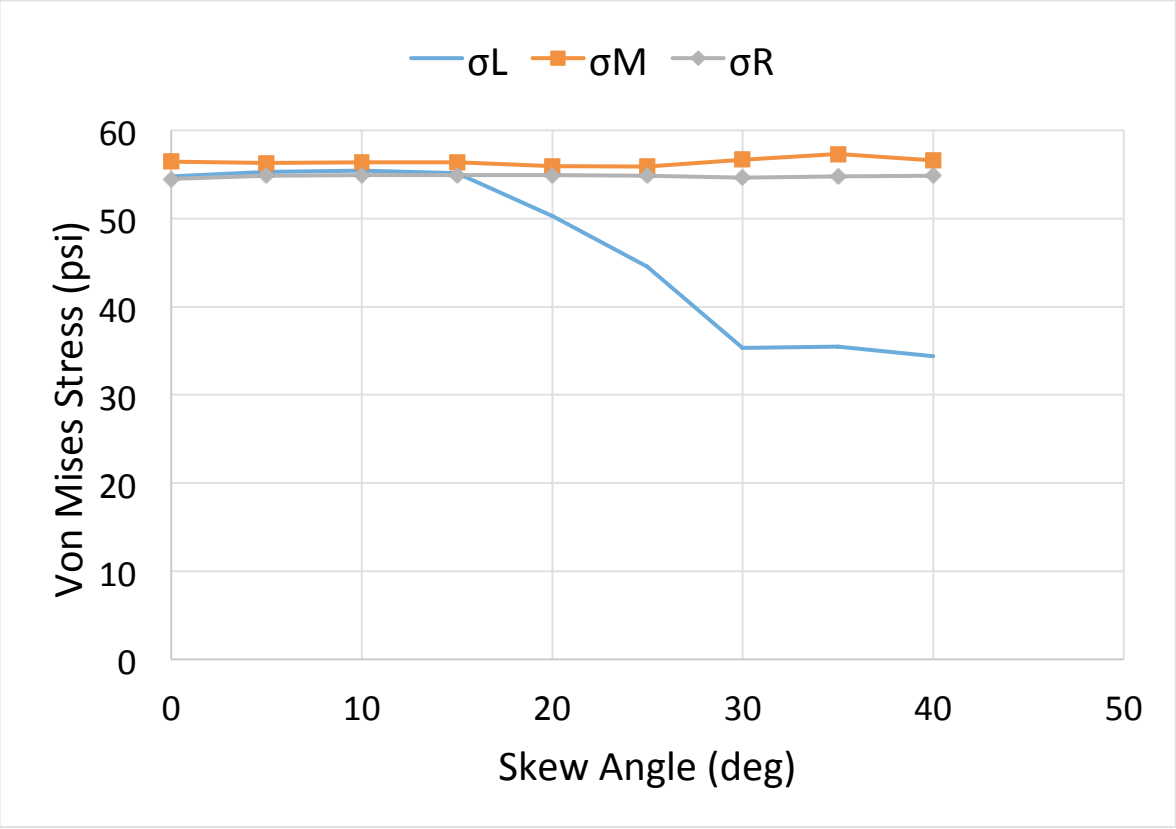


**Figure 6-35: Von Mises stress values within the RBS with radius cut parallel to the column flange for skewed configurations at first yield.**

At 50% of the yield moment as calculated by dividing the moment associated with the first indication of non-linearity by 2, the stress values were recorded corresponding to a moment of 14295 k-in. The stress values were plotted with respect to the skewed angle in Figure 6-36. The stress concentration in the left of the radius cut region decreases for each increase in skew angle. The stress concentration in the middle of the radius cut essentially remains unchanged as the skew angle increases. The stress concentration in the right side of the radius increases for each increase in skew angle.

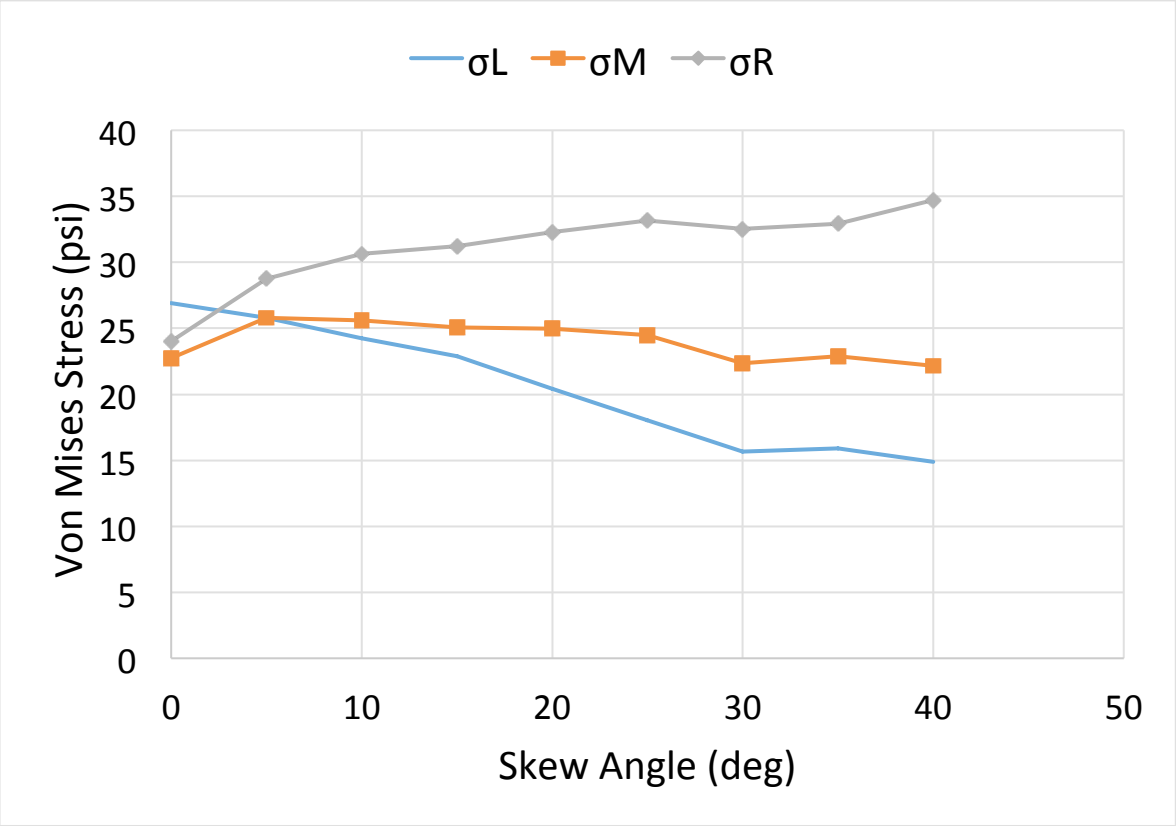


**Figure 6-36: Von Mises stress values within the RBS with radius cut parallel to the column flange for skewed configurations at 50% yield.**

For skewed configurations with RBS radius cut perpendicular to the beam, the strain demands are concentrated within the radius cut region as shown in Figures 6-37 through 6-44. However, localized strain demands occur in the flanges at the acute angle formed between the beam and column at skew angles exceeding 10 degrees, as shown in Figure 6-34. For a 10-degree skew configuration, the strain demand in the flanges near the connection reaches approximately 17% of the maximum observed strain. The effect increases for each increasing skew angle. For the extreme case of a 40 degree skew configuration, this strain demand at the face of the column reaches approximately 67% of the maximum observed plastic strain.

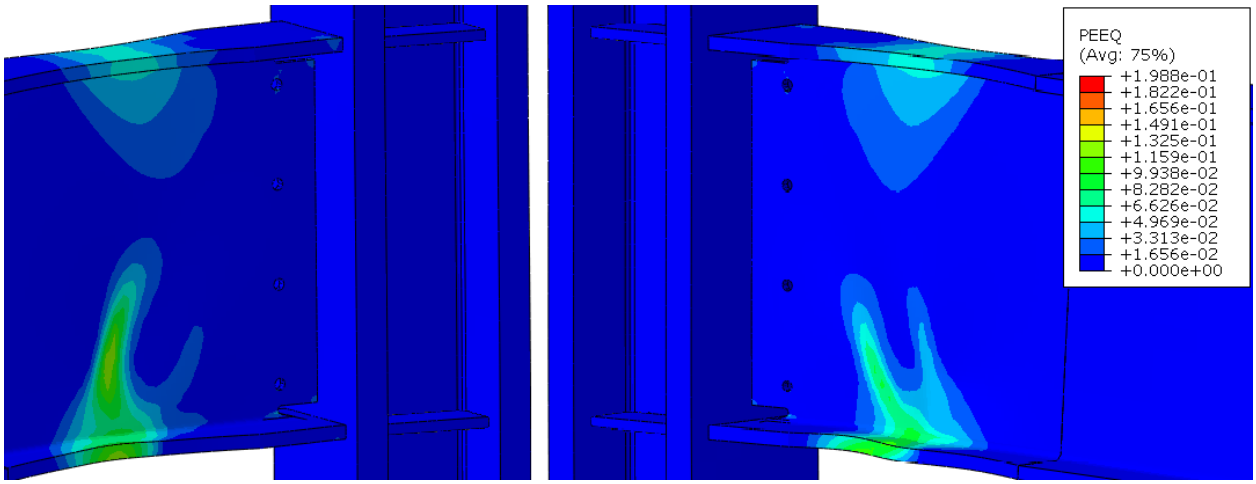


**Figure 6-37: PEEQ of the RBS connection with 5 degree skew and radius cut parallel to the column section**

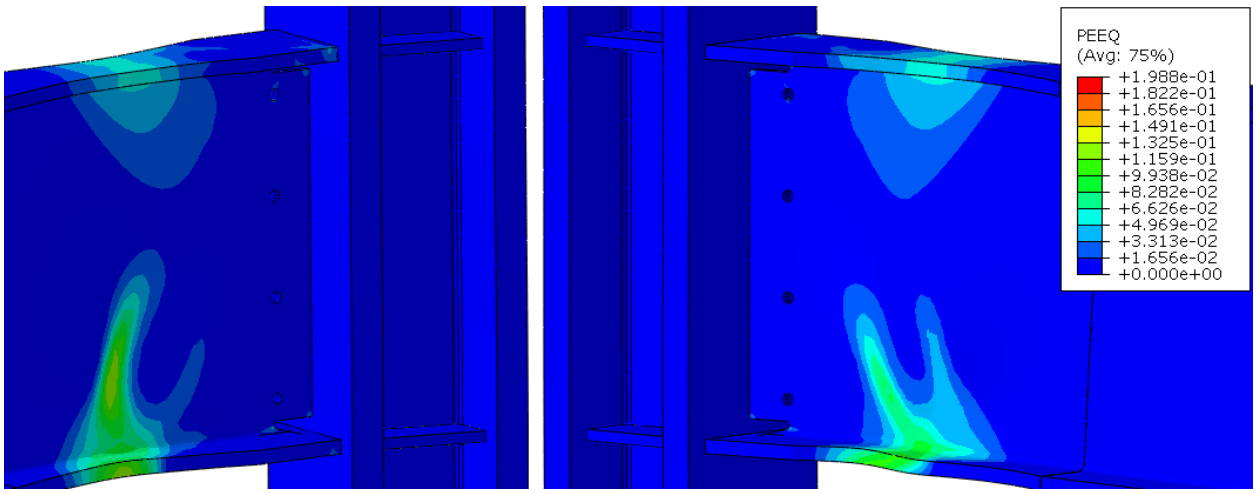


**Figure 6-38: PEEQ of the RBS connection with 10 degree skew and radius cut parallel to the column section**

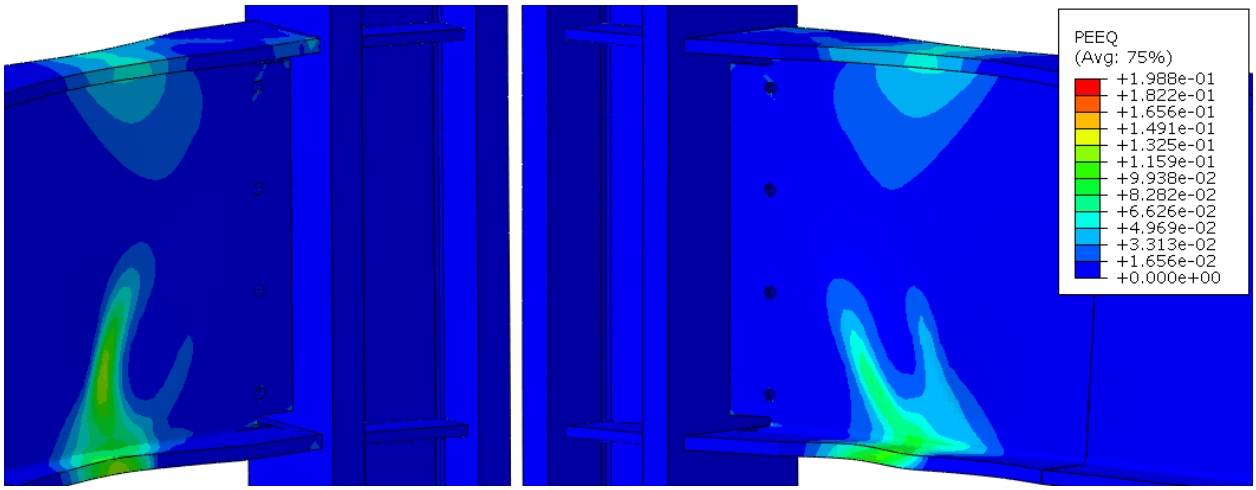


**Figure 6-39: PEEQ of the RBS connection with 15 degree skew and radius cut parallel to the column section**

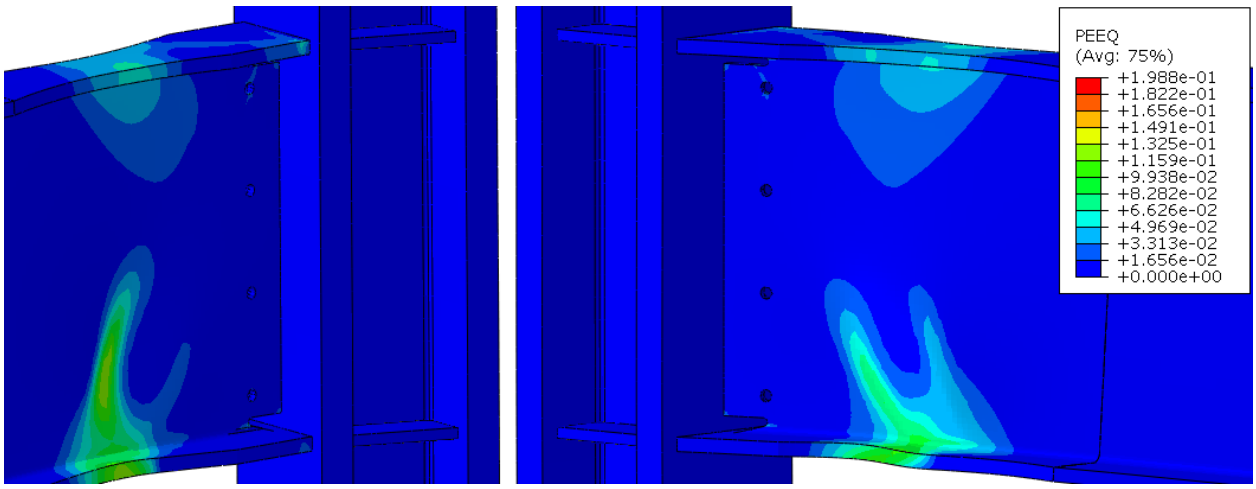


**Figure 6-40: PEEQ of the RBS connection with 20 degree skew and radius cut parallel to the column section**

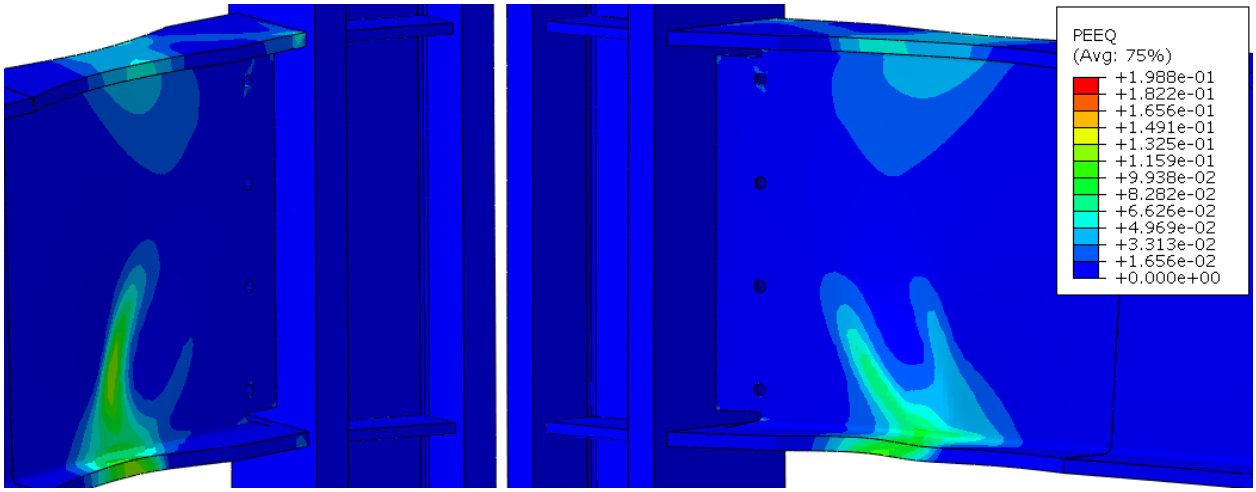


**Figure 6-41: PEEQ of the RBS connection with 25 degree skew and radius cut parallel to the column section**

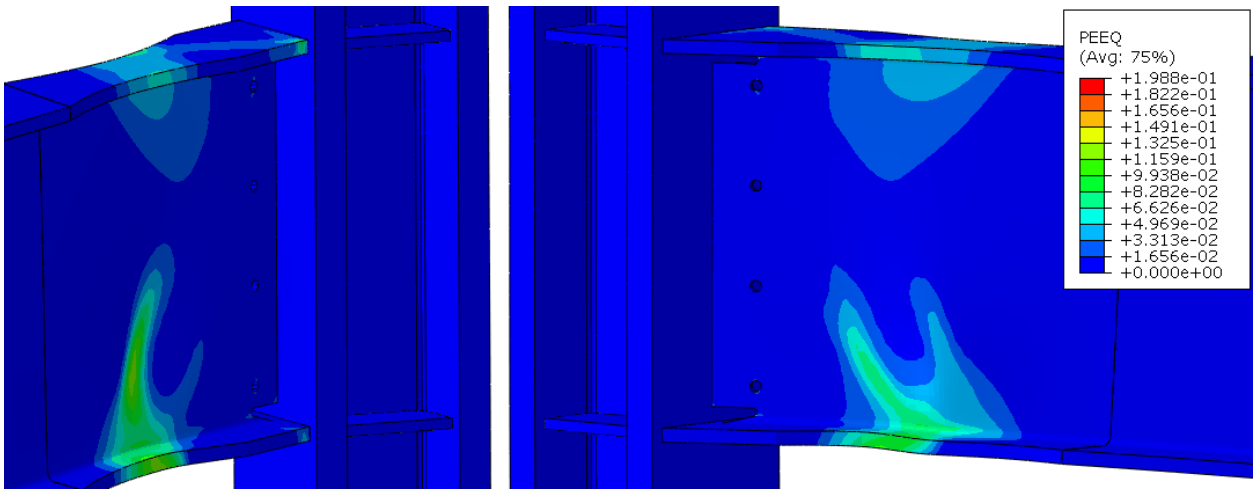


**Figure 6-42: PEEQ of the RBS connection with 30 degree skew and radius cut parallel to the column section**

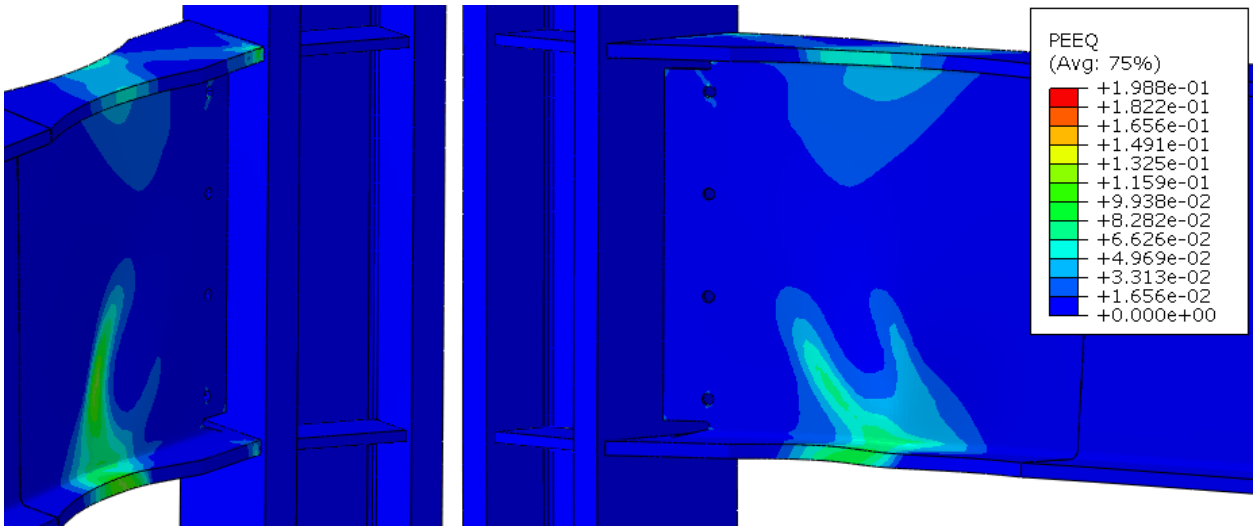


**Figure 6-43: PEEQ of the RBS connection with 35 degree skew and radius cut parallel to the column section**

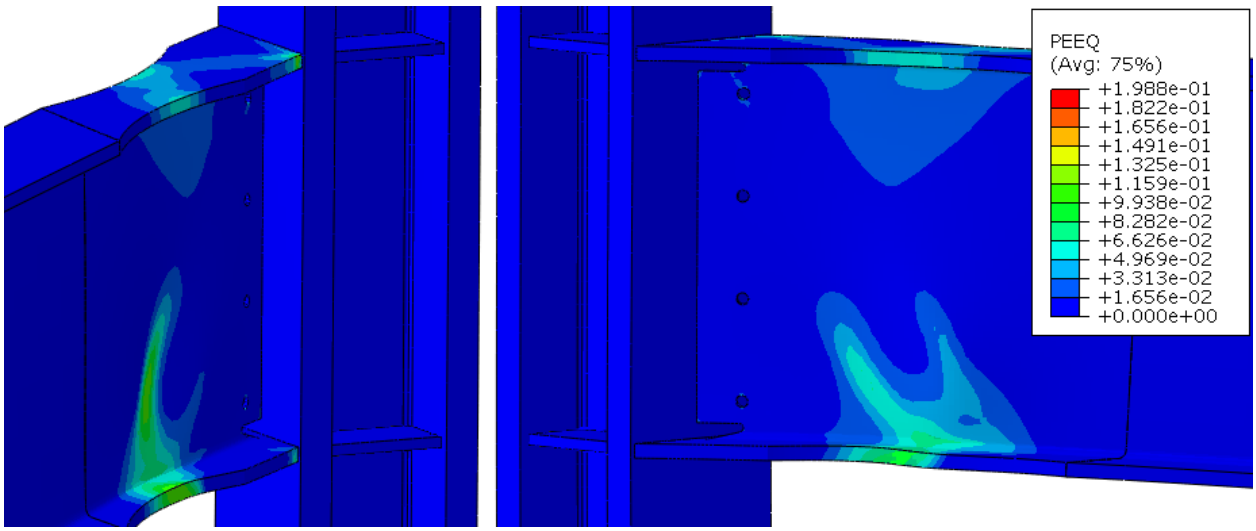


**Figure 6-44: PEEQ of the RBS connection with 40 degree skew and radius cut parallel to the column section**

## 6.2 RBS with Sloped Configurations

The RBS connection models with sloped configurations were subject to a negative moment as well as a positive moment to observe the effects on the connection in a manner similar to the WUF-W connection. A negative moment was applied by inducing a downwards vertical beam tip displacement while a positive moment was applied by inducing an upward vertical beam tip displacement. Both of the previously discussed radius cut arrangements were investigated for the sloped configurations.

### 6.2.1 RBS with Radius Cut Perpendicular to the Beam Section and Subject to a Negative Moment

An increase in slope angle increases the plastic moment capacity of the RBS connection, as shown in Figure 6-45. For each increasing slope angle, the initial stiffness and plastic moment capacity increase. Similar to the WUF-W connection details with slope configurations, the increase in capacity is most likely attributed to an increase in effective depth of the beam cross-section.

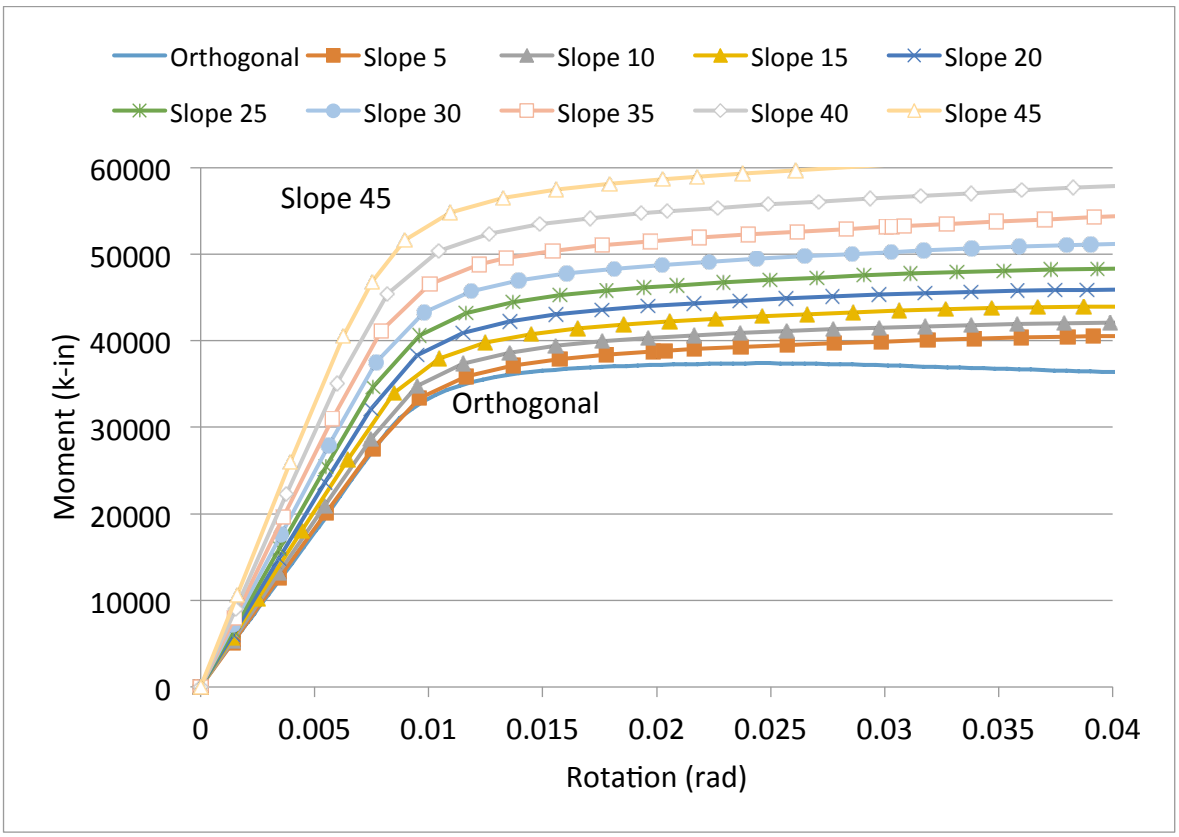


**Figure 6-45: Moment versus rotation of the RBS connection with sloped configurations and radius cut perpendicular to the beam section subject to a negative moment**

For the RBS connection detail with sloped configurations subject to a negative moment, the stress distribution remains perpendicular to the beam section as shown in Figures 6-46 through 6-54. This effect does not appear to be impacted by the sloped geometry. The radius cut region is successful at concentrating the stress distribution for slope angles up to 20 degrees. However, there are localized stress concentrations in the beam bottom flange near the beam/column interface in as the stress distribution is perpendicular to the beam section. The radius cut region is less successful at concentrating the stress distribution within the beam for skew

angles exceeding 30 degrees. The stress distribution in the beam bottom flange concentrates at the beam/column interface. For the extreme case of a 45 degree slope, the radius cut is incapable of concentrating the majority of the stress in the beam bottom flange.

The column flange at the beam/column interface experiences greater stress concentrations as the slope angle increases. As the slope angle increases, the stress distribution in the column flange concentrates at the beam top and bottom flanges. The panel zone of the connection is also impacted by the sloped configurations. As the slope angle increases, the stress distribution in the column web concentrates towards the bottom of the panel zone.

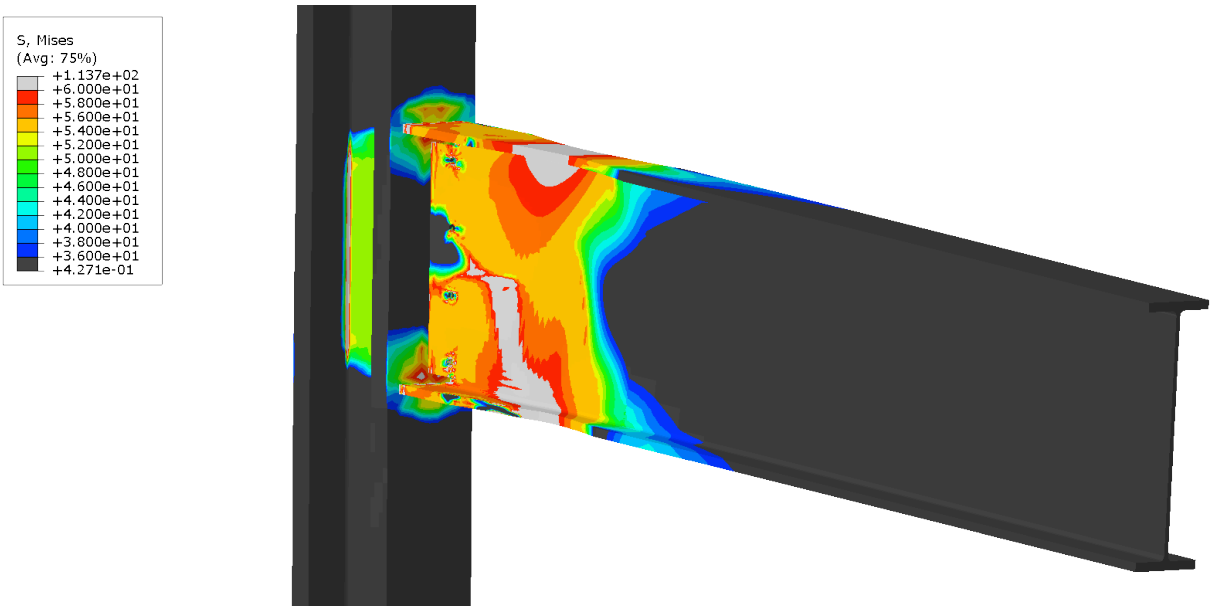


**Figure 6-46: Von Mises stress distribution of the RBS connection with 5 degree slope and radius cut perpendicular to the beam section subject to a negative moment**

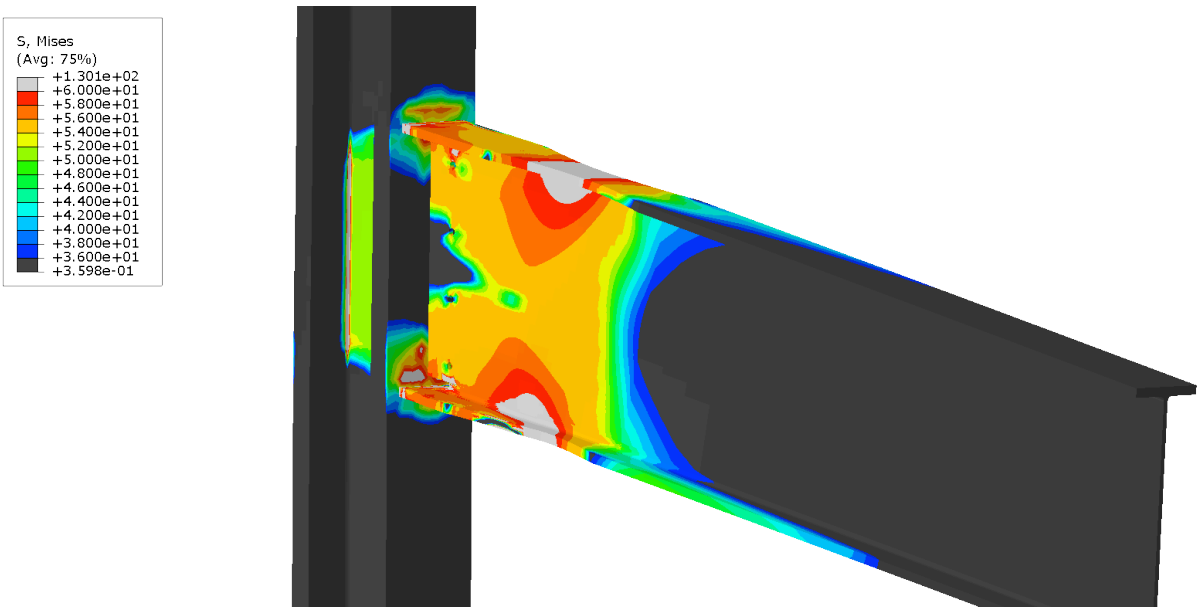


**Figure 6-47: Von Mises stress distribution of the RBS connection with 10 degree slope and radius cut perpendicular to the beam section subject to a negative moment**

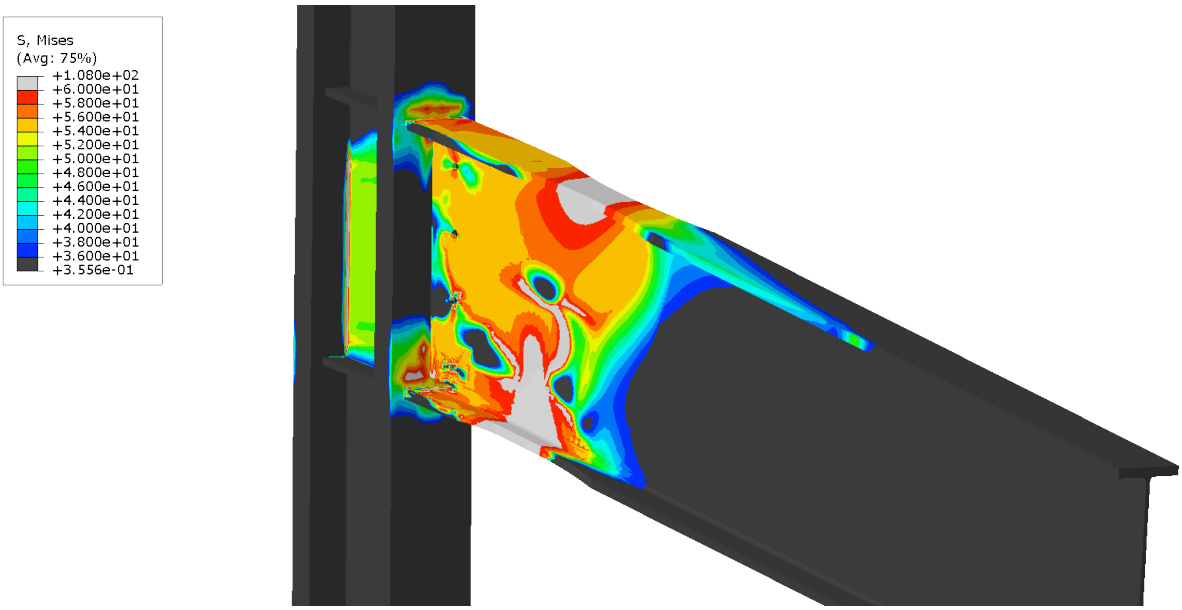


**Figure 6-48: Von Mises stress distribution of the RBS connection with 15 degree slope and radius cut perpendicular to the beam section subject to a negative moment**

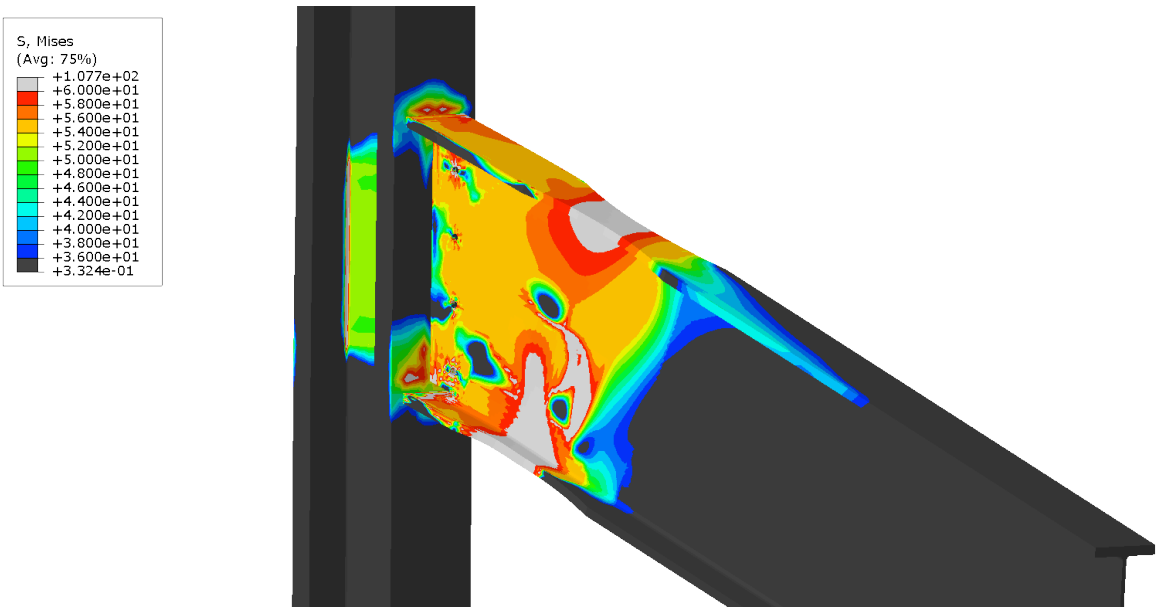


**Figure 6-49: Von Mises stress distribution of the RBS connection with 20 degree slope and radius cut perpendicular to the beam section subject to a negative moment**

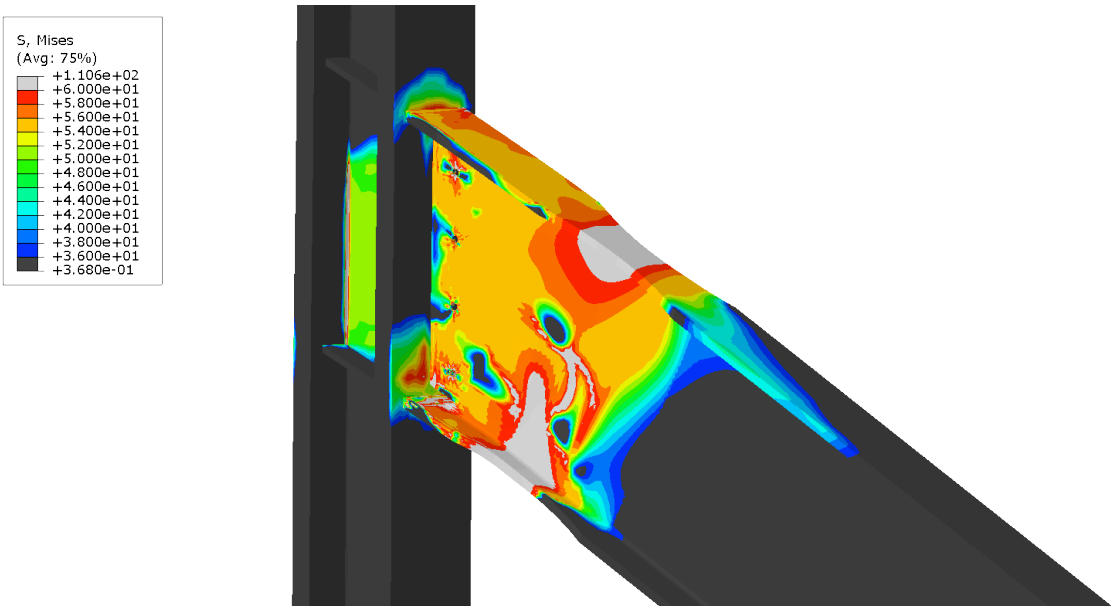


**Figure 6-50: Von Mises stress distribution of the RBS connection with 25 degree slope and radius cut perpendicular to the beam section subject to a negative moment**

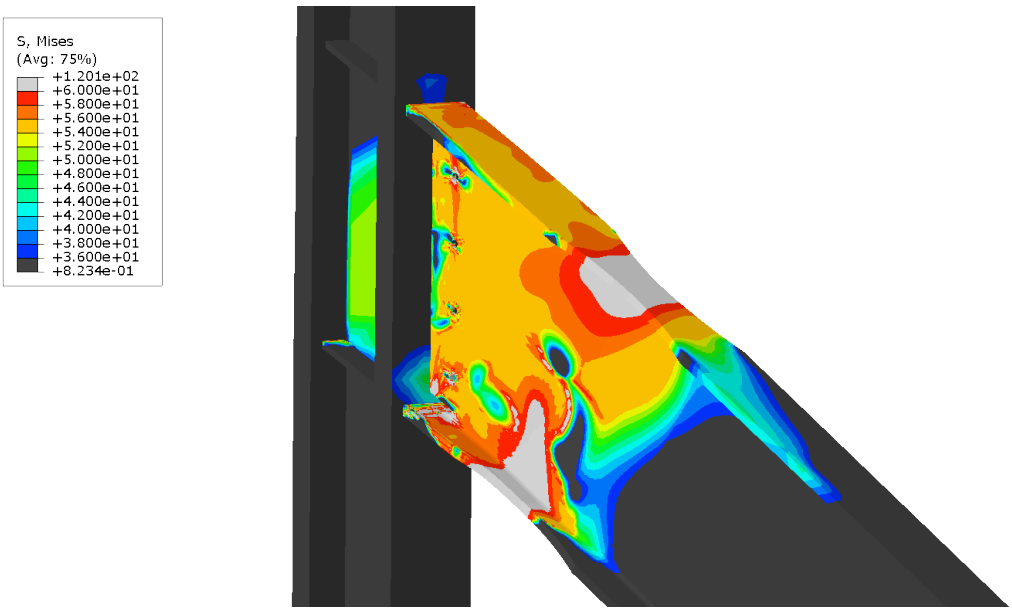


**Figure 6-51: Von Mises stress distribution of the RBS connection with 30 degree slope and radius cut perpendicular to the beam section subject to a negative moment**

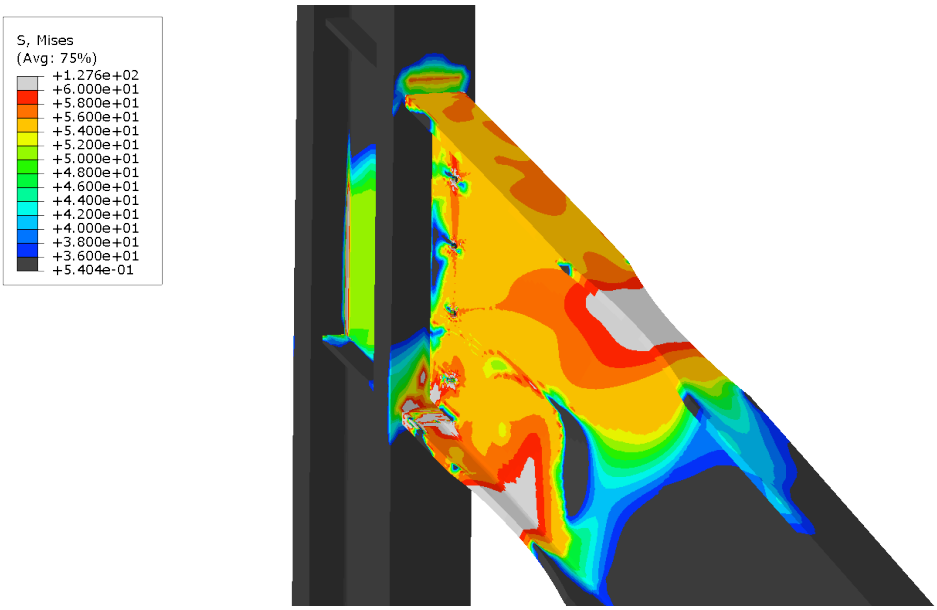


**Figure 6-52: Von Mises stress distribution of the RBS connection with 35 degree slope and radius cut perpendicular to the beam section subject to a negative moment**

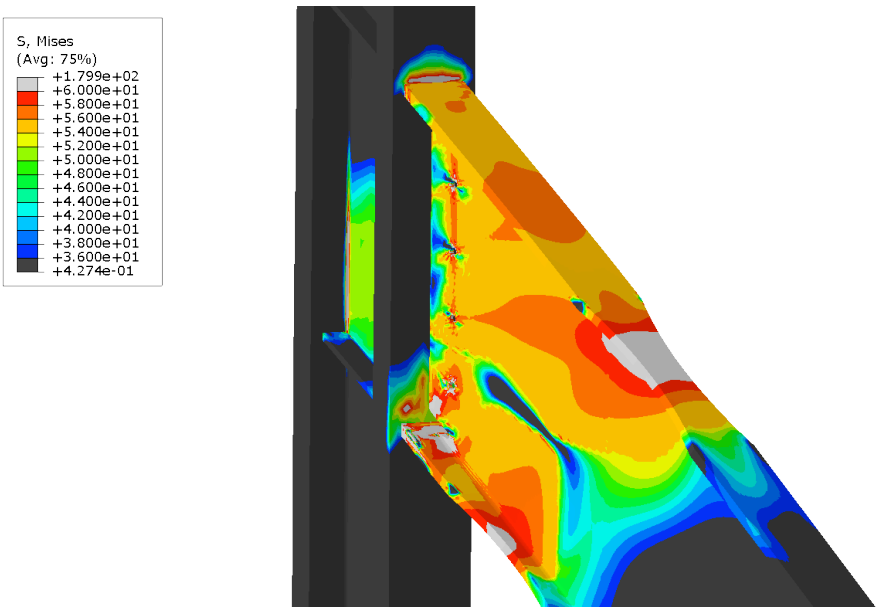


**Figure 6-53: Von Mises stress distribution of the RBS connection with 40 degree slope and radius cut perpendicular to the beam section subject to a negative moment**

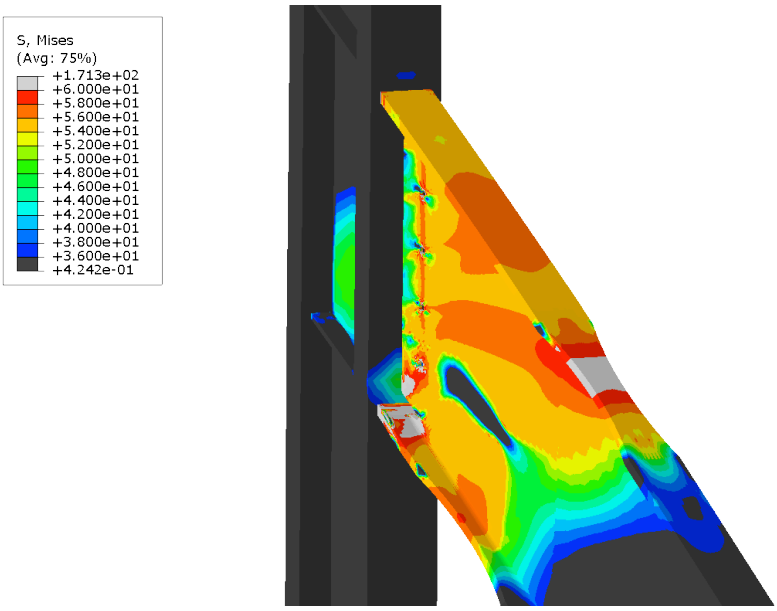


**Figure 6-54: Von Mises stress distribution of the RBS connection with 45 degree slope and radius cut perpendicular to the beam section subject to a negative moment**

The first indication of non-linearity from the moment vs. rotation relationship occurs at a moment of 32125 k-in. The stress values associated with that moment were recorded and plotted with respect to the sloped angle in Figure 6-55. The stress concentration within the beam flange remains essentially unchanged for slope angles up to 20 degrees. For slope angles exceeding 20 degrees, the stress concentration in the beam flange decreases for each increase in slope angle.

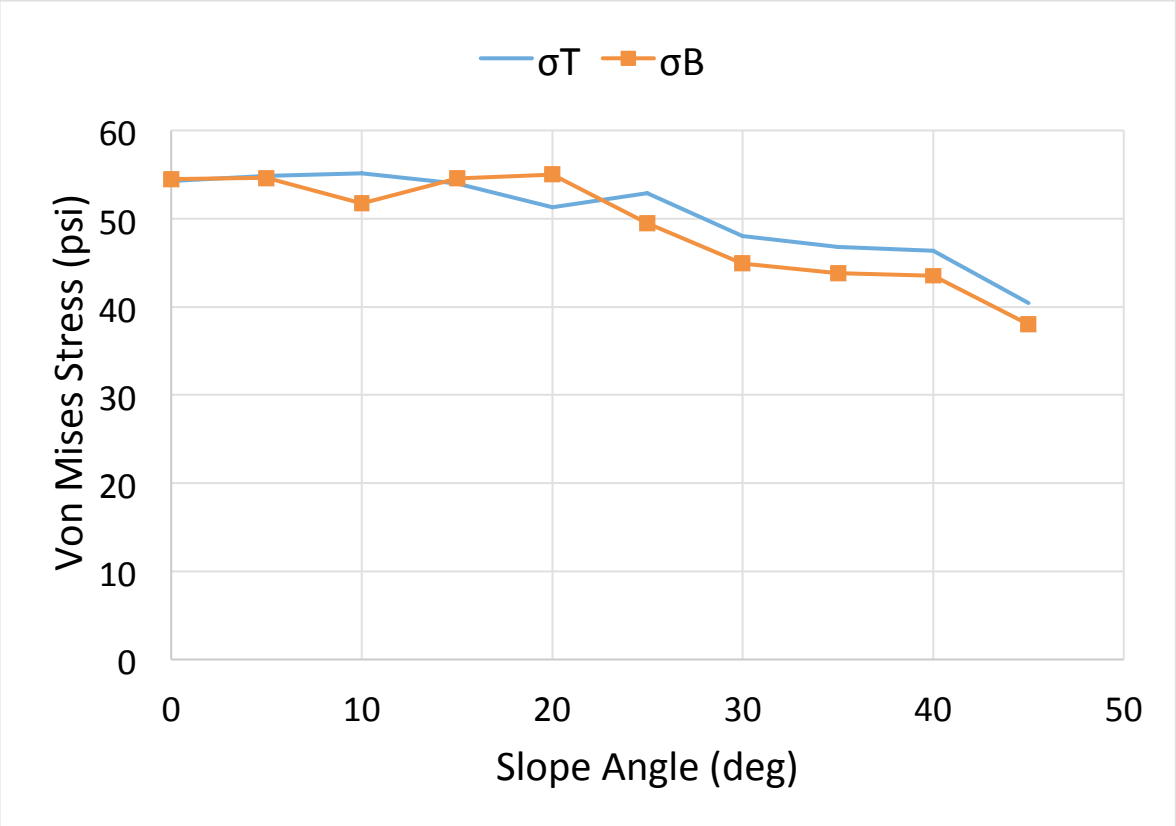


**Figure 6-55: Von Mises stress values within the RBS with radius cut perpendicular to the beam with slope configurations subject to a negative moment at first yield.**

At 50% of the yield moment as calculated by dividing the moment force associated with the first indication of non-linearity by 2, the stress values were recorded corresponding to a moment force of 14295 k-in. The stress values were plotted with respect to the skewed angle in Figure 6-56. The stress concentration within the beam flange remains essentially unchanged for slope angles up to 20 degrees. For slope angles exceeding 20 degrees, the stress concentration in the beam flange decreases for each increase in slope angle.

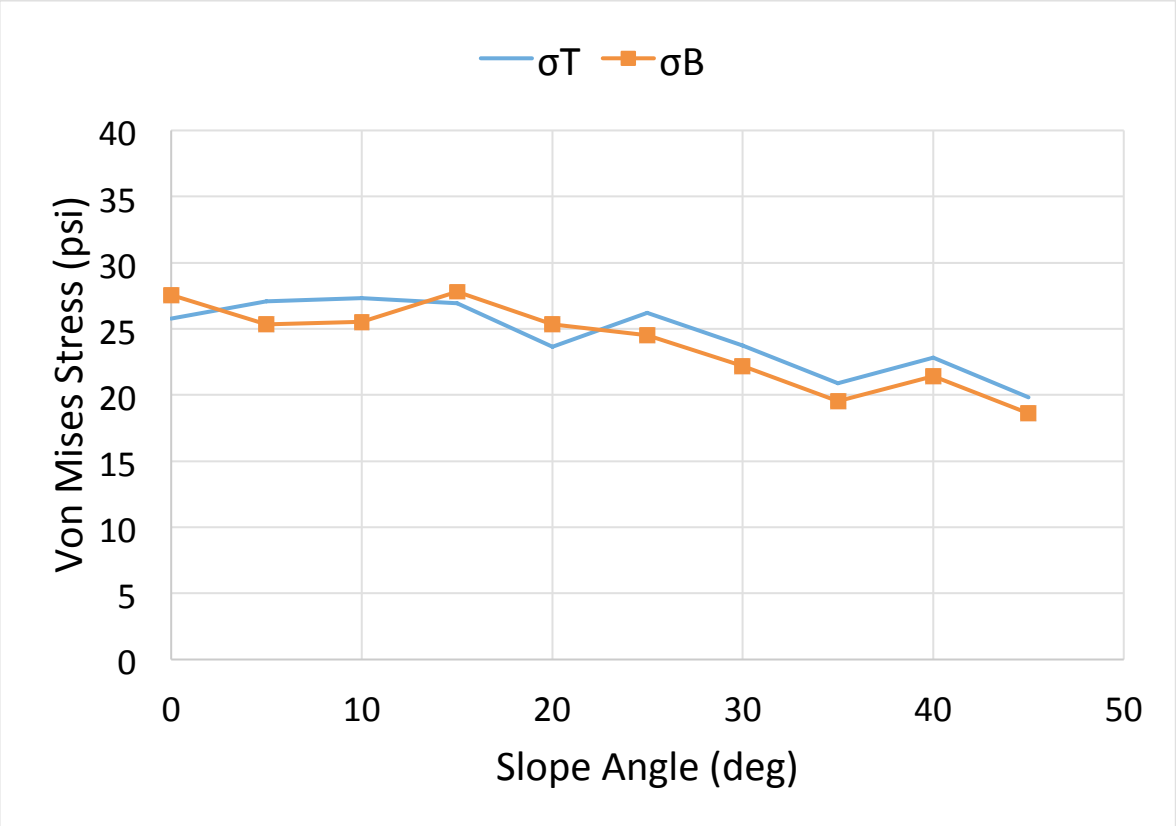


**Figure 6-56: Von Mises stress values within the RBS with radius cut perpendicular to the beam with slope configurations subject to a negative moment at 50% yield.**

The sloped configurations of the RBS connection were able to concentrate most of the strain demand within the radius cut region for angles less than 10 degrees. For slope angles between 10 and 30 degrees, localized strain demands occur in the flanges near the beam/column interface. Additionally, some strain demand localizes in the bottom of the web near the connection. The observed plastic strain reached approximately 33% of the maximum observed strain at these slope angles. The plastic strain distribution for the sloped configurations are shown in Figures 6-57 through 6-65.

Once the slope angle exceeds 30 degrees, the radius cut region becomes less effective at concentrating the strain demand. Furthermore, the strain demand in the bottom flange, at the bottom of the web, and at the weld access hole exceed the strain demand in the radius cut region.

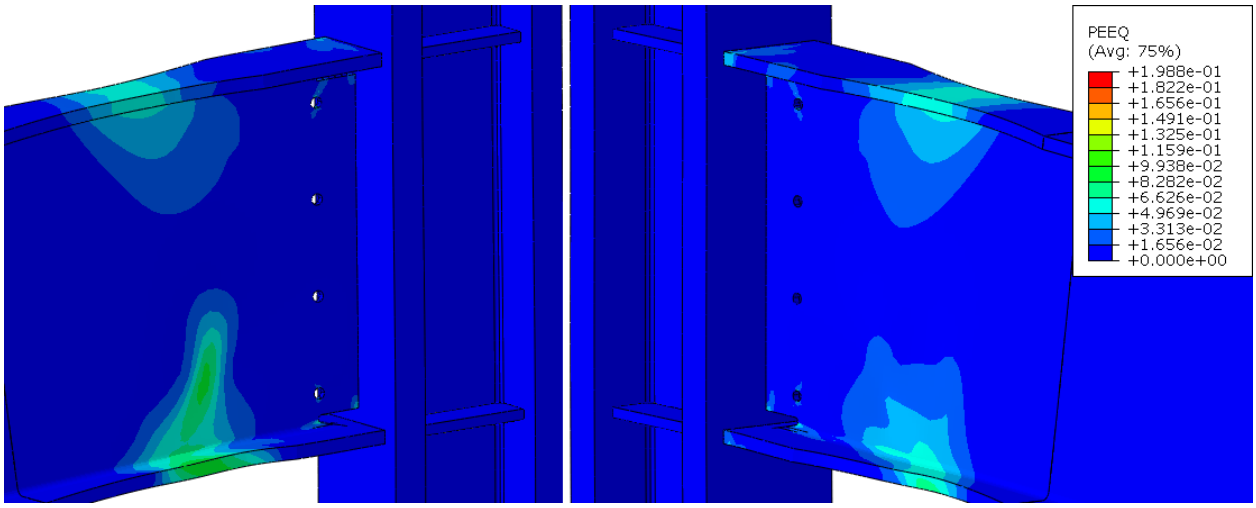


**Figure 6-57: PEEQ of the RBS connection with 5 degree slope and radius cut perpendicular to the beam section subject to a negative moment**

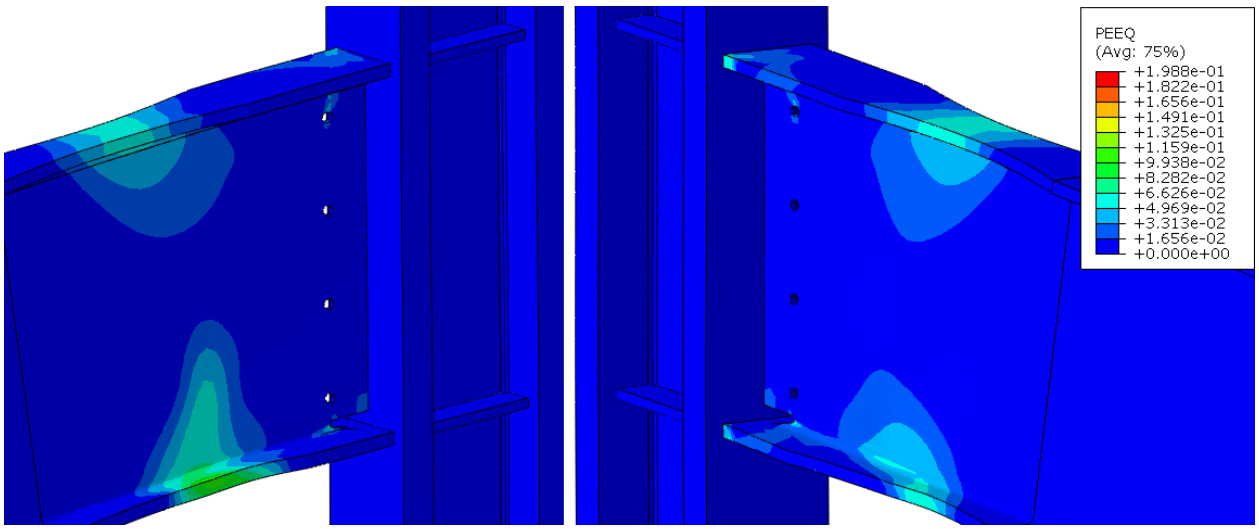


**Figure 6-58: PEEQ of the RBS connection with 10 degree slope and radius cut perpendicular to the beam section subject to a negative moment**

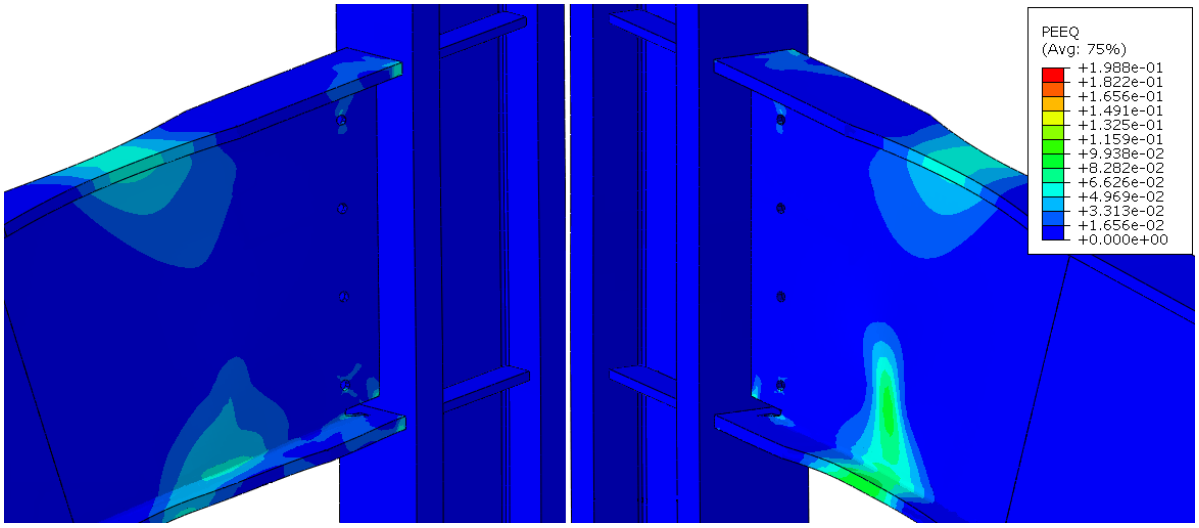


**Figure 6-59: PEEQ of the RBS connection with 15 degree slope and radius cut perpendicular to the beam section subject to a negative moment**

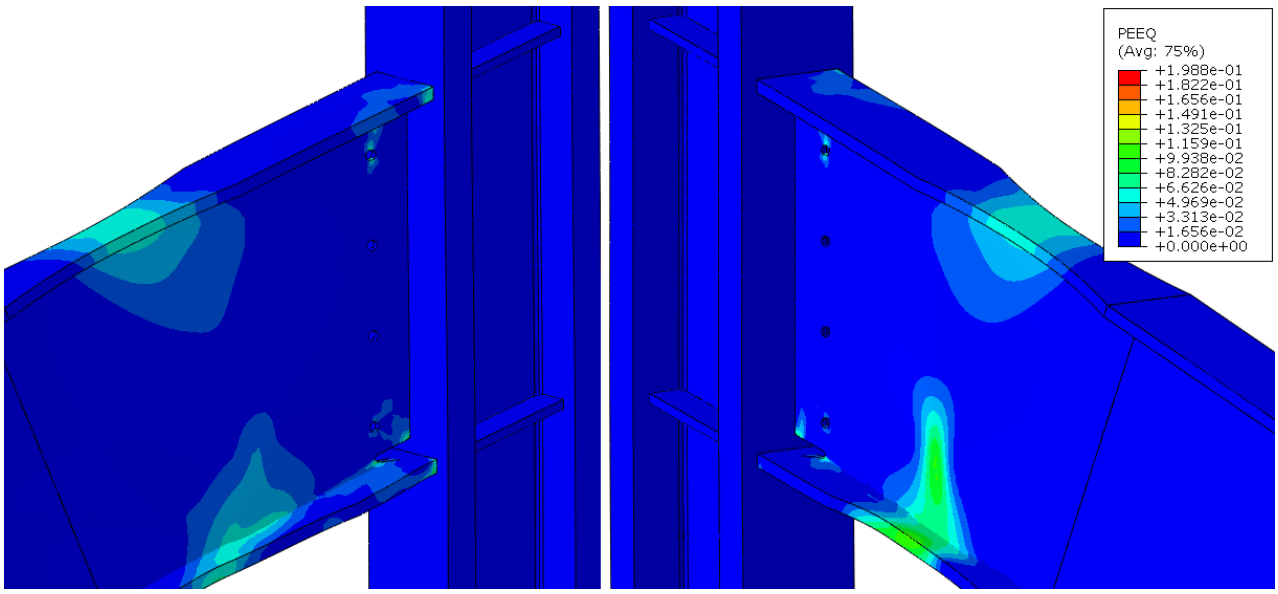


**Figure 6-60: PEEQ of the RBS connection with 20 degree slope and radius cut perpendicular to the beam section subject to a negative moment**

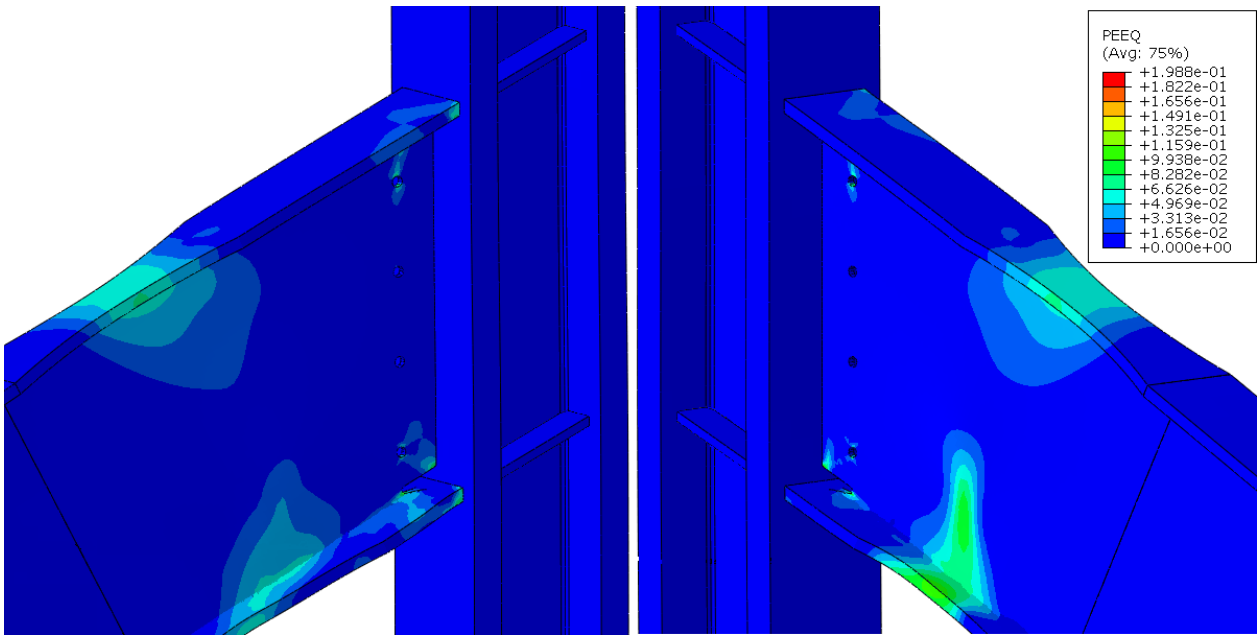


**Figure 6-61: PEEQ of the RBS connection with 25 degree slope and radius cut perpendicular to the beam section subject to a negative moment**

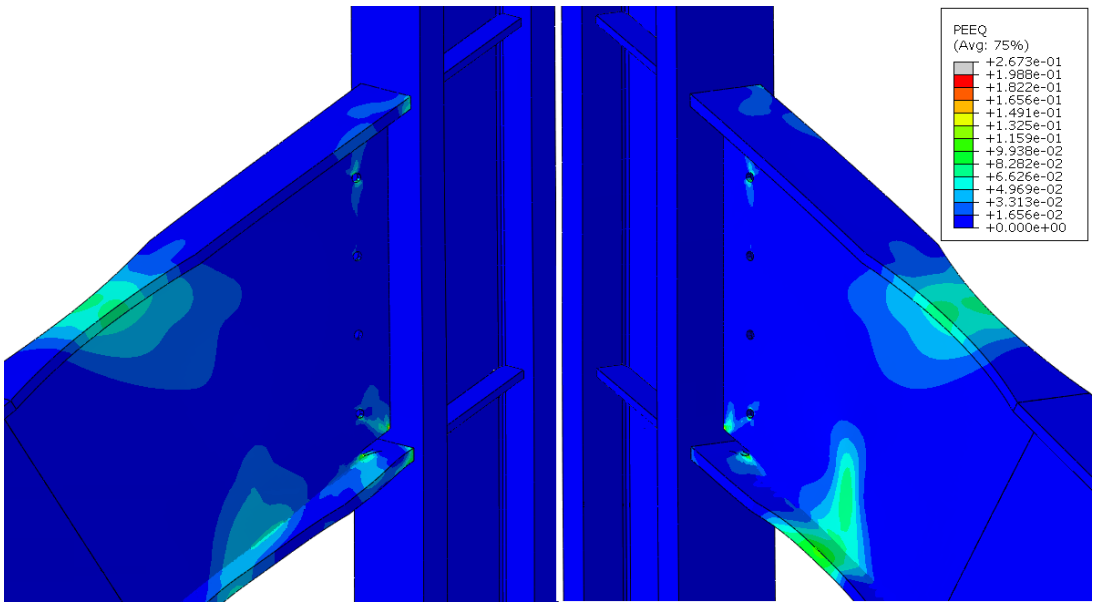


**Figure 6-62: PEEQ of the RBS connection with 30 degree slope and radius cut perpendicular to the beam section subject to a negative moment**

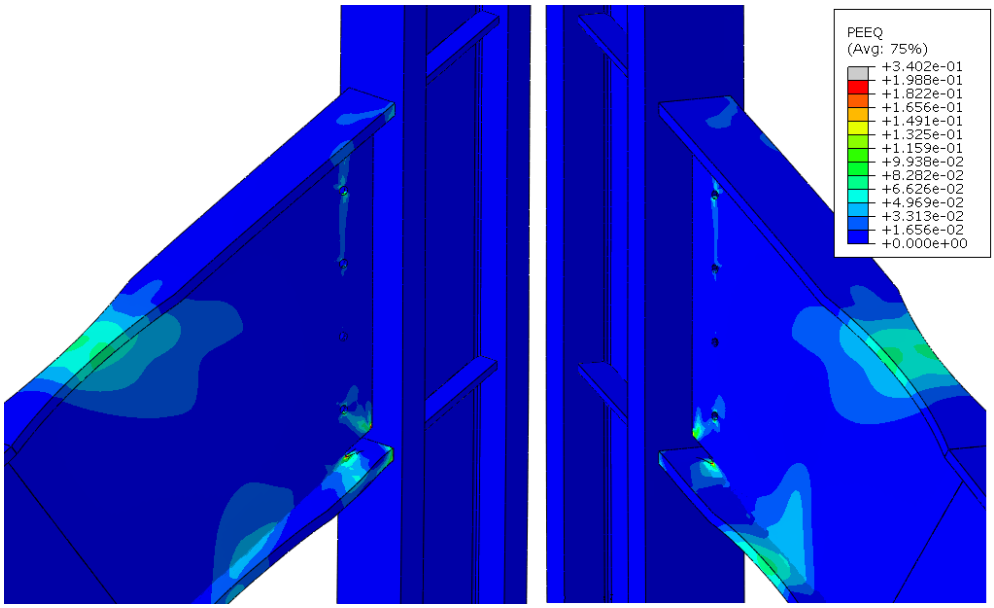


**Figure 6-63: PEEQ of the RBS connection with 35 degree slope and radius cut perpendicular to the beam section subject to a negative moment**

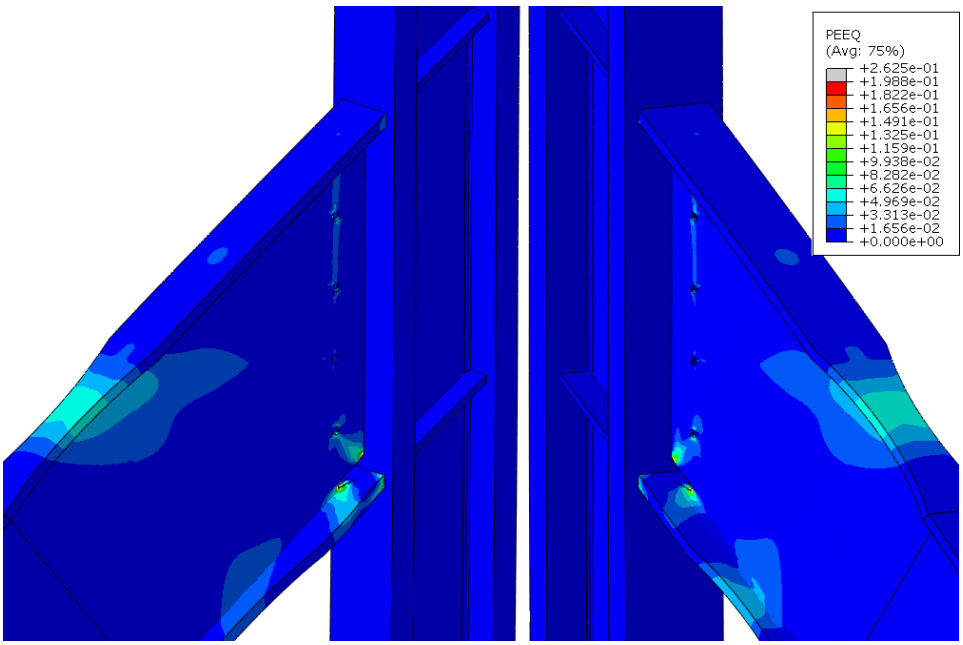


**Figure 6-64: PEEQ of the RBS connection with 40 degree slope and radius cut perpendicular to the beam section subject to a negative moment**

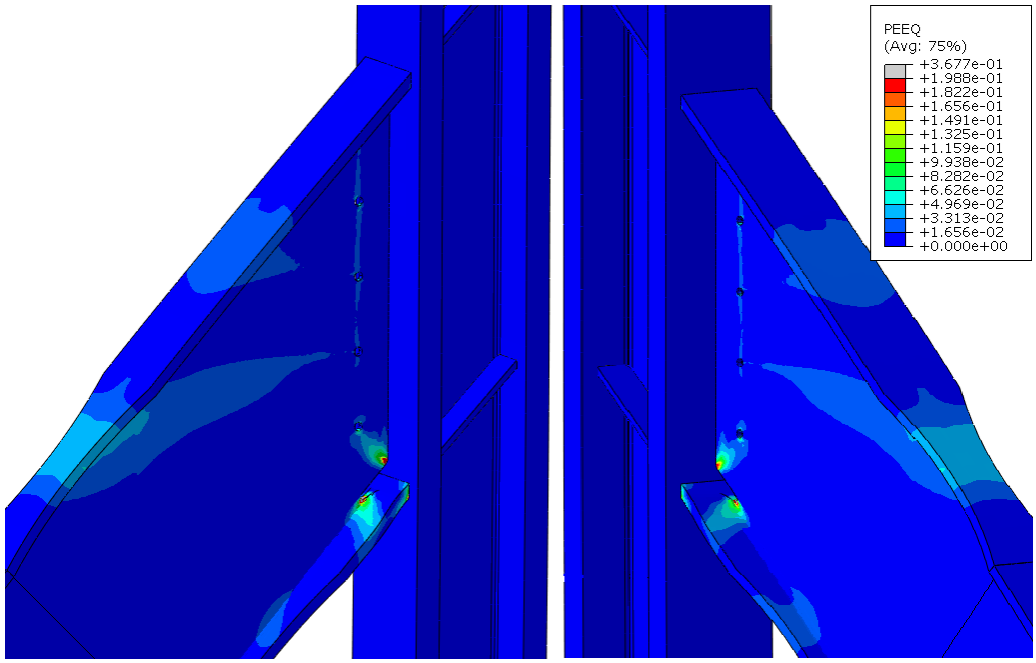


**Figure 6-65: PEEQ of the RBS connection with 45 degree slope and radius cut perpendicular to the beam section subject to a negative moment**

### 6.2.2 RBS with Radius Cut Perpendicular to the Beam Section and Subject to Positive Moment

The plastic moment capacity in this case increases with an increase in slope angle as shown in Figure 6-66. Much like the case of a negative moment, the overall effective depth is increased with the slope angle. This in turn increases the moment of inertia about the beam strong axis and consequently the capacity of the connection. However, the connection stiffness and plastic moment capacity is slightly reduced in comparison with the case of a negative moment. The radius cut region buckles after yielding, as can be surmised by the decrease in post-yield stiffness.

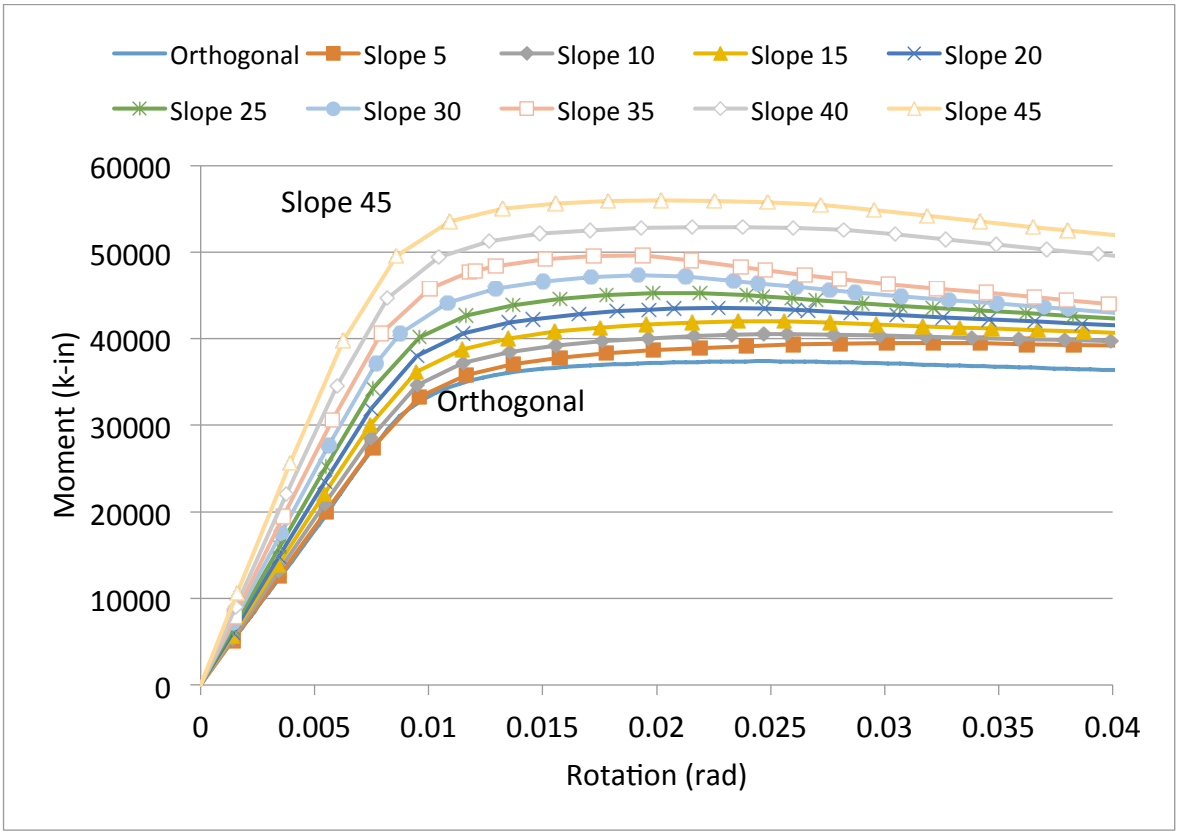


**Figure 6-66: Moment versus rotation of the RBS connection with sloped configurations and radius cut perpendicular to the beam section subject to a positive moment**

Similar to the RBS connection detail with sloped configurations subject to a negative moment, the stress distribution remains perpendicular to the beam section as shown in Figures 6-67 through 6-75. This effect does not appear to be impacted by the sloped geometry. For the RBS connection detail subject to a positive moment, the radius cut region is successful at concentrating the stress distribution for slope angles up to 30 degrees. As the slope angle exceeds 30 degrees, the stress distribution in the beam top flange concentrates closer to the beam/column interface but also within the radius cut region. Additionally, the stress distribution

in the beam bottom flange progressively concentrates closer to the beam/column interface for slope angles exceeding 30 degrees. For the extreme case of a 45 degree slope, the radius cut is incapable of concentrating the stress distribution in the beam bottom flange. Also, the stress distribution in the beam top flange concentrates closer to the beam/column interface.

The column flange at the beam/column interface experiences greater stress concentrations as the slope angle increases. As the slope angle increases, the stress distribution in the column flange concentrates at the beam top and bottom flanges. The panel zone of the connection is also impacted by the sloped configurations. As the slope angle increases, the stress distribution in the column web concentrates towards the bottom of the panel zone. Contrary to the RBS subject to a negative moment, this stress concentration reduces as the slope angle increases.

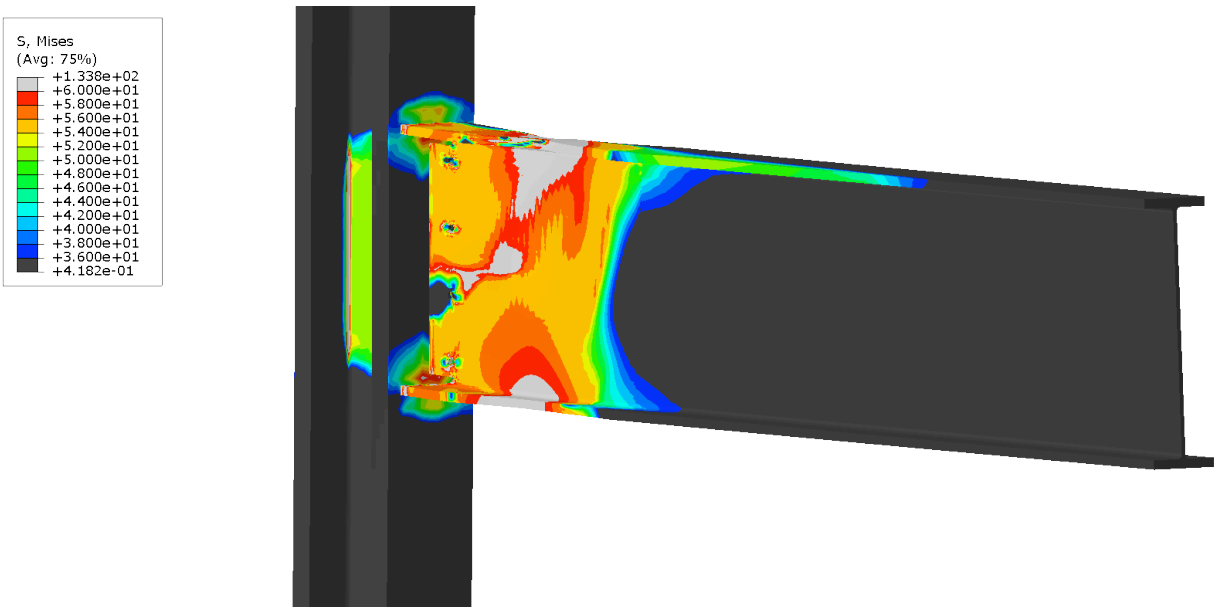


**Figure 6-67: Von Mises stress distribution of the RBS connection with 5 degree slope and radius cut perpendicular to the beam subject to a positive moment**

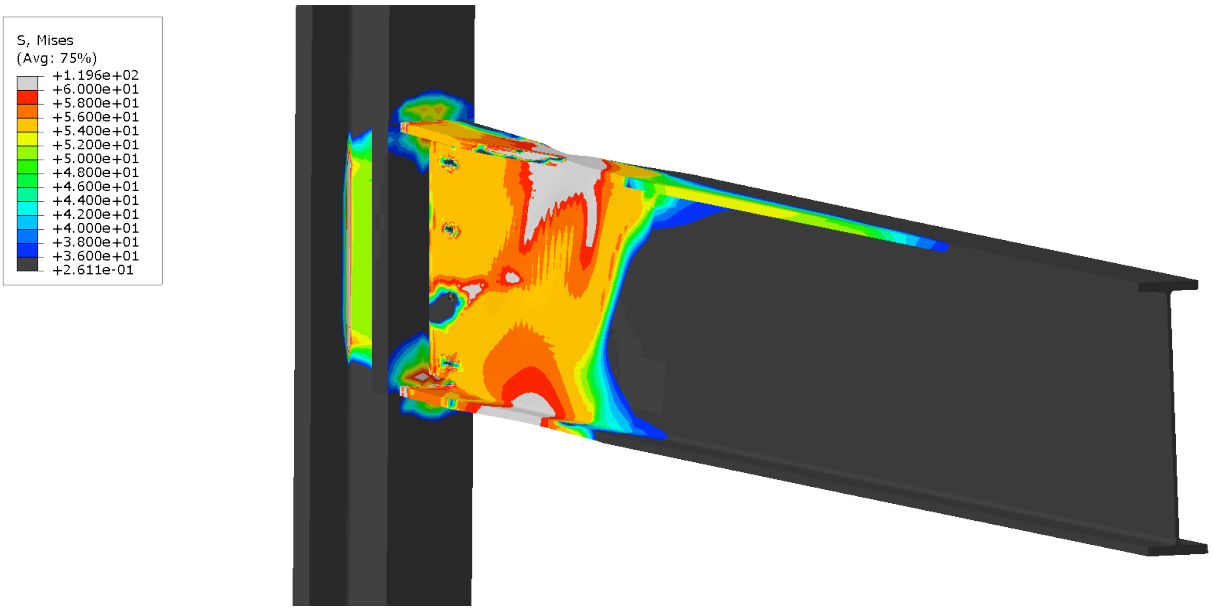


**Figure 6-68: Von Mises stress distribution of the RBS connection with 10 degree slope and radius cut perpendicular to the beam subject to a positive moment**

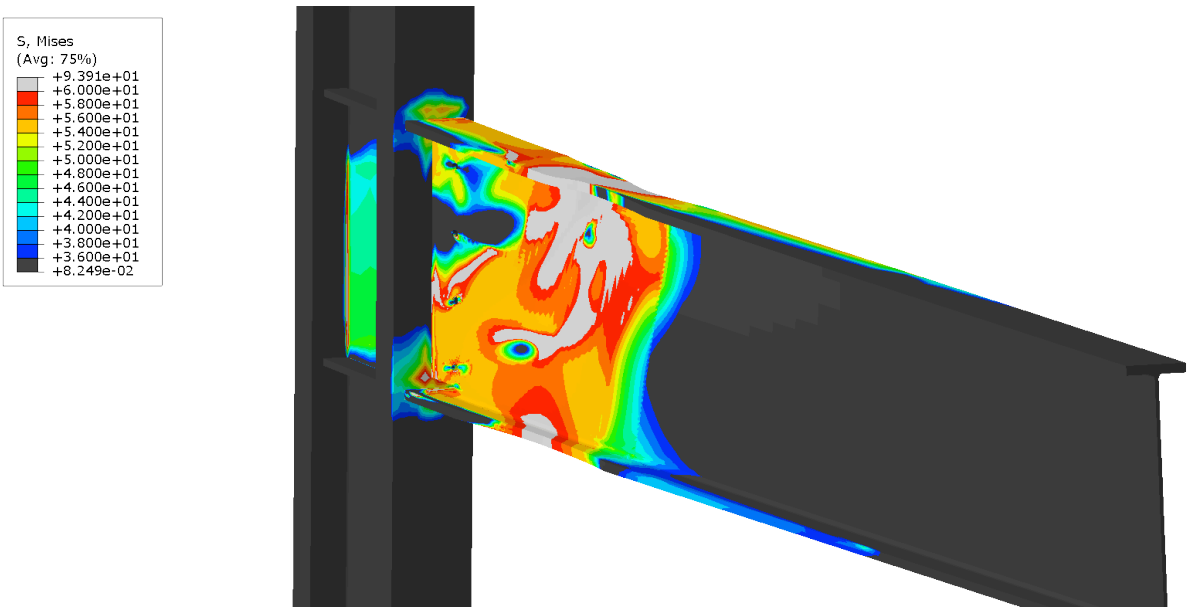


**Figure 6-69: Von Mises stress distribution of the RBS connection with 15 degree slope and radius cut perpendicular to the beam subject to a positive moment**

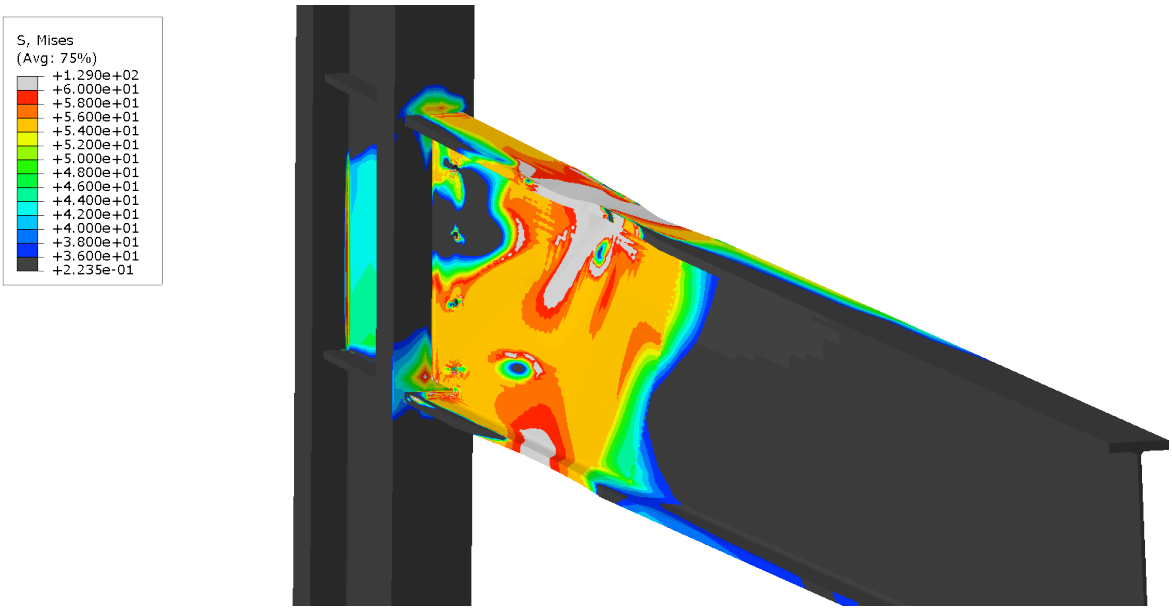


**Figure 6-70: Von Mises stress distribution of the RBS connection with 20 degree slope and radius cut perpendicular to the beam subject to a positive moment**

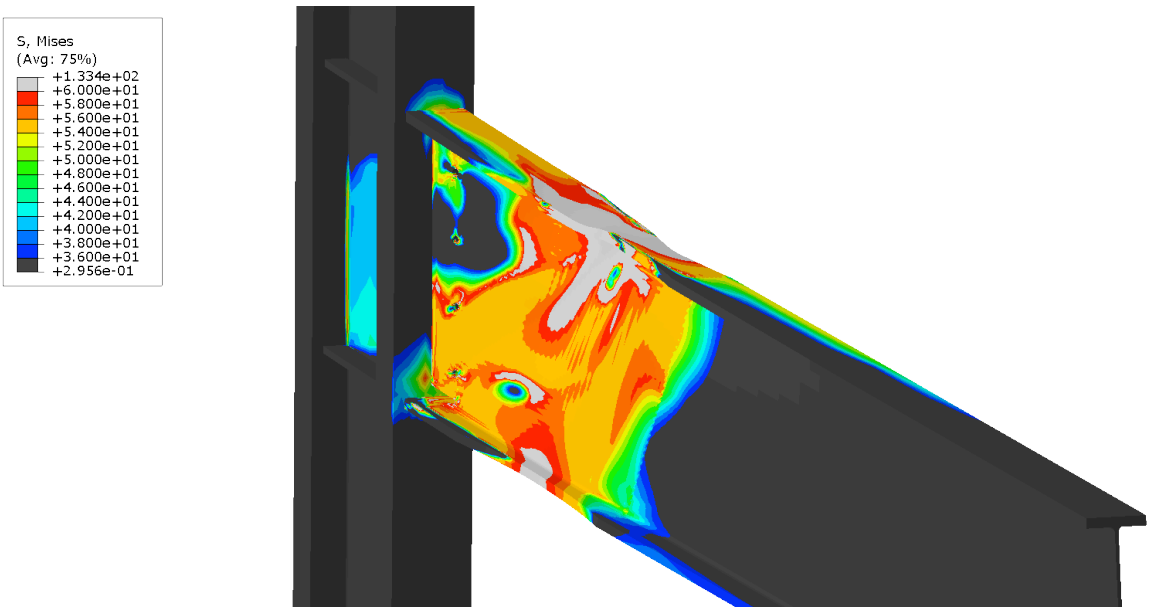


**Figure 6-71: Von Mises stress distribution of the RBS connection with 25 degree slope and radius cut perpendicular to the beam subject to a positive moment**

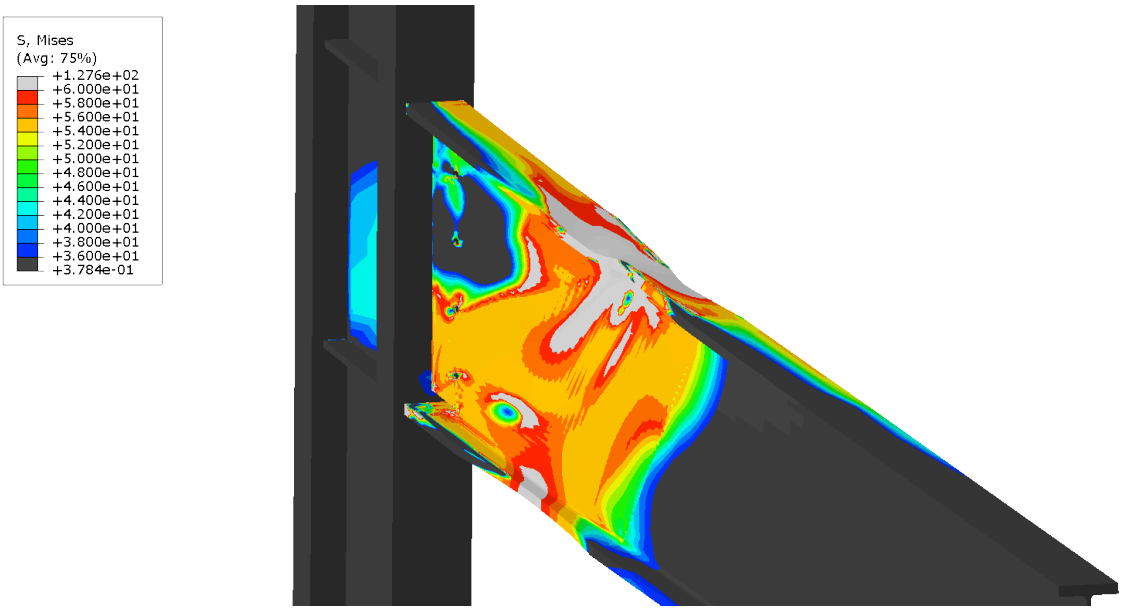


**Figure 6-72: Von Mises stress distribution of the RBS connection with 30 degree slope and radius cut perpendicular to the beam subject to a positive moment**

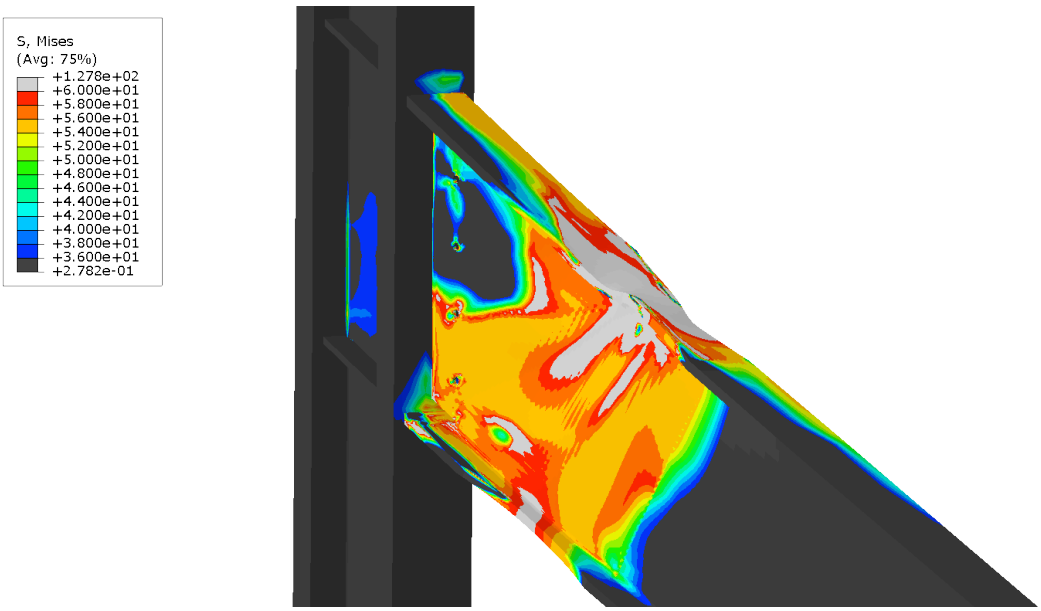


**Figure 6-73: Von Mises stress distribution of the RBS connection with 35 degree slope and radius cut perpendicular to the beam subject to a positive moment**

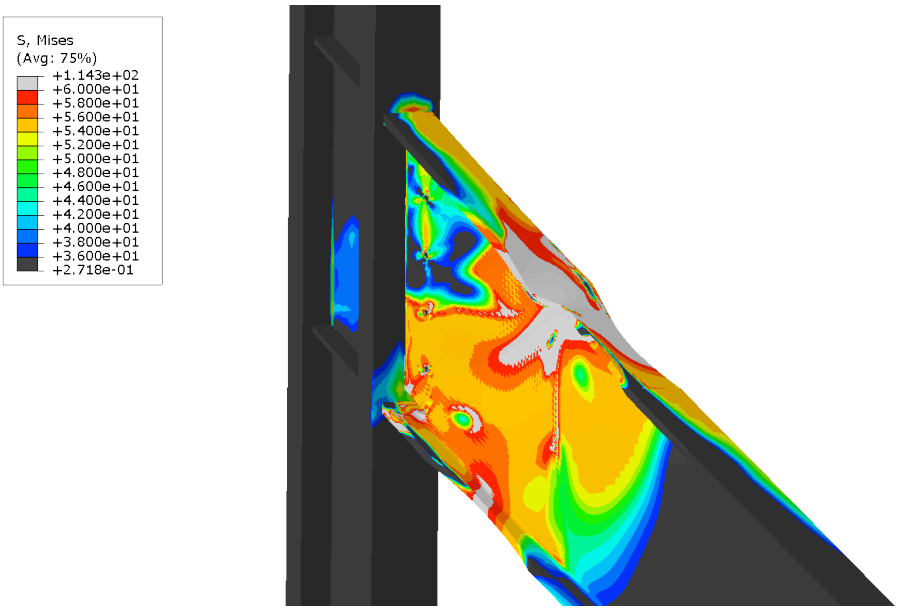


**Figure 6-74: Von Mises stress distribution of the RBS connection with 40 degree slope and radius cut perpendicular to the beam subject to a positive moment**

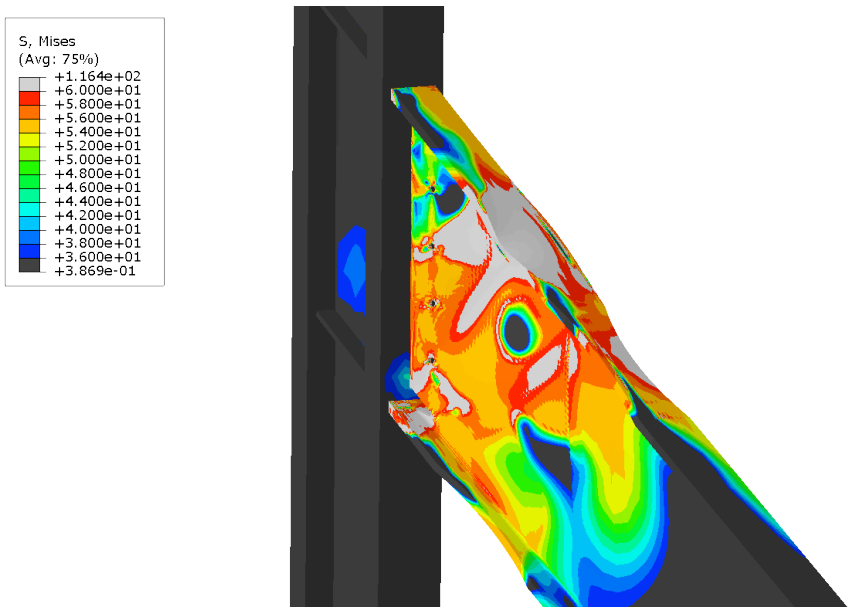


**Figure 6-75: Von Mises stress distribution of the RBS connection with 45 degree slope and radius cut perpendicular to the beam subject to a positive moment**

The first indication of non-linearity from the moment vs. rotation relationship occurs at a moment of 32125 k-in. The stress values associated with that moment were recorded and plotted with respect to the slope angle in Figure 6-76. For each increase in slope angle, the stress concentration decreases in the beam flange. The distribution of stress throughout the beam flange remains essentially unchanged for any slope angle.

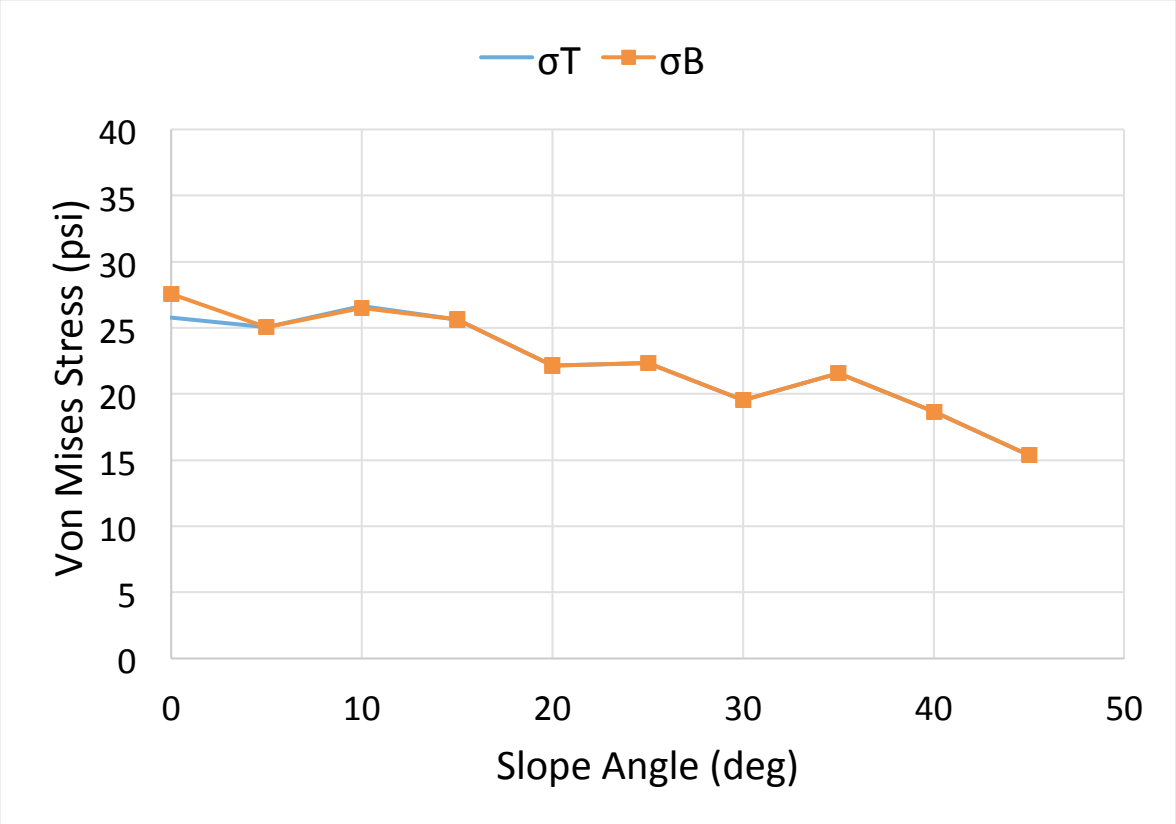


**Figure 6-76: Von Mises stress values within the RBS with radius cut perpendicular to the beam with slope configurations subject to a positive moment at first yield.**

At 50% of the yield moment as calculated by dividing the moment associated with the first indication of non-linearity by 2, the stress values were recorded corresponding to a moment of 14295 k-in. The stress values were plotted with respect to the slope angle in Figure 6-77. For each increase in slope angle, the stress concentration decreases in the beam flange. The stress concentration in the top of the flange is slightly lower than the bottom of the flange for slope angles exceeding 10 degrees.

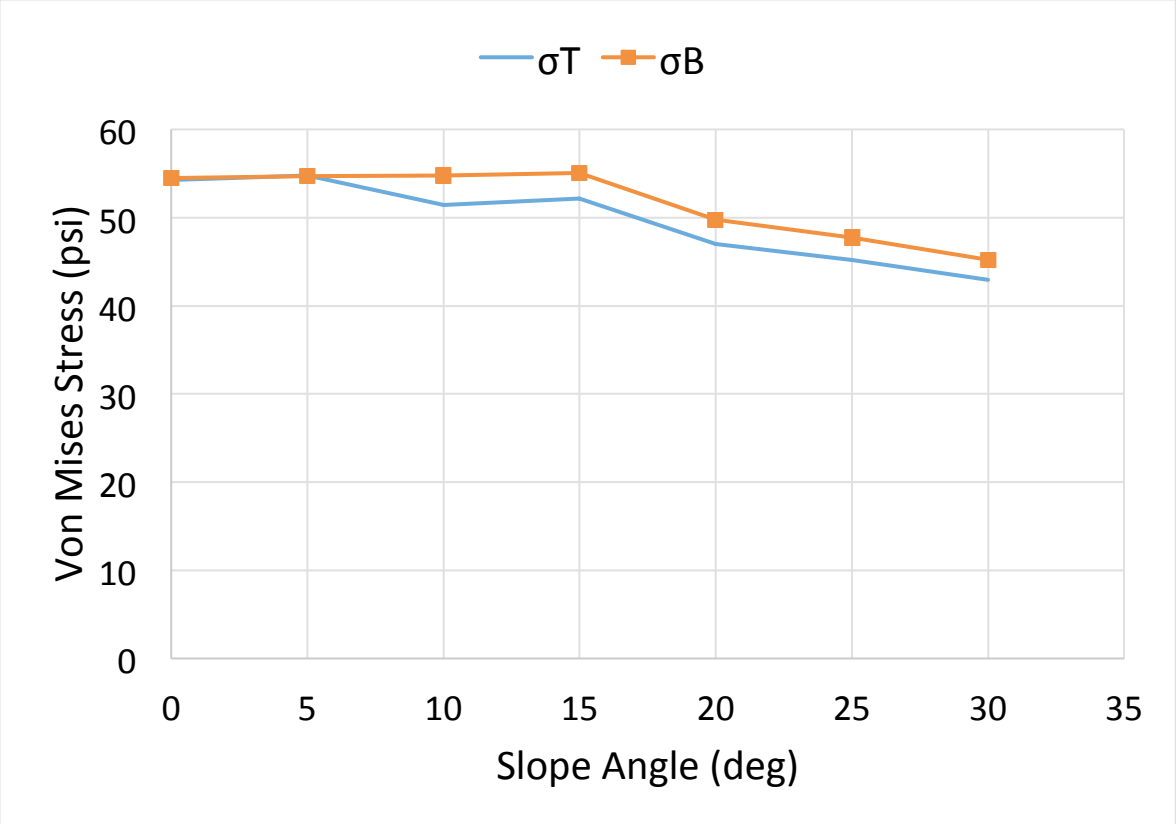


**Figure 6-77: Von Mises stress values within the RBS with radius cut perpendicular to the beam with slope configurations subject to a positive moment at 50% yield.**

The radius cut region is successful at concentrating the strain demand for slope angles less than 30 degrees, as can be seen in Figures 6-78 through 6-86. The radius cut region concentrates most of the strain demand, but there are localized strain demands occurring in the bottom flange near the beam/column interface. When the radius cut region buckles after yielding, the strain demand begins to concentrate in the bottom flange near the connection. For slope angles between 0 and 30 degrees, the strain demand that occurs near the connection in the bottom flange reaches the order of 25% of the maximum observed strain.

Once the slope angle exceeds 30 degrees, the radius cut region becomes increasingly less effective at concentrating the strain demand. Additionally, the strain demand reaches the values of 30% to 90% of the maximum observed strain. For the extreme case of a 45-degree slope, the bottom flange in the radius cut region is no longer capable of concentrating strain demand. The bottom flange along with the bottom of the web section near the connection experiences nearly all the strain demand.

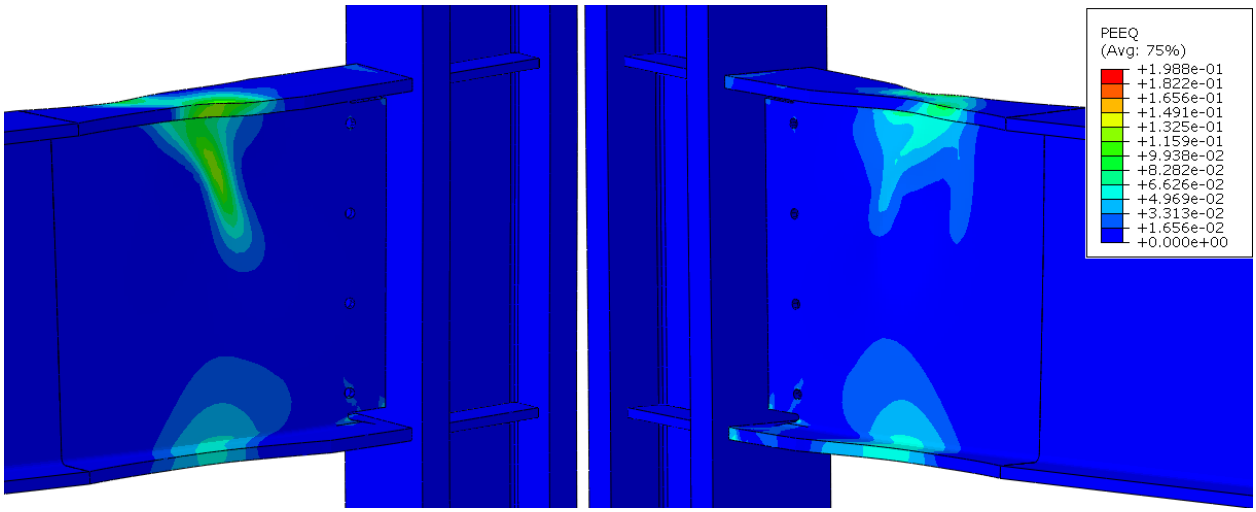


**Figure 6-78: PEEQ of the RBS connection with 5 degree slope and radius cut perpendicular to the beam subject to a positive moment**

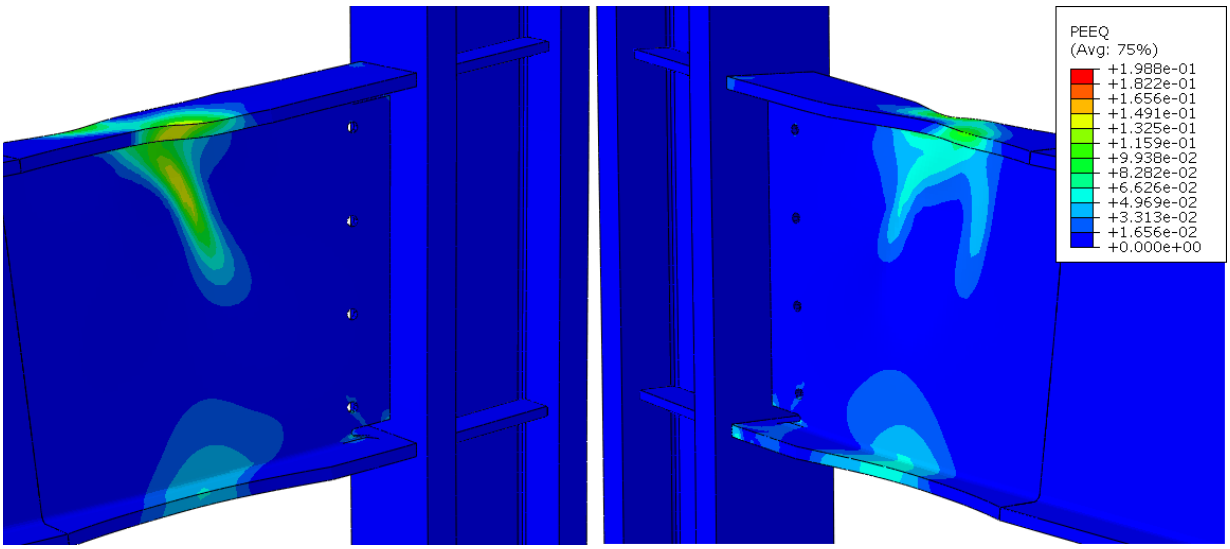


**Figure 6-79: PEEQ of the RBS connection with 10 degree slope and radius cut perpendicular to the beam subject to a positive moment**

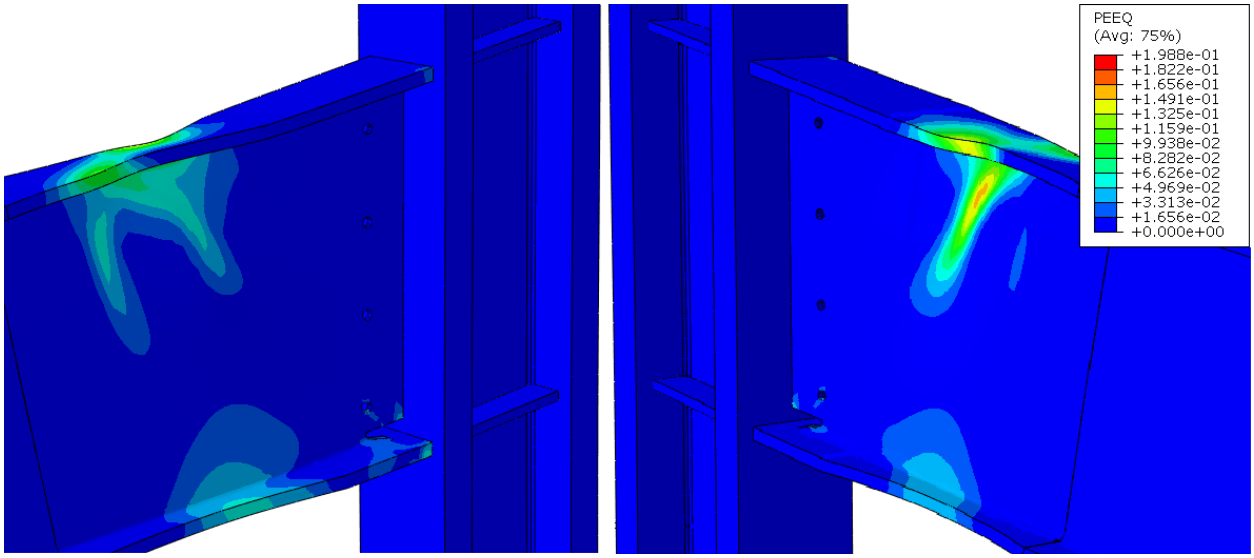


**Figure 6-80: PEEQ of the RBS connection with 15 degree slope and radius cut perpendicular to the beam subject to a positive moment**

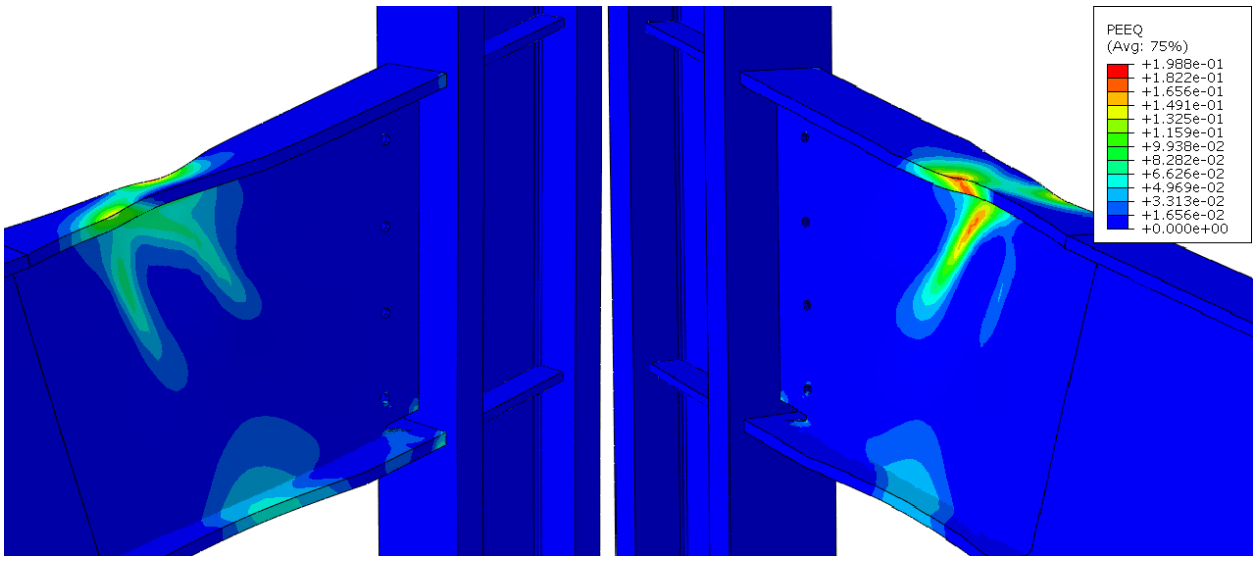


**Figure 6-81: PEEQ of the RBS connection with 20 degree slope and radius cut perpendicular to the beam subject to a positive moment**

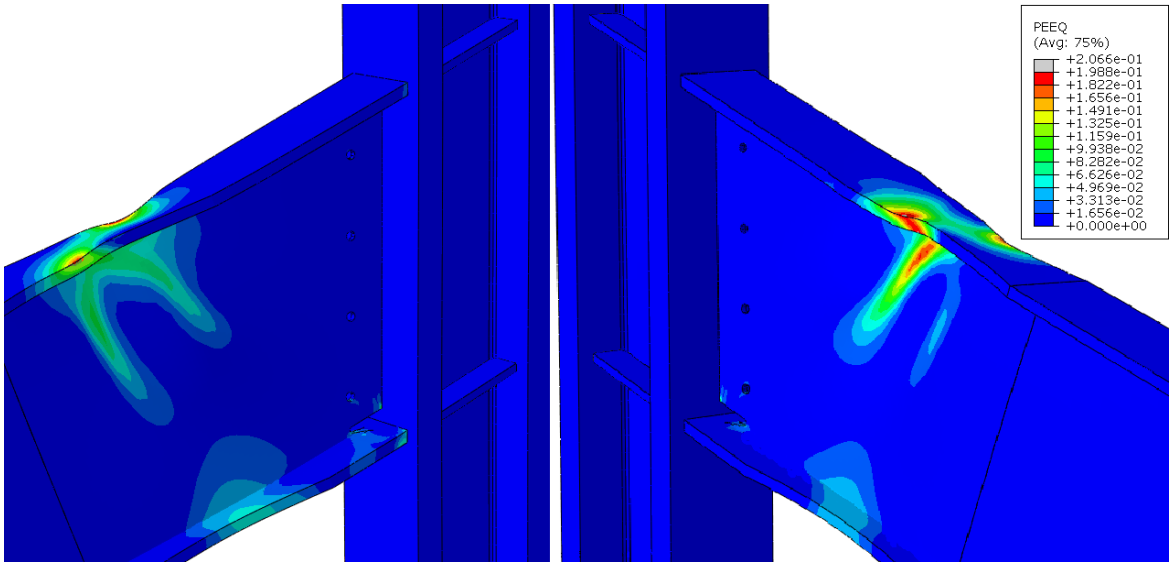


**Figure 6-82: PEEQ of the RBS connection with 25 degree slope and radius cut perpendicular to the beam subject to a positive moment**

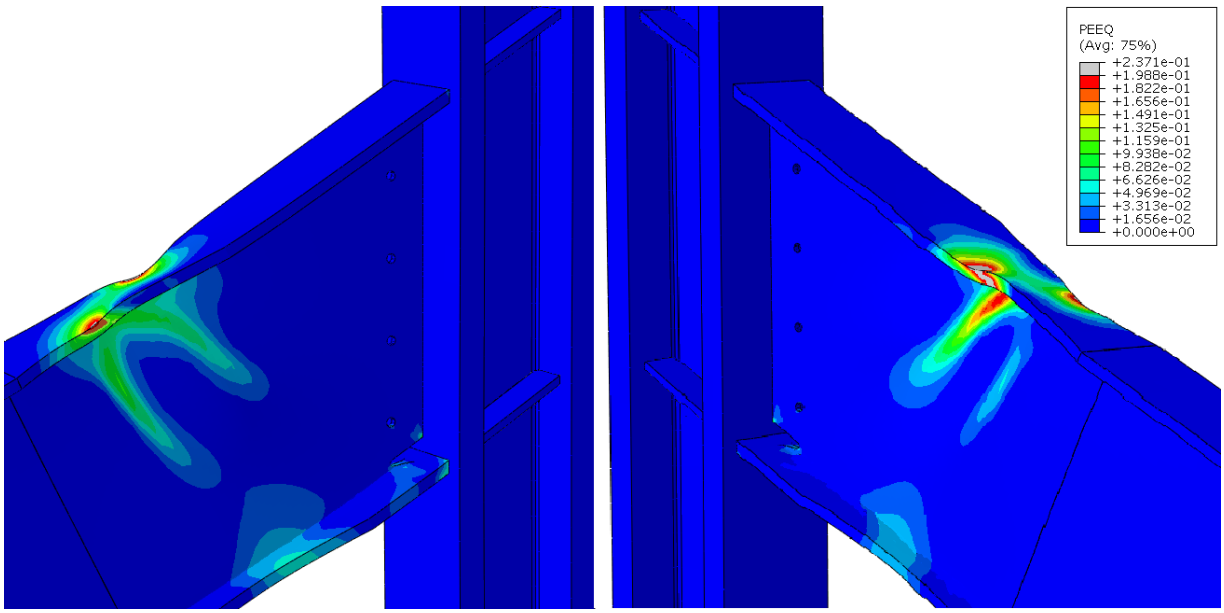


**Figure 6-83: PEEQ of the RBS connection with 30 degree slope and radius cut perpendicular to the beam subject to a positive moment**

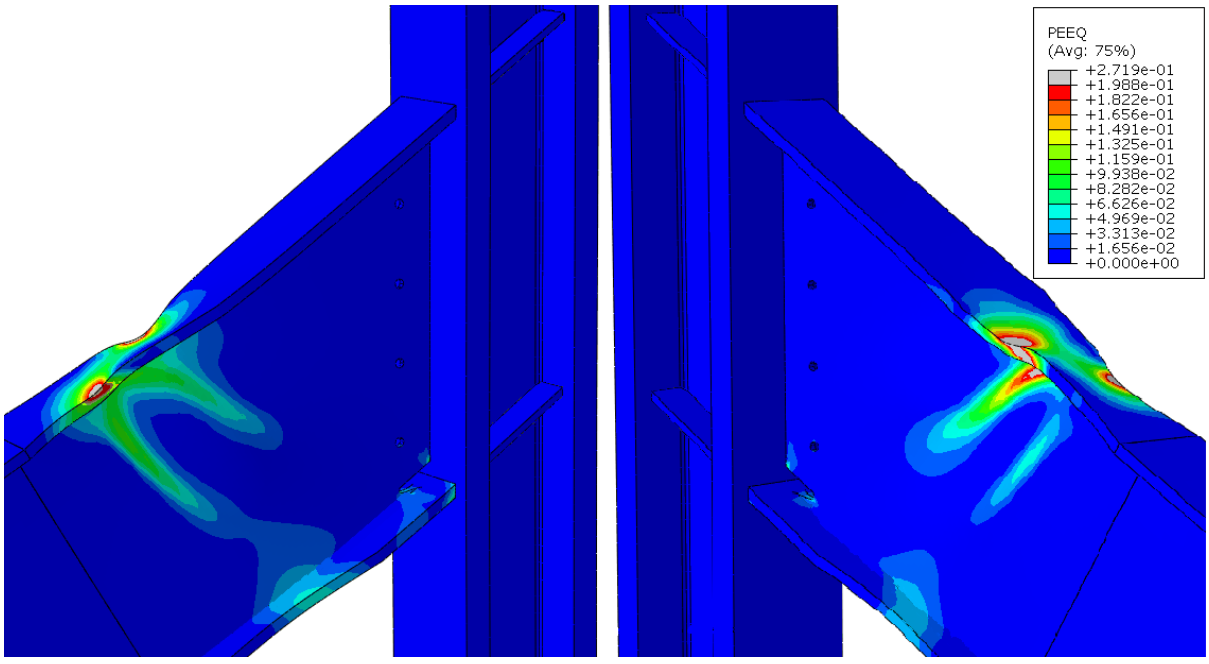


**Figure 6-84: PEEQ of the RBS connection with 35 degree slope and radius cut perpendicular to the beam subject to a positive moment**

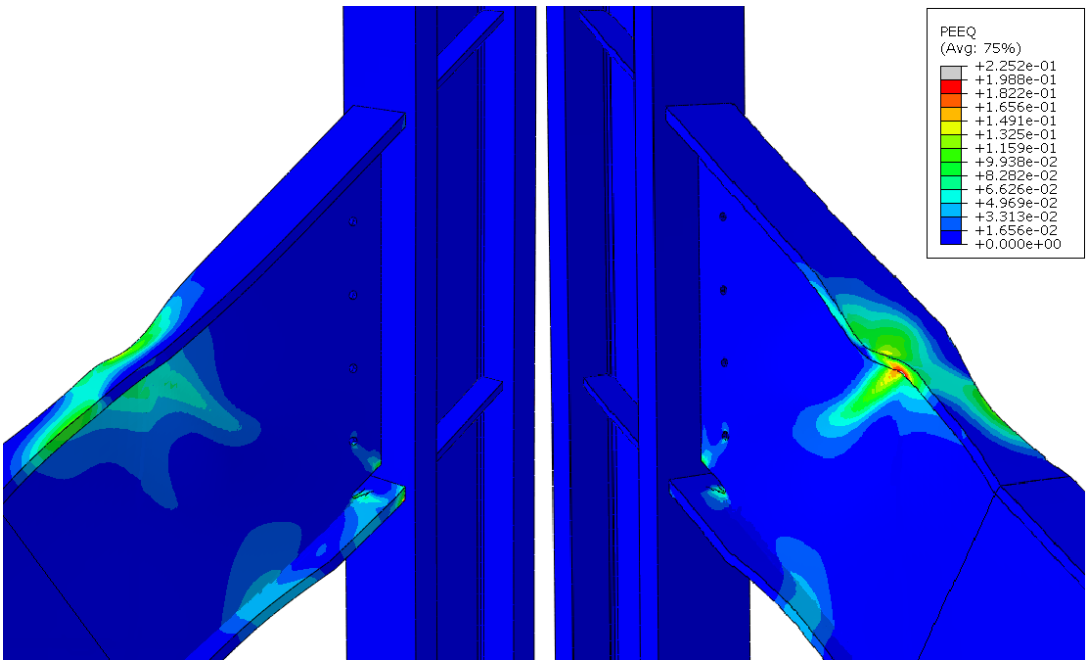


**Figure 6-85: PEEQ of the RBS connection with 40 degree slope and radius cut perpendicular to the beam subject to a positive moment**

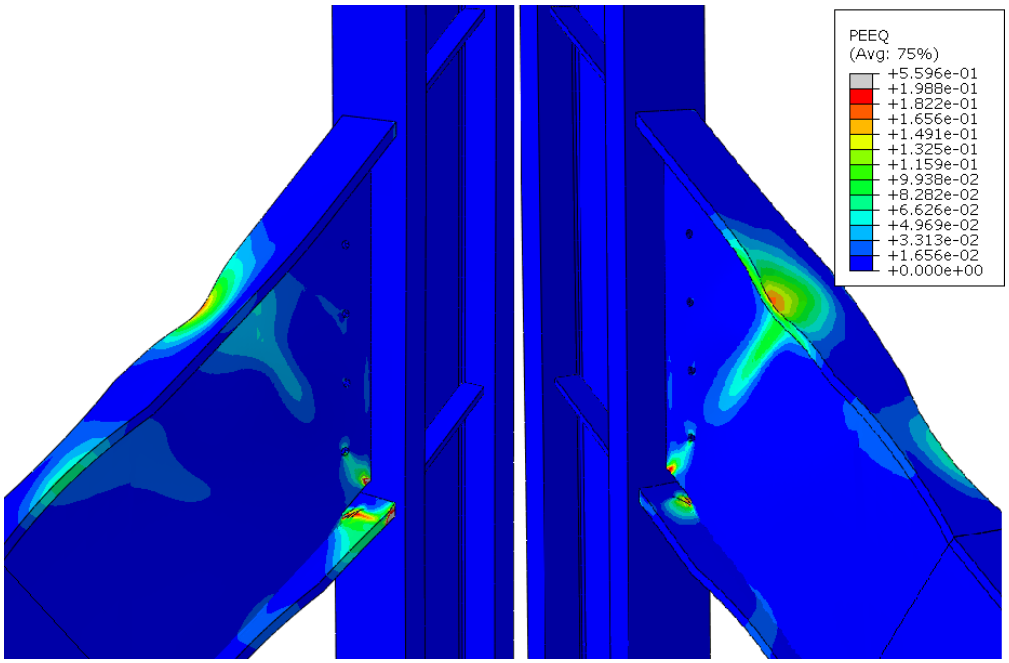


**Figure 6-86: PEEQ of the RBS connection with 45 degree slope and radius cut perpendicular to the beam subject to a positive moment**

### 6.2.3 RBS with Radius Cut Parallel to the Column Section and Subject to a Negative Moment

The models of configurations with radius cut arrangement parallel to the column section experienced convergence problems once the slope angle exceeded 20 degrees. The finite element analyses were unsuccessful in converging to a solution due to excessive element distortion. The limited results obtained are illustrated in this section.

The plastic moment capacity of the RBS connection with radius cut parallel to the column section subject to a negative moment increased for each increasing slope angle as shown in Figure 6-87. Similar to the other RBS models, this is most likely attributed to the increase in effective depth of the beam cross-section.

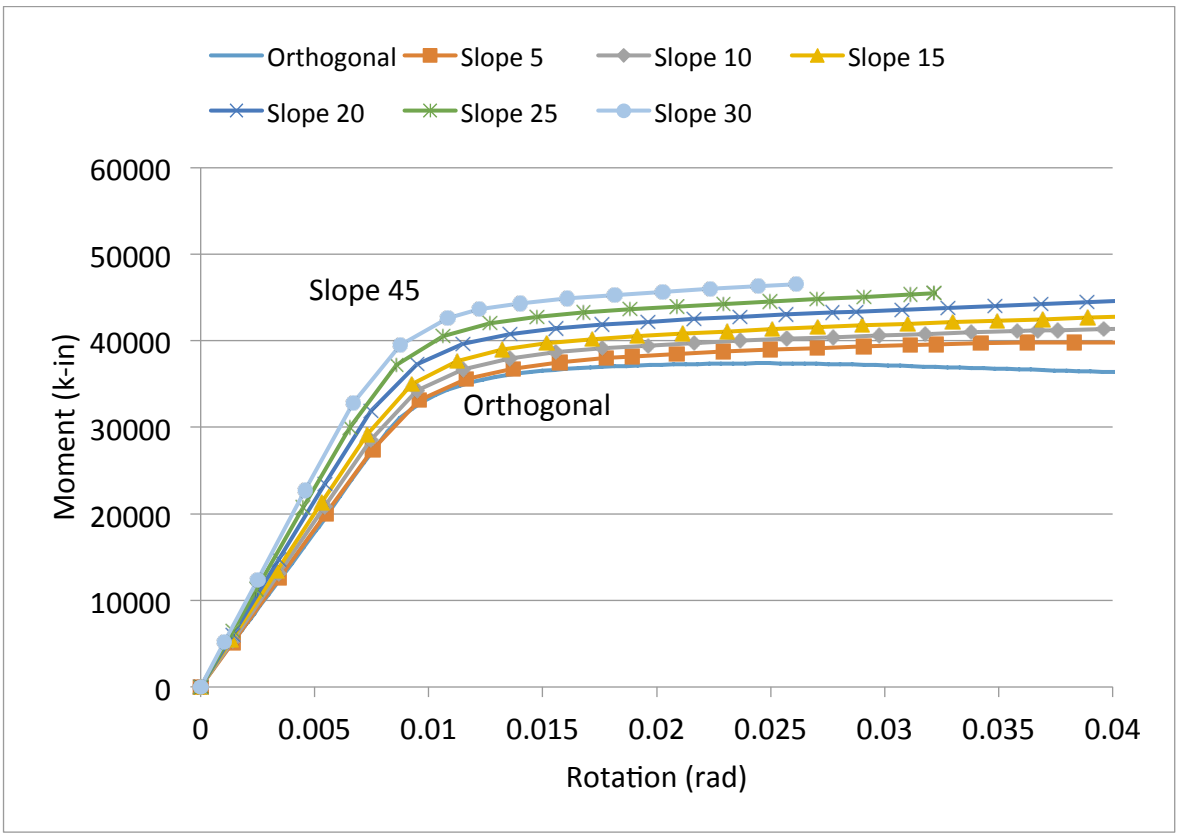


**Figure 6-87: Moment versus rotation of the RBS connection with sloped configurations and radius cut parallel to the column section subject to a negative moment**

For the RBS connection detail with sloped configurations subject to a negative moment, the stress distribution remains perpendicular to the beam section as shown in Figures 6-88 through 6-93. This effect does not appear to be impacted by the sloped geometry. For slope angles up to 15 degrees, the radius cut region is successful at concentrating the majority of the stress distribution. As the slope angle exceeds 15 degrees, the radius cut region in the beam bottom flange becomes increasingly less efficient at concentrating the stress distribution. This is likely attributed to the stress distribution in the beam remaining perpendicular to the

beam cross-section. As a result, the stress concentration in the beam bottom flange increases near the beam/column interface.

The column flange at the beam/column interface experiences greater stress concentrations as the slope angle increases. As the slope angle increases, the stress distribution in the column flange concentrates at the beam top and bottom flanges. The panel zone of the connection is minimally impacted for the RBS under these loading conditions.

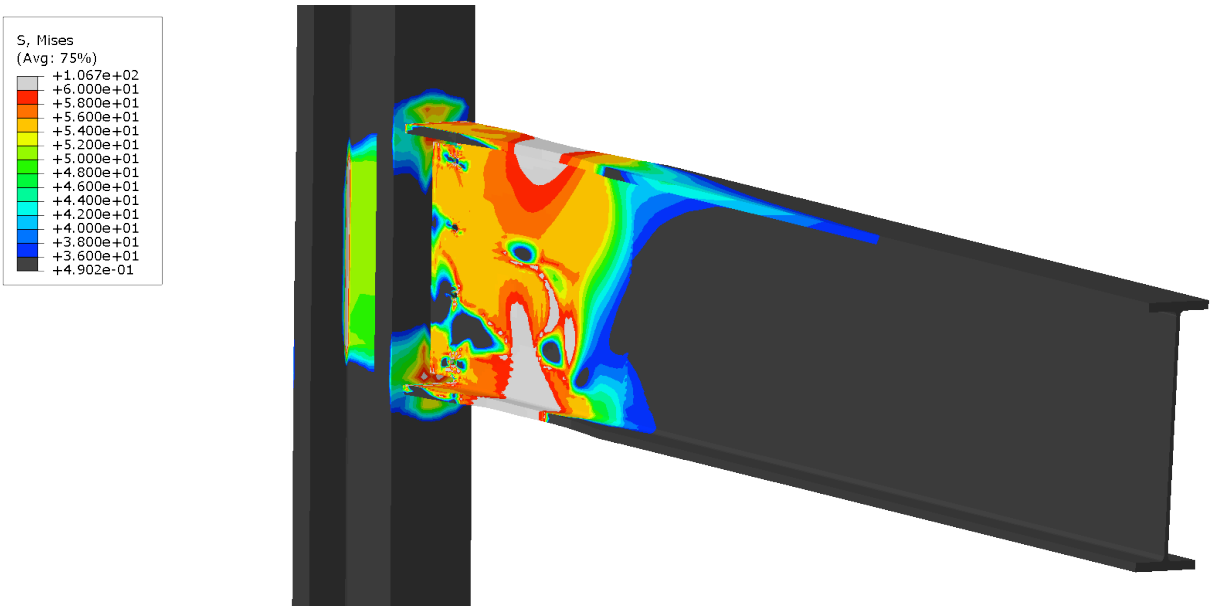


**Figure 6-88: Von Mises stress distribution of the RBS connection with 5 degree slope and radius cut parallel to the column section subject to a negative moment**

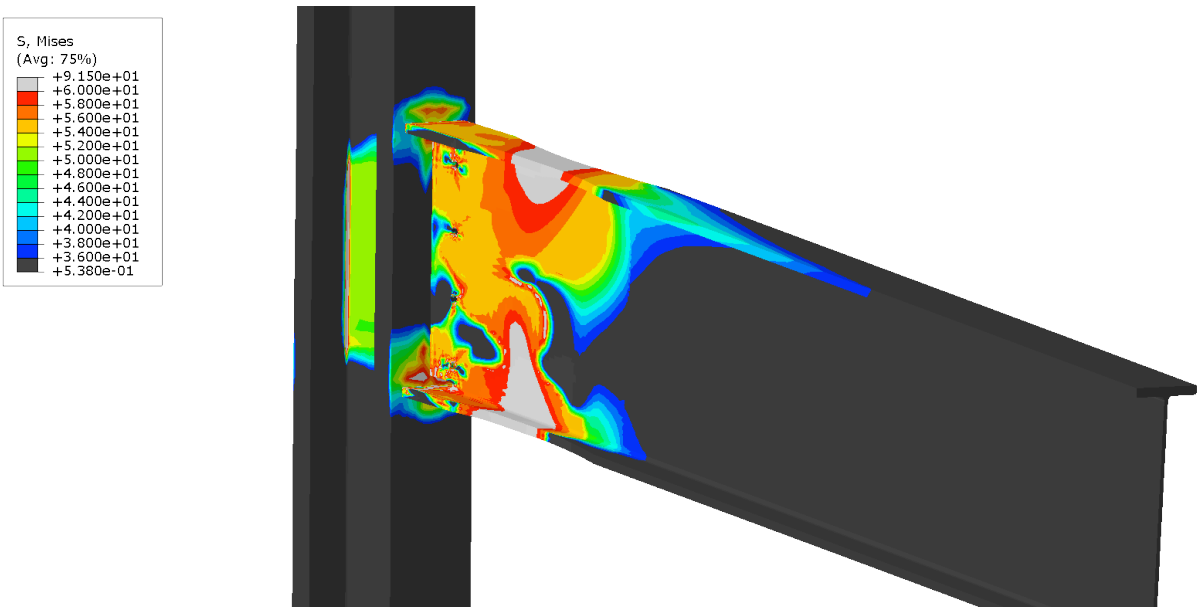


**Figure 6-89: Von Mises stress distribution of the RBS connection with 10 degree slope and radius cut parallel to the column section subject to a negative moment**

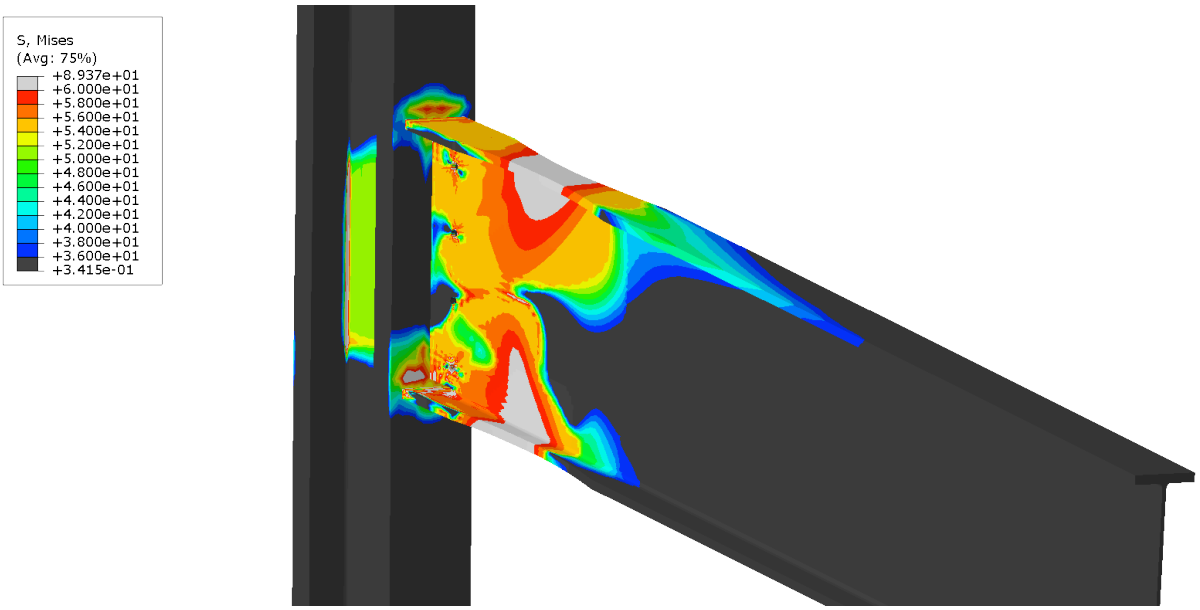


**Figure 6-90: Von Mises stress distribution of the RBS connection with 15 degree slope and radius cut parallel to the column section subject to a negative moment**

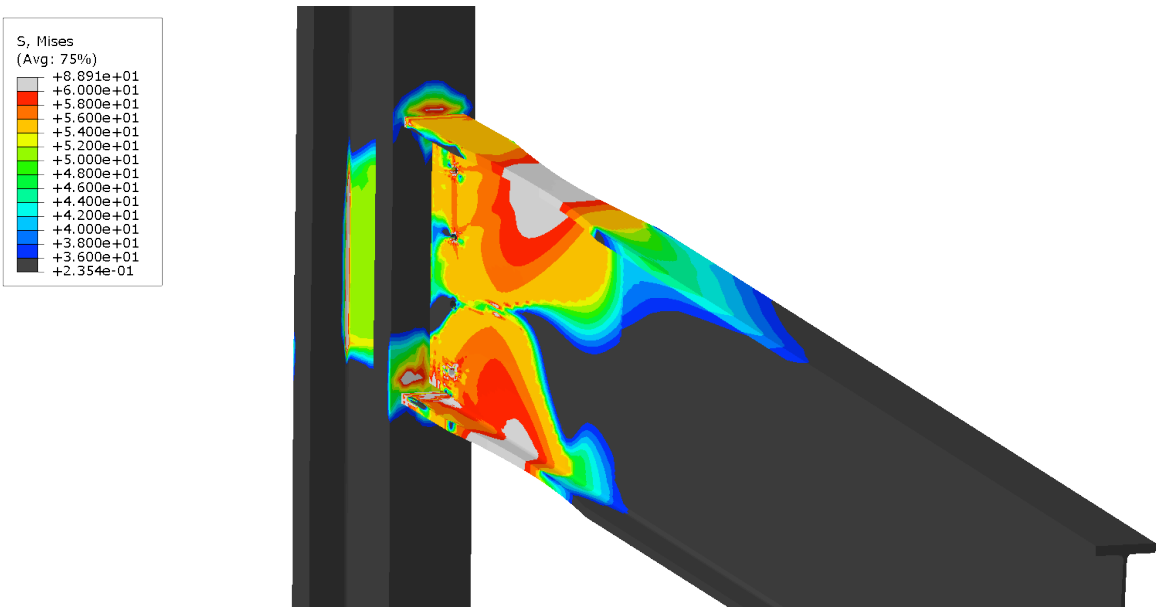


**Figure 6-91: Von Mises stress distribution of the RBS connection with 20 degree slope and radius cut parallel to the column section subject to a negative moment**

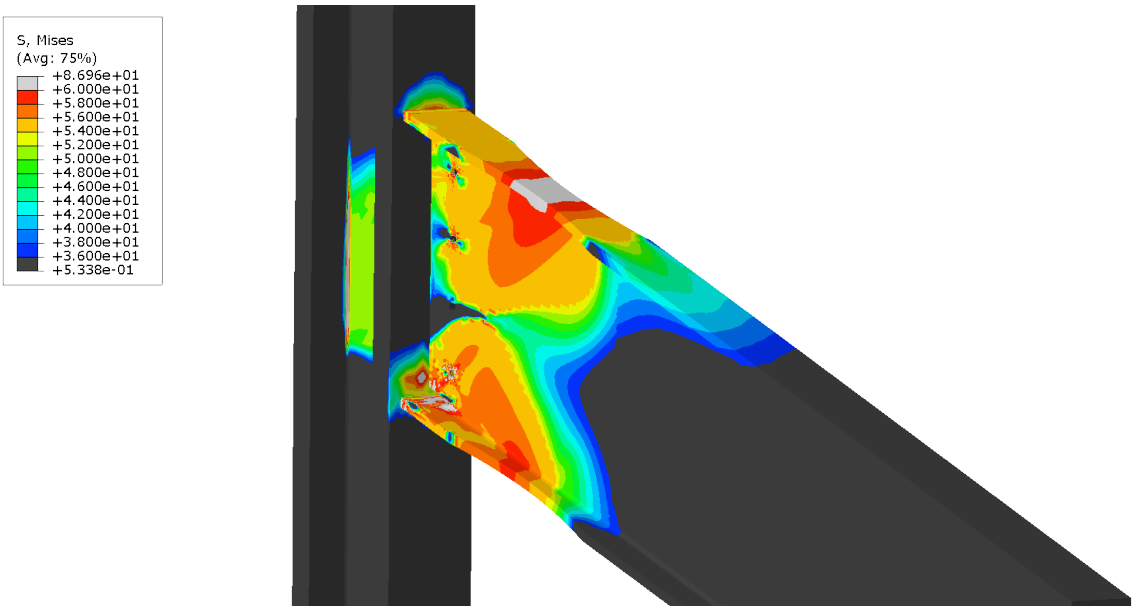


**Figure 6-92: Von Mises stress distribution of the RBS connection with 25 degree slope and radius cut parallel to the column section subject to a negative moment**

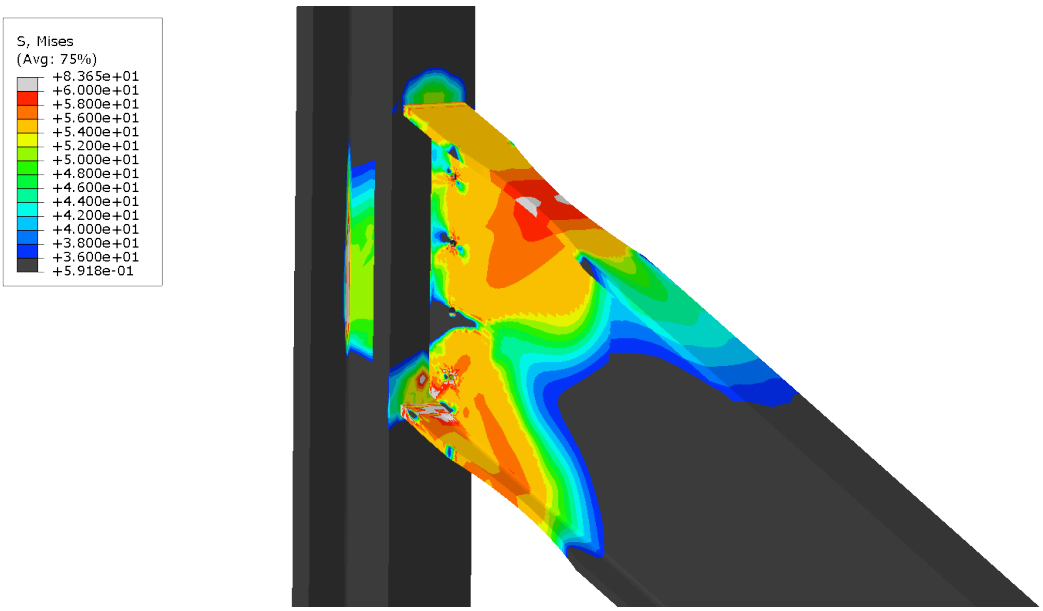


**Figure 6-93: Von Mises stress distribution of the RBS connection with 30 degree slope and radius cut parallel to the column section subject to a negative moment**

The first indication of non-linearity from the moment vs. rotation relationship occurs at a moment of 32125 k-in. The stress values associated with that moment were recorded and plotted with respect to the slope angle in Figure 6-94. For each increase in slope angle, the stress value within the beam flange associated with that moment indicated no noticeable difference.

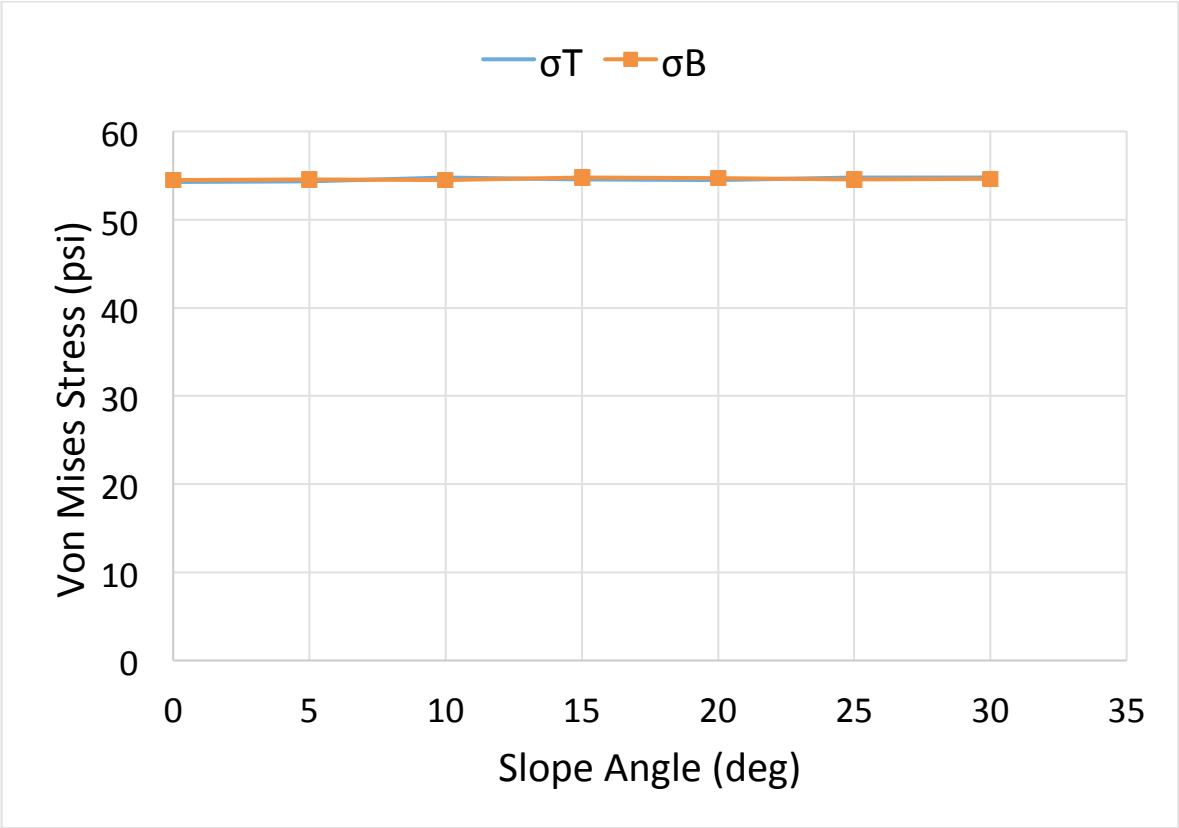


**Figure 6-94: Von Mises stress values within the RBS with radius cut parallel to the column with slope configurations subject to a negative moment at first yield.**

At 50% of the yield moment as calculated by dividing the moment associated with the first indication of non-linearity by 2, the stress values were recorded corresponding to a moment of 14295 k-in. The stress values were plotted with respect to the slope angle in Figure 6-95. For each increase in slope angle, the stress value within the beam flange associated with that moment indicated no noticeable difference.

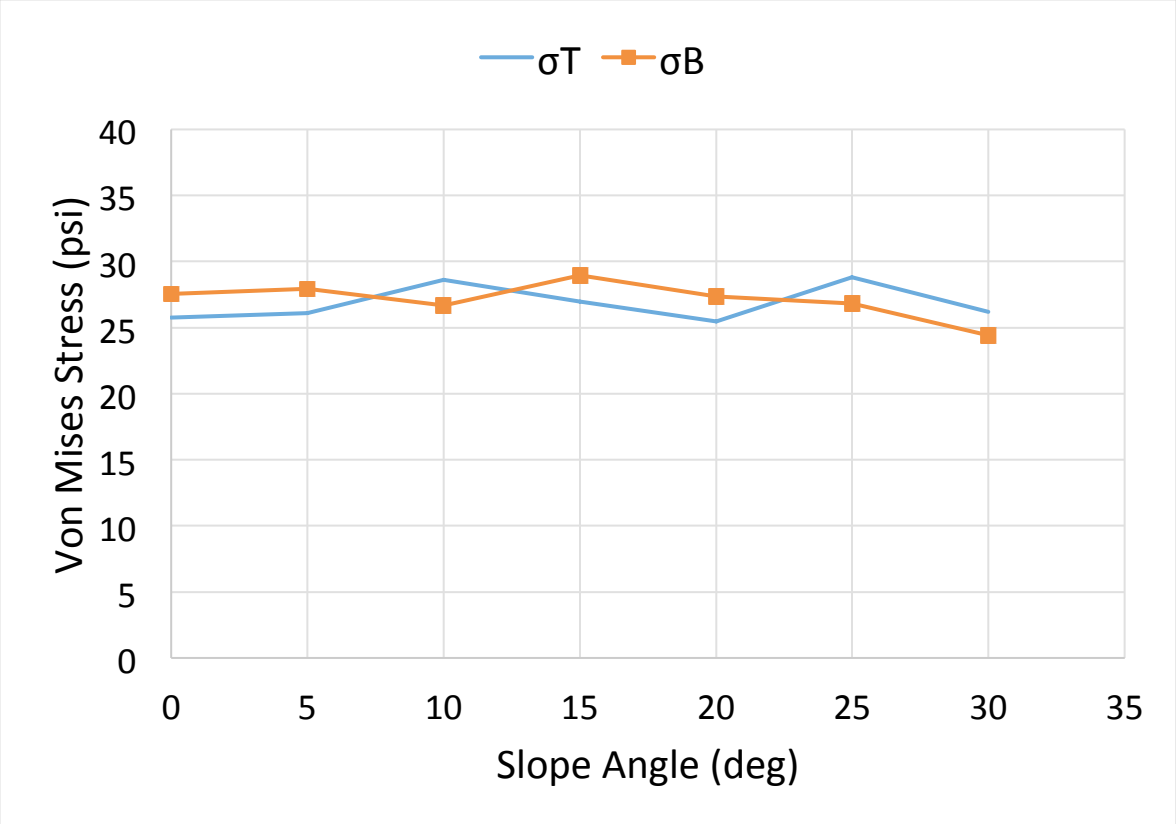


**Figure 6-95: Von Mises stress values within the RBS with radius cut parallel to the column with slope configurations subject to a negative moment at 50% yield.**

The radius cut region of the connection is successful in concentrating the strain demand for connection angles up to 10 degrees as shown in Figures 6-96 and 6-101. Localized strain demand begins to occur in the bottom flange near the beam/column interface in the 5- and 10-degree slope models. The strain reaches the value of approximately 20% of the maximum observed strain.

For slope angles exceeding 10 degrees, the strain demand begins to concentrate near the beam/column, away from the radius cut region, in the bottom flange. The radius cut region becomes increasingly less effective at concentrating

the strain demand as shown in Figures 6-88 through 6-91. Because the radius cut region is not perpendicular to the beam cross-section, the beam yields outside of the radius cut region in the bottom flange. This is because the beam tends to yield perpendicular to the beam cross-section.

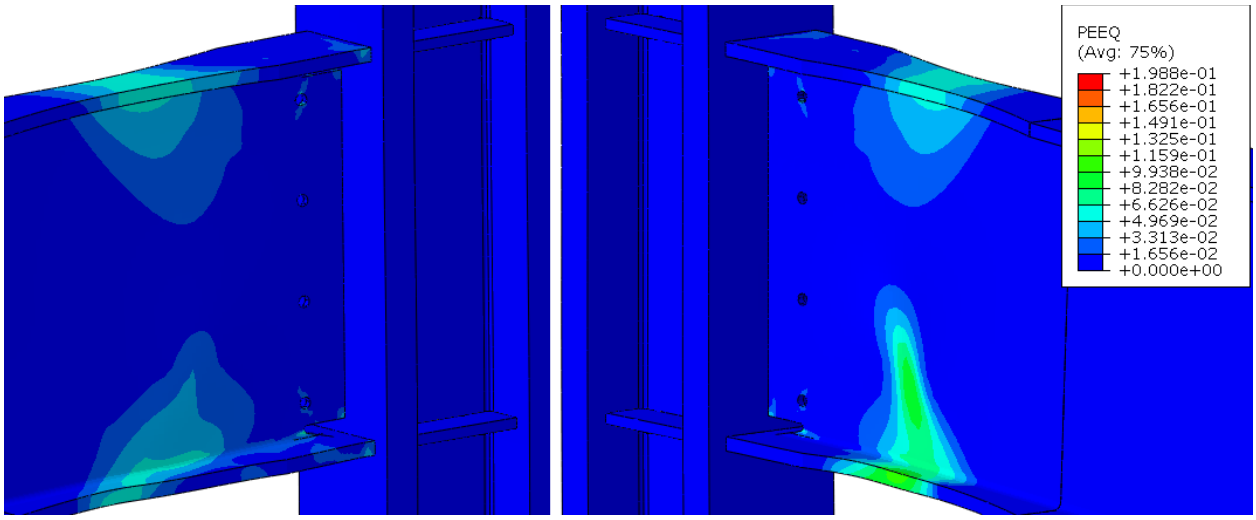


**Figure 6-96: PEEQ of the RBS connection with 5 degree slope and radius cut parallel to the column section subject to a negative moment**

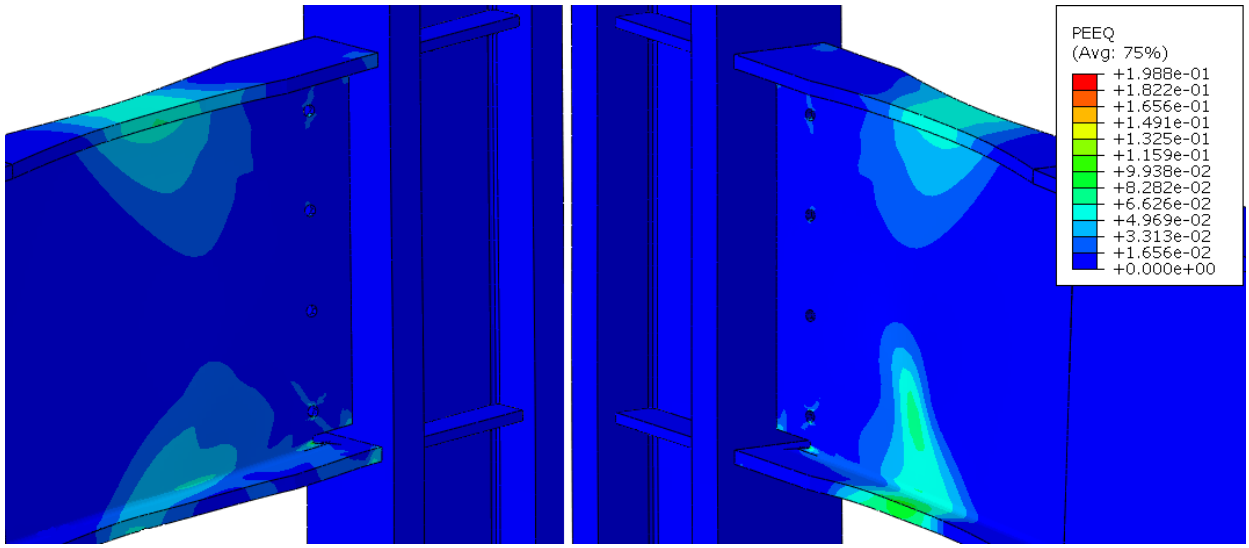


**Figure 6-97: PEEQ of the RBS connection with 10 degree slope and radius cut parallel to the column section subject to a negative moment**

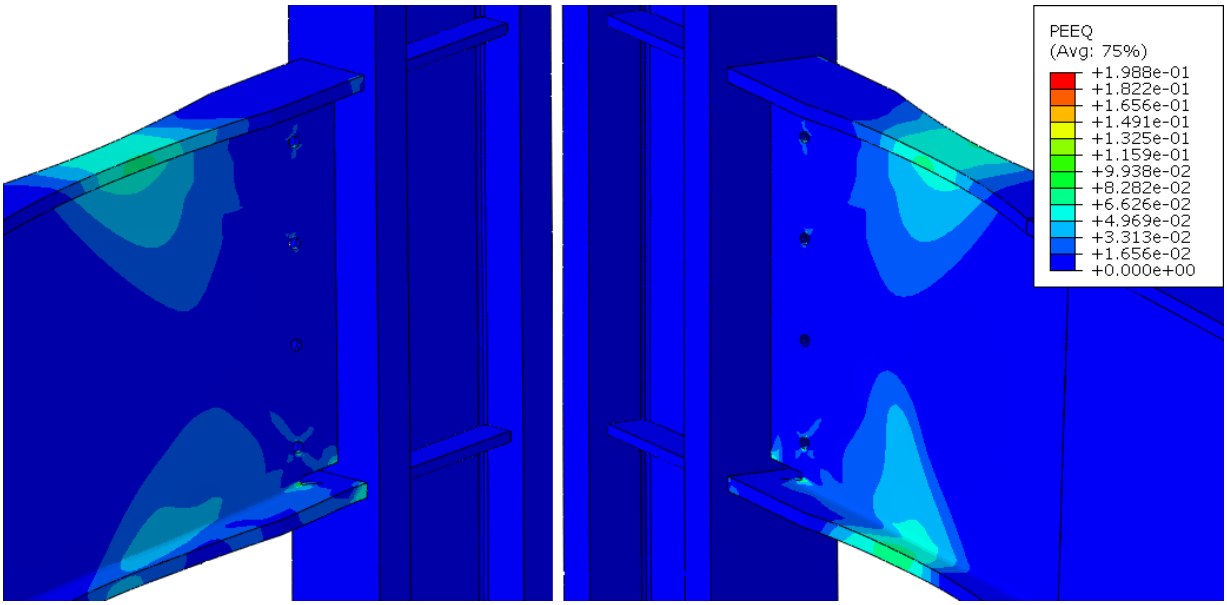


**Figure 6-98: PEEQ of the RBS connection with 15 degree slope and radius cut parallel to the column section subject to a negative moment**

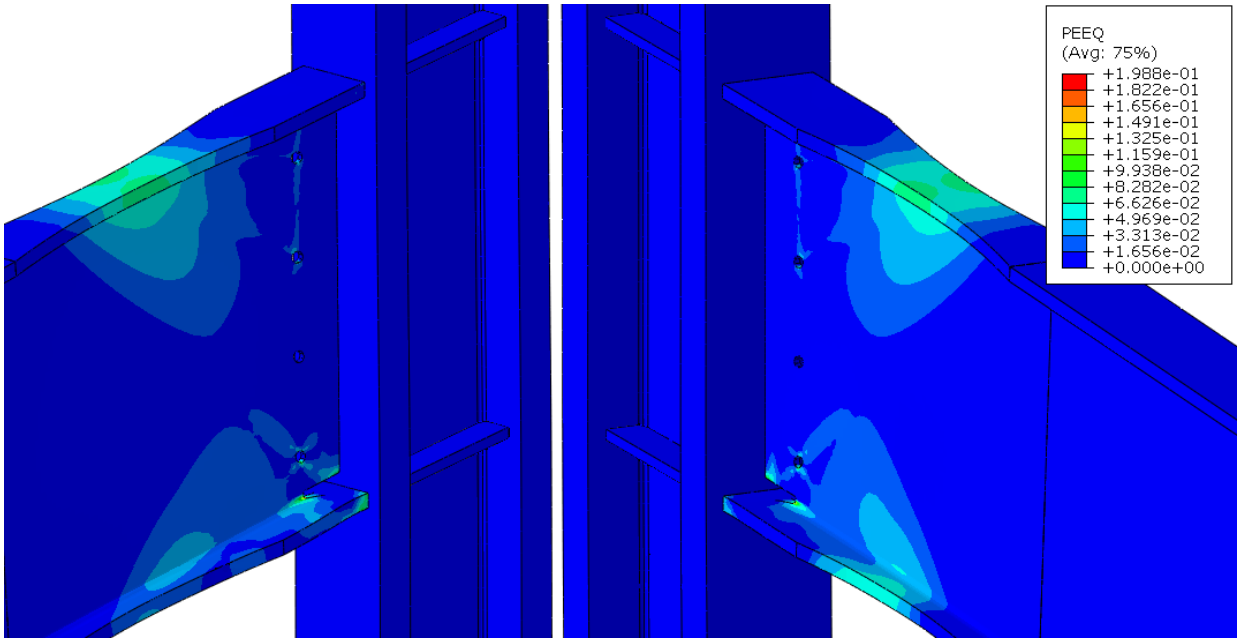


**Figure 6-99: PEEQ of the RBS connection with 20 degree slope and radius cut parallel to the column section subject to a negative moment**

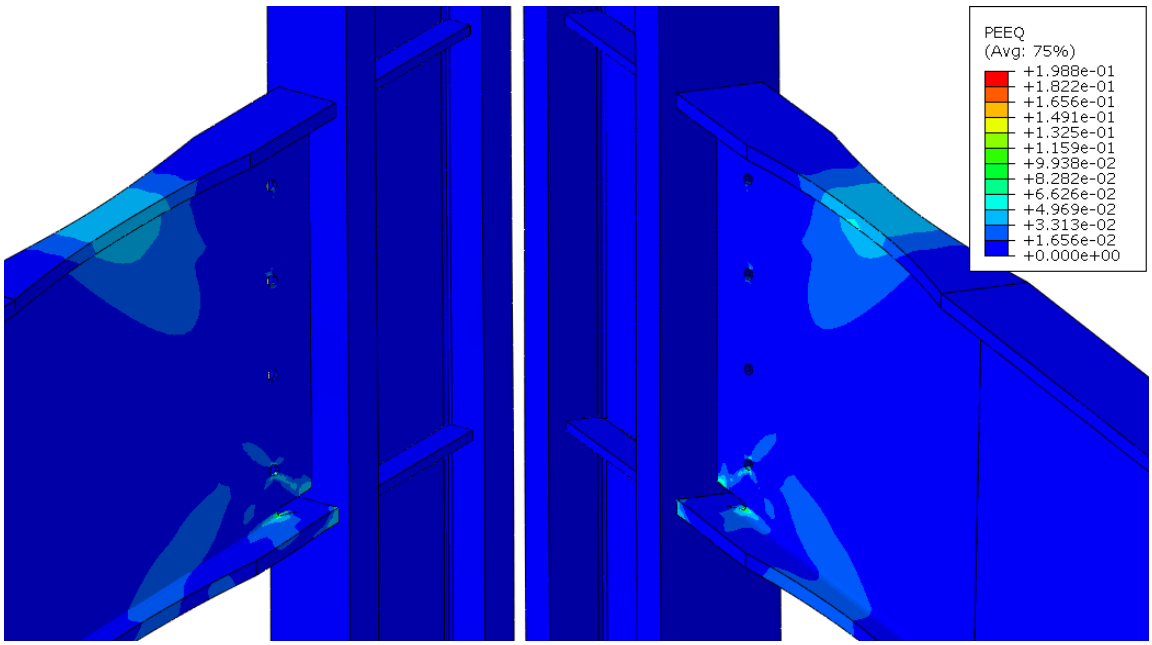


**Figure 6-100: PEEQ of the RBS connection with 25 degree slope and radius cut parallel r to the column section subject to a negative moment**

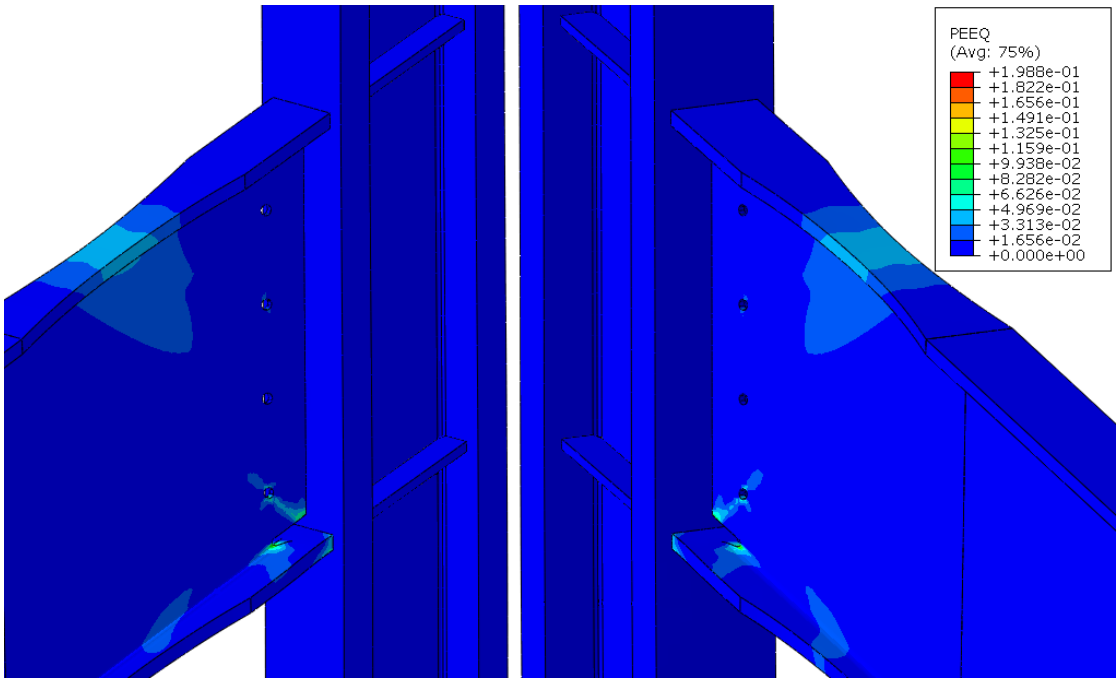


**Figure 6-101: PEEQ of the RBS connection with 30 degree slope and radius cut parallel to the column section subject to a negative moment**

### 6.2.4 RBS with Radius Cut Parallel to the Column Section and Subject to a Positive Moment

The models of configurations with the radius cut arrangement parallel to the column section experienced convergence problems. When subject to a positive moment, the finite element analysis was able to converge up to 30 degree slope. The finite element analyses were unsuccessful in converging to a solution due to excessive element distortion in cases with slope angle in excess of a 30 degree slope. The limited results obtained are illustrated in this section.

The plastic moment capacity increases as the slope angle increases as shown in Figure 6-102. The overall increase in plastic moment capacity is less than that observed for the configurations with the radius cut perpendicular to the beam section. The beam section within the radius cut region buckles after yielding which can be seen by the decrease in post-yield stiffness.

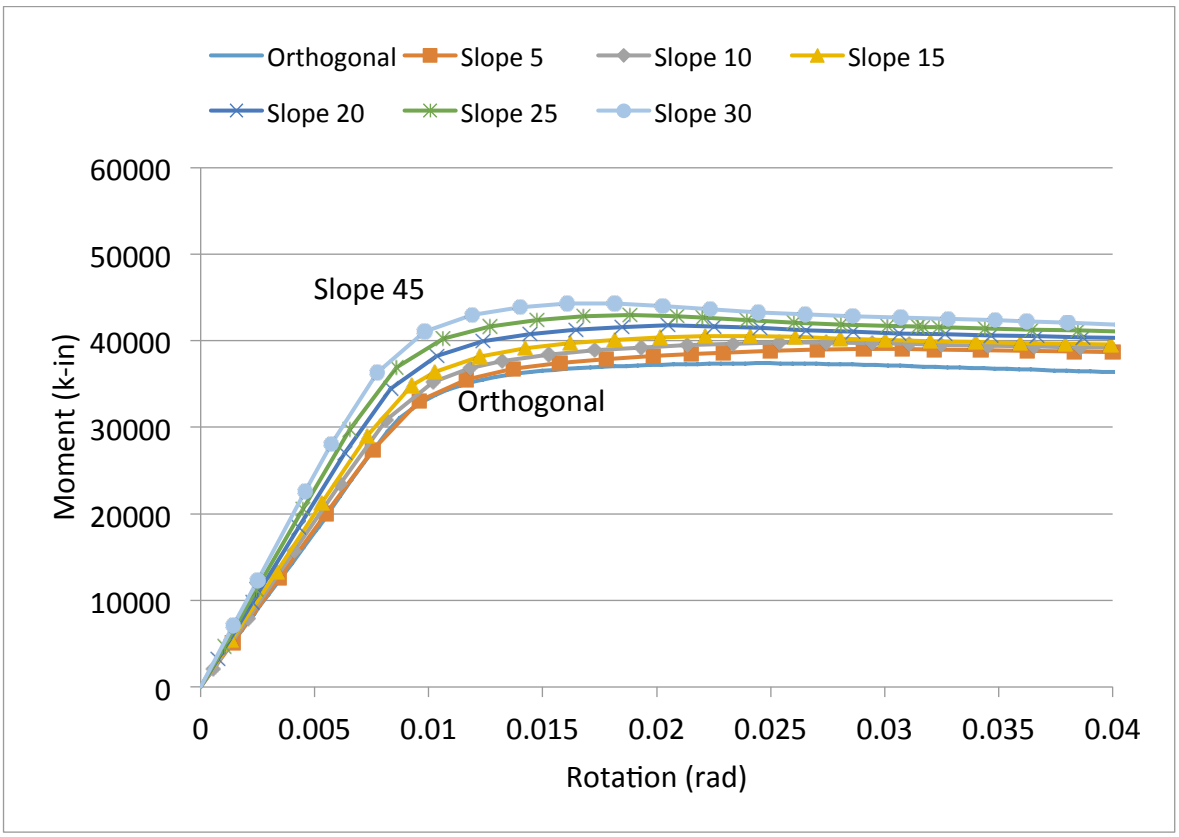


**Figure 6-102: Moment versus rotation of the RBS connection with sloped configurations and radius cut parallel to the column section subject to a positive moment**

For the RBS connection detail with sloped configurations subject to a positive moment, the stress distribution remains perpendicular to the beam section as shown in Figures 6-103 through 6-108. This effect does not appear to be impacted by the sloped geometry. For slope angles up to 15 degrees, the radius cut region is successful at concentrating the majority of the stress distribution. However, localized stress concentrations near the beam/column interface in the beam bottom flange occur for slope angles. As the slope angle exceeds 15 degrees, the radius cut region in the beam bottom flange becomes increasingly less efficient

at concentrating the stress distribution. This is likely attributed to the stress distribution in the beam remaining perpendicular to the beam cross-section. As a result, the stress concentration in the beam bottom flange increases near the beam/column interface. The beam top flange is successful at concentrating the stress distribution for slope angles up to 30 degrees.

The column flange at the beam/column interface experiences greater stress concentrations as the slope angle increases. As the slope angle increases, the stress distribution in the column flange concentrates at the beam top and bottom flanges. The panel zone of the connection is also impacted by the sloped configurations. As the slope angle increases, the stress distribution in the column web concentrates towards the bottom of the panel zone. Contrary to the RBS subject to a negative moment, this stress concentration reduces as the slope angle increases.

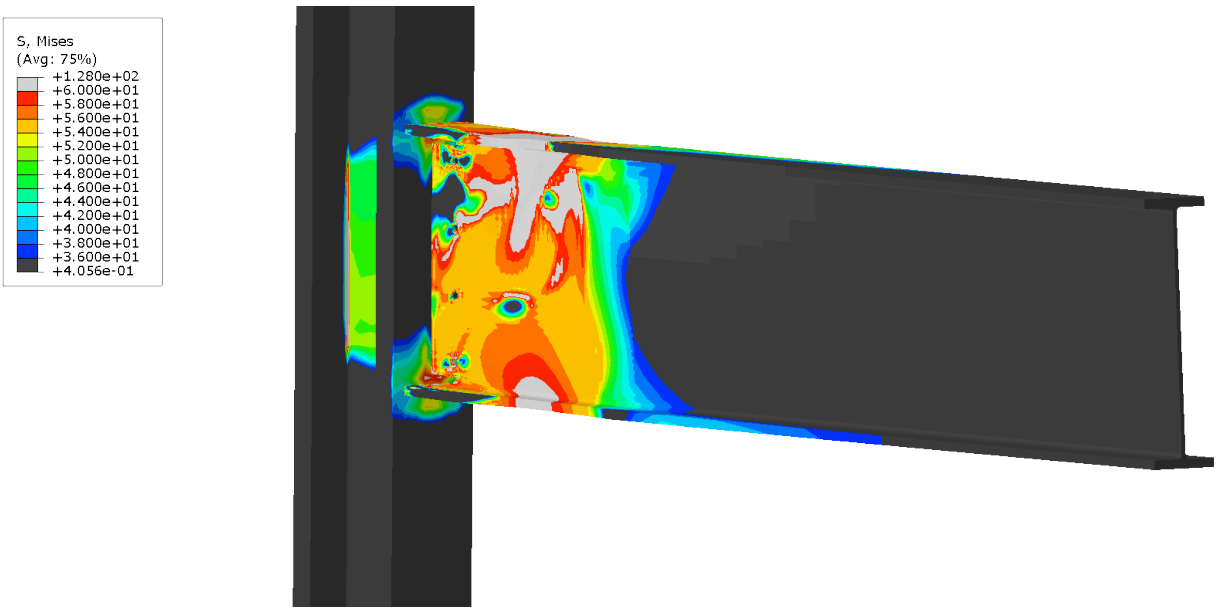


**Figure 6-103: Von Mises stress distribution of the RBS connection with 5 degree slope and radius cut parallel to the column section subject to a positive moment**

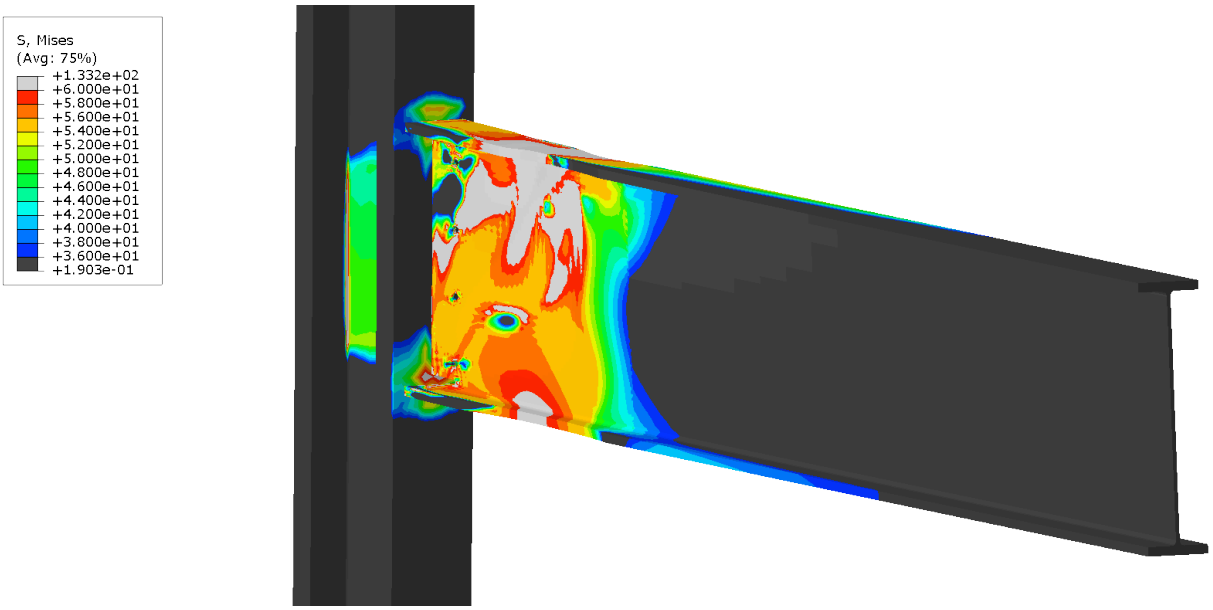


**Figure 6-104: Von Mises stress distribution of the RBS connection with 10 degree slope and radius cut parallel to the column section subject to a positive moment**

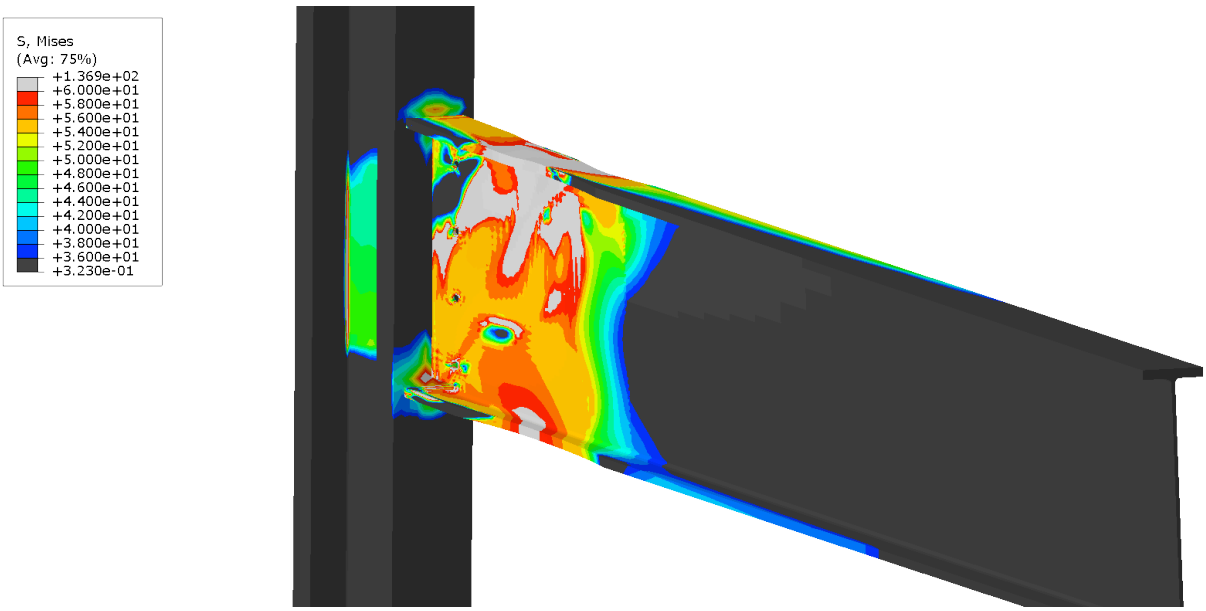


**Figure 6-105: Von Mises stress distribution of the RBS connection with 15 degree slope and radius cut parallel to the column section subject to a positive moment**

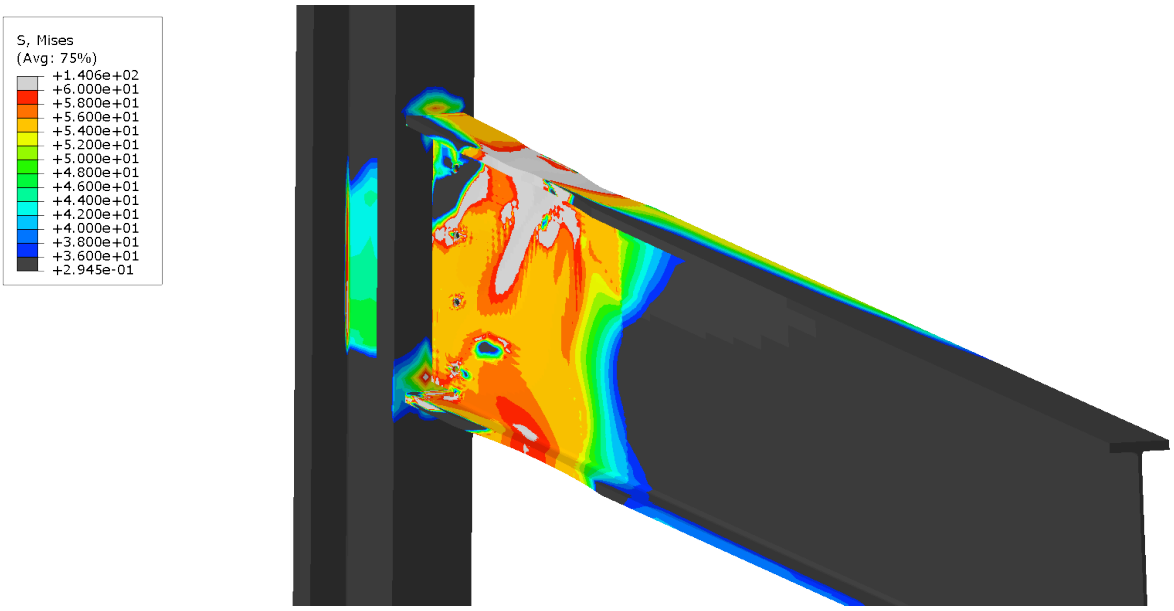


**Figure 6-106: Von Mises stress distribution of the RBS connection with 20 degree slope and radius cut parallel to the column section subject to a positive moment**

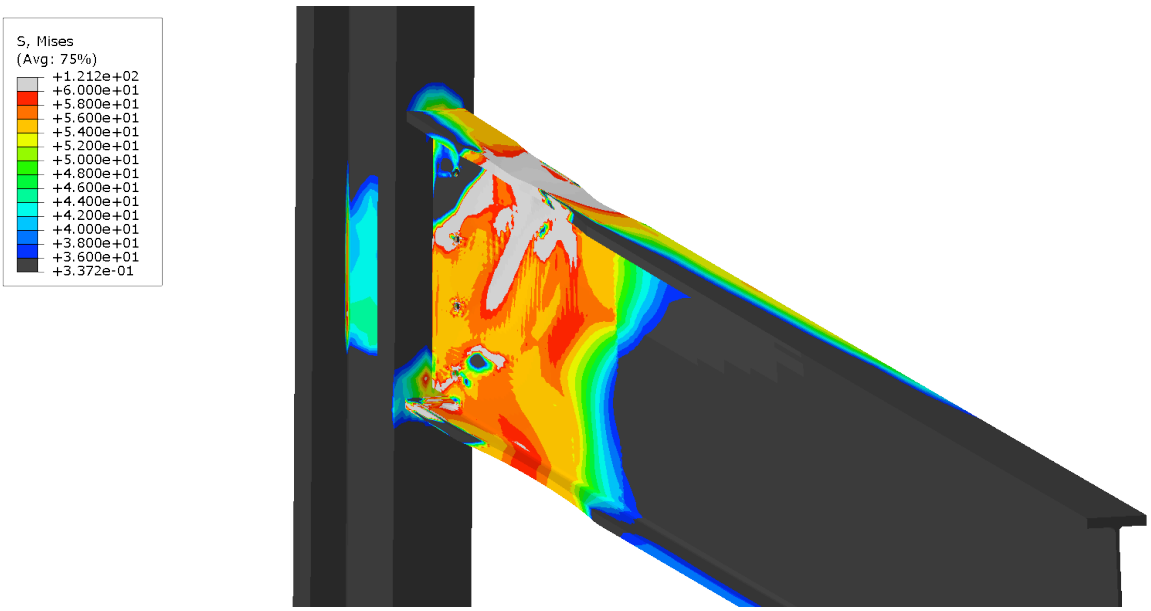


**Figure 6-107: Von Mises stress distribution of the RBS connection with 25 degree slope and radius cut parallel to the column section subject to a positive moment**

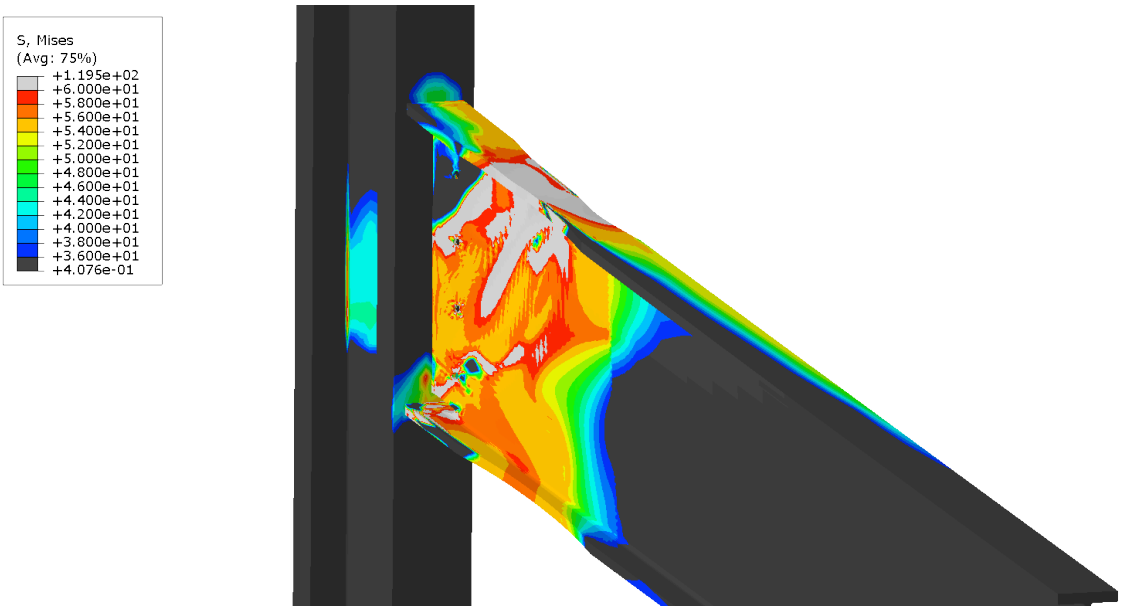


**Figure 6-108: Von Mises stress distribution of the RBS connection with 30 degree slope and radius cut parallel to the column section subject to a positive moment**

The first indication of non-linearity from the moment vs. rotation relationship occurs at a moment of 32125 k-in. The stress values associated with that moment force were recorded and plotted with respect to the sloped angle in Figure 6-109. The stress concentration in the beam flange remains essentially unchanged for slope angles up to 10 degrees. For slope angles exceeding 10 degrees, the stress concentration decreases for each increase in slope angle.

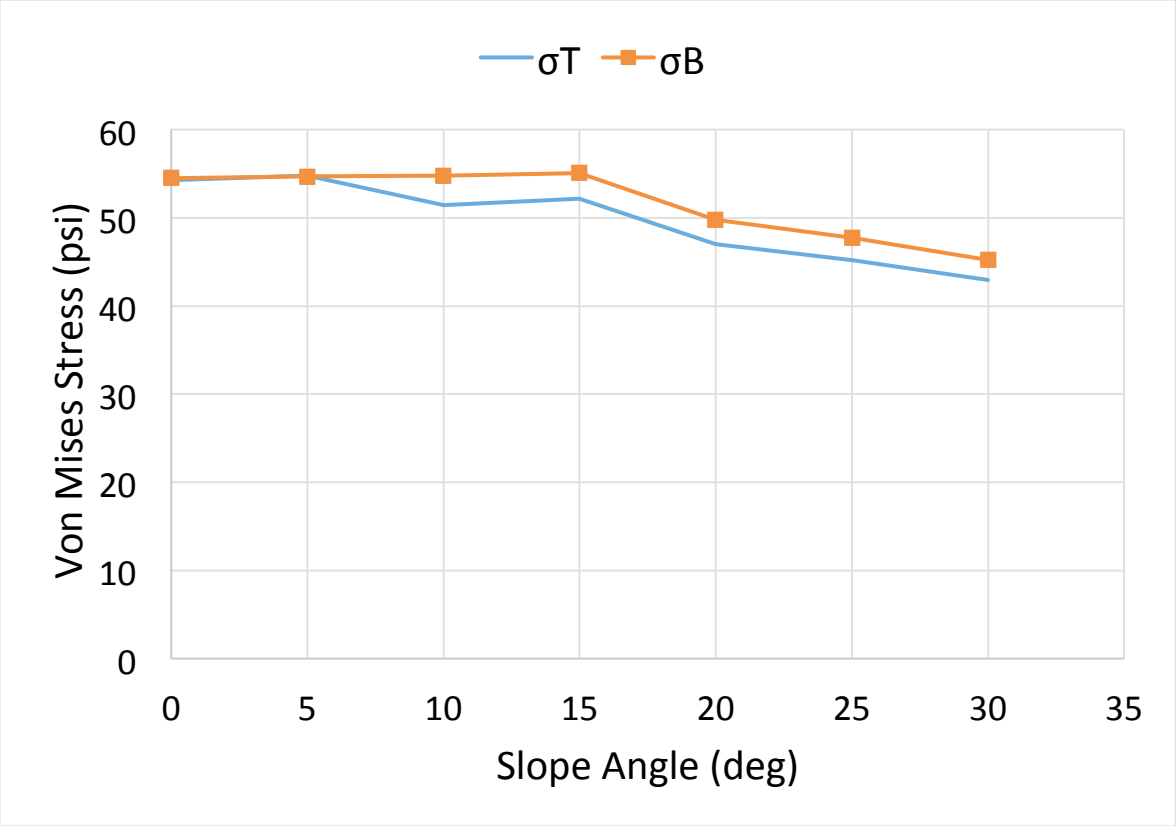


**Figure 6-109: Von Mises stress values within the RBS with radius cut parallel to the column with slope configurations subject to a positive moment at first yield.**

At 50% of the yield moment as calculated by dividing the moment associated with the first indication of non-linearity by 2, the stress values were

recorded corresponding to a moment of 14295 k-in. The stress values were plotted with respect to the slope angle in Figure 6-110. The stress concentration in the beam flange remains essentially unchanged for slope angles up to 15 degrees. For slope angles in excess of 15 degrees, the stress concentration decreases throughout the beam flange.

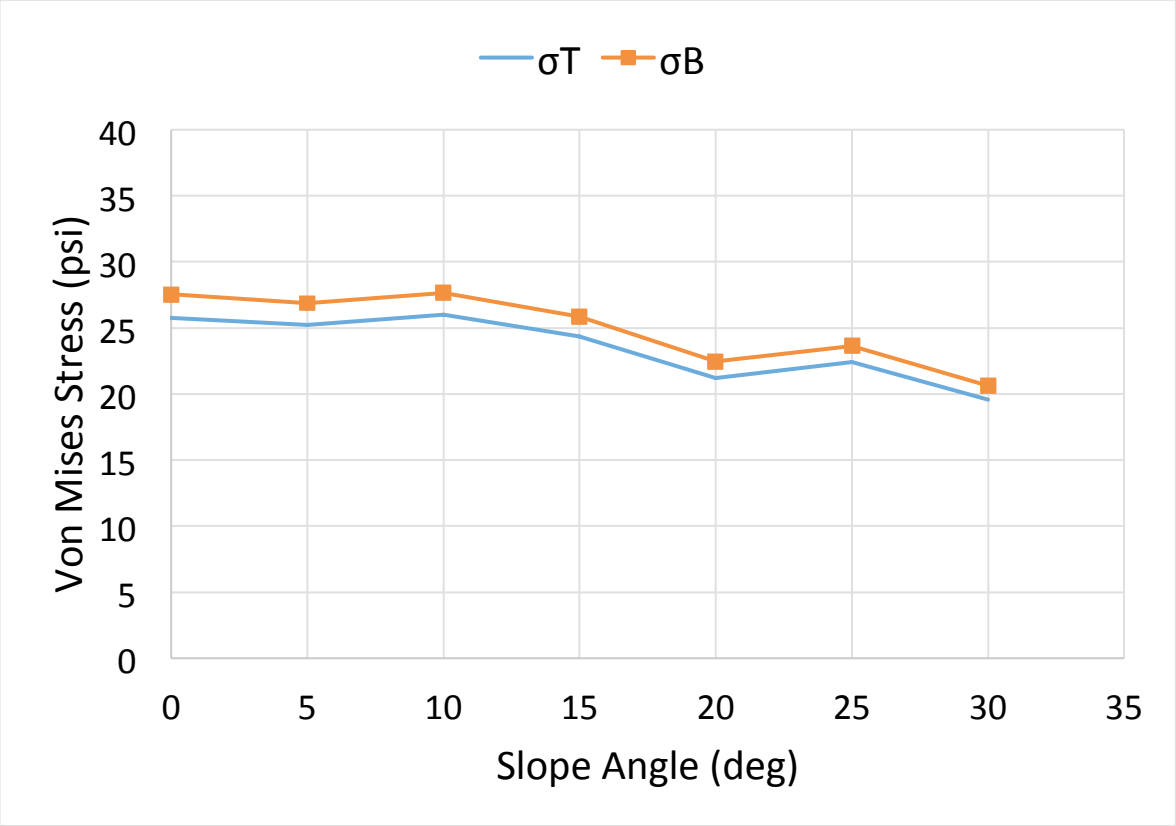


**Figure 6-110: Von Mises stress values within the RBS with radius cut parallel to the column with slope configurations subject to a positive moment at 50% yield.**

The radius cut region was successful in concentrating the strain demand for slope angles up to 10 degrees as shown in Figure 6-111 and 6-116. Localized strain demand begins to occur in the bottom flange near the beam/column interface in the

5- and 10-degree slope models. This reaches the order of approximately 20% of the maximum observed strain.

For slope angles exceeding 10 degrees, the strain demand begins to concentrate near the beam/column interface, away from the radius cut region, in the bottom flange. The radius cut region becomes increasingly less effective at concentrating the strain demand as the slope angle exceeds 10 degrees. Because the radius cut region is not perpendicular to the beam cross-section, the beam yields outside of the radius cut region in the bottom flange. This is once again because the beam tends to yield perpendicular to the beam cross-section.

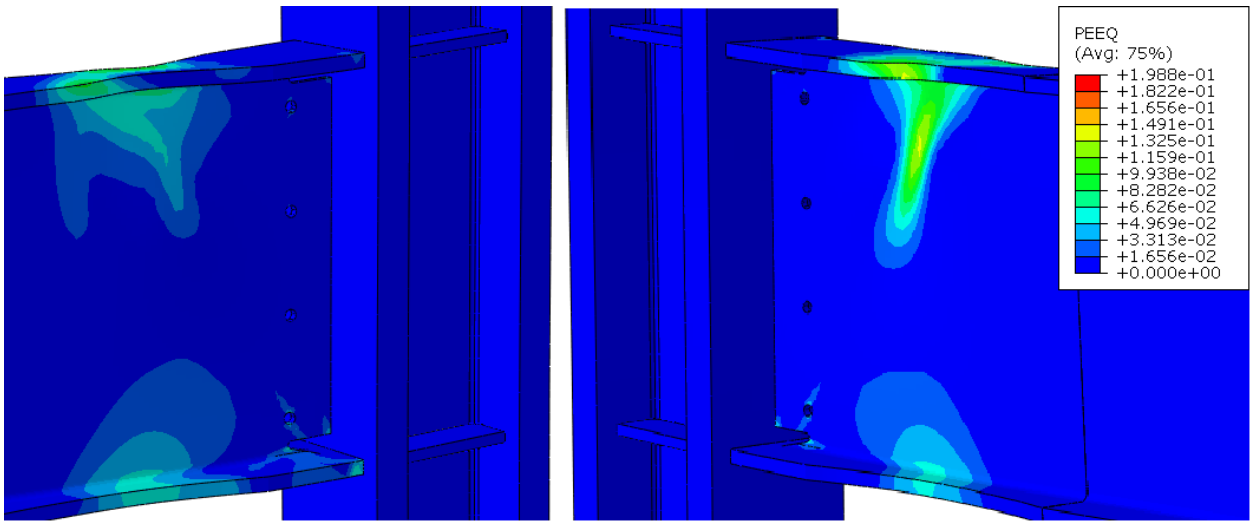


**Figure 6-111: PEEQ of the RBS connection with 5 degree slope and radius cut parallel to the column section subject to a positive moment**

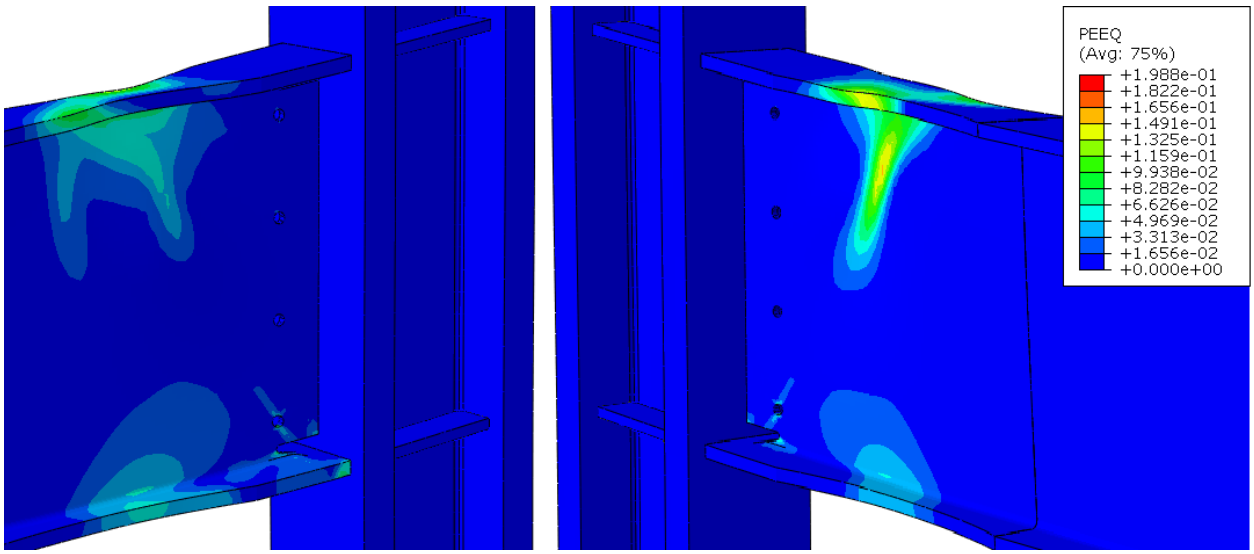


**Figure 6-112: PEEQ of the RBS connection with 10 degree slope and radius cut parallel to the column section subject to a positive moment**

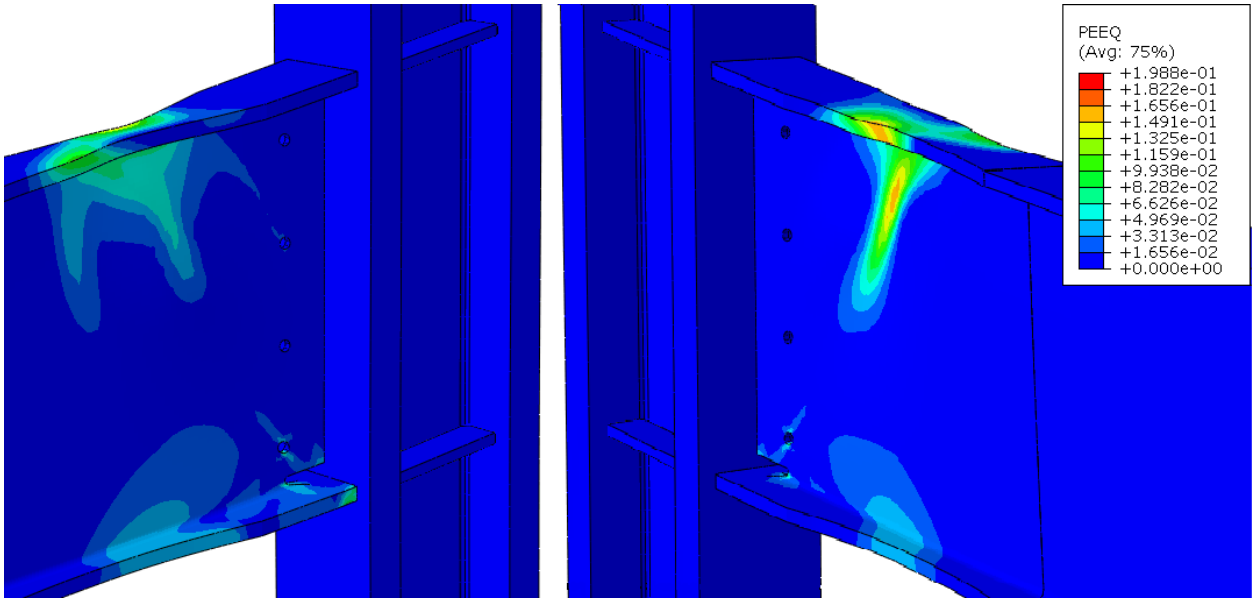


**Figure 6-113: PEEQ of the RBS connection with 15 degree slope and radius cut parallel to the column section subject to a positive moment**

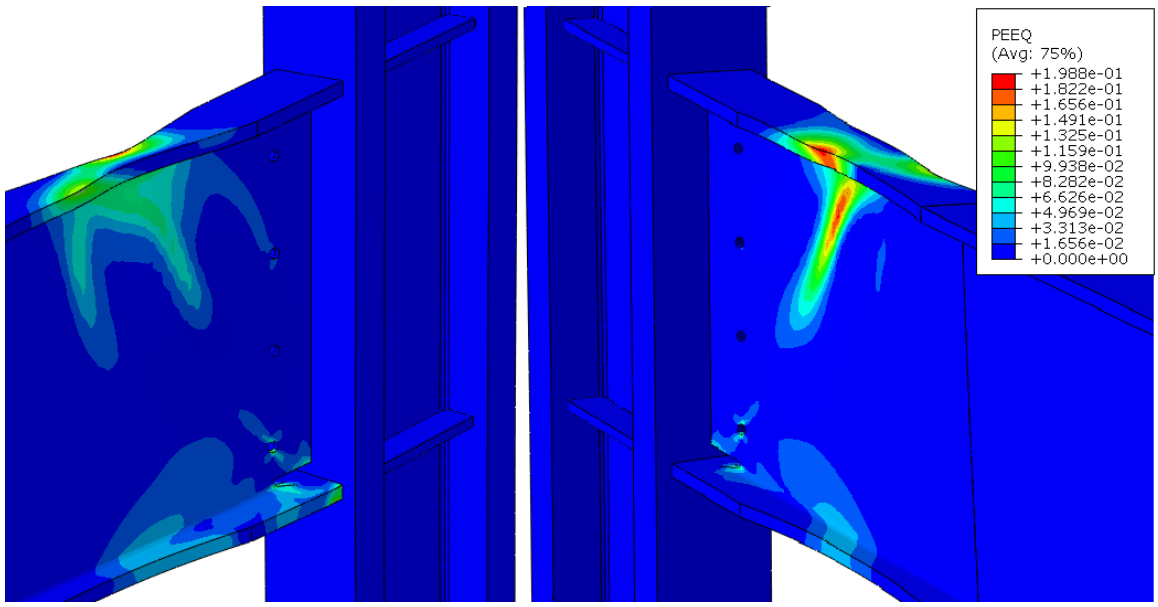


**Figure 6-114: PEEQ of the RBS connection with 20 degree slope and radius cut parallel to the column section subject to a positive moment**

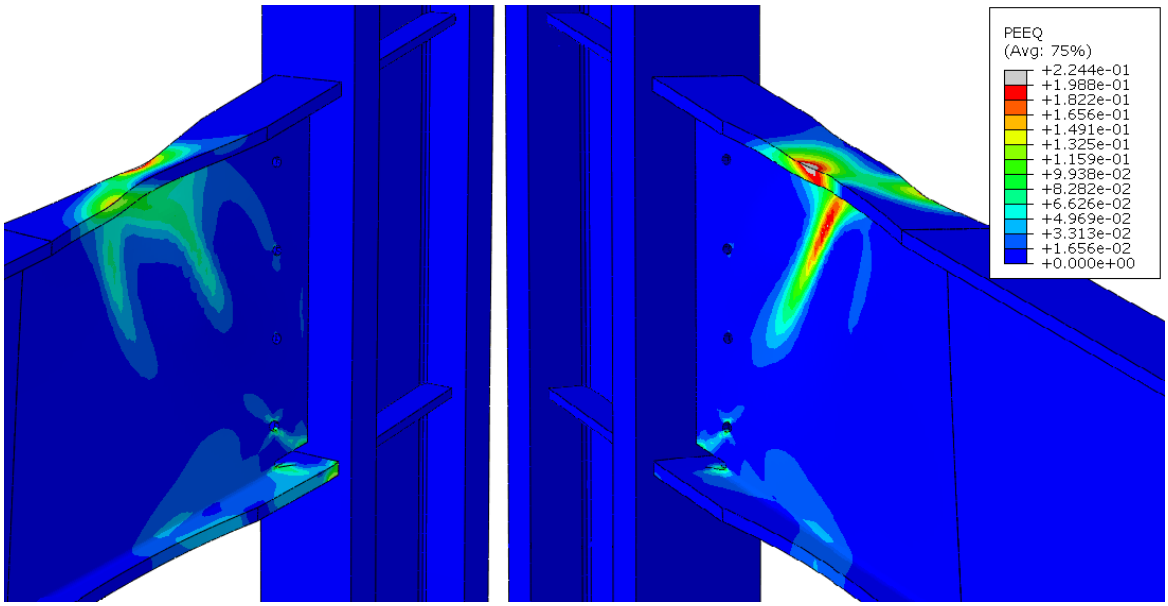


**Figure 6-115: PEEQ of the RBS connection with 25 degree slope and radius cut parallel to the column section subject to a positive moment**

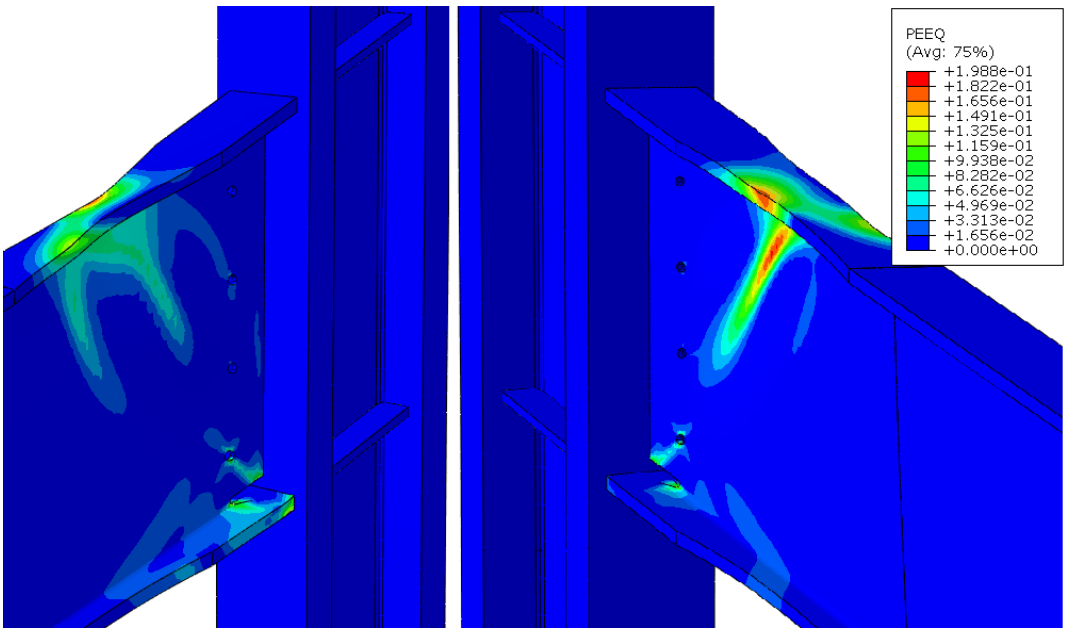


**Figure 6-116: PEEQ of the RBS connection with 30 degree slope and radius cut parallel to the column section subject to a positive moment**

# Chapter 7: Conclusions

## 7.1 Recommendations for the WUF-W Moment Connection with Skewed Configurations

A skewed configuration results in a negligible difference in initial stiffness and plastic moment capacity. The full plastic moment capacity of the beam can be obtained for angles of 0 to 45 degrees. However, as the skew angle increases, the yielding point becomes less well defined as indicated by the more gradual transition from elastic to plastic behavior. This is most likely attributed to the additional out-of-plane forces such as torsion and minor axis bending present in the skewed configurations.

The stress distribution is largely impacted by the skew angle in the beam. The stress distribution in the column flange progressively increases near the acute angle formed between the beam and the column for each increase in skew angle. For skew angles less than 10 degrees, the stress concentration in the column flange is negligible. Additionally, as the skew angle exceeds 20 degrees, the stress distribution in the column flange at the beam/column interface begins concentrating at both the acute and obtuse angle formed between the beam and the column. Within the beam flanges, the stress distribution progressively concentrates within at the acute angle formed between the beam and the column for each

increase in skew angle. For skew angles less than 10 degrees, this effect is negligible.

The stress distribution within the beam flange in tension is impacted by the skew angle of the beam. As the skew angle increases, the stress concentration in the beam flange increases near the acute angle formed from the beam/column interface. Conversely, the stress concentration decreases near the obtuse angle formed from the beam/column interface. The effect on the stress distribution throughout the beam flange is negligible for skew angles less than 10 degrees.

The plastic strain distribution is highly impacted by the skew angle of the connection. As the connection angle increases, the strain demand in the top and bottom flanges concentrates near the acute angle formed by the beam-to-column connection. Therefore, it is not recommended that skew angles greater than 10 degrees be designed without considering the effects of increased localized strain demands near the beam/column interface.

## 7.2 Recommendations for the WUF-W Moment Connection with Sloped Configurations

As the slope angle of the beam increases, the initial stiffness and plastic moment capacity increase. This is because the effective depth of the beam cross-section is proportional to the slope angle. Therefore, as the slope angle increases, the effective depth of the beam increases. This increases the moment of inertia

about the beam strong axis which increases the beam stiffness and plastic moment capacity.

The stress distribution within the beam section remains perpendicular to the beam section regardless of slope angle. As a result, the stress distribution progressively concentrates near the beam/column interface in the beam bottom flange for each increase in slope angle exceeding 10 degrees. Conversely, the stress distribution in the beam top flange concentrates further away from the beam/column interface and distributes over a larger region as the slope angle increases.

The stress concentration within the beam flange in tension is minimally impacted by the slope angle of the beam. As the slope angle increases, the stress concentration in the beam flange increases for slope angles up to 20 degrees. For slope angles in excess of 20 degrees, the stress concentration progressively decreases. The stress distribution throughout the beam flange remains uniform for sloped configurations.

When the connection detail has a sloped beam configuration, the plastic strain demand increases in the bottom flange near the acute angle formed between the beam/column interface. In the beam top flange, the strain demand distributes over a larger region. For slope angles less than or equal to 10 degrees, the increase in strain demand near the beam/column interface is negligible. Therefore, slope

angles greater than 10 degrees are not recommended for design without the consideration of increased localized strain demands near the beam/column interface.

## 7.3 Recommendations for the RBS Moment Connection with Skewed Configurations

### 7.3.1 RBS with Radius Cut Perpendicular to the Beam Section

For each increase in skew angle, the impact on the plastic moment capacity is minimal, resulting in a slight increase in plastic moment capacity. The yielding point is unaffected by the skew angle. No gradual change of slope is observed in the RBS moment connection with skewed configurations.

The stress distribution in the RBS connection detail is largely impacted by the skew angle in the beam. The stress concentration increases within the column flange at the acute angle formed between the beam and the column as the skew angle increases. For skew angles not greater than 10 degrees, this effect is negligible. As the skew angle exceeds 20 degrees, the stress distribution in the column flange concentrates at both the acute and obtuse angles formed between the beam and the column. Within the beam, the radius cut region is successful at concentrating the majority of the stress distribution for each increase in skew

angle. As the skew angle increases, the stress concentration in the beam flanges at the acute angle formed between the beam and the column minimally increases.

The stress distribution within the beam flange in tension is highly impacted by the skew angle of the beam. At 50% of the yield moment, the stress distribution in the beam flange progressively concentrates near the side of the radius cut region corresponding to the acute angle formed between the beam and column. At first yield, the stresses in the radius cut region remain essentially unchanged up to skew angles of 15 degrees. Upon exceeding a skew angle of 15 degrees, the stress concentration in the beam flange near the radius cut region corresponding to the obtuse angle formed from the beam and column progressively decreases.

The skewed configurations were successful in concentrating the strain demand within the radius cut region for angles up to 30 degrees. For skew angles in excess of 30 degrees, localized strain demands occur in the top and bottom flanges near the connection. Skew angles greater than 10 degrees are not recommended due to the expected increase in stress concentration in the column flanges and the increased localized strain demands near the beam/column interface.

### 7.3.2 RBS with Radius Cut Parallel to the Column Section

In this case, the plastic moment capacity increases minimally as the skew angle increases. The yielding point is unaffected by the skew angle. No gradual

change of slope is observed in the RBS moment connection with skewed configurations.

The stress distribution in the RBS connection detail is largely impacted by the skew angle in the beam. The stress concentration increases within the column flange at the acute angle formed between the beam and the column as the skew angle increases. For skew angles not greater than 10 degrees, this effect is negligible. As the skew angle exceeds 20 degrees, the stress distribution in the column flange concentrates at both the acute and obtuse angles formed between the beam and the column. Within the beam, the radius cut region is successful at concentrating the majority of the stress distribution for each increase in skew angle. As the skew angle increases, the stress concentration in the beam flanges at the acute angle formed between the beam and the column increases. For skew angles less than or equal to 10 degrees, the effect of increased stress concentration in the beam flanges near the beam/column interface is negligible.

The stress distribution within the beam flange in tension is highly impacted by the skew angle of the beam. At 50% of the yield moment, the stress distribution in the beam flange progressively concentrates near the side of the radius cut region corresponding to the acute angle formed between the beam and column. At first yield, the stresses in the radius cut region remain essentially unchanged up to skew angles of 15 degrees. Upon exceeding a skew angle of 15 degrees, the stress

concentration in the beam flange near the radius cut region corresponding to the obtuse angle formed from the beam and column progressively decreases.

The skewed configurations were successful in concentrating the strain demand within the radius cut region for angles up to 10 degrees. For skew angles exceeding 10 degrees, strain demand begins to concentrate near the beam/column interface in the top and bottom flanges away from the radius cut region. The strain demand near the beam/column increases for each increasing skew angle. Therefore, the use of skew angles in excess of 10 degrees is not recommended unless the localized strain demands near the connection are considered in the design.

## 7.4 Recommendations for the RBS Moment Connection with Sloped Configurations

### 7.4.1 RBS with Radius Cut Perpendicular to the Beam Section

An increase in initial stiffness and plastic moment capacity is observed for a connection subject to both a negative and positive moment. This is attributed to the increase in effective depth of the beam cross-section. The effective depth of the beam cross-section is proportional to the slope angle of the beam. As the slope angle increases, the effective depth of the beam cross-section increases. This

increases the moment of inertia about the beam strong axis and in turn increases the beam stiffness and plastic moment capacity.

For both cases of the RBS connection detail with sloped configurations subject to a negative and positive moment, the stress distribution remains perpendicular to the beam section. This effect is not impacted by the slope angle in the beam. The radius cut region is successful at concentrating the stress distribution for slope angles up to 20 degrees when the connection is subject to a negative moment and up to 30 degrees when the connection is subject to a positive moment. However, localized stress concentrations within the beam bottom flange are observed as the stress distribution tends to remain perpendicular to the beam section. For slope angles exceeding 20 degrees under both loading conditions, the radius cut region becomes progressively less effective at concentrating the stress distribution as localized stress concentrations in the beam bottom flange near the beam/column interface increase.

The stress concentration within the beam flange in tension is minimally impacted by the slope angle of the beam. As the slope angle increases, the stress concentration in the beam flange progressively decreases for each increase in slope angle. The stress distribution throughout the beam flange remains uniform for sloped configurations.

For sloped configurations subject to a negative moment, the radius cut region is successful in concentrating the strain demand for slope angles not exceeding 10 degrees. For sloped configurations subject to a positive moment, the radius cut region is successful in concentrating strain demands for slope angles up to 30 degrees. Because a seismic event may induce cyclical loading on the connection, it is not recommended to use sloped configurations in excess of 10 degrees without the consideration of localized stress concentrations and strain demands near the beam column interface.

### 7.4.2 RBS with Radius Cut Parallel to the Column Section

An increase in initial stiffness and plastic moment capacity is observed for a connection subject to both cases of a negative moment and positive moment. This is attributed to the increase in effective depth of the beam cross-section. The effective depth of the beam cross-section is proportional to the slope angle of the beam. As the slope angle increases, the effective depth of the beam cross-section increases. This increases the moment of inertia about the beam strong axis and in turn increases the beam stiffness and plastic moment capacity.

For the RBS connection detail with sloped configurations subject to both a negative and positive moment, the stress distribution remains perpendicular to the beam cross-section. This effect is not impacted by the slope angle in the beam. For both loading conditions and slope angles up to 15 degrees, the radius cut region is

successful at concentrating the majority of the stress distribution. However, localized stress concentrations are observed in the beam bottom flange near the beam/column interface. As the slope angle exceeds 15 degrees, the radius cut region in the beam bottom flange becomes increasingly less effective at concentrating the stress distribution. As a result, the stress concentration within the beam bottom flange increases near the beam/column interface.

The stress concentration within the beam flange in tension is minimally impacted by the slope angle of the beam. As the slope angle increases, the stress concentration in the beam flange progressively decreases for each increase in slope angle. The stress distribution throughout the beam flange remains uniform for sloped configurations.

For sloped configurations subject to a negative moment, the radius cut region is successful in concentrating the strain demand for slope angles not exceeding 10 degrees. For sloped configurations subject to a positive moment, the radius cut region is successful in concentrating strain demands for slope angles up to 30 degrees. Because a seismic event may induce cyclical loading on the connection, it is not recommended that sloped configurations with angles exceeding of 10 degrees be designed without the consideration of localized stress concentrations and strain demands near the beam/column interface.

## 7.5 General Recommendations for the Radius Cut Arrangement

The radius cut arrangement impacts the performance of the connection. Because there are two possible arrangements for the radius cut, it is important that the arrangement be considered in the design and detailing of an RBS connection.

The radius cut oriented perpendicular to the beam section appears to perform better for skew configurations. The radius cut region is successful at concentrating the stress distribution and strain demands away from the connection up to 30 degrees of skew. For the radius cut arrangement parallel to the column section, the stress distribution progressively concentrates at the acute angle formed between the beam and the column when the skew is greater than of 10 degrees. Additionally, localized strain demands are observed at the acute angle formed between the beam and the column when the skew is greater than of 10 degrees.

The radius cut arrangement perpendicular to the beam section appears to perform better for slope angle configurations. This is mostly attributed to the fact that the plastic hinge tends to form perpendicular to the beam section. If the radius cut arrangement is made perpendicular to the beam section, the strain demand is more successfully concentrated within the radius cut region. Cases with the radius cut parallel to the column section observed higher strain demands near the connection.

## 7.6 Future Research

A seismic event creates dynamic loads on the building system. A stable cyclical response of a moment connection is of paramount importance in the performance of a building system. A finite element analysis capable of applying cyclical loading on a full-scale moment connection would better help understand the response of a non-orthogonal moment connection. Using solid elements would demand an incredible amount of computational power and time to perform. An alternative would be to incorporate elements with fewer degrees of freedom such as shell elements which would reduce the computational demand. However this could also impact the level of accuracy in the analysis.

Perhaps the most difficult, but potentially the most useful research would be the application of damage mechanics. A finite element model of a moment connection incorporating damage mechanics could help better understand the effects of increased strain demands. Full penetration welds are susceptible to the increased localized strain demands of non-orthogonal connection framing. The application of damage mechanics can help better understand where the strain demands would be critical and where a failure would be suspected in the connection.

## Chapter 8: References


ANSI/AISC (2010). *"ANSI/AISC 341-10: Seismic Provisions for Structural Steel Buildings."* American Institute of Steel Construction. Chicago, Ill.

ANSI/AISC (2010). *"ANSI/AISC 358-10: "Prequalified Connections of Special and Intermediate Steel Moment Frames for Seismic Applications."* American Institute of Steel Construction. Chicago, Ill.

ANSI/AISC (2010). *"ANSI/AISC 360-10: Specification for Structural Steel Buildings."* American Institute of Steel Construction. Chicago, Ill.

ASCE/SEI (2010). *"ASCE/SEI 7-10: Minimum Design Loads for Buildings and Other Structures."* American Society of Civil Engineers. Reston, VA.

Ball, S. (2011) "Steel Non-Orthogonal Reduced Beam Section Moment Connections – A Case Study." *The Structural Design of Tall and Special Buildings,* Vol. 20, Wiley-Blackwell, Hoboken, NJ.

Engelhardt, M., Winneberger, T., Zekany, A., Potyraj, T. (1998) "Experimental Investigation of Dogbone Moment Connections." *AISC Engineering Journal*, 12-21. Chicago, Ill.

Hassan, T. (2012). "An Innovative Seismic Performance Enhancement Technique for Steel Building Beam-Column Connections." *National Science Foundation,* #0936547, Arlington, VA.

Kim, D.W., Ball, S., Sim, H.B., Uang, C.M. (2015). "Evaluation of Sloped RBS Moment Connections." *ASCE Journal of Structural Engineering,* In Review.

Prinz, G., Richards, P. (2014). "Demands on Reduced Beam Section Connections with Out-of-Plane Skew." *ASCE Journal of Structural Engineering,* In Review.

Ruffley, D. (2011). *"A Finite Element Approach for Modeling Bolted Top-and-Seat Angle Components and Moment Connections."* M.S. Thesis, Univ. of Cincinnati, Cincinnati, OH.

Schrauben, C. (1999). *"Behavior of Full-Scale Bolted Beam-to-Column T-Stub and Clip Angle Connections under Cyclic Loading."* M.S. Thesis, Georgia Institute of Technology, Atlanta, GA.